



N° 2006-ISAL-00101



2006

Ph.D.

Jointly awarded at the
University of Rome 'La Sapienza'
Dottorato di ricerca in Meccanica Teorica ed Applicata
XIX ciclo
and at the
'Institut National des Sciences Appliquées' of Lyon
Ecole doctorale: Mécanique, Energétique, Génie Civil, Acoustique
(MEGA)
Spécialité: Mécanique

Dynamic and tribological analysis of brake squeal

Francesco MASSI

On December 5, 2006

PhD Committee:

Examiner	Y. BERTHIER	Research director (CNRS) (INSA of Lyon)
Examiner	P. CAPPA	Professor (University of Rome 'La Sapienza')
Examiner / Tutor	A. SESTIERI	Professor (University of Rome 'La Sapienza')
Examiner / Tutor	L. BAILLET	Professor (Université Joseph Fourier, Grenoble)
Guest	A. AKAY	Professor (National Science Foundation, USA)

Reviewers:

Reviewer	P. DUFRENOY	Professor (Ecole Polytechnique, Lille)
Reviewer	J.E. MOTTERSHEAD	Professor (University of Liverpool)

Research laboratory:
Dipartimento di Meccanica ed Aeronautica (DMA)
and
Laboratoire de Mécanique des Contacts et des Solides (LaMCoS)

SIGLE	ECOLE DOCTORALE	NOM ET COORDONNEES DU RESPONSABLE
	CHIMIE DE LYON Responsable : M. Denis SINOÛ	M. Denis SINOÛ Université Claude Bernard Lyon 1 Lab Synthèse Asymétrique UMR UCB/CNRS 5622 Bât 308 2 ^{ème} étage 43 bd du 11 novembre 1918 69622 VILLEURBANNE Cedex Tél : 04.72.44.81.83 Fax : 04 78 89 89 14 sinou@univ-lyon1.fr
E2MC	ECONOMIE, ESPACE ET MODELISATION DES COMPORTEMENTS Responsable : M. Alain BONNAFOUS	M. Alain BONNAFOUS Université Lyon 2 14 avenue Berthelot MRASH M. Alain BONNAFOUS Laboratoire d'Economie des Transports 69363 LYON Cedex 07 Tél : 04.78.69.72.76 Alain.bonnafous@ish-lyon.cnrs.fr
E.E.A.	ELECTRONIQUE, ELECTROTECHNIQUE, AUTOMATIQUE M. Daniel BARBIER	M. Daniel BARBIER INSA DE LYON Laboratoire Physique de la Matière Bâtiment Blaise Pascal 69621 VILLEURBANNE Cedex Tél : 04.72.43.64.43 Fax 04 72 43 60 82 Daniel.Barbier@insa-lyon.fr
E2M2	EVOLUTION, ECOSYSTEME, MICROBIOLOGIE, MODELISATION http://biomserv.univ-lyon1.fr/E2M2 M. Jean-Pierre FLANDROIS	M. Jean-Pierre FLANDROIS UMR 5558 Biométrie et Biologie Evolutive Equipe Dynamique des Populations Bactériennes Faculté de Médecine Lyon-Sud Laboratoire de Bactériologie BP 1269600 OULLINS Tél : 04.78.86.31.50 Fax 04 72 43 13 88 E2m2@biomserv.univ-lyon1.fr
EDIIS	INFORMATIQUE ET INFORMATION POUR LA SOCIETE http://www.insa-lyon.fr/ediis M. Lionel BRUNIE	M. Lionel BRUNIE INSA DE LYON EDIIS Bâtiment Blaise Pascal 69621 VILLEURBANNE Cedex Tél : 04.72.43.60.55 Fax 04 72 43 60 71 ediis@insa-lyon.fr
EDISS	INTERDISCIPLINAIRE SCIENCES-SANTE http://www.ibcp.fr/ediss M. Alain Jean COZZONE	M. Alain Jean COZZONE IBCP (UCBL1) 7 passage du Vercors 69367 LYON Cedex 07 Tél : 04.72.72.26.75 Fax : 04 72 72 26 01 cozzone@ibcp.fr
	MATERIAUX DE LYON http://www.ec-lyon.fr/sites/edml M. Jacques JOSEPH	M. Jacques JOSEPH Ecole Centrale de Lyon Bât F7 Lab. Sciences et Techniques des Matériaux et des Surfaces 36 Avenue Guy de Collongue BP 163 69131 ECULLY Cedex Tél : 04.72.18.62.51 Fax 04 72 18 60 90 Jacques.Joseph@ec-lyon.fr
Math IF	MATHEMATIQUES ET INFORMATIQUE FONDAMENTALE http://www.ens-lyon.fr/MathIS M. Franck WAGNER	M. Franck WAGNER Université Claude Bernard Lyon1 Institut Girard Desargues UMR 5028 MATHEMATIQUES Bâtiment Doyen Jean Braconnier Bureau 101 Bis, 1 ^{er} étage 69622 VILLEURBANNE Cedex Tél : 04.72.43.27.86 Fax : 04 72 43 16 87 wagner@desargues.univ-lyon1.fr
MEGA	MECANIQUE, ENERGETIQUE, GENIE CIVIL, ACOUSTIQUE http://www.lmfa.ec-lyon.fr/autres/MEGA/index.html M. François SIDOROFF	M. François SIDOROFF Ecole Centrale de Lyon Lab. Tribologie et Dynamique des Systèmes Bât G8 36 avenue Guy de Collongue BP 163 69131 ECULLY Cedex Tél : 04.72.18.62.14 Fax : 04 72 18 65 37 Francois.Sidoroff@ec-lyon.fr

ACCORD DE COOPERATION POUR LA MISE EN OEUVRE D'UNE COTUTELLE DE THESE

L'Université de Rome "La Sapienza", Piazzale Aldo Moro n. 5, Rome, Italie, représentée par son Recteur, professeur Giuseppe D'Ascenzo, agissant en qualité et en vertu des pouvoirs qui lui sont conférés, d'une part

ET

L'INSA, Institut National des Sciences Appliquées de Lyon, représenté par son Délégué aux Etudes Doctorales, Adjoint à la Direction de la Recherche, Professeur Jean-Michel JOLION agissant en qualité et en vertu des pouvoirs qui lui sont conférés, d'autre part

VU

- La convention cadre franco-italienne entre la Conférence des Présidents d'Université (CPU) et la Conferenza dei Rettori delle Università Italiane (CRUI) sur la reconnaissance des diplômes et validation des titres universitaires, signée en date 18 janvier 1996;
- La convention cadre franco-italienne entre la Conférence des Présidents d'Université (CPU) et la Conferenza dei Rettori delle Università Italiane (CRUI) sur la co-tutelle de thèse signée le 13 février 1998;

Pour la partie italienne:

- Vu la loi n. 210 du 3 juillet 1998 art. 4 – docteur de recherche;
- Vu le D.M. 224/99 relatif aux normes en matière de doctorat de recherche;
- Vu le Règlement de l'Université en matière de doctorat de recherche;

Pour la partie française:

- Les modalités de dépôt, signalement et reproduction des thèses sont régies en France par l'arrête du 22 Avril 2002 relatif aux travaux présentés en soutenance en vue de l'obtention du Doctorat.

désireux (désireuses) de contribuer à l'instauration et/ou le développement de la coopération scientifique entre équipes de recherche italiennes et françaises en favorisant la mobilité des doctorants

ont convenu(e)s des dispositions suivantes

Titre I – Modalités Administratives

Art. 1 – L'Université de Rome "La Sapienza" et l'INSA de Lyon désigné(e)s ci-après "les établissements" décident, dans le respect des lois et règlements en vigueur dans chacun des pays et/ou établissements, d'organiser conjointement une cotutelle de thèse au bénéfice de l'étudiant(e) désigné(e) ci-après :

nom et prénom: MASSI Francesco

spécialité: Ingénieur Mécanique – Doctorat en Meccanica Teorica ed Applicata

sujet de thèse: Les bruits de crissement – Application au Freinage.

Le but de ce projet est l'étude et la compréhension des phénomènes d'instabilité à l'origine des bruits de crissement lors du freinage. Ce projet comportera une partie expérimentale et une partie numérique qui seront menées en parallèle.

La première partie du projet est la conception d'un banc d'essais de freinage, dans lequel la simplification du mécanisme entourant la plaquette et le disque permettra une comparaison et une validation des résultats expérimentaux et numériques. Cette première étape de conception d'un tel banc d'essais prenant en compte l'interaction de la plaquette et du disque avec des conditions aux limites du mécanisme "connues", constitue un challenge. Les résultats expérimentaux obtenus avec ce banc d'essais, tels que les fréquences expérimentales de crissement, les forces normales et tangentielles, seront ensuite confrontés dans une seconde partie avec les deux différents modèles numériques suivants.

Le premier modèle linéaire devra prédire les mêmes fréquences de crissement obtenues expérimentalement, et indiquer les régimes d'instabilité à l'origine du crissement. Les paramètres modaux seront identifiés lors d'essais expérimentaux dans le domaine des fréquences pour chacun des deux corps (plaquette et disque) pris séparément. Enfin, une analyse modale complexe du couplage des deux premiers corps (similaire à celle effectuée par Giannini lors de son doctorat effectué à Rome) sera menée.

Le second modèle non-linéaire utilisant le code d'éléments finis PLAST3 permettra l'étude en temps du système de freinage en régime stable ou instable. Les simulations du freinage par éléments finis en 3D permettront de quantifier les phénomènes de relais entre les zones instantanées de contact, la mise en vibration des premiers corps (plaquette et disque), la répartition des pressions de contact et la cinématique des surfaces de contact. Pour chaque régime, les conditions de contact (adhérence ou glissement) et de non contact (décollement), entre les deux surfaces de contact de la plaquette et du disque seront analysées. La connaissance des phénomènes à la source des vibrations dans les premiers corps devra permettre dans un premier temps la compréhension du phénomène du crissement, et donc sa réduction dans un second temps. Le code d'éléments finis PLAST3 est développé par L.Baillet pour ce qui concerne les algorithmes de contact avec frottement, et a été utilisé lors du DEA de S.D'Errico à l'INSA de Lyon pour la modélisation du freinage.

Les principes et les modalités administratives et pédagogiques de cette cotutelle sont définis par le présent accord.

Art. 2 - La durée prévue pour la préparation de la thèse en cotutelle est normalement de 3 ans, à partir du 1/11/2003

En cas de nécessité, cette durée peut être prolongée en conformité avec la réglementation en vigueur dans les deux établissements.

Art. 3 - La préparation de la thèse s'effectue par périodes alternatives, dans chacun des deux établissements partenaires. La durée de ces périodes sera fixée avec l'accord des deux directeurs de thèse.

Art. 4 – L'étudiant MASSI Francesco

est tenu à s'inscrire régulièrement dans les deux établissements. L'étudiant paiera les droits d'inscription à l'Université de Rome "La Sapienza" et en sera dispensé auprès de l'INSA de Lyon

Art. 5 – Pendant la période de préparation de la thèse, l'étudiant MASSI Francesco

bénéficiera du régime de couverture sanitaire italienne, en usage en France selon les règlements communautaires en vigueur en la matière (fascicule E 128). Le doctorant veillera à sa couverture de responsabilité civile.

Titre II – Modalités Pédagogiques

Art. 1 – Le travail de thèse de l'étudiant MASSI Francesco sera réalisé sous la responsabilité de deux directeurs de thèse:

- SESTIERI Aldo (Professeur dans le Département de Meccanica e Aeronautica), Directeur de thèse à l'Université "La Sapienza";

- BAILLET Laurent (Maître de Conférence, H.D.R. (Habilité à diriger des recherches), dans le Laboratoire de Mécanique des Contacts et des Solides), Directeur de thèse à l'INSA de Lyon

qui s'engagent à exercer pleinement leur fonction auprès du doctorant.

Art. 2 - La soutenance de la thèse est unique et aura lieu à l'Université de Rome "La Sapienza".

Art. 3 – Le jury de soutenance, désigné par les Recteurs des deux établissements sera composé à parité par des représentants scientifiques des deux pays.

Le jury sera composé au moins de quatre membres et au maximum de six membres qui appartiennent aux secteurs disciplinaires du Doctorat. Parmi ces membres il doit y avoir les deux directeurs de thèse (pour la partie italienne avec les modalités prévues dans le Règlement de l'Université en matière de Doctorat de Recherche).

Art. 4 – Le Centre de Dépense auquel se réfère le Cours de Doctorat de Recherche en: Meccanica Teorica ed Applicata

se chargera des éventuelles dépenses de mission du directeur de thèse, ainsi que des propres du Jury, sauf si accord avec l'établissement partenaire.

Art. 5 – La thèse sera rédigée et soutenue en langue anglaise; le résumé sera rédigé en langue française et sera présenté oralement en cette langue pendant la soutenance de la thèse.

Art. 6 – Chacun des deux établissements s'engage à conférer le titre de docteur de recherche pour la même thèse, sur rapport de soutenance unique et avis favorable du jury de soutenance.

l'Université de Rome "La Sapienza" s'engage à conférer le grade de docteur de recherche en Meccanica Teorica ed Applicata

l'INSA de Lyon

s'engage à conférer le grade de docteur de recherche en Mécanique.

Titre III – Conclusion

Art. 1 – L'étudiant(e) doctorant est tenu(e) de respecter les règlements et les usages de l'établissement d'accueil.

Art. 2 – Les deux établissements contractants, par l'intermédiaire des directeurs de thèse respectifs concernés, s'engagent à se communiquer mutuellement toutes les informations et documentations utiles pour l'organisation de la cotutelle de thèse faisant l'objet du présent accord.

informations et documentations utiles pour l'organisation de la cotutelle de thèse faisant l'objet du présent accord.

Art. 3 – Les modalités dépôt signalement et reproduction de la thèse seront effectuées dans chaque pays, selon la réglementation en vigueur.

La protection du sujet de thèse ainsi que la publication, l'exploitation et la protection des résultats issus des travaux de recherche du doctorant dans les deux établissements seront assujetties à la réglementation en vigueur et assurées conformément aux procédures spécifiques à chaque pays impliqué dans la cotutelle.

Lorsque requis, les dispositions relatives à la protection de droits de propriété intellectuelle pourront faire l'objet de protocoles ou documents spécifiques.

Art. 4 – Le présent accord prend effet à compter de la date de signature de représentant légal de chacun établissement contractants et sera valide jusqu'à la fin de l'année universitaire au cours de laquelle la thèse (ou les travaux) sera (seront) soutenue (soutenus).

Dans le cas où l'étudiant(e) ne serait pas inscrit(e) dans l'un et/ou l'autre des deux établissements contractants, ou renoncerait par écrit à poursuivre, ou, en vertu d'une décision d'au moins l'un des deux directeur de thèse ou de travaux, ne sera pas autorisé(e) à poursuivre la préparation de la thèse en cotutelle, les deux établissements mettront fin, sans délai, aux dispositions du présent accord par décision conjointe.

Art. 5 – Le présent accord est établi en quatre exemplaires originaux, dont deux en langue italienne et deux en langue français, faisant également foi.

Fait à Rome le _____

Pour l'Université de Rome "La Sapienza"

Pour l' INSA de Lyon

Le Recteur
(Prof. Giuseppe D'Ascenzo)

Le Président/Recteur/Directeur

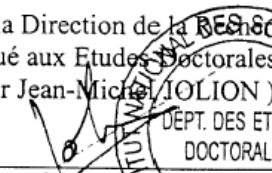


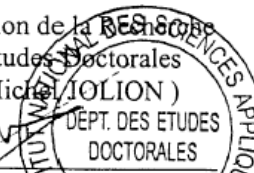


Le Responsable de l'école doctorale
(Prof. L. De Socio)

Adjoint à la Direction de la Recherche
Délégué aux Etudes Doctorales
(Professeur Jean-Michel IOLION)

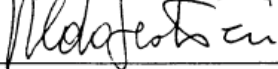






Le Directeur de thèse
(Prof. A. Sestieri)

Le Directeur de thèse
(Maître de Conférence/HDR Laurent Barillet)





riferirsi confluire

CONVENZIONE PER UNA CO-TUTELA DI TESI DI DOTTORATO DI RICERCA

L'Università degli Studi di Roma "La Sapienza" con sede in Roma (Italia), Piazzale Aldo Moro, 5 rappresentata dal Rettore prof. Giuseppe D'Ascenzo, che opera in virtù dei poteri che gli sono conferiti

E

L'INSA di Lione, rappresentata dal Professore Jean-Michel JOLION, Addetto alla direzione della ricerca, Direttore della scuola di dottorato,

che opera in virtù dei poteri che gli sono conferiti

VISTA

- La convenzione quadro franco-italiana tra la Conférence des Présidents d'Université (CPU) e la Conferenza dei Rettori delle Università Italiane (CRUI) sul riconoscimento dei Diplomi e la convalida dei titoli universitari firmata in data 18 gennaio 1996;
- La convenzione quadro franco-italiana tra la Conférence des Présidents d'Université (CPU) e la Conferenza dei Rettori delle Università Italiane (CRUI) per la co-tutela di tesi firmata il 13 febbraio 1998;

Per la parte italiana:

- Vista la Legge 210 del 3 luglio 1998 art. 4 – dottorato di ricerca;
- Visto il D.M. 224/99 recante norme in materia di dottorato di ricerca
- Visto il Regolamento di Ateneo in materia di dottorato di ricerca;

Per la parte francese:

- Visto il decreto del 25 settembre 1985 relativo ai lavori presentati per l'ottenimento del dottorato di ricerca

nell'intento di contribuire ad instaurare e/o sviluppare la cooperazione scientifica tra équipes di ricerca italiane e francesi attraverso la mobilità dei dottorandi

convengono e stipulano quanto segue

Parte prima – Modalità amministrative

Art. 1 – L'Università degli Studi di Roma "La Sapienza" e l'INSA di Lione denominati qui di seguito "Istituzioni" concordano, nel rispetto delle leggi e dei regolamenti in vigore in ciascun Paese e/o Istituzione, di organizzare congiuntamente una co-tutela di tesi di dottorato a beneficio del dottorando sottoindicato:

nome e cognome: Francesco Massi

iscritto al corso di Dottorato di Ricerca in: Meccanica Teorica ed Applicata

titolo della tesi: Emissione sonora di Squeal-Applicazione ai sistemi frenanti

Programma iniziale del progetto:

Lo scopo di questo progetto di tesi è lo studio e la comprensione dei fenomeni di instabilità che sono all'origine del rumore di squeal nei sistemi frenanti. Il progetto prevede sviluppi sperimentali e sviluppi teorici che saranno portati avanti parallelamente.

In primo luogo verrà progettato e costruito un set-up sperimentale semplificato di un freno da laboratorio che includa solamente la pasticca del freno ed il disco. I risultati sperimentali di questo sistema, relativamente alle frequenze di squeal del freno, verranno confrontati con due diversi modelli. Il primo è un modello lineare che dovrà essere in grado di riprodurre le stesse frequenze di squeal del set-up e dovrà indicare fundamentalmente l'insorgere dell'instabilità: questo modello verrà realizzato utilizzando i parametri modali identificati dalle prove sperimentali di risposta in frequenza ottenuti, separatamente, per il disco e la pasticca del freno, utilizzando un'analisi modale complessa, già sviluppata da Giannini durante la sua tesi di dottorato in Roma. Il secondo modello utilizzerà un modello non lineare agli elementi finiti che dovrà essere in grado di mostrare, nel dominio del tempo, la risposta della pasticca e del freno nella zona di contatto e dovrà essere in grado di determinare la distribuzione della pressione di contatto dopo l'insorgere delle condizioni di instabilità, al fine di controllare condizioni di stick and slip e di indicare eventuali metodologie di controllo per la riduzione o l'eliminazione del rumore di squeal. Questo modello verrà sviluppato utilizzando il software sviluppato dal dr. Baillet PLAST3 e provato precedentemente, su un modello più semplice, da D'Errico per il suo lavoro di tesi di DEA presso l'INSA di Lione.

I principi e le modalità amministrative e didattiche di tale co-tutela sono definiti dalla presente convenzione.

Art. 2 - La durata per la preparazione della tesi è di 3 anni, a partire dal 1/11/2003

In caso di necessità tale durata potrà essere prorogata in conformità con la regolamentazione vigente nelle due Istituzioni.

Art. 3 - La preparazione della tesi si effettuerà in periodi alterni, pressoché equivalenti, in ciascuna delle due Istituzioni. La durata di tali periodi sarà fissata in comune accordo dai due Direttori di tesi.

Art. 4 - Il dott. Francesco Massi sarà iscritto in entrambe le Istituzioni. Corrisponderà i regolari diritti di iscrizione all'Università degli Studi di Roma "La Sapienza" e ne sarà esonerato presso l'INSA di Lione.

Art. 5 - Per tutto il periodo di preparazione della tesi il dott. Francesco Massi beneficerà della copertura sanitaria italiana, valida in Francia secondo i regolamenti comunitari vigenti in materia (modello E128). Per tutto quel che concerne gli ulteriori rischi non coperti da assicurazione prevista per legge, il/la dottorando/a provvederà autonomamente tramite una propria assicurazione personale.

Parte seconda – Modalità didattiche

Art. 1 - Il dott. preparerà la tesi sotto la direzione comune dei professori:

- Aldo Sestieri (Docente presso il Dipartimento di Meccanica e Aeronautica), direttore di tesi all'Università "La Sapienza";
 - Laurent Baillet (Maître de Conférence, HDR (habilité à diriger des recherches), près le Laboratoire de Mécanique des Contacts et des Solides), direttore di tesi a l' INSA di Lione
- che si impegnano ad esercitare pienamente la funzione di tutori del dottorando.

Art. 2 - La discussione della tesi, unica, avrà luogo presso l'Università di Roma "La Sapienza".

Art. 3 - La Commissione giudicatrice è nominata dai Rettori delle due Istituzioni ed è composta da rappresentanti scientifici dei due Paesi in numero pari.

Essa comprende da un minimo di quattro ad un massimo di sei membri appartenenti ai settori scientifico-disciplinari del Dottorato, tra cui i due direttori di tesi, (per la parte italiana con le modalità previste dal Regolamento di Ateneo in materia di Dottorato di Ricerca.)

Art. 4 - Il Centro di Spesa cui afferisce il Corso di Dottorato di Ricerca in Meccanica Teorica ed Applicata sosterrà le eventuali spese di missione del direttore di tesi, nonché dei propri membri di Commissione, se non diversamente convenuto con l'Istituzione partner.

Art. 5 – La tesi sarà redatta e discussa in italiano; il riassunto sarà redatto in francese e sarà presentato oralmente in tale lingua in sede di discussione della tesi medesima. Il Collegio dei Docenti può autorizzare la redazione della tesi in lingua inglese o in altra lingua dell’Unione Europea.

Art. 6 – Ognuna delle due Istituzioni si impegna a conferire il titolo di dottore di ricerca per la stessa tesi, in seguito ad una relazione favorevole della Commissione giudicatrice.

L’Università degli Studi di Roma “La Sapienza” conferirà il titolo di dottore di ricerca in Meccanica Teorica ed Applicata

L’INSA di Lione conferirà il titolo di dottore di ricerca in Mécanique.

Parte terza - Conclusioni

Art. 1 – I dottorandi dovranno rispettare i regolamenti e le consuetudini dell’Istituzione ospitante.

Art. 2 – Le Istituzioni contraenti, attraverso l’intermediazione dei rispettivi direttori di tesi, si impegnano a comunicarsi rispettivamente tutte le informazioni e la documentazione utile per l’organizzazione della co-tutela di tesi oggetto della presente convenzione.

Art. 3 – Le modalità di presentazione, di deposito e riproduzione della tesi saranno effettuati in ogni paese secondo i regolamenti in vigore.

La protezione dell’oggetto della tesi, così come la pubblicazione, lo sfruttamento e la protezione dei risultati ottenuti con lo studio di ricerca del/la dottorando/a nelle Istituzioni contraenti saranno assoggettati alla normativa in vigore e assicurati conformemente alle procedure specifiche di ciascun Paese coinvolto nella co-tutela.

Qualora richiesto, le disposizioni relative alla protezione dei diritti di proprietà intellettuale potranno costituire oggetto di protocolli o documenti specifici.

Art. 4 – La presente convenzione entra in vigore dalla data di firma del rappresentante legale di ciascuna Istituzione contraente e sarà valido fino alla fine dell’anno accademico nel corso del quale la tesi o lo studio saranno discussi.

Nel caso in cui il dottorando non fosse iscritto in una e/o l’altra delle Istituzioni contraenti, oppure rinunciasse per iscritto a proseguire, oppure, in virtù della decisione di almeno uno dei due direttori di tesi, non fosse autorizzato a proseguire la preparazione della tesi in co-tutela, le Istituzioni contraenti porranno fine, congiuntamente e senza ritardo, alle disposizioni del presente accordo.

Art. 5 – La presente convenzione è redatta in quattro esemplari originali, di cui due in lingua italiana e due in lingua francese, aventi valore legale.

Roma, li _____, li

_____ , li

Per l’Università “La Sapienza”

Per l’INSA di Lione

IL RETTORE
(Prof. Giuseppe D’Ascenzo)

IL PRESIDENTE/RETTORE/DIRETTORE

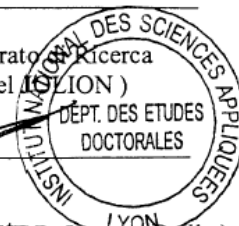


Il Coordinatore del Dottorato di Ricerca
(Prof. L. De Socio)

Il Coordinatore del Dottorato di Ricerca
(Professeur Jean-Michel LION)

Il Direttore di tesi
(Prof. A. Sestieri)

Il Direttore di tesi
(Maître de Conférence, HDR, Laurent Barillet)



To my family

To Erica

Acknowledgments

This thesis has been developed in cotutelle at the “Dipartimento di Meccanica ed Aeronautica” (DMA) of the University of Rome “La Sapienza” and at the “Laboratoire de Mécanique des Contacts et des Solides” (LaMCoS) of the INSA of Lyon, in the framework of a French-Italian agreement between the doctoral course in Theoretical and Applied Mechanics of the University of Rome “La Sapienza” and the doctoral school MEGA (Mécanique, Energétique, Génie Civil, Acoustique) of Lyon. I acknowledge the directors of the two doctoral schools, François Sidoroff and Luciano de Socio, for accepting and supporting this program.

I would like to express my deepest gratitude to Professors Laurent Baillet and Aldo Sestieri for their constant guidance throughout the development of this work and the scientific and personal support during my research in Lyon and Rome. My thanks go also to Professor Yves Berthier for introducing me into the tribological problems and for his precious advices and support. A special thank is due to Professor Adnan Akay who followed and encouraged my work starting from the beginning of my Master thesis at Pittsburgh and during his visits to Rome and Lyon. A sincere thanks to Claude Godeau for the excellent realization of the experimental set-up and to Mr. Xu for his help during my first year of experimental research.

I am sincerely grateful to the members of the committee and in particular to Professors Philippe Dufrenoy and John E. Mottershead for their careful revision of the thesis and to Professor Paolo Cappa for his interest in my work.

I would like to express my heartfelt thanks to the research group at the DMA: their useful advices and their friendship have supported me, making pleasant three stressful years of research. A particular thanks to Oliviero Giannini who introduced me to the squeal problem during my Master thesis. Sincere thanks to Antonio Culla for his friendship and reciprocal esteem. I want to mention as well my esteem to Professors Annalisa Fregolent and Antonio Carcaterra.

I would like to extend my thanks to all the people and friends who made my working environment at LaMCoS stimulating and pleasant. Among them, Anissa, Guillaume, Haytam, Aurélien, Claire, Benoit, Rachelle and all the others.

The development of this thesis would have never been possible without the support and the encouragement of my family. As well, I will never forget the support of all my friends in Rome. Still, I would like to thank Sandro, Ruggero, Rosario and the others ‘Italian’ who were close to me during my staying in Lyon.

This acknowledgments would not be completed without my full gratitude to Erica, who shared with me these years, encouraging and supporting me day after day, wherever I was, permitting me to forget any distance and separation.

Abstract

The squeal problem, concerning high frequency noise vibrations of brake systems, is a major research topic since several decades. This thesis is addressed to understand the physics of the instability that is at the origin of the problem. Due to the interdisciplinary nature of this issue, involving especially dynamic and tribological aspects, the work is organized into four main branches, developed parallelly. i) A linear finite element model of a simplified brake system is developed to predict the squeal frequencies by a parametrical analysis (complex eigenvalue analysis), and to underline the dynamic conditions of the system that lead to instability. ii) The unstable values of the system parameters are introduced into a nonlinear finite element model specifically developed for contact problems and based on the augmented Lagrange multipliers formulation. The contact nonlinearities are thus accounted for and a transient dynamic analysis allows to study the system vibrations and the behaviour of the contact stresses with and without squeal (difficult to retrieve experimentally). iii) A dynamic experimental analysis is performed to understand the macroscopic behaviour of the system and to link the squeal instability with the dynamics of the brake apparatus. The design of a simplified brake set-up, characterized by a dynamics that can be simply monitored and modified, allows to highlight that the modal coupling (lock-in) is the cause of the squeal phenomenon and to understand several squeal features. iv) A tribological experimental analysis is developed to understand the role of the components of the tribological triplet (mechanism, first bodies, third body). The topography of the contact surfaces after brake phases with and without squeal, and the STTs (Superficial Tribological Transformations) observed after the squeal vibrations, allow to validate the numerical results and to evidence fatigue phenomena due to the local oscillation of the contact stresses.

The results obtained from the four branches of the research converge together, characterizing the squeal as a dynamic instability of the brake system due to unstable couplings between two modes of the brake components. The coupling occurs at the contact surface where the oscillations of the local contact stresses and the friction coefficient couple the normal and tangential vibrations of the brake components, causing auto-excited vibrations of the system.

Résumé

Le problème du crissement, concernant les systèmes de freinage, est l'objet de recherche depuis plusieurs décades. Le but de cette thèse est l'étude des phénomènes d'instabilités à l'origine des bruits de crissement lors du freinage. L'interdisciplinarité du sujet qui traite majoritairement des aspects tribologiques et dynamiques, est prise en compte. Le rapport est structuré en quatre parties principales, menées en parallèle. i) Un modèle numérique linéaire basé sur la méthode des éléments finis est développé pour prédire les fréquences de crissement avec une analyse paramétrique (analyse aux valeurs propres complexes), et pour étudier les conditions de la dynamique du système qui mènent à l'instabilité. ii) Les valeurs instables des paramètres sont alors introduites dans un modèle numérique nonlinéaire développé pour les problèmes de contact et basé sur la méthode des multiplicateurs de Lagrange avant. Les nonlinéarités du contact sont donc prises en compte et la simulation numérique dans le domaine temporel permet d'analyser les vibrations du système et le comportement local des contraintes de contact en régime stable ou instable (ce qui est difficile à mesurer expérimentalement). iii) Une analyse dynamique expérimentale est effectuée pour comprendre le comportement macroscopique du système et lier l'instabilité de crissement à la dynamique du système de freinage. La conception d'un banc d'essais de freinage dans lequel la simplification du mécanisme a permis ainsi de comprendre et de contrôler la dynamique du système, d'identifier le couplage modal (lock-in) comme la cause du phénomène du crissement, et de déterminer plusieurs caractéristiques du phénomène. iv) Une analyse tribologique expérimentale est conduite pour comprendre les rôles des éléments du triplet tribologique (mécanisme, premier corps et troisième corps). L'étude de la topographie des surfaces de contact après le freinage en régime stable et instable et les STTs (Superficial Tribological Transformations) observées après le crissement permet la validation des résultats numériques et met en évidence les phénomènes de fatigue dus à l'oscillation locale des contraintes de contact.

Les résultats obtenus dans chacune des quatre parties de ce travail convergent et permettent l'interprétation de la physique du phénomène du crissement: l'instabilité est due au couplage entre deux vecteurs propres du système. Le couplage s'initie dans la surface du contact où l'oscillation local des contraintes de contact et le coefficient de frottement assurent le couplage entre les vibrations tangentielles et normales des composants du système de freinage, et causent ainsi les vibrations auto-excitées du système.

Summary

Summary	21
Introduction	25
Chapter 1. Brake squeal noise: an interdisciplinary issue	29
1.1 Introduction.....	31
1.2 Experimental works.....	32
1.2.1 <i>Experimental dynamic analysis</i>	32
1.2.2 <i>Experimental tribological analysis</i>	34
1.3 Theories for brake squeal.....	35
1.3.1 <i>Squeal instability: global dynamic theories</i>	35
Negative friction coefficient-sliding velocity slope.....	35
Sprag-slip theory.....	37
Squeal as a result of symmetry: splitting the double modes.....	38
Self-excited vibrations with constant μ : mode lock-in.....	39
1.3.2 <i>Squeal instability: tribological theories</i>	40
Local hammering.....	40
1.4 Analytical models of brake squeal.....	42
1.4.1 <i>Lumped parameters models</i>	42
1.4.2 <i>Models of plate vibrations</i>	43
1.5 Finite elements models.....	44
1.5.1 <i>Numerical formulation of the contact</i>	44
Linear contact elements.....	45
Treatment of contact constraints for transient analysis.....	46
1.5.2 <i>Numerical analysis</i>	47
Complex eigenvalue analysis.....	47
Transient dynamic analysis.....	48
Combined analysis.....	49
1.6 Remarks.....	50
Chapter 2. Approach to the squeal problem	53
2.1 Introduction.....	55
2.2 Dynamic analysis on simplified brake systems.....	56
2.2.1 <i>The beam-on-disc set-up</i>	56
Description of the set-up.....	56
Experimental results.....	57
Models of the Beam-on-disc.....	58
Outputs.....	61
2.2.2 <i>The Laboratory Brake set-up</i>	62
Description of the set-up.....	62
Experimental results.....	63
Model of the Laboratory Brake.....	66
Outputs.....	68
2.3 Numerical contact analysis.....	69
2.3.1 <i>Transient analysis for contact problems</i>	69
Description of the FE method.....	69
Transient simulations with contact.....	71
Outputs.....	73
2.4 The TriboBrake COLRIS.....	74
2.4.1 <i>Design of the test rig</i>	74
2.4.2 <i>Methodology for squeal investigation</i>	78
Chapter 3. Linear and nonlinear numerical analysis	81

3.1	Introduction	83
3.2	Finite Element Models	85
3.2.1	<i>Geometry of the models</i>	85
3.2.2	<i>Linear model</i>	86
3.2.3	<i>Nonlinear model</i>	88
3.2.4	<i>Dynamic comparison</i>	89
3.3	Linear analysis for the detection of system instabilities	91
3.3.1	<i>Complex eigenvalue analysis</i>	91
3.3.2	<i>Stability analysis</i>	95
3.3.3	<i>Propensity to instability</i>	98
3.4	Time analysis with the nonlinear contact model: braking simulation	101
3.4.1	<i>Stability analysis</i>	101
3.4.2	<i>Local contact analysis</i>	105
3.5	Comparison of results	108
3.5.1	<i>Prediction of the unstable regions of the parameters</i>	108
3.6	Conclusions	110
<u>Chapter 4. Dynamic analysis</u>		<u>113</u>
4.1	Introduction	115
4.2	Experimental set-up	116
4.2.1	<i>Geometry of the TriboBrake</i>	116
4.2.2	<i>Dynamics of the set-up</i>	117
Disc dynamics	117
Support dynamics	119
Pad dynamics	120
4.2.3	<i>Natural frequencies modulation for "modal tuning"</i>	122
4.3	Squeal phenomena	125
4.3.1	<i>Pad-disc squeal coupling</i>	126
4.3.2	<i>Support-disc squeal coupling</i>	128
4.4	Effects of modal damping on squeal instability	130
4.4.1	<i>Squeal suppression with damping</i>	131
4.4.2	<i>Increase of squeal propensity with modal damping</i>	132
4.4.3	<i>Phase of the squeal vibrations</i>	137
4.5	Conclusions	140
<u>Chapter 5. Tribological analysis</u>		<u>143</u>
5.1	Introduction	145
5.2	Dry friction contact between pad and disc	146
5.2.1	<i>First bodies</i>	146
5.2.2	<i>The role of the third body</i>	148
5.2.3	<i>Mechanism behaviour with and without squeal</i>	151
5.3	Contact surface topography	152
5.3.1	<i>Pad surface topography without squeal</i>	152
5.3.2	<i>Pad surface topography after squeal</i>	153
5.3.3	<i>Analysis of the superficial material of the pad after squeal</i>	155
5.3.4	<i>Disc surface topography</i>	158
5.4	Conclusions	159
<u>Chapter 6. Concluding remarks</u>		<u>161</u>
6.1	Summary	163
6.2	Original contributions	166
6.3	Future work	168
<u>References</u>		<u>171</u>

<u>Appendix A.</u>	<u>Eigenvalues plots with different friction coefficients</u>	<u>181</u>
<u>Appendix B.</u>	<u>Locus plots of the unstable regions</u>	<u>187</u>
<u>Appendix C.</u>	<u>Acquisition details.....</u>	<u>191</u>
<u>Appendix D.</u>	<u>Modes of the disc under braking pressure</u>	<u>195</u>
<u>Appendix E.</u>	<u>Linear model updating.....</u>	<u>199</u>
E.1	Updating of the linear FE model	201
E.2	Prediction of squeal instabilities	203
E.2.1	<i>Support-disc squeal coupling</i>	204
E.2.2	<i>Pad-disc squeal coupling</i>	205
E.2.3	<i>Remarks</i>	207

Introduction

The present thesis deals with squeal noise of disc brake systems. Brake noise is an example of noise caused by vibration induced by friction forces: during the brake operation, the contact forces between the pad and the disc can induce a dynamic instability in the system. Different types of noises and vibrations induced by friction are reported in the literature. Aircraft brakes involve generally lower frequencies: walk (5-20 Hz), chatter (50-100 Hz), and squeal (100-1000 Hz). Automotive and rail brake noises reach much higher frequencies and are classified in the literature according to the covered ranges of frequencies or the generating mechanism. Among them, squeal was, since the 30s, object of several studies, partly because of its fugitive nature, partly because of the interest of the automotive industry. Warranty costs, due to noise and vibration in brake systems, overcome one billion dollars each year just in North America.

Brake squeal is a harmonic noise emission that in automotive brakes usually occurs in the frequency range between 1 kHz and 20kHz, and even over. It is usually classified as high-frequency squeal and low-frequency squeal. The former typically involves the higher-order modes of the disc, and ranges between 5 and 20 kHz. The wave length of the excited modes is comparable or less than the dimension of brake pads. The low-frequency squeal involves modes of the system characterized by wave length larger than the dimensions of the pads. It usually ranges between 1 and 5 kHz.

Friction-induced vibrations and noise radiated by brake discs is a difficult subject partly because of its strong dependence on many parameters and partly because the mechanical interactions in the brake system are very complicated, including non-linear contact problems at the friction interface. Despite decades of research on such issue, it remains an unresolved problem. Different approaches have been adopted in the past to study the squeal issue: analytical simplified models, numerical models, experimental investigations on real brake apparatus, experimental works on simplified set-ups. These simplified rigs are appropriately designed to allow an easy measurement of the most significant parameters of interest and to simplify theoretical and numerical modelling. Despite brake squeal is, because of its nature, an interdisciplinary topic involving, in particular, dynamics and tribology, the approaches to the problem are usually confined to the dynamic domain (dynamics of the mechanism) or the tribological domain (analysis of the contact surfaces). Until now, four main mechanisms of friction-induced noise in disc brake systems are reported in the literature: stick-slip, sprag-slip, negative friction-velocity slope and modal coupling. Some tribological work tries to address squeal generation to an effect of local hammering, at micro-scale level, due to the actual topography of the contact surfaces.

The University of Rome "La Sapienza", in collaboration with the Carnegie Mellon University of Pittsburgh, has recently developed a research project based on a dynamic analysis of the problem. Such project, using a simplified experimental set-up, allows to predict the onset of squeal through a complex eigenvalue analysis on a reduced model of the set-up and the interpretation of the results on the base of the "mode lock-in" theory. Contemporarily, a group of research at LaMCoS (Laboratoire de Mécanique des Contacts et des Solides at the INSA of Lyon) has promoted a nonlinear numerical study of the problem, developing a FE code, specific for the simulation of the local dynamics of the contact by the method of Lagrange multipliers.

Aim of this thesis is to give a combined overview of the phenomenon. The work includes both two different numerical approaches to the problem, linear and nonlinear, and a dynamic and tribological experimental analysis carried out on a simplified brake system.

Two different numerical methodologies are available on the literature to predict and analyze squeal by using finite element methods: the complex eigenvalue analysis and the dynamic transient analysis. An integration of these two different numerical approaches to the problem, respectively in the linear field (complex eigenvalue analysis of the brake system) and in the nonlinear field (analysis of the contact dynamics in the time domain), is here presented. The first approach performs a finite element modal analysis of the system to identify its eigenvalues and to relate them to the squeal occurrence. The second uses a specific finite element code, Plast3, appropriate for a nonlinear dynamic analysis in the time domain, and particularly addressed to contact problems with friction between deformable bodies. The use of this program allows to analyze the contact stresses and the dynamics of the system along the contact surface, both in the linear and in the nonlinear states. These two methodologies are used separately in the squeal literature. Aim of this part of the work is to use them simultaneously and predict the onset of squeal both in the frequency domain by the linear model and in the time domain by the nonlinear one. The time behaviour of the system vibration during squeal, characterized by the limit-cycle of harmonic squeal oscillations is reproduced by introducing contact nonlinearities.

A tribological and dynamic experimental analysis on an appropriately designed brake system, named "TriboBrake COLRIS", is performed to investigate the squeal phenomenon and to validate the results obtained by the numerical models. The set-up is designed, on the experience of the previous researches, to have a geometry and dynamics that can be controlled and easily understood, to correlate the onset of squeal with the actual dynamics of the system in operating conditions. Particular attention is addressed to the measurement of the contact forces and the topography of the contact surfaces

under both silent and squealing conditions. The TriboBrake is designed to be closer to a real brake apparatus, than earliest simplified set-ups, like the beam-on-disc, but adopts yet some simplifying characteristic on its dynamics that permits to correlate clearly the appearance of squeal with the lock-in conditions between two modes of the three main substructures of the brake systems: caliper, pad and disc. The robustness of the squeal events, reproducible on the set-up, permits to investigate the relationship between squeal tendency and modal damping, by introducing the concept of the “tune in” frequency band defined as the frequency range where two appropriate modes can couple to give instability, around their natural frequencies. The analysis of the contact surfaces after the braking phase, either with and without squeal, points out the different characteristics of the third body and the STTs (Superficial Tribological Transformations) at the friction interface, in the two cases. After squeal occurrence, the topography of the surface and the internal structure of the pad material, close to the contact, show several signs of fatigue that can be related to the system vibrations and to the oscillations of the local contact forces.

Finally, the results obtained by the numerical simulations, either with the linear and the nonlinear models, and the experimental results, obtained by both the dynamic and the tribological analysis, are discussed and linked together in order to point out a general understanding of the physical mechanism that causes squeal.

The thesis is carried on in the framework of a “cotutela” thesis between the PhD course in “Meccanica Teorica ed Applicata” at the university of Rome “La Sapienza” and the Doctorate in “Génie Mécanique” of the “Ecole Doctorale Mega” at the LaMCoS-INSA of Lyon. The project is also supervised by prof. Adnan Akay of the Carnegie Mellon University of Pittsburgh.

Chapter 1. Brake squeal noise: an interdisciplinary issue

Chapter 1.	Brake squeal noise: an interdisciplinary issue	29
1.1	Introduction.....	31
1.2	Experimental works.....	32
1.2.1	<i>Experimental dynamic analysis</i>	32
1.2.2	<i>Experimental tribological analysis</i>	34
1.3	Theories for brake squeal.....	35
1.3.1	<i>Squeal instability: global dynamic theories</i>	35
	Negative friction coefficient-sliding velocity slope.....	35
	Sprag-slip theory.....	37
	Squeal as a result of symmetry: splitting the double modes.....	38
	Self-excited vibrations with constant μ : mode lock-in.....	39
1.3.2	<i>Squeal instability: tribological theories</i>	40
	Local hammering	40
1.4	Analytical models of brake squeal	42
1.4.1	<i>Lumped parameters models</i>	42
1.4.2	<i>Models of plate vibrations</i>	43
1.5	Finite elements models	44
1.5.1	<i>Numerical formulation of the contact</i>	44
	Linear contact elements.....	45
	Treatment of contact constraints for transient analysis	46
1.5.2	<i>Numerical analysis</i>	47
	Complex eigenvalue analysis.....	47
	Transient dynamic analysis	48
	Combined analysis	49
1.6	Remarks	50

1.1 Introduction

Friction-induced noise is observed frequently during braking. A wide range of brake noise and vibration phenomena are reported in literature: squeal, groan, chatter, judder, hum, squeak, etc. Among them squeal is the most prevalent, disturbing both vehicle passengers and environment, and expensive for brake and automotive manufacturers in terms of warranty costs [AKAY 02]. Brake squeal is one of the most difficult concerns associated with brake systems. Even if the development of brakes has focused primarily on increasing the braking performances, in the last decades the attention to acoustics and comfort of vehicles, together with the increasing regard for environmental concerns, encouraged several studies on such issue. Different theories have been formulated to explain the squeal mechanisms, and several works have been developed to highlight the main features of the phenomenon. In 2003 Kinkaid et al. [KINK 03], in their extensive review paper on brake squeal, concluded that *“despite a century of developing disc brake systems, disc brake squeal remains a largely unresolved problem”*.

Since squeal is a friction-induced instability, it is affected by many different factors on both the micro and macro scales. Phenomena at small scales both in length (microscopic contact effects) and in time (high-frequency vibrations), affects and are affected by phenomena at large scales (wear, behaviour of the tribological triplet* and dynamics of the whole brake system). Thus, squeal is an interdisciplinary issue, and a correct approach to the problem should include jointly a tribological and dynamic analysis. Despite this, different approaches have been adopted to analyze the problem mainly confined to the dynamic analysis or to the tribological one only. Many of them treated the squeal phenomenon as an instability of the brake mechanism, introducing a global friction coefficient to model the coupling force between the substructures of the system. Complete different approaches have been adopted by the tribological analyst: their attention was focused on investigations (manly post-mortem) of the contact surfaces of both the pad and the disc. Thus, the analysis is developed mainly on the STTs (Superficial Tribological Transformations) study and on the role of the third body (wear particles trapped at the interface).

This chapter provides some references of the experimental, analytical, and numerical methods used for the investigation on brake squeal and presents

* Mechanism, the two first bodies (parts in contact) and the third body (wear particles trapped at the interface) [BERT 01]

the main theories proposed to explain the physics of the problem, underlining the different approaches adopted by tribological and dynamic researchers.

1.2 Experimental works

1.2.1 Experimental dynamic analysis

The experimental analysis has been the most successful approach to investigate squeal, obtaining important results that highlighted some of its main features. Therefore each research group carried out experiments on a particular brake assembly, so that, because of the wide range of designs and material selections that are possible for brake components, it is almost impossible to compare results and conclusions from different groups. Considering also the dispersion of data in experimental studies, there is a large amount of different suggestions on the causes of squeal. Consequently, different experiences and, sometimes, contradictory results are reported.

The experimental work on brake squeal noise is non-trivial, because of its fugitive nature. Since it is not possible to design a squeal free brake, for the same reason it is not possible to design a brake which squeals all the time. This explain why several researchers adopted simplified brake apparatus in order to be able to control the driving parameters of the phenomenon.

One of the first experimental investigations was carried out by Mills in 1938 [MILL 38], trying to correlate squeal occurrence with a negative friction coefficient-sliding velocity slope. However he didn't reach any definitive conclusion.

With the same aim Fosberry and Holubecki [FOSB 59 61] tested a disc brake system, finding a good, but not complete, correlation between squeal occurrence and the decreasing slope between friction coefficient and relative velocity. They also noted that the disc is the resonant member, vibrating with bending modes characterized by nodal diameters. While the pad and disc vibrations are of the same magnitude, the caliper vibrates much less.

In experiments by Spurr [SPUR 61], brake pads were machined to have a partial contact zone with the disc. Spurr was aimed to provide confirmation of its sprag-slip theory (§ 1.3.1).

In 1972 North [NORT 72] worked on a commercial brake apparatus, to correlate experimental results with his model (§ 1.4.1), asserting a good agreement.

In the mid-1970s the dual pulsed holographic interferometry (DPHI) was introduced to capture the deformed shapes of the brake system during

squeal. This technique increased the interest on squeal investigation and a large number of works were carried out [KINK 03].

By measuring the operating deformed shapes, Felske et al. [FELS 78] established that the entire brake apparatus vibrated during squeal and that the mechanism causing squeal was the coupled vibration of the brake assembly. Another interesting finding in Felske's work was the highlighting that the larger is the friction coefficient, the higher the likelihood of squeal events. They also concluded that the pads of friction material vibrate with various bending modes, and that the main contribution to audible noise was the vibration of the pads and the caliper.

Also Murakami et al. [MURA 84] used the holographic technique and concluded that the squeal is generated by the coupled vibrations of the disc and the pads, and that squeal likelihood increased when the natural frequencies of the brake components were close to each other; they also found a higher propensity to squeal when the friction coefficient decreases as the relative velocity increases.

In 1989 Nishiwaki et al. [NISH 89] compared the squealing deformed shapes with the modes of the stationary rotor and found the two to be very close one another. They found that, during squeal, both pads and rotor vibrate with their bending modes, and that the squealing deformed shapes are stationary while the disc rotates.

Ichiba and Nagasawa [ICHI 93] performed experimental studies on brake discs: they put a series of accelerometers on the backplate of a pad and measured both the normal and the tangential accelerations of the pad. They found that the pad vibrates as a rigid body at low frequencies and with bending modes at higher frequencies; they also found a phase difference between the normal acceleration and the tangential one.

Fieldhouse and Newcomb [FIEL 93 96] using a holographic technique, found that the disc brake vibrates with deformed shapes characterized by nodal diameters, and observed instances when the deformed shapes are not stationary but traveling waves.

In 1993 Matsuzaki et al. [MATZ 93] presented evidence that squeal in disc brakes is the result of longitudinal vibrations rather than transverse vibrations of the disc; Chen et al. [CHEN 02a] found experimentally that the coupling between in-plane and bending modes of the disc was the key-factor for the squeal.

Since a real brake apparatus is characterized by geometry and dynamics that can be hardly controlled and understood, in the last years some researchers moved toward experimental studies of simplified experimental set-ups, helped by the new measurement possibilities offered by the laser scanner vibrometer. Van der Auweraer et al. [VAN 01] worked on a simplified disc brake.

Akay et al. [AKAY 00] worked on an evolution of the cantilever-disc set-up proposed by Jarvis and Mills [JARV 63], called “the beam-on-disc” set-up. Akay’s work pointed out the “lock-in” phenomenon between two modes of the brake system, explaining squeal as an unstable modal coupling. This set-up was also used later by Allgaier et al. [ALLG 02] and Tuchinda et al. [TUCH 01 02].

A further evolution of the “beam-on-disc” set-up is the “Laboratory Brake” set-up, asserted by Giannini [GIAN 05a] to be a bridge between the beam-on-disc and real brakes. The beam-on-disc and the Laboratory Brake will be discussed in detail in § 2, being the basis of the dynamic work of this thesis.

Some works also attempted to correlate the squeal vibration with the acoustic field: among the others Cunefare and Rye [CUNE 01], Matsuzaky and Izumihara [MATS 93], and Fieldhouse and Newcomb [FIEL 93 96].

1.2.2 Experimental tribological analysis

Brake systems involve dry sliding contact. Particles, coming from the pad and the disc, constitute the third body [GODE 84] and have a key role on the behaviour of the contact triplet [BERT 01]. The third body transmits the load between the two first bodies and accommodates the relative velocity. Starting from the late 1980s, the interest focused on the role played by tribology in squeal generation.

In 1990 Rhee et al. [RHEE 90] asserted that the formation of friction films between pad and rotor, due to the wear debris removed from the contact surfaces, increases the friction coefficient until a steady level, and that brake squeal does not occur until the films are formed.

The real contact between brake pads and disc consists of a number of small contact plateaus [ERIK 02]. Results by Eriksson et al. [ERIK 99] indicated that pads with many small contact plateaus have a larger tendency to generate squeal than pads with few large plateaus. They also noticed a small effect of the disc temperature on the contact plateaus size and on the generation of squeal.

Bergman et al. [BERG 99] examined the surface of the disc brake rotors and examined the change in the friction coefficient as the braking system was running-up. They noted that it gradually increased from a value just above 0.2 and, after over one thousand brakings, began to stabilize at a value below 0.6. As the friction coefficient increased beyond a critical value, Bergman et al. observed that the squealing behaviour sharply increased.

Ibrahim et al. [IBRA 00] measured the average normal and friction forces acting on a friction element that was placed in contact with a rotating disc. They noted that neither the normal force nor the friction coefficient were

constant. In fact, these authors reported that the friction and normal forces acting on the friction element are random, non-Gaussian processes.

In their experimental analysis, performed on an experimental apparatus designed for the analysis of sliding surfaces, Chen et al. [CHEN 03] showed that squeal can occur with either negative or positive friction-velocity slopes. They showed that contact areas where squeal occurred were characterized by adhesively jointed asperities, whereas the surface topography without squeal was characterized by a “*mirror finished surface*”. They noted also the coincidence between the squeal frequency and a natural frequency of the system.

Sherif defined a squeal index in function of the ratio of the standard deviations of the height distribution of asperities to the mean radius of asperities [SHER 04].

Recently, at the university of Liverpool, researchers are trying to correlate some local contact features of the brake surfaces with the dynamics of the brake apparatus and the onset of squeal, in order to predict squeal by numerical models [ABU 05a]. In particular, they measured the contact pressure distribution, in static conditions (not rotation of the disc), between pad and disc surfaces [ABU 05b] and implemented such pressure distribution in the FE model for a complex eigenvalue analysis.

1.3 Theories for brake squeal

1.3.1 Squeal instability: global dynamic theories

As shown above, most of the experimental works concerning squeal deal with the dynamics of the system and focus on the macro-scale aspect of the problem. Consequently, since the first studies on brake squeal, several theories tried to explain squeal as a phenomenon linked to the dynamics of the whole brake system. The micro-scale at the contact surface is not considered and the friction forces are modelled by introducing a global friction coefficient μ , either constant or variable in function of other global parameters, as the sliding velocity vr .

In the following, the main features of the dynamic theories for squeal instability are described. A detailed description of these theories can be found in the review by Kinkaid et al. [KINK 03].

Negative friction coefficient-sliding velocity slope

Since the work of Mills [MILLS 38] concerning brake systems characterized by decreasing μ - vr slope, several researchers started to link the

rise of squeal with such relationship between friction coefficient and relative velocity. In fact, systems where μ is a decreasing function of v_r can have negative damping and be unstable.

Experimental studies, e.g. Popp et al. [RUDO 01], correlated the friction coefficient with the relative velocity, and different laws of dependency for μ were introduced to fit experimental results. Generally polynomial laws were introduced in the form

$$\mu = \mu(v_r) = \mu_1 - \mu_2 \cdot v_r \dots \pm \mu_k \cdot v_r^k \quad (1-1)$$

where μk are constants.

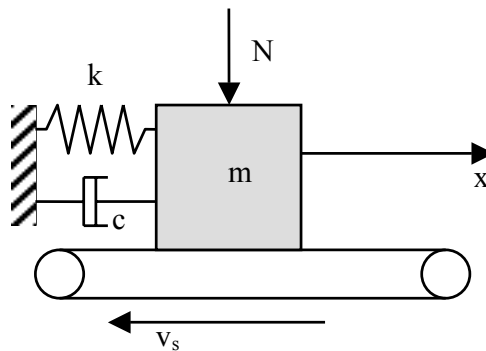


Figure 1.1 Spring-mass-damper system mounted on a moving surface

Considering the system in Figure 1.1, and a linear approximation of equation (1-1), the governing equation can be written

$$m\ddot{x} + c\dot{x} + kx = \mu_1 N - \mu_2 (v_r - \dot{x})N \quad (1-2)$$

where x is the horizontal displacement of the mass m from the equilibrium, c the viscous damping, k the spring stiffness and N the normal load. The term of the friction force that is proportional to the velocity of the mass introduces an additional term to the damping coefficient that brings to an “apparent” damping value

$$(c - N\mu_2) \quad (1-3)$$

When $\mu_2 > c/N$, the apparent damping results to be negative and causes self-excited vibration of the system.

In 1961 Fosberry and Holubecki [FOSB 61] advocated the same approach to the generation of squeal by considering either a static coefficient of friction higher than the dynamic coefficient, or a dynamic coefficient that decreases with the increase of sliding velocity. In fact, another similar approach

to squeal considers it to be due to a phenomenon of *stick-slip*, i.e. the friction coefficient varying between the static and dynamic value. The relationship between friction coefficient and velocity is, in such case, a Heaviside step function.

This approach to squeal generation has not received much attention in recent years, and different experimental studies proved that squeal can occur without negative slope of the μ - v function [CHEN 03][ERIK 01] and without stick-slip [MASS 03]. Lang and Smales [LANG 93] suggested that this mechanism is not the cause of squeal, but can eventually produce low frequency noise (<100Hz).

Sprag-slip theory

In 1961 Spurr linked squeal to unstable oscillations of the system even with the friction coefficient independent of the sliding velocity [SPUR 61]. In its *sprag-slip* theory the variation of the friction force is achieved by varying the normal force, due to the actual geometry of the system.

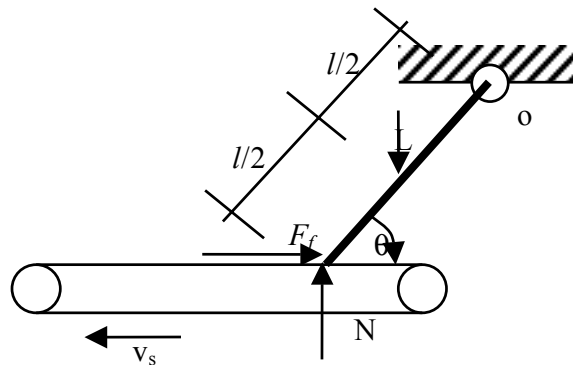


Figure 1.2 The rigid system by Spurr. A rigid massless rod is loaded on a rigid moving plane.

Spurr illustrated that the constrained interaction of various degrees-of-freedom of a system can increase the value of the contact force that can become unbounded when considering rigid bodies. By considering the system in Figure 1.2 Spurr demonstrated that the friction force

$$F_f = \mu \cdot \frac{L}{2(1 - \mu \cdot \operatorname{tg}(\theta))} \quad (1-4)$$

becomes unbounded ($F_f \rightarrow \infty$) when $\theta \rightarrow \operatorname{tg}^{-1}(1/\mu)$. He named this critical condition *spragging*.

To link its theory with brake squeal, Spurr noted that, by introducing elasticity of the brake components, “the assembly then deflects, reducing the

frictional force and returns to its first state to repeat the cycle". In this way Spurr explained the loading cycle that brings to the limit-cycle of squeal vibrations. Spurr also explained the randomness of squeal onset by the changes of the geometry of the system, due to wear (changes over long time periods) and thermal deformations (changes over short time periods).

The sprag-slip theory was followed also by Earles and co-workers [EARL 77], and Jarvis and Mills [JARV 63], among others. Murakami et al. [MURA 84] hypothesized that squeal is generated by a combination of the sprag-slip mechanism and the negative μ - νr slope.

Squeal as a result of symmetry: splitting the double modes

Mottershead and Chan [MOTT 95] introduced a further possible explication of brake vibrations during squeal. They asserted that the splitting of the double modes of an axial symmetric structure, i.e. the disc, could lead to flutter instability due to the frictional follower forces. This mechanism, that can lead to unstable behaviour of the disc, is related to the angular velocity of the disc loaded in the transversal directions. If one considers the vibration of a disc, vibrating with its i^{th} diametral mode, it is possible to write its response $w(r, \theta, t)$ along the axial direction as follows:

$$w(r, \theta, t) = R_i(r) \sin(i\theta) \cos(\omega_{ni} t) \quad (1-5)$$

where r and θ are the polar coordinates with respect to the centre of the disc and ω_{ni} the natural frequency. This equation can be expressed as:

$$w(r, \theta, t) = \frac{R_i(r)}{2} [\sin(i\theta - \omega_{ni} t) + \sin(i\theta + \omega_{ni} t)] \quad (1-6)$$

that is the sum of two traveling waves at speed $v = \pm \omega_{ni} / i$. These two waves are called the forward and the backward traveling waves. If the disc is rotating at an angular velocity Ω , since the two waves travel with the disc, for a fixed observer the deformed shape of the disc can be expressed as:

$$w(r, \theta, t) = \frac{R_i(r)}{2} [\sin(i\theta' - (\omega_{ni} - i\Omega)t) + \sin(i\theta' + (\omega_{ni} + i\Omega)t)] \quad (1-7)$$

where θ' is the angular coordinate on the disc for a fixed observer.

If the disc is excited with a sinusoidal force, fixed in space, with a frequency Ω_f , two resonance conditions for each disc mode can be observed:

$$\begin{aligned} \omega_1 &= \omega_{ni} - i\Omega \\ \omega_2 &= \omega_{ni} + i\Omega \end{aligned} \quad (1-8)$$

A critical speed Ω_c is defined as $\Omega_c = \omega_{ni} / i$. If the disc is rotating at one of its critical speeds a stationary load can destabilize the disc vibration.

Such instability mechanism occurs for a standard brake rotor at high angular velocity, that is generally outside the range of interest for the brake squeal, occurring usually at low angular velocities. Therefore, the rotation of the disc in a squeal model can lead to parametric resonances and can induce instability because of the effect of the friction at speed below the critical speeds, as shown, among others, by Chan et al. [CHAN 94].

Self-excited vibrations with constant μ : mode lock-in

The first researcher to consider squeal as a self-excited vibration with constant μ was North [NORT 72] in 1972. In his eight-degrees-of-freedom model North described the contact forces as follower forces, introducing asymmetry in the stiffness matrix of the system.

The equations of motion of the system can be written as

$$M\ddot{x} + Kx = 0 \quad (1-9)$$

with M the mass matrix and K the stiffness matrix. The latter includes both the stiffness parameters of the system and the components due to the friction forces, becoming asymmetric. When the equilibrium of the system is stable the eigenvalues consist of complex conjugate purely imaginary pairs (or with negative real part if damping is introduced). Varying the parameters of the system, it is possible for the pairs to coalesce (equal imaginary part) and split, so that a pair results to have positive real part, i.e. negative damping. The equilibrium is then said to be unstable in flutter instability.

The instability occurring in dynamic models when two eigenfrequencies of the system, due to asymmetry in the stiffness matrix, coalesce and become unstable, was named by Akay as *mode lock-in* [AKAY 00].

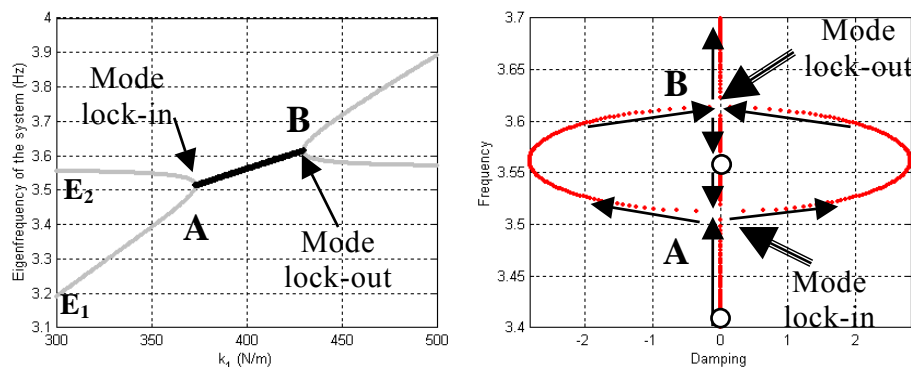


Figure 1.3 Complex eigenvalue analysis.

Figure 1.3 shows the results of the complex eigenvalue analysis performed on North's two degrees-of-freedom model proposed in [NORT 76]; the left graph shows that, when one parameter of the analysis varies (k_1 here), the first eigenfrequency of the system increases. When the two eigenvalues (E_1, E_2) approach each other, they coalesce and the system becomes unstable. The coalescence point (A) is called the mode lock-in point. The right-hand graph shows the same results in the locus plot; the axes are scaled to plot the effective damping on the x axis and the frequency of the eigenvalues on the y axis. The two eigenvalues move one toward the other along the zero damping axes (imaginary axis). When they reach the lock-in point they coalesce and become conjugate. One eigenvalue moves toward the negative damping semi-plane (positive real part of the eigenvalue), while the other moves in the positive damping semi-plane. The negative effective damping is considered related to the squeal unstable behaviour. By varying the parameters, they move to the lock-out point (B), where the two eigenvalues split again to different frequencies.

Several researchers adopted North's approach, applied to different models.

1.3.2 Squeal instability: tribological theories

Local hammering

Rhee et al [RHEE 89] pointed out that the proposed mechanisms of friction-induced noise in disc brakes can only describe the parameters spaces in which squeal may occur, but cannot clearly define the physical phenomena that cause squeal. The same claim was supported by Chen et al [CHEN 03]. They hypothesized that squeal can be due to an effect of *local hammering* at the contact surface that excites a mode of the brake system. Several hammering mechanisms were proposed by Rhee et al.: among them, disc imperfections and *local spragging*. They also noticed that stick slip interaction associated with waves of detachment can also be considered as a series of impulses acting at the contact interface. Chen et al [CHEN 03] hypothesized that the *local hammering* is due to a “*serious pit-like material detachment or formation of adhesively joined asperities and asperity deformations*”.

These impulses can excite natural frequencies of the brake system.

It is worth to notice that this approach, confined at the micro-scale level, can be easily integrated to the models of squeal instability described above. In fact, the dynamic theories for squeal describe the mechanism of the whole system that bring to the auto-excited vibrations, and the *local hammering* might be seen as the modality of excitation that can trigger the instability. Akay in its extensive review on friction noise and vibration [AKAY 02] discusses about the “friction noise” caused by sliding surfaces. This noise might be linked

to the *local hammering* that can trigger the unstable eigenfrequency of the system that falls inside the wide range of frequencies excited by the friction noise.

Chen et al. [CHEN 02b] tried to relate the variation of the friction coefficient to the topography of the friction surface, in function of the braking cycles. They considered the friction-cycles curve (Figure 1.4) proposed by Suh and Sin [SUH 81] and retraced by their experimental results.

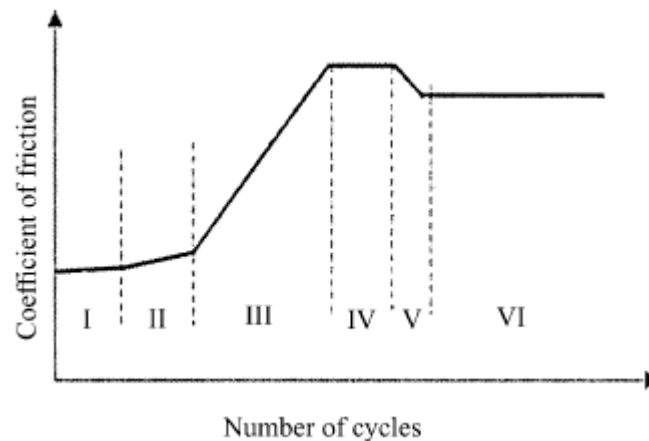


Figure 1.4 Friction coefficient vs. braking cycles.

The friction-cycles curve was divided by Suh and Sin in six stages, and the dependency of the friction coefficient in each of these stages was explained by considering the formation of the third body at the friction interface and the topography of the contact area. According to Suh and Sin's theory at stage IV the rheology [BERT 01] of the third body is in equilibrium and the internal flow of the third body is constant. At such stage there are "*very strong plowing action, asperity deformation and adhesion*" [SUH 81]. Chen et al. noticed that squeal starts to occur at this stage and asserted that "*this strong plowing action, asperity deformation and adhesion bring about strong fluctuation of the friction force to lead to vibration and associated squeal*".

This tribological behaviour is reached in the advanced phase of the braking, when the friction coefficient reaches a larger value with respect to the starting value, and this explains the critical friction coefficient proposed by Bergman et al. [BERG 99], that is the result of the local contact phenomena at this braking phase.

Moreover, this approach could explain why new pads need to perform several brake cycles before squeal occurs. According to Eriksson et al. [ERIK 02] surface variations are related to both rapid and slow processes, the latter due to the result of numerous brakings.

1.4 Analytical models of brake squeal

1.4.1 Lumped parameters models

This section deals with several models proposed in the literature to reproduce analytically brake squeal. Each model attempts to apply one of the dynamic theories described above. Since the 1960s, models for squeal have featured an increased number of degrees-of-freedom, increased complexity, and different contact laws; subsequently plate models of the rotor were introduced to arrive, finally, to detailed finite element models. The first detailed analysis of a model was presented by Jarvis and Mills in 1963 [JARV 63], on a three-degrees-of-freedom model, championing Spurr's sprag-slip theory. With their model of a cantilever beam loaded against a rotating disc, they showed that a decreasing friction velocity slope had a negligible effect in generating unstable vibrations in such a system.

Earls and co-workers [EARL 77 84 87] used a pin-on-disc system to investigate and quantify the sprag-slip mechanism for squeal. They conducted linear stability analyses on lumped parameter models to predict the flutter boundaries in the parameters space.

In 1972 North [NORT 72] proposed an eight-degrees-of-freedom linear system, where the friction was modeled as a follower force, and he found a possible instability using a constant friction coefficient. He equated this instability to the squeal occurrence and found a good agreement with his experimental work on a real brake apparatus. North is also the author of a review paper about the early models of the brake squeal [NORT 76] where he proposed also a two-degrees-of-freedom system to predict squeal.

In 1978 Millner [MILL 78] developed a model for a fixed calliper disc brake, modelling each component with two-degrees-of-freedom. He found that the geometry was extremely important, and that if the friction coefficient had a value sufficiently high, and the caliper's stiffness was in a certain range, instability could be excited in almost any contact configuration. He also found that the more the contact between piston and pad is close to the trailing edge, the more a propensity to squeal is obtained.

A division of the brake squeal phenomena into two different categories was proposed by Lang and Smales [LANG 93] in 1993: the low frequency squeal (LFS) and the high frequency squeal (or squeak) (HFS). The low frequency squeal is characterized by a wavelength of the squealing deformed shape of the disc larger than the length of the pad. In this case it is possible to model the pad as a rigid body and this line of research was also followed by Nishiwaki [NISH 93] and Denou and Nishiwaki [DENO 01]. In the latter work the authors proposed a four-degrees-of-freedom system (two for the disc and one for each pad) and presented an interesting analysis of their results when some of

the parameters in their model were changing. They correlated also the numerical results with experiments performed on a disc brake that was modified with the purpose of changing the effective contact points between the pad and the disc, and the pad and the caliper. They traced the stability maps as a function of the position of this contact point, finding a good agreement with experimental results. In the model they used a constant friction coefficient and the stability of the system was studied by a complex eigenvalue analysis.

An analogous approach was followed, among the others, by Rudolph and Popp [RUDO 01]. They proposed in 2001 a fourteen-degrees-of-freedom system that models the disc, the caliper the pads, and their connection with the frame. The disc is considered vibrating as a rigid body. The main difficulty of these approaches is to find the numerical values of the parameters to insert into the model, necessary to obtain significant results. Thus, an experimental work was performed to build the model and to correlate numerical results with experimental occurrence of squeal.

Recently Giannini and Sestieri [GIAN 05c] proposed a reduced model of a brake apparatus by introducing the modal parameters of the disc and the caliper, obtained experimentally, and modeling the friction pad of reduced dimensions with one further degree-of-freedom. They conducted a parametric complex eigenvalue analysis to reproduce squeal frequencies obtained experimentally, achieving a good agreement with the experimental results (§ 2.3.3).

1.4.2 Models of plate vibrations

In order to study the high frequency squeal, the models must include the flexibility of both the disc and the pads. Many models used an analytical formulation for the brake rotor considered as a flat, homogeneous annular plate, clamped on the internal radius and free on the external one.

Among the others, Mottershead and his co-workers presented, over the past decade, many papers that were considering this description of the disc vibration. These papers are summarized by Mottershead in an extensive survey paper [MOTT 98] on friction-induced instability in discs. The models suggested for the brake pad were different, showing a trend of increasing complexity through the years.

In their early models the disc was considered fixed and the pads were rotating: in 1994, Chan and Mottershead [CHAN 94] proposed a one degree of freedom system (mass-spring-damper) to model the pad, and the friction was modeled as a follower force. Through a multiple time-scale analysis, they find two different set of instabilities: the first set produces instabilities at subcritical parametric resonances; the second set is caused by the friction interaction,

destabilizing the backwards waves of all the modes with nodal diameters, regardless of the value of the angular velocity.

Ouyang et al. [OUYA 98] modeled the pad as a two degree of freedom system: they added a second degree of freedom along the tangential direction for the pad, and used a negative friction-velocity relationship for the contact. They found that the in-plane damper induces instability in additional parametric resonances while it reduces the unstable regions in correspondence to other resonances.

To have a more realistic description of the brake pad, Mottershead et al. [MOTT 97] proposed also a distributed model of the pad. Finite elements were used to describe both the disc and the pad and they applied a multiple time-scale analysis to the FEM equations to study the parametric resonances. They found that the friction follower force destabilizes significantly the parametric resonances, while the effect of the mass and the stiffness of the pad is that of providing the supercritical parametric resonances. In 2000, Ouyang et al. [OUYA 00] proposed a mixed model for the brake apparatus: the rotating disc was described as a thin plate, and the values of the parameters were derived from an experimental modal analysis of a commercial disc brake, while the stationary pad was described by a finite element model. The stability of the system was studied by the state-space method. Their conclusions are that the friction coefficient is highly destabilizing, while the damping of both the disc and the pads have a stabilizing effect; the unstable behaviour is also highly speed-dependent.

Tseng and Wickert [TSEN 98] used another plate model for the disc, which was loaded by a tangential stress field: they determined linearized equations of small transverse vibrations of the disc and concluded that only modes with nodal diameter can become unstable.

1.5 Finite elements models

1.5.1 Numerical formulation of the contact

Because the continuous increase of the computational resources, starting from the first '90s several works implementing FE (Finite Element) models to investigate squeal have been carried out. Nowadays FEM (Finite Element Method) has become an indispensable tool to model disc brake systems and provide new insights into the problem. With respect to the traditional lumped parameter models, the FEM allows for accurate representation of complex geometries and boundary conditions. In particular the modelling of the contact between the pad and the disc is of major relevance in FE models of

brakes, due to the role played by the friction forces on the onset of the system instability.

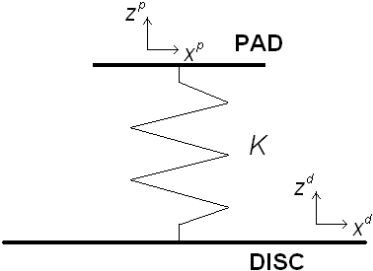
Several friction laws have been adopted by researchers: from the simplest Coulomb law with constant friction coefficient, to more complicated friction laws that consider the dependence of the friction coefficient on the sliding velocity, temperature, or relative sliding displacement. Therefore, sophisticated friction laws developed in tribology have not yet been adopted by the researchers. Wear and actual distribution of the contact pressures has not been yet considered. This is due to the actuality of studies on tribological friction laws regarding brake materials, and to the complicated modelling of brake systems. Moreover, FE models implementing simple friction laws (e.g. Coulomb friction law) permitted already to predict and reproduce squeal instabilities, as discussed in § 1.4.2.

The contact between two bodies in a FE model must be introduced through appropriate elements, able to simulate the behaviour at the contact interface. Depending on the type of analysis, different contact elements have been used in brake models. The most commonly treatments of contact constraints in brake modelling are described below.

Linear contact elements

In order to perform a complex eigenvalue analysis of the brake assembly linear elements must be introduced to simulate the contact. Thus, an extremely nonlinear component such as the contact interface, due to contact nonlinearities, must be approximated by linear elements. This approximation is aimed to linearize properly the contact in the vicinity of an equilibrium point like the steady sliding position. Such models are aimed to capture the onset of instability, by assuming it to rise in linear condition.

The most commonly used linear schematization of the contact surface is through a geometric coupling. This can be obtained by a spring element that links each pair of nodes at the contact surface between the disc and the pad. The element stiffness matrix results to be asymmetric:

$$\begin{Bmatrix} F^p \\ N^p \\ F^d \\ N^d \end{Bmatrix} = \begin{bmatrix} 0 & \mu k & 0 & -\mu k \\ 0 & k & 0 & -k \\ 0 & -\mu k & 0 & \mu k \\ 0 & -k & 0 & k \end{bmatrix} \begin{Bmatrix} x^p \\ z^p \\ x^d \\ z^d \end{Bmatrix} \quad (1-10)$$


where F and N are the tangential and normal contact forces, x and z are the tangential and normal displacements of the nodes, of the disc d and the pad p ; k is the normal stiffness of the contact element. Such schematization introduces

tangential and normal contact forces proportional to the normal relative displacement between the disc and the pad:

$$\begin{aligned} N^d &= k \cdot (z^d - z^p) & N^p &= -k \cdot (z^d - z^p) \\ F^d &= -\mu \cdot k \cdot (z^d - z^p) & F^p &= \mu \cdot k \cdot (z^d - z^p) \end{aligned} \quad (1-11)$$

By introducing these contact elements, the stiffness matrix of the system become asymmetric and a complex eigenvalue analysis can results in unstable eigenvalues.

Treatment of contact constraints for transient analysis

The solution of a contact problem in which the motion of the bodies is constrained by the condition of non-penetration, brings to the so-called *variational inequality*. Considering the energy of the system $\Pi(u)$, function of the displacement u , because of the restriction of the solution space by the non-penetration condition, the solution of the energy equation is not at the minimum point associated with $\Pi(u)_{\min}$. On the contrary it is at the point associated with $\Pi(u)_{\min}^c$, which denotes the minimal energy within the admissible solution space.

Different methods can be used to fulfil the constraint equations in the normal direction at the contact interface, and, by introducing constitutive relations, in the tangential direction.

The *Lagrange multipliers* method adds to the energy of the system a term Π_c^{LM} due to the contributions of the contact constraints:

$$\Pi_c^{LM} = \int_{\Gamma_c} (\lambda_N \cdot g_N + \lambda_T \cdot g_T) dA \quad (1-12)$$

where λ_N and λ_T are the Lagrange multipliers, g_N and g_T are the normal and tangential gap functions, Γ_c is the contact area. The variation of $\Pi(u)$ then includes the constraint formulation due to the variation of Π_c^{LM} . In this formulation λ_N can be identified as the contact pressure pN , while the tangential stress vector tT , to be calculated, needs the introduction of the constitutive law (friction law) depending on the stick or slip condition. The Lagrange multipliers method introduces additional variables in the system (the Lagrangian multipliers), but fulfils the constraint equation correctly.

Another commonly applied method in finite element analysis of contact problems is the *penalty* approach. In this formulation a penalty term Π_c^P due to the constraint condition is added to the energy of the system $\Pi(u)$:

$$\Pi_c^P = \frac{1}{2} \int_{\Gamma_c} (\varepsilon_N (g_N)^2 + \varepsilon_T (g_T \cdot g_T)) dA \quad \varepsilon_N, \varepsilon_T > 0 \quad (1-13)$$

where ε_N and ε_T are the penalty parameters. As it can be seen from equation (1-13), the penalty parameter ε_N can be interpreted as a spring stiffness at the contact interface between the two surfaces. This is due to the fact that the energy of the penalty term has the same structure as a potential energy of a simple spring. The solution obtained by this formulation converges to the solution obtained with the Lagrange multiplier (exact fulfillment of the constraint) for $\varepsilon_N \rightarrow \infty$ and $\varepsilon_T \rightarrow \infty$; however, large values of ε_N and ε_T lead to an ill-conditioned numerical problem. As for the Lagrange multiplier formulation, the friction laws have to be introduced in the case of slip condition.

A further method is the *augmented Lagrange formulation*. The main idea is to combine either the penalty method or the constitutive interface laws with the Lagrange multiplier method.

Several other variants for the formulations of the energy term Π_c due to the contact constraint are described in the literature [WRIG 02]. Most standard FE codes which are able to handle contact problems use either the penalty or the Lagrange multiplier method.

1.5.2 Numerical analysis

Early numerical works on brake squeal used finite element models to obtain a description of the deformed shapes of the rotor at its natural frequencies [NISH 89]. Wickert et. al. [BAE 00][TZOU 98] used a finite element model to explore how the thickness of the disc or the dimension of the hat influence the dynamic behaviour of the disc. For a disc-hat structure they determined different modes at different frequencies characterized by the same number of nodal diameter.

Finite element models can be used to describe the complex geometry of a brake and, once extracted, the modal parameters can be used to build a reduced order model of the system that is generally more suitable for parametric analysis [TUCH 02][GIAN 06c].

An extensive review of the numerical works concerning squeal was proposed by Ouyang et al. [OUYA 05]. Nowadays two major numerical approaches are adopted in research concerning squeal: the complex eigenvalue analysis and the transient dynamic analysis.

Complex eigenvalue analysis

The complex eigenvalue analysis is the most commonly used technique to predict squeal propensity of a brake system. The real parts of the extracted eigenvalues dictate the stability, or instability, of the system at the

eigenfrequencies obtained by the imaginary parts. If the real part of an eigenvalue is positive, the corresponding imaginary part is indicated as a possible squeal frequency.

The contact is usually modelled as a geometry coupling, providing an asymmetric stiffness matrix of the system. Therefore, different methods to construct the friction stiffness were used by researchers. The first work dealing with a complex eigenvalue analysis on a FE model is due to Liles [LILE 89]. Other researchers treated squeal as a moving load problem [OUYA 00]. During the last two decades several works [OUYA 05] correlating squeal prediction by complex eigenvalue analysis with experimental squeal occurrence, have been carried out, providing some good agreement. Such agreement supports the hypothesis that the onset of squeal starts in linear conditions, which is the necessary hypothesis to treat the problem with a linear model for such analysis.

Recently, some researchers [ABU 05a 05b] introduced into the FE model the non-uniformity of the contact pressure distribution, due to the surface topography of the pad, by measuring the contact pressure in static condition (applied brake pressure without rotation of the disc).

Nowadays the complex eigenvalue analysis is the preferred approach for industry and researchers, because it is more mature analysis than the dynamic transient analysis and because the lower computational effort permits to perform a parametric analysis, useful in phase of design, to understand the influence of the system parameters on the squeal propensity. Several commercial software for dynamic analysis (e.g. ABACUS, Ansys, etc.) include built-in procedures to perform complex eigenvalue analysis of systems including contact preloaded surfaces.

Transient dynamic analysis

In 1994 Nagy et al. [NAGY 94] published the first work describing a transient analysis of disc brakes using FEM, finding the instability of the system to be mainly influenced by the friction coupling. They modelled the contact by incorporating a penalty function.

Chern et al. [CHER 02] simulated the brake squeal limit-cycle using LS-DYNA software, providing the operational deflection shapes (ODSs) of the brake components during squeal.

In recent years, because of the increasing interest on the nonlinear behaviour of brake vibration during squeal, and thanks to the increasing power of actual computational tools, the transient analysis has been adopted and developed for brake squeal simulation. Mayor works are listed in the review paper by Ouyang et al. [OUYA 05].

The main advantage of the transient analysis with respect to the complex eigenvalue analysis is the possibility of introducing contact (stick, detachment, not constant friction coefficient) and material nonlinearities.

Moreover, the transient analysis allows to simulate the real behaviour of the system vibration including the limit-cycle motion that characterizes squeal vibrations and that is due to the nonlinearities of the system. The complex eigenvalue analysis allows only to predict the growth rate of an oscillation at the starting linear stage.

A further advantage of the transient analysis is the possibility to follow the behaviour of the local contact stresses during squeal, providing new insights into the unstable mechanism due to the action of the friction forces. This point is of particular importance because such behaviour can not be analyzed experimentally, due to the difficulty to reach the contact zone by experimental instrumentation.

Commercial softwares start to include several packages to model contact problems and perform either explicit or implicit transient analysis. However, this approach has still the mayor drawback of an important computing time for each single simulation, so that it is not yet useful for design interactions.

Combined analysis

Nowadays a standard integration of the two methods is based on a preliminary transient nonlinear analysis to simulate the contact in operating conditions (applied brake pressure and disc rotation) and recover the contact boundary conditions and interfacial contact distribution to introduce in the linear model, that is then used for the complex eigenvalue analysis [LEE 03a 03b 03c].

Therefore, in the literature it seems that the transient and the complex eigenvalues approaches are performed separately in order to predict or simulate squeal, and their correlation was not much investigated. Some work dealing with both the methods to predict squeal have been conducted on reduced order models; Mahajan et al. [MAHA 99] in 1999 ran both complex eigenvalue analysis and transient analysis using the FEM, but it was not made any comparison between them. In a recent work Abu Bakar et al. [ABU 06] examined the correlation between the two methodologies for a large degrees-of-freedom model, comparing the results of the complex eigenvalue analysis and the transient analysis performed with three different treatments of the contact available in ABACUS. They concluded that *“even though transient analysis is capable of predicting squeal events and frequencies of disc brakes in theory, it may not be so in reality because of lack of sophistication in the modelling and algorithms that are available in the Explicit version of ABAQUS.”*

The work presented in this thesis includes the development and the correlation of the two models to simulate squeal instability of a brake apparatus: a linear FE model for complex eigenvalue analysis developed by Ansys and a nonlinear FE model for transient dynamic analysis developed with a specific finite element program, Plast3 [BAIL 02], particularly addressed to contact

problems with friction between deformable bodies. The former is aimed to find the unstable regions of the system parameters; the latter is aimed to study the time nonlinear behaviour of the system and the contact stresses during the squeal steady state.

1.6 Remarks

As reported above, an extensive literature on disc brake squeal was produced over the last decades. Different theories have been proposed to explain the physics of the phenomenon, but there is yet neither an exhaustive understanding of the problem nor a general agreement on its nature.

The main results on this topic have been obtained by the numerous experimental analyses. Despite the different schools of thought, the following experimental results are generally accepted:

- brake squeal is a harmonic sound emission due to vibration of the brake components, with main harmonic ranging from 1 to 20 kHz;
- the vibration of the disc brake during squeal can be either a standing or a travelling wave;
- the squeal frequencies are strongly linked to the natural frequencies of the brake assembly;
- by increasing the friction coefficient between disc and pad, the propensity to squeal increases;
- an important role in generation of squeal is played by the topography of the friction surface, i.e. by the friction noise [AKAY 02].

A distinction between works confined in the domain of tribology and works confined in the domain of structure dynamics emerges from the literature. A prevalence of dynamic works is present, due to the general thought that squeal is due to an instability of the brake system. Therefore, such instability has its genesis at the contact interface, where the micro-scale physics of the phenomenon can not be neglected. A combined approach to the tribological and dynamic analysis has to be performed to understand the roles of the micro and macro-scale mechanisms in squeal generation.

Starting from the experimental evidences, numerous models for squeal simulation have been proposed, by modelling the dynamics of the brake assembly and introducing different laws of the global friction force. Few analyses in the brake squeal literature have incorporated complex tribological processes in their models. In fact, despite the effects discussed in tribological studies are undoubtedly important, it is not clear how to incorporate them into predictive models for disc brake squeal.

In recent years, FEM has become an indispensable tool for brake modelling, thanks to the increasing computational tools, and new insights on squeal features have been reached. Two different approaches have been adopted in FE squeal analysis: the complex eigenvalue analysis and the transient analysis. However, the two methods were performed separately rather than simultaneously to investigate squeal generation and features.

In such contest, the work object of this thesis is aimed to combine both dynamic and tribological experimental analyses with numerical simulations in the linear domain, through the complex eigenvalues tool, and in the nonlinear domain, through the transient dynamics analysis. The final goal is to obtain a general description of the topic including micro and macro-scales and linear and nonlinear features of squeal.

Chapter 2. Approach to the squeal problem

Chapter 2.	Approach to the squeal problem	53
2.1	Introduction.....	55
2.2	Dynamic analysis on simplified brake systems.....	56
2.2.1	<i>The beam-on-disc set-up</i>	56
	Description of the set-up	56
	Experimental results.....	57
	Models of the Beam-on-disc.....	58
	Outputs	61
2.2.2	<i>The Laboratory Brake set-up</i>	62
	Description of the set-up	62
	Experimental results.....	63
	Model of the Laboratory Brake.....	66
	Outputs	68
2.3	Numerical contact analysis	69
2.3.1	<i>Transient analysis for contact problems</i>	69
	Description of the FE method.....	69
	Transient simulations with contact	71
	Outputs	73
2.4	The TriboBrake COLRIS	74
2.4.1	<i>Design of the test rig</i>	74
2.4.2	<i>Methodology for squeal investigation</i>	78

2.1 Introduction

One of the main difficulties encountered in studying brake squeal is the high complexity of the brake apparatus. Such complexity, together with the everpresence of data dispersion in experimental studies, is one of the main reasons that did not permit yet to have an efficient control of brake squeal. For this reason, in the past some research groups decided to tackle the problem by conducting experiments on a simplified test rig [AKAY 00][TUCH 01 02][ALLG 02 01], the Beam-on-disc set-up, in order to acquire a clear understanding of the squeal mechanism.

The beam-on-disc is the evolution of the cantilever-disc set-up proposed by Jarvis and Mills [JARV 63] and was designed at the Carnegie Mellon University by Akay et al. [AKAY 00]. This set-up was aimed at creating a brake squeal-like friction interaction between bodies in sliding contact that, unlike real brake systems, may have good repeatability and could be easily modeled.

A further evolution of the Beam-on-disc set-up is the “Laboratory brake” set-up [GIAN 05a 05c], designed with the aim to be a “trait d’union” between the Beam-on-disc and commercial brakes. The main change of this new rig is the introduction of the third substructure characterizing a brake apparatus: the friction pad. Moreover, a schematic calliper was designed to provide the braking pressure.

Despite the simple modelling of these “brake-like” set-ups allowed to have new insights into squeal and to relate squeal occurrence with the brake dynamics, such systems did not allow to investigate nonlinear conditions and evaluate the contact stresses during squeal.

To overcome this gap and account for such features that are important for a physical interpretation of the problem, a FE code, Plast3 [BAIL 02], was used to reproduce squeal instabilities and analyze the contact conditions in the time domain [DERR 03]. The local behaviour of the contact stresses and the vibrations of the system in the time domain are analyzed by the numerical transient analysis.

The work presented in this thesis is aimed to develop and join together different methodologies and is constituted of four main substructures:

- a dynamic analysis is performed on a simplified set-up to relate its dynamics (macro-scale) with the squeal occurrence;
- a parallel experimental analysis is aimed to highlight the tribological features of the problem (micro-scale);
- a nonlinear FE analysis on large degrees-of-freedom model is performed with Plast3 to investigate the behaviour of the system

vibrations during squeal, with particular attention on its nonlinear features and on the analysis of the contact interface;

- parallelly, a linear FE parametrical analysis is performed for squeal prediction by the complex eigenvalue analysis performed with Ansys.

Considering that the present thesis is strictly related to the previous works mentioned above, a summary of the main features obtained with these set-ups are reported in the following.

2.2 Dynamic analysis on simplified brake systems

2.2.1 The beam-on-disc set-up

Description of the set-up

The beam on disc is a development of the pin-on-disc proposed by Earles and Soar [EARL 71 77] in the sixties.

The beam-on-disc consists of a cantilever beam (representing the brake pad) and a rotating disc (the brake rotor) pushed one against the other. Figure 2.1 shows a picture and a scheme of the set-up: the disc (diameter 358 mm, thickness 25 mm) and the cantilever beam are both made in aluminum. The angle of incidence of the beam can be adjusted as well as its length. The beam cross section is 9.5 mm square. The cantilever beam is mounted on a guide plate which moves on two linear bearings, allowing the cantilever beam to be pre-loaded against the disc at a specified normal load.

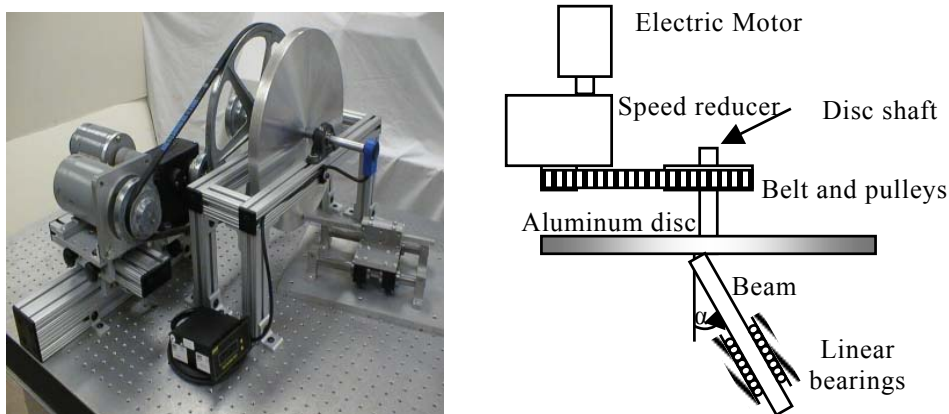


Figure 2.1 The beam-on-disc set-up.

The main difference of this set-up with respect to the pin on disc is the beam flexibility that introduces a coupling between the dynamics of two bodies and permits unstable conditions. The beam on disc was proposed by Akay et al [AKAY 00], and later used, with the same basic geometry, by Tuchinda et al. [TUCH 01 02] and Allgaier et al. [ALLG 02].

This set-up, even if far away from a real brake, is able to capture features of the friction interaction between two deformable bodies. In particular, the beam-on-disc is particularly appropriate to reproduce and study the mode-lock-in phenomenon which is widely considered to be the cause of squeal instability in brakes.

Experimental results

The squeal tests performed on the beam-on-disc were addressed to have repeatable squeal conditions by varying the length of the beam, the angle between the disc and the beam and the normal load. Figure 2.2 summarizes the main results obtained with the beam-on-disc: the vertical lines are the natural frequency of the disc alone, the transverse curves the natural frequencies of the beam, in function of the beam length (vertical axes), and the black dots are the squeal frequencies obtained during the experiment.

The results show that in general squeal occurs at the disc or beam natural frequencies, when they are close each other.

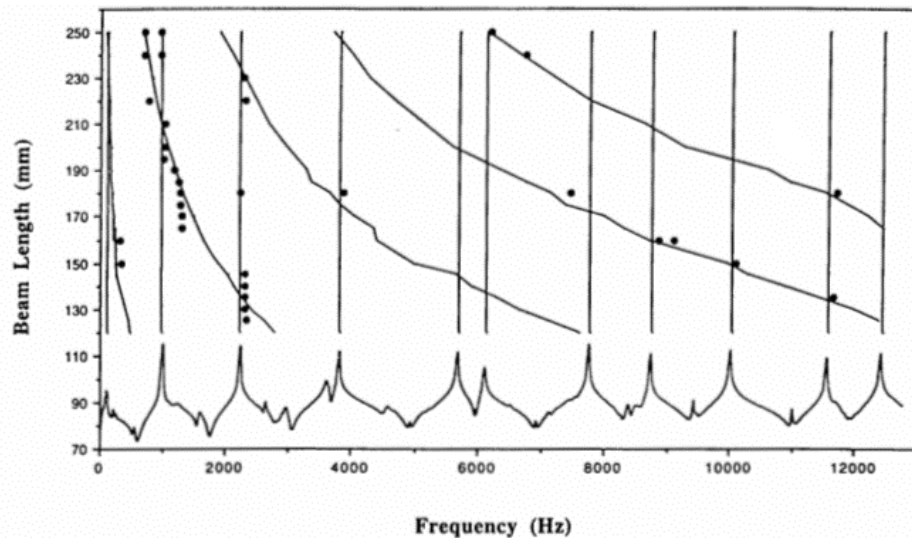


Figure 2.2 *Beam-on-disc mode lock-in ([AKAY 00])*

Moreover, all the squeal conditions determined during the experiments involve a cosine mode of the disc, i.e. a mode with an antinode at the contact point, also referred as a (n,m^+) mode.

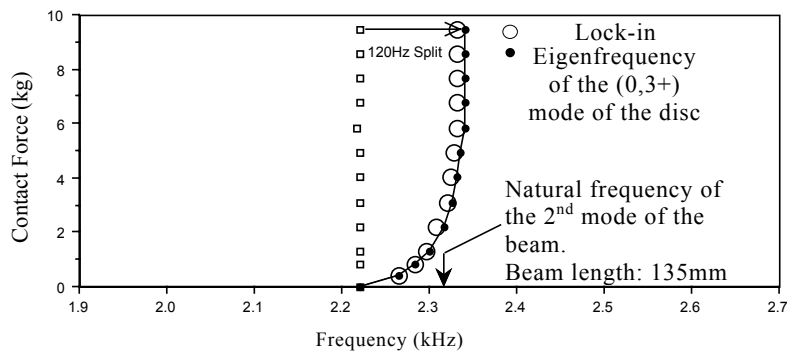


Figure 2.3 Mode lock-in and split when the normal contact force increases (without disc rotation): 2nd mode of the beam and mode (0,3+) of the disc ([AKAY 00])

Since the frequency of the second peak of a split mode increases when the normal load increases, the squeal frequencies also increase with the normal load. Figure 2.3 shows the coincidence between the split frequency of the (0,3+) mode and the squealing frequency. The figure shows also the dependence between contact force and squeal frequency.

Models of the Beam-on-disc

Tuchinda et al. [TUCH 01 02] built a copy of the beam-on-disc, called Pin-on-disc, and carried out experiments obtaining the same results of Akay, and developed two different models to predict the squeal occurrence.

The first model describes the disc as a thin plate and uses three equations: the transverse vibration of a plate w , the longitudinal vibration of a beam u and the transverse vibration of a beam v .

The authors set the following boundary conditions:

- the center of the disc is clamped in the w direction, and both torque and shear are equal to zero along the external circumference of the disc;
- the beam end is clamped at the opposite end to the contact.

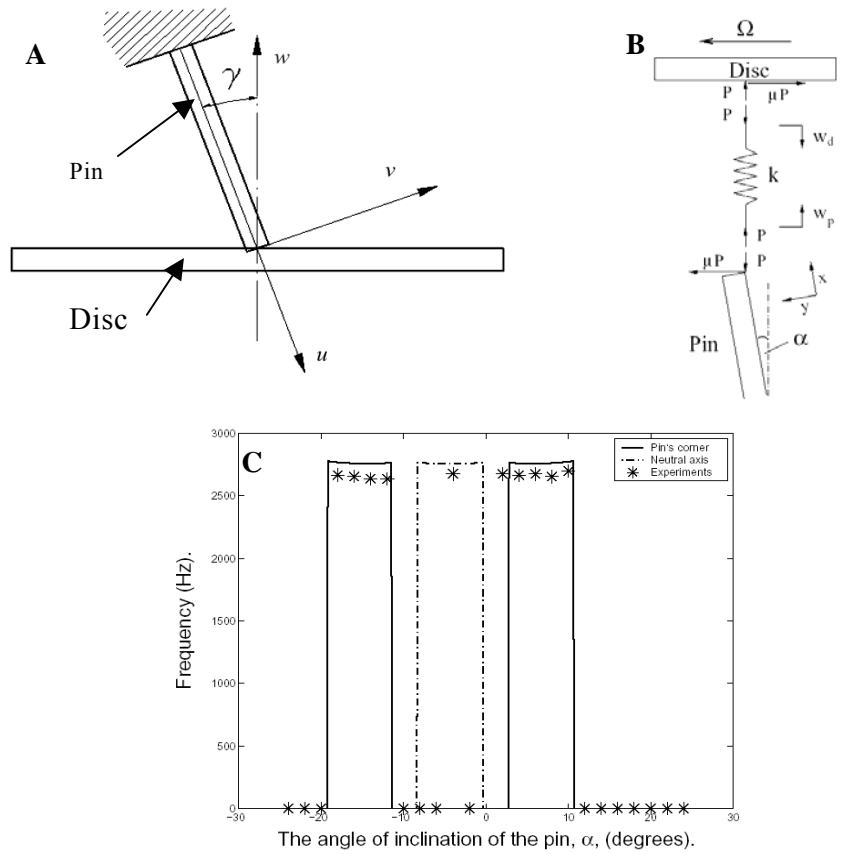


Figure 2.4 a) Pin on disc model; b) contact model; c) comparison between numerical and experimental instabilities [TUCH 02].

The theoretical modes, with the proposed boundary conditions, are computed up to 16kHz. The coupling conditions are expressed by equations (2-1), where P is the preload between the disc and the beam, μ a constant friction coefficient and γ the angle between the beam (pin) and the disc axes.

$$\begin{cases} f_w = -P \\ f_u = P(\mu \sin \gamma - \cos \gamma) \\ f_v = P(\mu \cos \gamma + \sin \gamma) \end{cases} \quad (2-1)$$

The kinematic constraint, imposing that disc and beam are in contact, is expressed as:

$$u(l, t) \cos \gamma - v(l, t) \sin \gamma + w(r_0, \vartheta_0, t) = 0 \quad (2-2)$$

where l is the length of the pin, t is the time, $u(l,t)$ is the axial displacement of contact end of the pin, $v(l,t)$ is the transverse displacement, r_0 and θ_0 are the polar coordinates of the contact location on the disc surface.

These equations, expressed in modal coordinates, provide the coupling terms between the bending modes of the disc and the longitudinal and bending modes of the beam.

The model assumes the homogeneous form:

$$M \cdot \ddot{z} + K \cdot z = 0 \quad (2-3)$$

where M and K are the mass and stiffness matrix respectively and z is response of the combined system. The eigenvalues of the system are extracted in function of the friction coefficient μ . This model does not provide results (squeal frequencies prediction) comparable with the experiments. However, it is able to show instabilities caused by lock-in between the modes of the disc and the modes of the beam.

To refine the model and obtain better predictions of squeal occurrence, three major improvements were performed:

- the disc is described by an updated FE model, obtaining in this way a better correspondence between the experimental and numerical eigenvalues;
- a contact stiffness k between the beam tip and the disc is introduced;
- the finite width of the beam is considered, allowing the contact point to occur away from the beam axis. This effect is relevant to reproduce squeal when the incidence angle is close to zero.

After these modifications, the model was able to reproduce the experimental results presented in Figure 2.4-c

Allgaier et.al. [ALLG 02] describe the system by a finite element model of the beam-on-disc set-up. For the contact, few assumptions are made that can be summarized as follows:

- an elastic contact of metallic surfaces is considered;
- the contact points do not interfere among them;
- an isotropic surface roughness is considered;
- the surface parameters do not change with time;
- dry friction is considered.

In order to obtain realistic surface parameters in the simulations, a contact interface model based on a statistical description of the surface roughness is used to derive a non-linear constitutive description for the normal and tangential contacts.

The macroscopic friction coefficient resulting from these assumptions is a function of both the relative velocity and normal pressure (Figure 2.5).

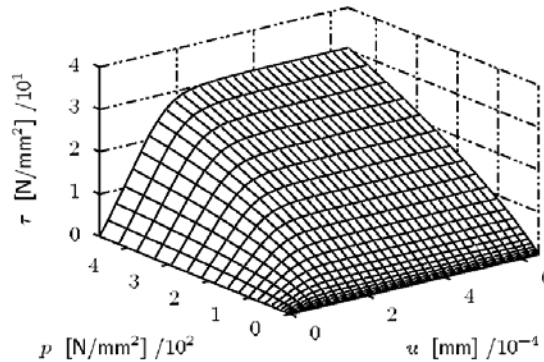


Figure 2.5 Tangential stress in function of the normal pressure and the relative velocity [ALLG 02].

With this model, after an updating process aimed to minimize the difference between experimental and numerical modes of the system, a good agreement is found between experimental and numerical results. The agreement is good both in the frequency domain, where the unstable modes are predicted through the complex eigenvalue analysis, and in the time domain, giving the grow rate of the unstable vibrations.

Outputs

The beam-on-disc set-up provides wide sets of data correlating the dynamic characteristics of the set-up with the squeal occurrence and a good experimental base for the lock-in theory. Some mode lock-in characteristics are found and can be reproduced by either linear or non-linear models. These characteristics are:

- the contact between the beam and the disc causes some disc nodal diameter modes to split into two different frequencies. Lock-in tends to occur near the frequencies of the disc's split cosine mode (the higher frequency one);
- the mode lock-in response occurs easily when the natural frequencies of the disc and the beam are coincident. The occurrence rate of lock-in depends on how close the subsystems' frequencies are;
- both the theoretical and numerical models are suitable to predict the squeal frequencies, provided that a good updating of the model is performed.

The experiments show that, usually, at large contact angles the system tends to lock-in with higher frequency modes and vice versa. Moreover, at

intermediate contact angles, the contact force appears to be the determining factor, and the lowest damping mode has the highest likelihood lock-in.

2.2.2 The Laboratory Brake set-up

Description of the set-up

The study of the squeal events using the beam-on-disc set-up allowed modeling the friction interaction between a beam and a disc that leads to unstable conditions. The models are able to predict the conditions necessary for the squeal event, but such good results can not be extended to the analysis of complex disc brakes by applying a similar methodology.

Thus, the need for a new experimental set-up, “trait d’union” between the beam-on-disc and a commercial brake, led to the design of a new experimental rig, called “Laboratory Brake” [GIAN 04].

The Laboratory Brake is an experimental rig designed to be, on one hand, reliable to produce squeal in a controlled and reproducible way and, on the other hand, to be as close as possible to a commercial brake.

The set-up consists of a disc constrained on a rotating shaft, a pair of beams that represent the caliper, and two small pads, obtained by machining commercial brake pads, that connect the disc and the beams (**Figure 2.6**).

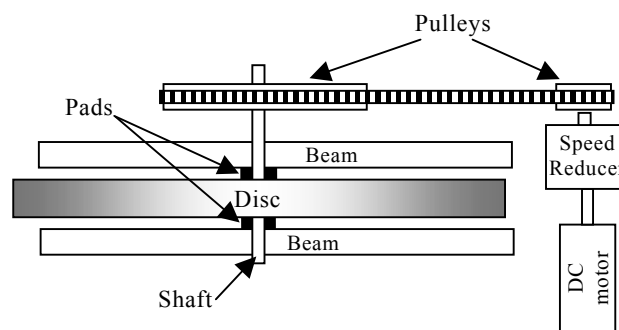


Figure 2.6 Schematic of the laboratory brake [GIAN 05a].

Depending on the specific version of the set-up, the physical dimensions may change. Moreover, the dimensions of the pad may change: in [GIAN 06a] a small brake pad is used, in [GIAN 05] two small brake pads are mounted on each beam, in [MASS 05b] commercial brake pads are used. Also the shape of the disc may change and can be either a machined disc [GIAN 06a] or a commercial brake disc [MASS 05b].

With respect to the beam-on-disc, the laboratory-brake is characterized by four major improvements:

- the materials in contact are analogous to a real brake pair;

- the laboratory-brake has two beams (representing the caliper) almost parallel to the disc plane and, thus, a geometry much closer to a real brake, characterized by a weak coupling between in and out-of-plane vibrations. On the contrary, in the beam-on-disc the angle between the beam and the disc was close to 45° , providing a high coupling;
- the beam-on-disc is characterized by two low-damped structures interacting through the friction force. In the laboratory-brake the brake pads are characterized by a high damping loss factor;
- the laboratory-brake may host pads with different dimensions, allowing the study of high frequency, squeal characterized by a large contact area between disc and pad.

Experimental results

Tests performed on the lab brake provide interesting insights into squeal. The squeal frequency can be related to the dynamics of the system. Figure 2.7 shows the frequency response function of the lab brake and the squeal occurrences when small brake pads are used (1cm^2 contact area). It can be noted that, like in the beam on disc, squeal involves the cosine modes of the disc, labelled as $(n,m+)$ mode, but it can also involve frequencies corresponding to bending modes of the beam.

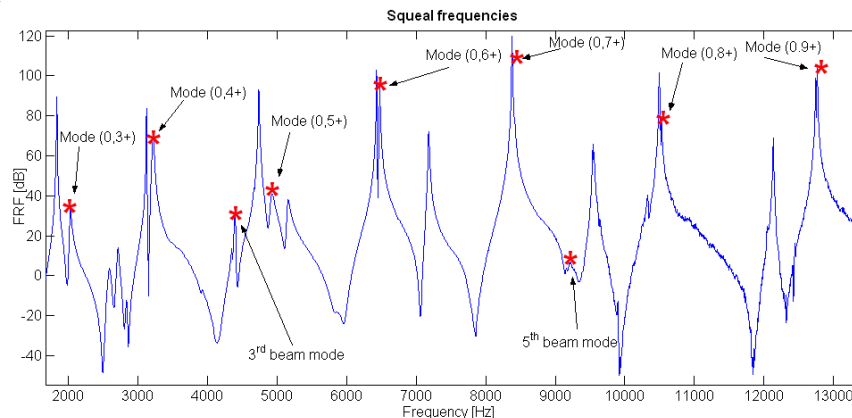


Figure 2.7 FRF of the coupled system and squeal frequencies (stars) [MASS 03].

A quite different behaviour occurs when two small brake pads are mounted on the same beam at a distance D [GIAN 05]. The mode involved in the squeal mechanism depends, in this case, on the value of the ratio between such distance and the circumferential wavelength of the disc mode shape: $R=D/\lambda$. The results are provided in Table 2.1.

Distance Mode	D= 0	D= 36	D= 42	D= 51	D = 74	D= 106	D= 134	D = 160	D=168
(0,4)					R=0.28				
(0,4+)	R=0	A		R=0.20					
(0,5)				R=0.24	R=0.35	R=0.49			
(0,5+)	R=0								
(0,6)			Rotating	R=0.29	R=0.42	R=0.59	Rotating		
(0,6+)	R=0		R=0.25				R=0.76	C	
(0,7)		Rotating	R=0.29	B	R=0.50				
(0,7+)	R=0	R=0.25				R=0.69	R=0.85		R=1.11
(0,8)		R=0.28	R=0.33	R=0.39	R=0.56	Rotating		Rotating	R=1.28
(0,8+)	R=0					R=0.77	R=0.97	R=1.27	D
(0,9)			R=0.37	R=0.44				R=1.52	R=1.43
(0,9+)	R=0					R=0.90	R=1.1		

Table 2.1 Squeal occurrences during experiments on high frequency squeal [GIAN 05].

The table is divided into four regions, depending on the values of R . Squeals in zones A and C are characterized by a cosine squealing mode $(n,m+)$, while in the regions B and D the sine modes $(n,m-)$ become unstable. This reflects a characteristic of the dynamic behaviour of the lab brake: for $0 < R < 0.25$ and $0.75 < R < 1.25$ the cosine modes are at higher frequencies than the respective sine modes. Therefore, it is possible to generalize what it was previously found with the beam-on-disc, by stating that, between the two split double modes of the disc, it is generally the higher frequency one that squeals.

Moreover, another kind of squeal is obtained at the boundaries between these zones. In fact, at the boundaries ($R=0.25$, $R=0.75$, $R=1.25$), the two split modes become again coincident in frequency so that both may squeal together, implying that the squeal deformed shape is not anymore stationary, but the nodal lines rotate during a squeal period as found in commercial brakes by Fieldhouse et al. [FIEL 93 96].

Another important result obtained by using the lab brake is the identification of a key role in squeal mechanism played by the in-plane dynamics of the pad. Figure 2.8 shows the power spectral density of the acceleration of the pad in the in-plane (black line) and in the out-of-plane direction (grey line). The out-of plane acceleration peaks are in correspondence to the modes of the system, while the in-plane acceleration presents low peaks at frequencies corresponding to the $(m,n+)$ modes of the disc and a high damped peak related to the pad in-plane dynamics, ranging between 8 and 11KHz. These peaks move toward higher frequencies if the normal load increases, while the out-of plane peaks do not move consistently.

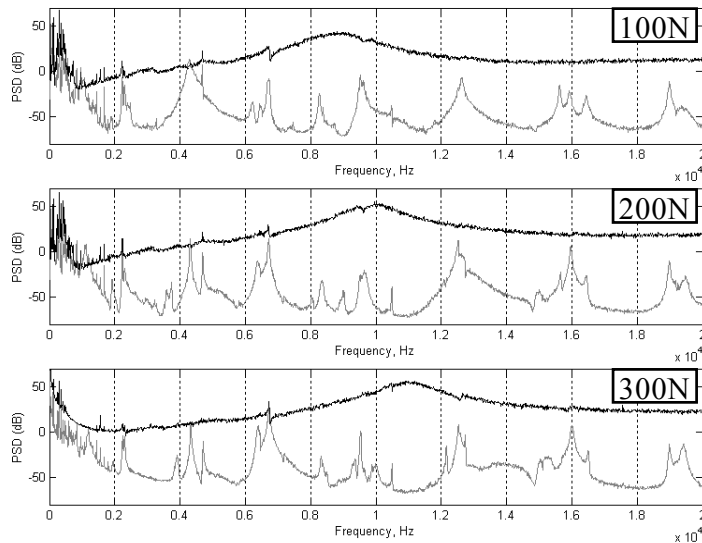


Figure 2.8 PSD of the pad for 3 normal loads and $10 \times 10 \text{ mm}^2$ of contact area: in-plane (black) out-of-plane (grey). After 100 cycles [MASS 03].

Therefore, changes in the normal load have two effects on squeal:

- it increases consistently the in-plane eigenfrequency of the pad, allowing higher frequency modes to become unstable: this explains a documented [GIAN 06a] tendency of higher order modes to squeal for higher normal loads.
- it increases by a small amount the out-of-plane eigenfrequency of the pad that causes the squeal frequency in a single cluster to increase with the normal load [GIAN 06a].

A further important finding obtained by using the laboratory brake [MASS 03] is the experimental evidence of no stick-slip behaviour during squeal instability. These measurements are summarized in Figure 2.9, when the normal load is equal to 120 N. By increasing the normal load the system can reach stick-slip conditions, but it is no more in squeal condition [MASS 03].

The plot shows that the average velocity of the disc, ranging from 242mm/s down to 42mm/s in 7 steps (grey horizontal lines), is always higher than the maximum in-plane vibration velocity of the pad (black line).

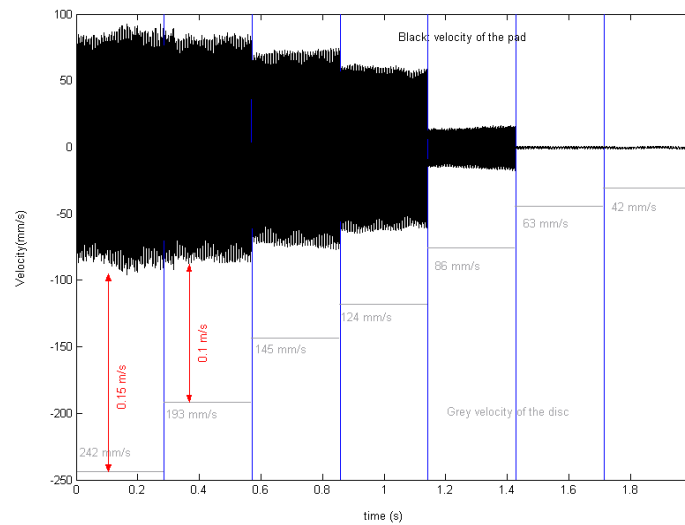


Figure 2.9 Relative velocity between disc and pad [MASS 03].

Moreover, the absence of stick-slip behaviour corroborates the mode lock-in theory as a reliable explanation of the squeal instability.

Model of the Laboratory Brake

The experimental study on the laboratory brake provided guide-lines for building a reduced model [GIAN 06c] of the squeal behaviour occurring in this set-up:

- since the squeal frequencies depend on the out-of plane dynamics of the system, the transverse modes of the disc and the beams within the range of interest are included in the model;
- the double modes of the disc are included in the model (the disc is symmetric when uncoupled to the rest of the system);
- considering that the experimental tests showed no stick-slip conditions during instabilities, it is possible to assume that the relative velocity between disc and pads does not change its direction, and the friction between disc and pads can be modelled by the Coulomb law with constant μ .

Such considerations leads to a linear description of the interaction between disc and pads that, together with a reduced number of degrees of freedom obtained from a modal description of the laboratory-brake, allows for a fast analysis of the model and, through a complex eigenvalue analysis, to the determination of the unstable conditions.

The model starts from the experimental modal description of the disc and the two beams, when they are not in contact. The pad is modelled (Figure 2.10) as a lumped stiffness in the normal direction and as a one degree-of-freedom system in the in-plane direction.

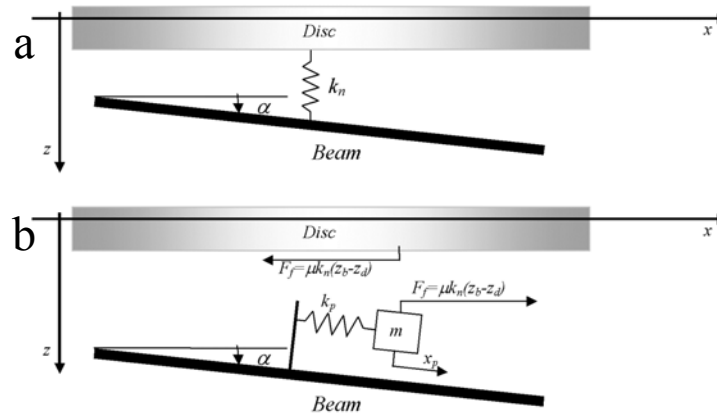


Figure 2.10 Model of the out-of-plane (a) and in-plane (b) dynamics of the pad [GIAN 06c].

The physical forces exchanged between disc and beam through the pad are expressed in terms of the modal coordinates of the beam and the disc in free conditions so that the equation of the coupled system assumes the homogeneous form:

$$M \cdot \ddot{q} + K \cdot q = 0 \tag{2-4}$$

The stability of the system is evaluated by a complex eigenvalue analysis. The stiffness matrix K is asymmetric due to the presence of the terms deriving from the description of the friction force in modal coordinates.

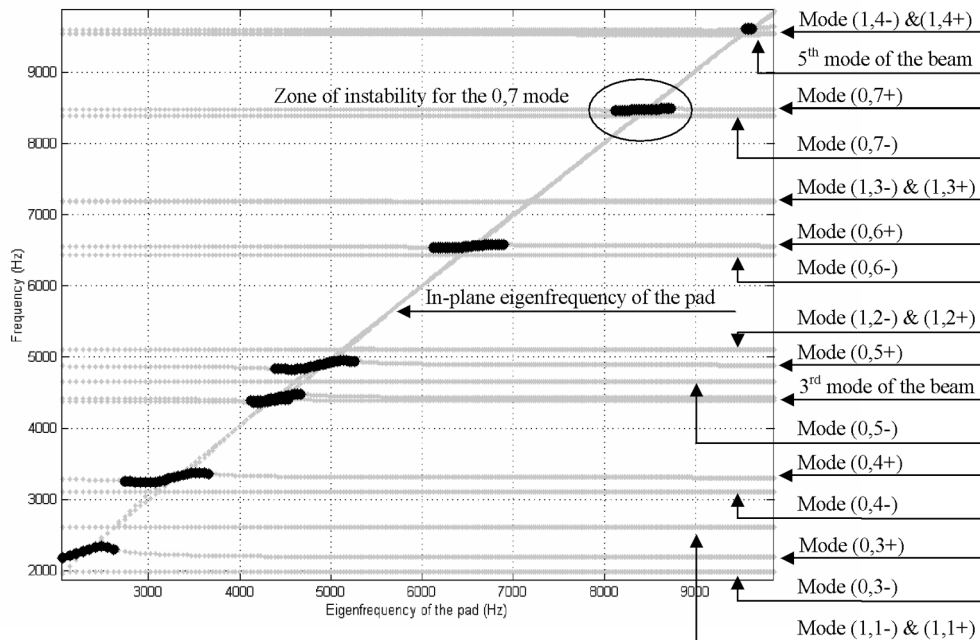


Figure 2.11 Result of the complex eigenvalue analysis [GIAN 06c].

Figure 2.11 shows the results of the complex eigenvalue analysis performed in function of the in-plane eigenfrequency of the pad. The horizontal lines are the modes of the disc and the beams that are not affected by the variation of the pad natural frequency unless they are close each other. When the eigenfrequency of the pad (the diagonal line) crosses some of the disc or beam eigenfrequencies, the real part of the eigenvalue becomes positive. A negative damping is assumed as the onset of squeal occurrence and the unstable points are marked as black dots in the graph.

The simulation shows a good agreement with the experimental results in the frequency range where the model is applicable.

Outputs

The main result obtained with the Laboratory Brake is the possibility to develop a reduced order model able to predict the squeal frequencies that occur during the experiments. Yet, the experimental setup is much more complex and brake-like with respect to the beam-on-disc.

Moreover, the onset of the squeal instabilities is obtained from a linear model of the brake. This supports the assumption that the non-linear aspects related to the contact between disc and pad, e.g. non constant friction coefficient, stick-slip or detachments, material nonlinearities, etc., are not necessary conditions to cause squeal occurrence.

The laboratory brake, with two pads are mounted provides insight into the characteristics of the high frequency squeal behaviour, allowing a correlation with the modal properties of the system.

In particular, the set-up is able to reproduce and study many squeal conditions; particularly interesting is the possibility of studying the rotating squeal by correlating its occurrence with specific values of the parameter R which seems to be the key to organize the different high frequency squeal behaviours. The results allows for a more consistent classification between low and high frequency squeal, based on the value of the ratio R : low frequency squeal occurs for $R < 0.25$, while, for $R \geq 0.25$, rotating squeals, that are characteristic of the high frequency squeal, can occur as well as squeals involving the (n,m-) modes of the disc. Nevertheless, attention should be placed to extend such classification, well defined for this particular test rig, to commercial brake systems.

The experiments and the model highlight that the squeal mechanism is driven mainly by the friction force that induces asymmetry in the stiffness matrix. The feedback force is related to the misalignment angle between disc and beams as well as to the rotational modes of the pad.

2.3 Numerical contact analysis

2.3.1 Transient analysis for contact problems

Several works concerning the dynamics and acoustics of brakes are reported in literature (§ 1) and several analytical and numerical models, characterized by an increasing complexity, are proposed. Nevertheless, the assumption of a global friction coefficient between the first bodies (disc and pad) is one of the main simplifications that allows for a formulation of the models. This macroscopic parameter, necessary for an easy modelling of the interaction between bodies in contact, hides the microscopic phenomena that take place at the contact interface where the instability rises. In particular models do not take in account the local behaviour of the contact and the role of the third body (wear particles trapped in the contact) in the arrangement of the relative velocity and the distribution of the contact pressure. The lack of a more precise modelling of the contact and its local effects is due to the experimental difficulties of measuring locally the surface behaviour, and to the few numerical works aimed to reproduce the contact constraint in time domain during squeal.

In order to overcome this lack and to analyze the local behaviour at the interface between disc and pad, the FE code Plast3 [BAIL 00], particularly addressed for contact problems between deformable bodies, was used to reproduce the contact instabilities. The explicit dynamic formulation and time scheme of this software allows to perform a transient analysis of the phenomenon and to introduce the contact nonlinearities into the model, by including algorithms, based on the formulation of Lagrange multipliers, that account for contact and friction phenomena.

Description of the FE method

Plast3 [BAIL 00 02] is an explicit dynamic finite element code based on an updated Lagrange formulation that uses a forward Lagrange multiplier method [CARP 91] for the treatment of the contact between deformable bodies. The code enables the evaluation of the normal and tangential contact stresses in the contact region as well as the determination of whether the contact surfaces stick, slide or separate locally. The formulation is discretized both spatially, by using the finite element method, and temporally, by using the β_2 method. The contact algorithm uses slave nodes and target surfaces described by quadrilateral (four nodes) elements. The deformable bodies are meshed in 3D with cubic elements of eight nodes with three translational degrees of freedom per node.

The elementary target surface is broken down into a bi-cubic Ferguson patch with C^1 continuity across the adjacent boundary [BAIL 00].

The forward increment Lagrange multiplier method is constructed using the equations of motion determined via the principle of virtual work at time step

t_n ($t_n = n \cdot \Delta t$), augmented by the displacement constraints acting at the contact surfaces at time t_{n+1} ($t_{n+1} = t_n + \Delta t$):

$$\begin{aligned} M \cdot \ddot{u}_{t_n} + C \cdot \dot{u}_{t_n} + F_{t_n}^{\text{int}} + {}^T G_{t_{n+1}} \cdot \lambda_{t_n} &= F_{t_n}^{\text{ext}} \\ G_{t_{n+1}} \cdot \{X_{t_n} + u_{t_{n+1}} - u_{t_n}\} &\leq 0 \end{aligned} \quad (2-5)$$

where λ_{t_n} is the contact force vector acting on the slave nodes at the contact surface, $G_{t_{n+1}}$ the global assembled matrix of the constraint elementary matrices, $X_{t_{n+1}} = (X_{t_n} + u_{t_{n+1}} - u_{t_n})$ the coordinate vector at time t_{n+1} , M and C the mass and damping matrices, F^{int} and F^{ext} the nodal vectors of internal and external forces, \dot{u}_{t_n} and \ddot{u}_{t_n} the velocity and acceleration vectors. The used friction law is the standard Coulomb friction model without regularization of the tangential stress versus the tangential velocity component.

At any time step, the velocity \dot{u}_{t_n} and acceleration \ddot{u}_{t_n} vectors are related to displacements and time increment Δt following the β_2 method ($\beta_2 \in [0.5; 1[$)

$$\left\{ \begin{aligned} \ddot{u}_{t_n} &= \frac{2}{\Delta t} (u_{t_{n+1}} - u_{t_n} - \Delta t \cdot \dot{u}_{t_n}) \\ \dot{u}_{t_n} &= \frac{1}{1 + 2\beta_2} \left\{ \dot{u}_{t_{n-1}} + \Delta t (1 - \beta_2) \ddot{u}_{t_{n-1}} + \frac{2\beta_2}{\Delta t} (u_{t_{n+1}} - u_{t_n}) \right\} \end{aligned} \right. \quad (2-6)$$

The classical central difference scheme can be found by imposing $\beta_2=0.5$. The coordinates of the nodes located at the contact surfaces are first computed with λ_{t_n} equal to zero. Then, an elementary constraint matrix is created for each slave node that has penetrated a target surface. The global assembled matrix $G_{t_{n+1}}$ enables the calculation of the contact forces λ_{t_n} and the new coordinates of the nodes. The resulting system is solved using the Gauss-Seidel method. The contact conditions during each internal iteration of the method are expressed by $\lambda_{t_n}^{\bar{n}} \leq 0$, and the standard Coulomb friction model, without regularization of the tangential stress with respect to the tangential velocity, is imposed:

$$\begin{aligned} \|\lambda_{t_n}^{\bar{t}}\| &\leq \mu |\lambda_{t_n}^{\bar{n}}| \\ \circ \text{ if } \|\lambda_{t_n}^{\bar{t}}\| &< \mu |\lambda_{t_n}^{\bar{n}}|, \quad v_t = 0 \text{ (stick)} \\ \circ \text{ if } \|\lambda_{t_n}^{\bar{t}}\| &= \mu |\lambda_{t_n}^{\bar{n}}| \quad \lambda_{t_n}^{\bar{t}} \cdot v_t \leq 0 \text{ (slip)} \end{aligned} \quad (2-7)$$

where v_t is the relative velocity of the slave node related to the target surface, and \bar{n} and \bar{t} are the normal and tangential vectors defining the contact.

Transient simulations with contact

The local contact instabilities are recognized in [OUES 03] by the onset of stick-slip-separation waves. These instabilities at the contact neighbouring are recognized to be a possible origin of system vibrations.

Different FE models of the pad-disc pair (first bodies) have been developed using the code Plast3, increasing the complexity of the model step by step. A first model includes a friction pad sliding on a beam that represents the disc [DERR 03], with a constant relative velocity and an imposed global contact force (Figure 2.12).

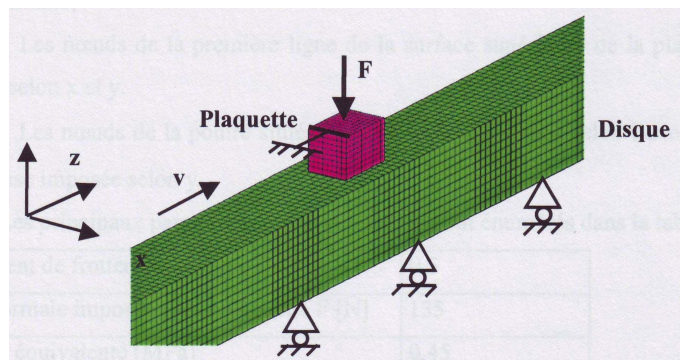


Figure 2.12 Preliminary pin-beam model [DERR 03].

The attention is focused on the local and global dynamics of the pad, by considering the disc rigid with respect to the pad. By this simple model an analysis of the contact stresses is developed and the rise of instabilities is related to the model parameters. The onset of instability is determined to be a function of both the friction coefficient and the sliding velocity. When one of these two parameters is fixed, a limit value of the other one is recognized to characterize the rise of the local instability.

Stick-slip-separation waves, propagating along the sliding direction, are also recognized in [BAIL 02], where the brake disc is modeled by an annular disc rotating with a constant angular velocity.

An analysis of the system vibrations during braking simulations on a similar model is presented in [DERR 03] and [BAIL 05a], and shows the brake rotor to vibrate with a mode at 15 kHz characterized by four nodal diameters and one nodal circumference (Figure 2.13-a). The system starts to vibrate with an harmonic spectrum when the imposed contact force reach the maximum value. When the instability starts the normal and friction forces begin to increase the amplitude of the oscillations until they reach a stable limit-cycle (Figure 2.13-b). The simulations show that such vibrations are associated with the squeal instability of brake systems.

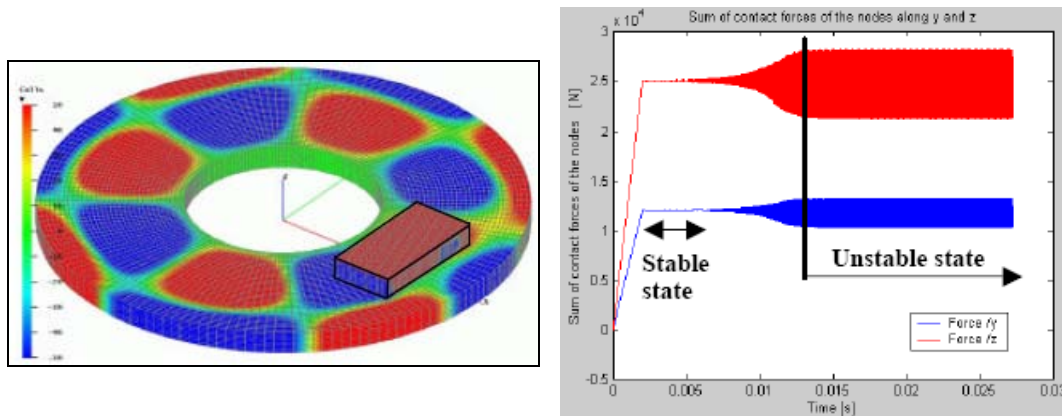


Figure 2.13 a) Velocity along the normal direction; b) Sum of the contact forces at the contact nodes [BAIL 05a].

The contact area between pad and disc shows four zones characterized by different behaviours during the unstable state (Figure 2.14): at the contact entry (Z1), the contact nodes slide, stick and separate periodically at the frequency of vibration; at zone (Z2), the contact area is slipping and sticking periodically; at the contact exit (Z3), the contact area is slipping and sticking; at zone (Z4) the pad is always slipping on the disc.

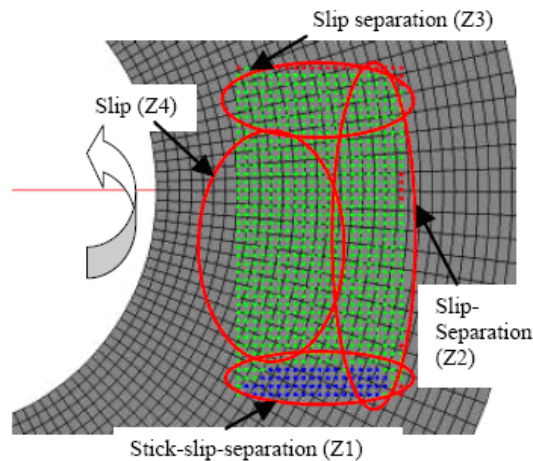


Figure 2.14 The different contact zones of the brake pad and their status [BAIL 05a].

A further analysis of the contact stresses during unstable conditions, simulated by the effort of the nonlinear contact numerical analysis, is shown in [BAIL 05b], where the FE model is developed to simulate the squeal events obtained on an experimental tribometer. The model is still composed by a pin and a disc in contact and the vibrations of the system are calculated in function of the main parameters. The unstable state is recognized again by the formation of zones in contact (slip or stick) and zones separated from the surface of the disc. The variation of the local contact status is accompanied by a variation of

the normal contact stress. These oscillations of the contact stresses are strictly correlated with the vibrations of the system.

A study on the variation of the macroscopic friction coefficient (ratio between the tangential and the normal forces calculated on the pin, far away from the contact) in function of the macroscopic relative velocity is reported in [BAIL 05b], where the variation is related to the local phenomena. Depending on the value of the local friction coefficient that is imposed to be constant with the velocity (Coulomb's friction law imposed at each contact node), the global friction coefficient can be or not function of the velocity. Figure 2.15 shows that, when the local friction coefficient is equal to 0.2 or less (no local instability), the global friction coefficient is constant and equal to the local one. On the contrary, with higher values of local friction coefficients, the global friction coefficient varies with the relative velocity.

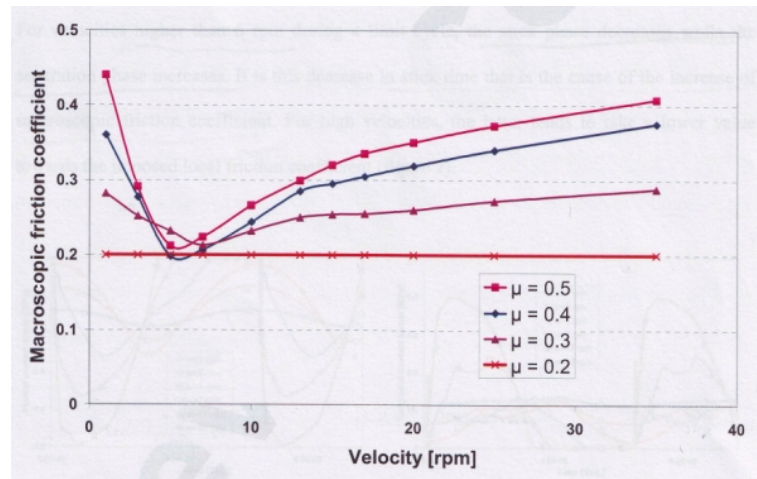


Figure 2.15 Macroscopic friction coefficient versus disc velocity for different local friction coefficients [BAIL 05b].

In particular, for low relative velocities ($\omega \leq 6$ rpm), the instabilities at the interface are characterized locally by stick-slip zones and the macroscopic friction coefficient decreases with the increase of the velocity. For disc velocities higher than 6 rpm, the instability is characterized by stick-slip-separation zones and the macroscopic friction coefficient increase with the relative velocity. The analysis of the contact stresses shows that this different trend is due to the increase (under 6 rpm) and then to the decrease (over 6 rpm) of the stick zones when the relative velocity increases.

Outputs

A main lack in squeal modelling was the characterization of the contact between the two first bodies (disc and pad). Analytical and numerical models simplified the friction interaction by introducing a global friction coefficient to

connect the substructures and simulate the friction force that acts tangentially to the contact surface. Moreover, in order to linearize the problem, simplified elements connecting the contact surfaces have been frequently adopted.

The nonlinear FE code Plast3, used to simulate the braking phase in the time domain, allows to introduce the nonlinearities due to the contact into the model. The modelling of the local contact constraints permits to overcome several assumptions previously adopted to reduce the order of the model and to linearize the solution. The prediction of the contact instabilities is obtained simply by imposing a local friction coefficient that is constant with the sliding velocity.

Moreover, the introduction of the contact nonlinearities allows to reproduce a steady state behaviour of the instability characterized by a limit-cycle of the system vibrations.

The friction coefficient, used in the previous analytical and numerical models as an adjusting parameters to connect the first bodies and to obtain the experimentally obtained behaviour, is treated by this FE code as a true parameter like the geometry of the first bodies, the rotational velocity, the load pressure, etc.

The nonlinear analysis of the transient behaviour during brake simulations permits to calculate the distribution of the contact stresses and their variation in time. Moreover, the tribological state of the instantaneous contact zones, i.e. sliding, sticking and separation (the zones where it would be necessary to take into account the action of the third body), can be predicted. The local analysis allows to link the variation of the global friction coefficient, in function of the relative velocity, with the local dynamics at the contact area (when the imposed local friction coefficient is constant).

In conclusion the transient analysis of the contact during brake simulations is proved to be a powerful tool to link the micro-scale phenomena (local contact state, small vibration wavelengths) with the macro-scale phenomena (vibration of the whole system).

2.4 The TriboBrake COLRIS

2.4.1 Design of the test rig

Considering the experience of the previous studies on simplified experimental set-ups (Beam-on-disc and Laboratory-brake) a new experimental rig is designed to be object of the work presented in this thesis. The design criteria focus the attention on the dynamics of the assembled brake system and on the behaviour of the tribological triplet (mechanism, bodies in contact, third

body). Moreover, the geometry of the system is conceived to be modelled in a simplified manner by the FE codes used for the numerical analysis of squeal.

The set-up, developed in collaboration between the University of Rome “La Sapienza” and the LaMCoS of Lyon, is conceived to be a tribometer test rig maintaining the main characteristic of a brake system, and is named TriboBrake COLRIS (COLlaboration Lyon-Rome for Investigation on Squeal).

The following criteria were accounted for the design of the system geometry:

- 1 the boundary conditions during the brake phase must be constant in order to have robust squeal events, durable in time;
- 2 the boundary conditions must be easily reproducible, in order to have reproducibility of squeal events;
- 3 the design must take into account the main characteristics of a real brake, e.g. the substructuring of the three main parts, that are the rotor, the calliper and the pad;
- 4 the dynamics of the substructures must be recognizable and easy to control, in order to analyze the dependence of squeal occurrence with respect to the system dynamics;
- 5 consequently, the dynamics of the single substructures have to be as simple as possible;
- 6 both tribological and dynamic measurements must be performed on the set-up, in order to analyze the data and compare them with numerical results, i.e. particular attention is focused on the measurability of the system;
- 7 the set-up must be modelled by a FEM, i.e. the geometry and connections between the substructures and the frame must be simple to schematize.

Figure 2.16 and Figure 2.17 show the side and front drafts of the TriboBrake assembly. The three main substructures are indicated: disc, calliper (support), and pad. The disc is clamped to the shaft by two thick hubs that guarantee a high stiffness to the connection. The friction pad is connected to its support (caliper) by a thin backplate that allows the dismounting of the pad itself without damage. Between the pad and the support a triaxial transducer is placed. It allows to measure the global normal and friction forces during the braking phase.

The support of the pad schematizes the brake caliper and is held in the tangential (friction) direction by two thin plates. Such solution permits to introduce a negligible stiffness in the normal direction, while opposing the tangential force due to the brake torque.

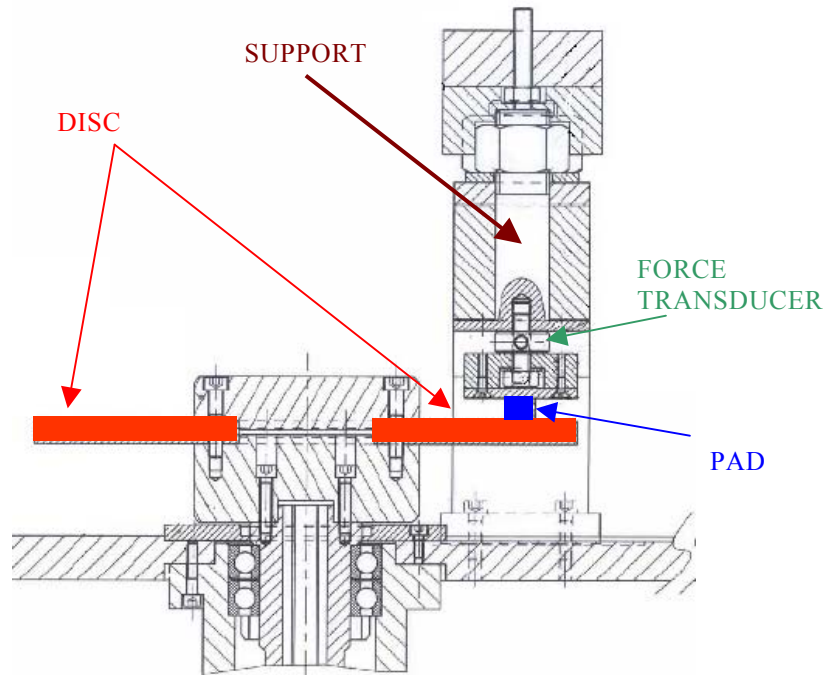


Figure 2.16 Side drawing of the TriboBrake COLRIS.

The normal force (brake pressure) can be adjusted by adding weighs on the top of the support; the negligible normal stiffness, introduced by the thin plates, allows the support to float and follow the misalignments of the disc.

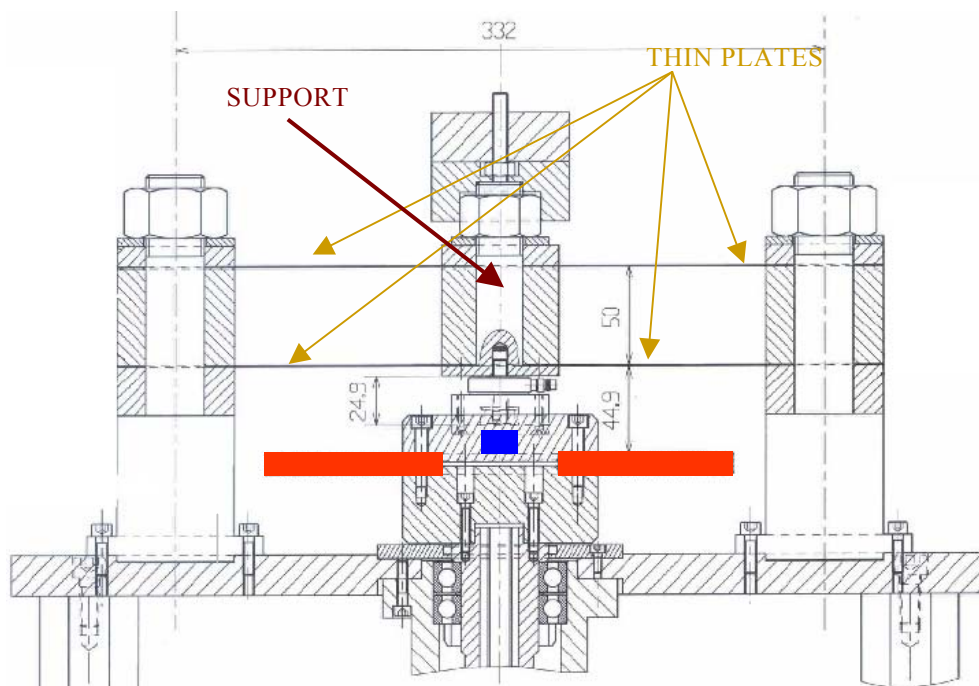


Figure 2.17 Front drawing of the TriboBrake COLRIS.

The design criteria 1 and 2 are assured by the way in which the load is applied: the floating support permits to have a constant normal force by following the misalignments of the rotating disc, i.e. by maintaining the same contour conditions during squeal.

Points 3, 4 and 5 are taken into account when designing the single substructures: the brake rotor is a flat disc without the hat shape at the inner radius (characteristic of the rotor of commercial brake systems), allowing to have a dynamics characterized mostly by bending (normal direction) modes with small in-plane component of vibration. The support, that represents the brake caliper, has a tangential dynamics that can be easily referred to the dynamics of a beam. The reduced dimensions of the friction pad allows to consider the dynamics of the assembly as the sum of the dynamics of the single substructures. Moreover, the simple geometry of the pad allows to recognize the tangential dynamics of the pad itself, that has a key role in the squeal generation. These properties satisfy the point 7 as well.

Point 6 is taken into account by positioning a tri-axial force transducer as close as possible to the contact surface, in order to have the time histories of the tangential and normal contact forces during the braking phase. The vibration of the system components can be acquired by accelerometers as well as by a laser vibrometer (in particular the rotating parts). The connecting backplate between pad and support allows a dismounting of the pad for tribological analyses of the contact surfaces (post-mortem analysis), while the horizontal position of the rotating disc permits to monitor the third body flows.

The TriboBrake can be consider an evolution of the previous simplified brake systems: it maintains the advantage to be close to a real brake, especially with respect to the Beam-on-disc, but introduces some further characteristics with respect to the Laboratory-brake. This permits to relate clearly the appearance of squeal with the lock-in conditions between two modes of the three substructures of the system: support, pad and disc. The following main improvements are thus introduced:

- the caliper is modeled by the cylindrical support having an in-plane dynamics that is clearly identifiable. This permits to distinguish the in-plane dynamics of the pad from the in-plane dynamics of the support, while in the Laboratory-brake the in-plane contribution of the beam could not be clearly determined;
- a tri-axial force transducer between the pad and the support permits to measure the normal and friction force time histories, that are necessary for a comparison with the numerical simulations;
- the floating support permits to have a constant normal force by following the misalignments of the rotating disc, i.e. by maintaining the same contour conditions during squeal;

- the set-up allows for tribological measurements, that are necessary because of the tribological nature of the issue;
- the out-of-plane dynamics of the support is not involved into the squeal modal coupling; such condition allows to reduce the squeal problem to an unstable coupling between the out-of-plane dynamics of the disc, with the in-plane dynamics of the support or the pad.

Such improvements, together with the easy FE modeling of the brake assembly, permits to have a more accurate and complete analysis of squeal and its relationships with the dynamic and the tribological features of the brake system under operating conditions.

2.4.2 Methodology for squeal investigation

The framework of the thesis includes different approaches to the squeal problem that are deeply connected one to the other. Experimental and numerical investigations are carried out and the results are compared. In particular, for clearness, the structure of the thesis consists of four main parts: the linear and the nonlinear numerical analyses (chapter 3 and appendix A), the experimental dynamic analysis (chapter 4), the tribological analysis (chapter 5). Nevertheless, each part should be read as a particular step of a more complex approach that links together the single analyses and is aimed to give a general understanding of the problem. *Figure 2.18* shows a scheme of the used methodology.

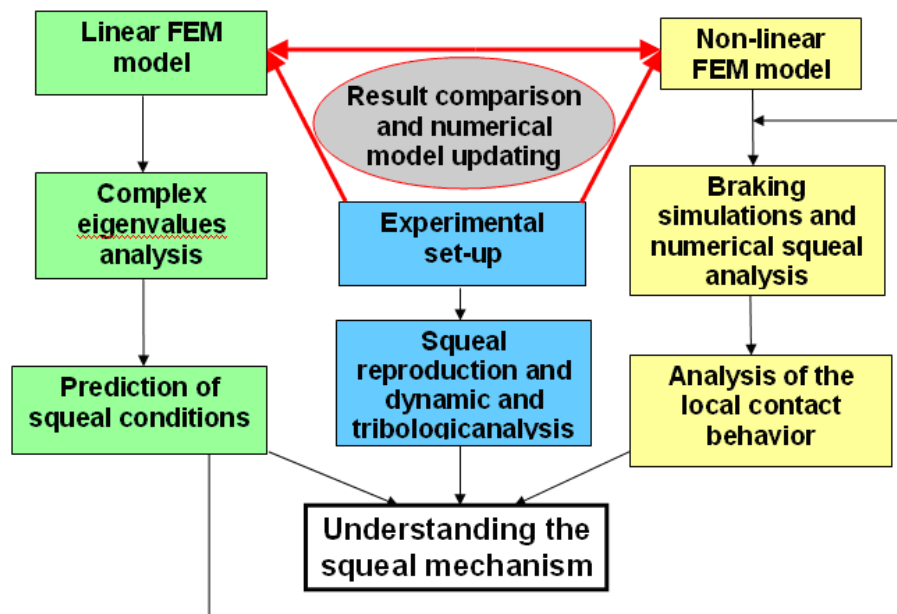


Figure 2.18 Scheme of research project

The core of the research is the experimental set-up that is designed to be appropriate for different analyses. The set-up design began in December 2003 and the experimental tests started in May 2005. An experimental dynamic analysis is performed to relate the squeal occurrence and its vibrational features to the system dynamics. A tribological experimental analysis is performed as well to investigate the role of the micro-scale effects at the contact surface with squeal and investigate the role of the contact triplet in the squeal generation. Then, the correlation between micro and macro scales features of squeal is investigated. The dynamic analysis of the set-up is also used for updating the numerical models.

A linear and a nonlinear FE model are developed parallelly: the linear FE model, developed with Ansys, is used to perform a parametrical complex eigenvalue analysis aimed to predict the values of the parameters that lead to instability; the nonlinear FE model, developed with Plast3, is used to simulate the braking phase in the time domain and analyze the system vibrations and the local contact behaviour during squeal. The values of the parameters that lead to instability are predicted by the linear complex eigenvalue analysis and introduced into the nonlinear model to simulate the instability in time. The two FE models are compared and a preliminary parallel analysis of the squeal prediction is performed with the two models, in order to verify the validity of each approach.

The results obtained from the linear and nonlinear numerical analyses and from the dynamic and tribological experimental analyses are compared to highlight the physics of the problem and characterize the squeal mechanism.

The developed work is reported in this thesis as follows:

- Chapter 3: the linear and the nonlinear FE models are presented and compared. The prediction of the squeal frequencies is performed with the linear model and the braking simulations in time domain are calculated by the nonlinear model. An analysis of the local contact features during squeal is performed.
- Chapter 4: the dynamic experimental analysis is presented. The squeal occurrence is linked to the dynamics of the system and the vibrational behaviour of the system during squeal is analyzed.
- Chapter 5: the tribological experimental analysis is presented and the analysis of the contact surface is linked to the squeal. The STTs (Superficial Tribological Transformations) and the third body are correlated with the numerical analysis of the contact stresses during squeal simulation.

- Chapter 6: all the numerical and experimental results are resumed and linked together to highlight the mechanism that bring to squeal instability and its main characteristics.

Chapter 3. Linear and nonlinear numerical analysis

Chapter 3.	<u>Linear and nonlinear numerical analysis.....</u>	81
3.1	Introduction.....	83
3.2	Finite Element Models.....	85
3.2.1	<i>Geometry of the models.....</i>	<i>85</i>
3.2.2	<i>Linear model.....</i>	<i>86</i>
3.2.3	<i>Nonlinear model</i>	<i>88</i>
3.2.4	<i>Dynamic comparison</i>	<i>89</i>
3.3	Linear analysis for the detection of system instabilities.....	91
3.3.1	<i>Complex eigenvalue analysis.....</i>	<i>91</i>
3.3.2	<i>Stability analysis.....</i>	<i>95</i>
3.3.3	<i>Propensity to instability</i>	<i>98</i>
3.4	Time analysis with the nonlinear contact model: braking simulation	101
3.4.1	<i>Stability analysis.....</i>	<i>101</i>
3.4.2	<i>Local contact analysis.....</i>	<i>105</i>
3.5	Comparison of results	108
3.5.1	<i>Prediction of the unstable regions of the parameters</i>	<i>108</i>
3.6	Conclusions.....	110

3.1 Introduction

The onset of squeal is due to an unstable behaviour that is supposed to occur in linear conditions, during the braking phase. Many researchers, North [NORT 72], Akay *et al.* [AKAY 00] in their studies on the dynamic behaviour of brake systems put in evidence a coincidence between the squeal frequencies and the natural frequencies of the system. Particularly, they associated the squeal phenomenon to the coalescence of two eigenfrequencies of the system. Their studies suggested the complex eigenvalue analysis of brake systems as a tool for squeal investigation. To study the stability of the system by the complex eigenvalue analysis, the friction effects between the pad and the disc are accounted for by introducing linear elements in an asymmetric stiffness matrix. The main limitation of these studies is the use of a linear model, despite the strong nonlinearities associated with the contact problems.

Nevertheless, linear models have been used to predict the onset of squeal [OUYA 05], and the good agreement with experimental experiences [GIAN 04] proves the assumption that the onset of the squeal instability occurs in linear conditions.

However, the nonlinear effects of the contact can not be neglected when investigating the squeal evolution, once squeal is developed. In particular, the linear model is not able to characterize the squeal response when it reaches its characteristic limit-cycle, and to analyze the local nonlinear effects at the contact surface. Moreover, the dynamics at the contact between disc and pad is also difficult to retrieve by experimental analysis. To overcome such drawback it is necessary to model appropriately the contact between the disc and the pad, considering the nonlinearities due to the contact between deformable bodies. This nonlinear modelling can be introduced in a FE model for simulation of the braking phase in the time domain.

In literature two different methodologies are envious for predicting brake squeal by finite elements models: the complex eigenvalue analysis and the transient analysis. The complex eigenvalue analysis has the advantage to be very efficient, but usually not all the frequencies predicted to be unstable can be founded experimentally. The transient analysis allows the reproduction of the time behaviour of the system vibrations but it is very time-consuming. A large number of studies consider either one or the other of such methodologies [ABU 06], so that the two methods were performed separately rather than simultaneously to predict and analyze the instability.

This chapter presents the integration of the numerical approaches to identify the mechanism leading to squeal instability and analyze its dynamics. The first approach performs a parametrical finite element modal analysis of the brake system to identify its eigenvalues and to relate them to the squeal

occurrence. The second uses a specific finite element program, Plast3, appropriate for nonlinear dynamic analyses in the time domain and particularly addressed to contact problems with friction between deformable bodies. The use of this program allows to analyze the contact stresses and the dynamics of the system along the contact surface, both in the linear and in the nonlinear range.

Two different FE models are therefore developed: the linear FE model, used to predict squeal “conditions” and squeal frequencies, and the nonlinear FE model developed for the contact problem, useful to investigate the characteristics of the contact in the time domain. The latter is, in fact, able to model the contact behaviour, with possible detachments and stick-slip conditions at the contact surface. In this work the Coulomb’s law with constant friction coefficient is used to model the friction force. Local and global normal friction forces can be directly determined during the braking simulation. The work wants to combine the linear numerical tool for squeal prediction and the nonlinear numerical code for squeal analysis. In particular, different brake simulations carried out with the nonlinear model, using different values of the parameters, allow to compare the ranges of the parameters that lead to instability with the ranges leading to instability using the linear model. The agreement between the results of the two models permits to assess that the instability conditions can be determined conveniently by the linear model that is computationally much more efficient. To simplify the dynamics of the brake components, the study is carried out on a simple model. The geometry of the model is related to the geometry of the TriboBrake that is used to validate the models and compare the numerical results with the experiments.

3.2 Finite Element Models

3.2.1 Geometry of the models

The system considered in this paper (Figure 3.1) represents a simplified brake, the TriboBrake set-up, that is designed for squeal reproduction and analysis.

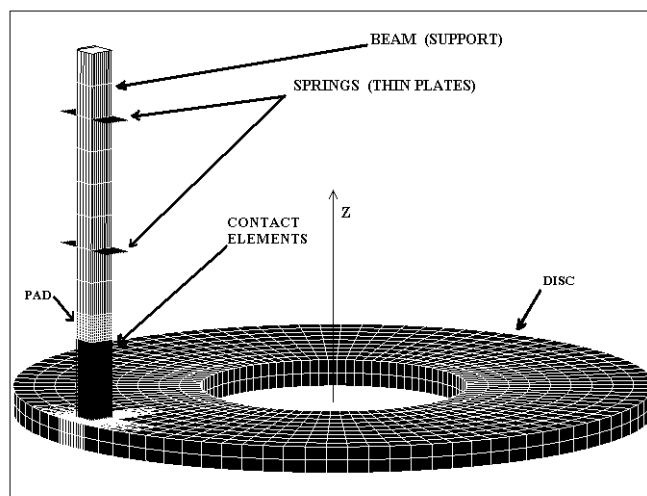


Figure 3.1 Finite element model.

The brake rotor consists of an annular disc with an external radius of 120mm, internal radius 50mm and thickness 10mm. Its Young modulus is equal to 210000 MPa and its density 7800 kg/m^3 . The brake pad consists of a cube $10 \times 10 \times 10 \text{ mm}$, with a material density of 2500 kg/m^3 and Young modulus variable between 1000 and 100000 MPa. The pad support is modelled by a beam $100 \times 10 \times 10 \text{ mm}$. Four rows of springs, two on each side, hold the beam in the horizontal (friction force) direction, and model the four thin aluminium plates that hold the pad support in the experimental set-up (Figure 3.2). The value of the springs stiffness ($8.422 \times 10^6 \text{ N/m}$ each spring, 11 springs each row) is determined by imposing the same normal stiffness of the thin plates. The other side of the springs is constrained along all the directions. A proportional structural damping is used for the whole model ($\alpha = 0.02$ and $\beta = 1e-7$). The normal force that pushes the pad against the rotor is generated in the experimental set-up by adding a weight: during the braking simulations it is modelled by a distributed force acting on the top of the pad support.

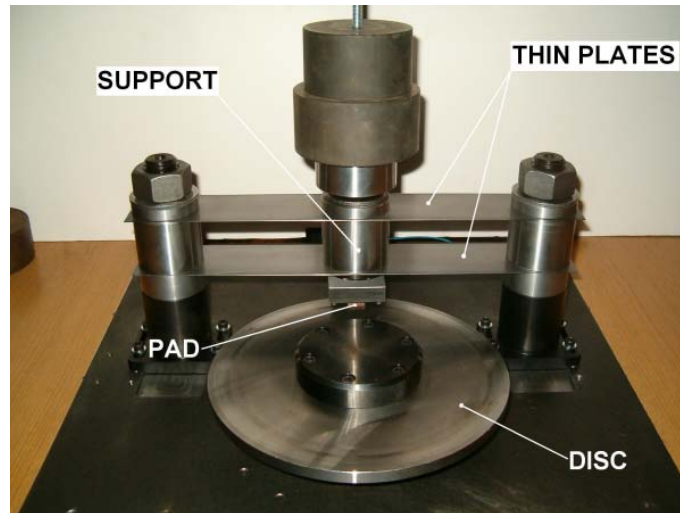


Figure 3.2 Experimental set-up.

Two different models of the contact surface, a linear and a nonlinear one, are used and described below. The main difficulty in the definition of the linear model is the need of using linear elements to account for the nonlinear behaviour of the contact. Since the two models must be appropriately compared the average value of the contact stiffness k_n that is introduced in the linear model is determined by the nonlinear model by applying a ramp contact force. A contact stiffness equal to 2.5895×10^8 N/m is determined, for a Young modulus of the pad equal to 16000 MPa. The variation of the contact stiffness in function of the Young modulus of the pad is not taken into account in the linear analysis, because it was checked that it has not a remarkable influence on the eigenvalues extraction in the considered range.

3.2.2 Linear model

Ansys®, a commercial FEM software, is used to investigate the dynamics of the system and to calculate its complex eigenvalues in function of the driving parameters. The Ansys element, SOLID45, is used to mesh all the solid components of the system. SOLID45 is a 3D brick element characterized by 8 nodes, with 3 translational degrees of freedom per node; the shape functions are linear.

The 3-D geometry of the subsystems is discretized with a mapped mesh. Compared with the free-mesh which uses tetragonal elements, the mapped mesh allows for a reduction of elements and computational resources. Moreover, the mapped mesh permits to generate an axial-symmetric grid of the disc. A non-axial symmetric mesh causes the modes of the disc that, under free conditions, are double modes, to split into different shapes and different frequencies. In order to reduce the computational time, a convergence study of the mesh is developed. Figure 3.3-a shows the same mesh used on the nonlinear FEM

model: it is completely axial symmetric, but it has a large number of elements (10240 disc elements). The mesh shown in Figure 3.3-b is not completely axial symmetric, but it has a lower number of elements (2412 disc elements) and a finer mesh of the disc surface is introduced at the contact area. This expedient allows to introduce a larger number of contact elements at the contact surface, to obtain a more uniform distribution of the contact stiffness.

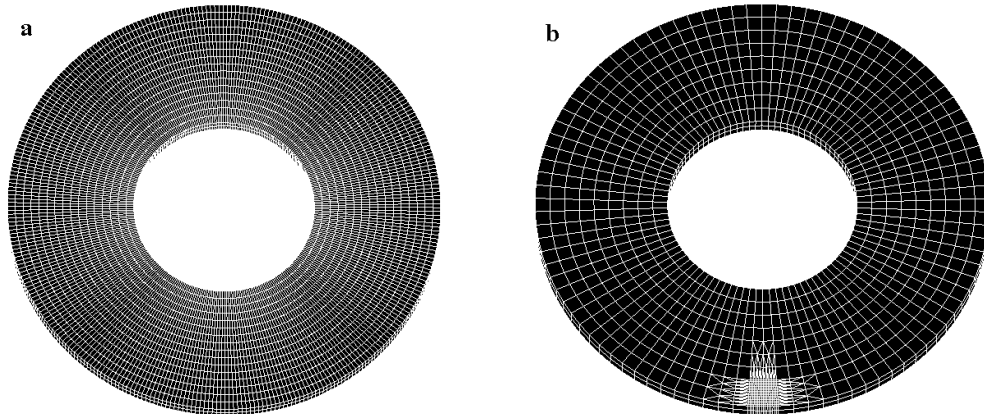


Figure 3.3 a) Disc mesh with 10240 elements; b) Disc mesh with 2412 elements

A comparison between the dynamics of the two models with different meshes has been performed. Although the use of a finer mesh on one sector of the disc modifies slightly the axial-symmetry of the disc, the percentage error in the frequency range of interest (1-20 kHz) is lower than 4% and lower than 2% up to 10 kHz (Figure 3.4). Therefore, because of the reduction of computational resources and because of the finer mesh in the contact area (where the contact elements have to be placed), the second mesh was preferred for the linear analysis.

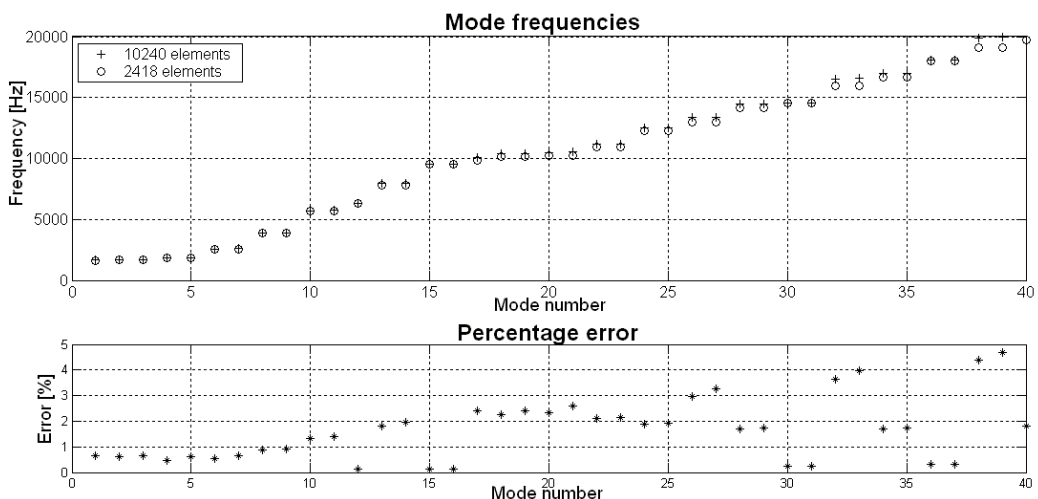


Figure 3.4 Error percentage between the eigenfrequencies obtained with the two meshes between 600 Hz and 20 kHz

The contact elements are implemented in the FEM code using the MATRIX27 element that produces an element stiffness matrix characterized by two nodes that can be non-symmetric.

For each couple of nodes of the pad and the disc at the contact area, the following force components are introduced in the element stiffness matrix MATRIX27:

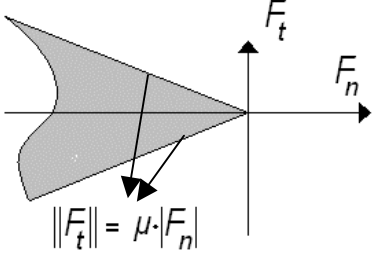
$$\begin{aligned} F_z^d &= k_n \cdot (z^d - z^p) & F_z^p &= -k_n \cdot (z^d - z^p) \\ F_y^d &= -\mu \cdot k_n \cdot (z^d - z^p) & F_y^p &= \mu \cdot k_n \cdot (z^d - z^p) \end{aligned} \quad (3-1)$$

where d denotes the disc, p the pad, k_n the contact normal stiffness between the two nodes, z the displacement in the direction normal to the contact surface. F_z and F_y are the contact forces in the normal and tangential (friction) direction, respectively, and μ is the Coulomb friction coefficient. At the contact area, the disc and the pad surfaces are meshed with 10x10 elements, 121 nodes for each surface, i.e. 121 stiffness elements are introduced over the nodes of the contact area, between the nodes of the disc surface and the nodes of the pad surface. The Coulomb law with a constant coefficient μ describes the friction interaction between disc and pad. The disc is constrained at the internal radius nodes along the x , y and z degrees of freedom. The lateral springs, modelling the thin plates of the experimental set-up, are introduced by the COMBIN14 element in Ansys.

3.2.3 Nonlinear model

The explicit dynamic three-dimensional finite element code Plast3 [BAIL 02] is used to simulate the behaviour of the system in the time domain. This software uses a forward incremental Lagrange multiplier method [CARP 91], that ensures the compatibility between the displacements of the slave nodes and the target surfaces at the contact area, enabling the evaluation of the normal and tangential contact stresses in the contact region as well as the determination of whether the contact surfaces stick, slide or separate locally (see § 2.3.1).

The displacement constraints, applied to the slave nodes to avoid penetration of the master surfaces at the time step $t + \Delta t$, permit to obtain the Lagrange multipliers and then the contact forces at the time step t . The used friction law is the standard Coulomb friction model without regularization of the tangential stress versus the tangential velocity component:



$$\begin{aligned} & \|F_t\| \leq \mu |F_n| \\ & \text{if } \|F_t\| < \mu |F_n|, \quad v_{\bar{i}} = 0 \quad (\text{stick}) \\ & \text{if } \|F_t\| = -\mu |F_n| \cdot \frac{v_{\bar{i}}}{|v_{\bar{i}}|} \quad (\text{slip}) \end{aligned} \quad (3-2)$$

where $v_{\bar{i}}$ is the sliding velocity, μ is the friction coefficient, F_n is the normal force and F_t is the tangential force.

The three deformable bodies, the disc, the pad, and the pad support, are meshed with cubic elements of eight nodes with three translational degrees of freedom per node. The model of the support has 400 elements, while the pad has 1000 elements, and the disc 10240 elements.

At time $t_0 = 0$, an increasing force, F , is applied along the z -direction until it reaches a pre-selected value corresponding to a uniformly distributed normal displacement on the top of the pad support. The application of this force puts the pad in contact with the disc whose rotational speed is kept constant throughout the simulation time. By using a force that increases starting from zero, it is possible to reduce the impulse response of the system due to the initial contact between disc and pad. Seemingly to the linear model, four rows of springs hold the beam in the horizontal (friction force) direction. Unlike the linear model where the disc is fixed, so that the internal radius is constrained along the three coordinates x , y and z , with the nonlinear model the nodes belonging to the inner radius of the disc are constrained only along the z -axis and are imposed to rotate with a constant rotational speed ω with respect to the disc axis. The material properties and bodies dimensions are the same of the linear model. Nonlinear properties of materials and thermal effects are not taken in account.

3.2.4 Dynamic comparison

The main purpose of this section is to compare the two models so that the linear one can be used to predict the squeal onset conditions, and the nonlinear one to investigate the squeal characteristics by studying the evolution of the contact dynamics in the time domain. Therefore, a frequency analysis of the nonlinear model is performed (when it is in linear conditions, i.e. $\omega = 0$ and small vibrations of the system are assumed) to compare the dynamic behaviour obtained by this model with the eigenvalues and eigenvectors of interest obtained by Ansys on the linear model. Aim of this comparison is to characterize the natural frequencies of the nonlinear model and to check the dynamic similarities between the two models.

With Plast3, the same increasing force F used in the runs for braking simulation is applied on the pad support, at the initial time, in the z -direction until it reaches the pre-selected value. This is done to have the same preloading conditions that are used for the braking simulations, so that the same normal force between disc and pad is obtained. Then, an impulse is applied at a node of the disc in the z -direction and the response of the system is calculated. The time results are elaborated with Matlab to obtain the Frequency Response Function on each node and to reconstruct the ODS at each eigenfrequency. The material properties are those listed in section 3.2.1, with the Young modulus of the pad equal to 25100 MPa ($10^{10.4}$ Pa). With the same parameters a modal analysis is performed with Ansys.

Here the attention is focused on those normal modes of the disc considered to be primarily involved in the squeal mechanism [MASS 06a]. The disc modes are characterized by nodal circumferences and nodal diameters: the (n,m) mode of the disc is characterized by n nodal circumferences and m nodal diameters. The disc is characterized by an axial symmetry: therefore the modes of the disc are generally double modes.

The following notation is used to name the modes of the coupled system that split the double modes of the disc:

- mode $(n,m-)$: a nodal diameter is coincident with the contact point;
- mode $(n,m+)$: an antinode is coincident with the contact point.

Table 3.1 lists the frequencies calculated by the linear model and by the nonlinear one, and the percentage error between them. In the frequency range of interest there is a percentage error less than 5%, and, below 15 kHz, less than 3%. This error is due to the different meshes and the different contact models. Moreover, the eigenfrequencies computed with Plast3 miss the modes with a nodal diameter at the contact point because the impulse is applied to a node of the contact area so that only the modes with an antinode at this point are excited. In fact the excitation point is chosen in order to excite modes that can be involved in the squeal phenomenon; in [MASS 06c] it is shown that, using pads with reduced dimensions, only modes with an antinode at the contact point are involved in squeal phenomena.

Figure 3.5-a and Figure 3.5-b show the deformed shapes related to the modes $(0,3+)$ and $(0,4+)$, when the normal load is applied, calculated with Matlab from the data obtained with Plast3. The deformation shapes are affected by the asymmetry due to the contact with the pad and the angle between the two nodal radiuses that include the contact area becomes larger, until a further node of vibration is detected at the contact radius. Such behaviour is also recovered by the modal analysis performed with Ansys (see Figure 3.8-b and Figure 3.8-d) and experimentally [MASS 05b].

MODE	Ansys	Plast3	ERR %	MODE	Ansys	Plast3	ERR %
(0,3-)	2594			(1,3)	12494	12348	1.169
(0,3+)	3492	3424	1.947	(0,8+)	13401	13179	1.657
(0,4-)	3918			(0,8-)	13700		
(0,4+)	4992	4877	2.304	(1,4-)	14437		
(0,5-)	5736			(1,4+)	14475	14216	1.789
(0,5+)	6659	6486	2.598	(0,9+)	16565	15980	3.532
(0,6-)	7956			(0,9-)	16724		
(0,6+)	8594	8353	2.804	(1,5-)	16970		
(1,0)	10126	10014	1.106	(1,5+)	17036	16603	2.542
(0,7)	10523	10636	-1.074	(0,10+)	19989	18938	5.258
(1,2)	11144	11155		(0,10-)	20018		

Table 3.1 Modes and frequencies (Hz) computed by Ansys and Plast3 (post-processing in Matlab), for a Young modulus equal to 25000 MPa ($10^{10.4}$ Pa) and friction coefficient 0.5.

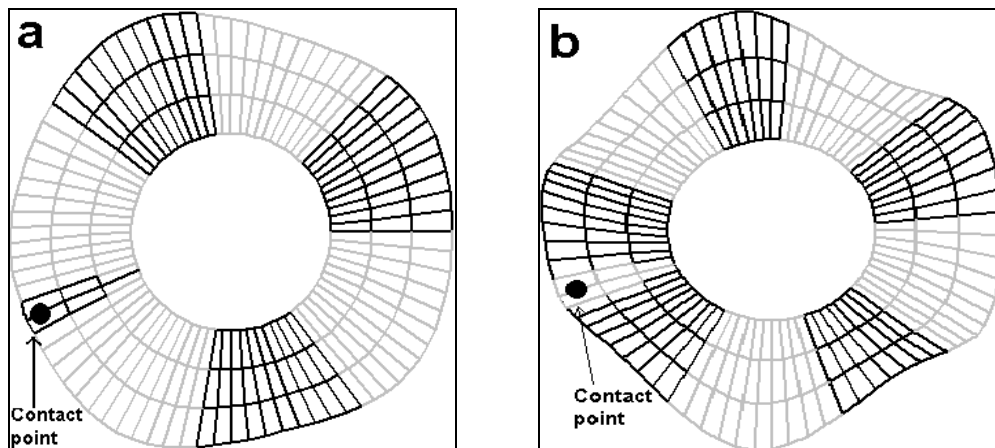


Figure 3.5 a) Deformed shape at 3424 Hz (0,3+); b) Deformed shape at 4877 Hz (0,4+). Obtained with Plast3 (postprocessing in Matlab).

3.3 Linear analysis for the detection of system instabilities

3.3.1 Complex eigenvalue analysis

Since brake squeal noise is characterized by extreme unpredictability due to the large number of parameters that influences it, a tool to locate the regions of the parameters bringing to squeal instability is necessary.

The analysis is performed here in function of two parameters, the friction coefficient and the Young modulus of the pad material that are the most influential and, at the same time, the most uncertain. In fact, the friction coefficient between pad and disc is the responsible for coupling the normal and

tangential stresses at the contact surface. The Young modulus of the pad material is very influential on the dynamics of the system at the contact zone. Moreover, the elastic properties of the brake pad materials are not well defined. In fact, an increase of the normal load in the experiments causes the natural frequencies of the system to shift. Such increase is here simulated by increasing the Young modulus of the pad material.

The complex eigenvalue analysis provides the tool to trace the regions of the parameter space that leads to an instability of the system. The extraction of the numerical eigenvalues is performed by the Damped Method of Ansys in function of the Young modulus of the pad material, ranging from 10^9 † to 10^{11} Pa (from 1000 to 100000 MPa). The eigenvalues extraction is repeated for six different values of the Coulomb friction coefficient, starting from 0.01 up to 0.7. For each value of the friction coefficient, the analysis is first performed in the whole frequency range of interest, i.e. from 900Hz to 20000Hz. Then, a more refined analysis is focused on the unstable regions.

Figure 3.6 shows the complex eigenvalues of the system in function of the Young modulus of the pad material for a friction coefficient equal to 0.01.

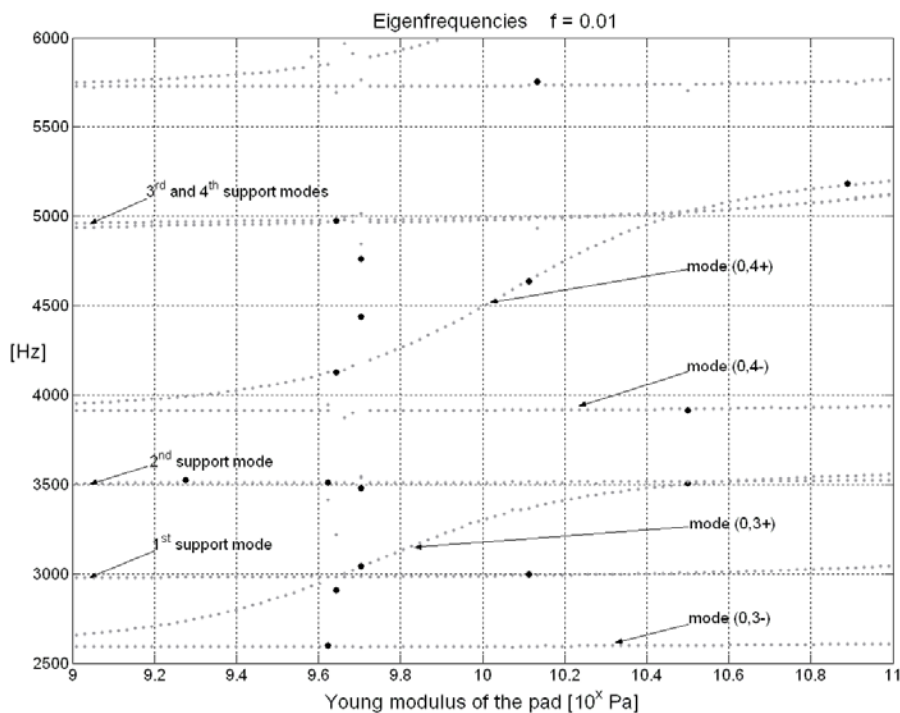


Figure 3.6 Eigenvalues analysis in function of the Young modulus of the pad (from 1 to 100 GPa) for a friction coefficient equal to 0.01.

† The reason for this unusual uniting of the Young modulus is related only to a clear plot of the stability regions when varying the Young modulus, that is plotted in logarithmic scale.

Figure 3.7 shows the modes of the support at 3 kHz, 3.5 kHz and 5 kHz, calculated with the Young modulus of the pad equal to 10^9 Pa (initial value). The mode at 3 kHz is characterized by a rigid rotation of the support and it is referred as the first (first in the reported frequency range) mode of the support (Figure 3.7-a). The mode at 3.5 kHz is characterized by a tangential translation of the support summed to its bending vibration (Figure 3.7-b). It is referred as the second mode of the support. The two modes of the support at 5 kHz are characterized by the same deformed shapes (the first bending mode of the support), but with the bending vibration in the tangential (friction) direction (Figure 3.7-c) and in the radial direction (Figure 3.7-d) with respect to the disc. The one with displacement in the tangential direction, at the contact surface, is involved in the mode coupling. In fact, the friction force that couples the normal vibration of the disc with the tangential vibrations of the pad, acts along such direction. This mode is referred as the third mode of the support.

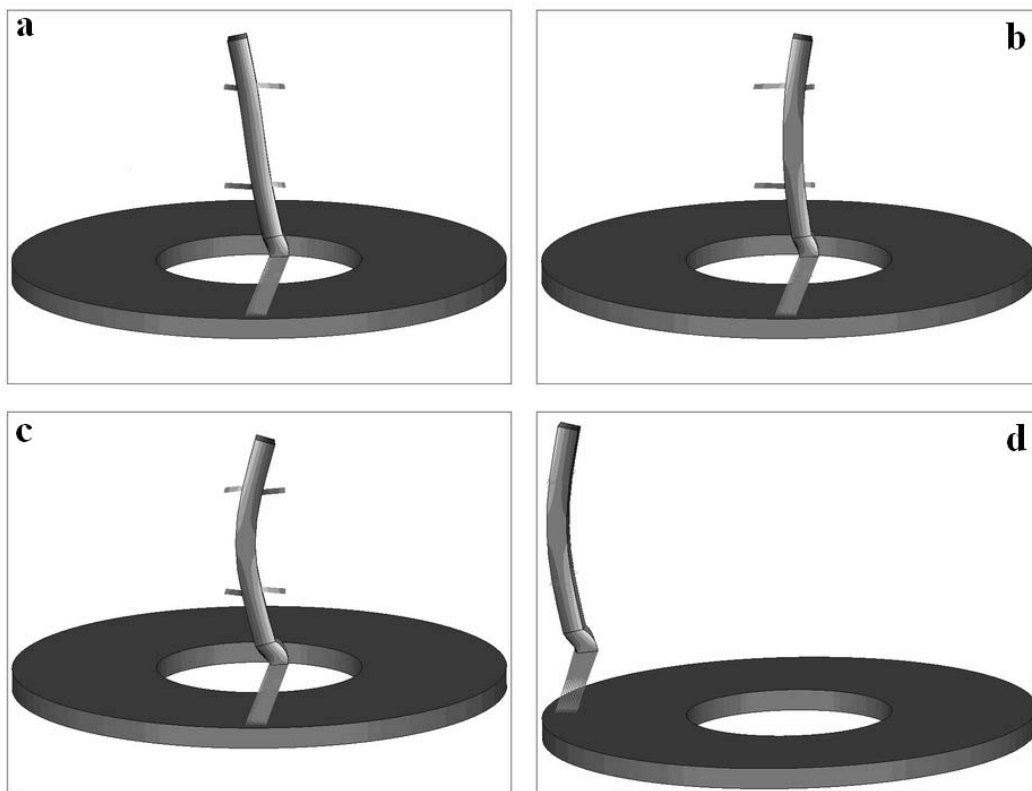


Figure 3.7 Support modes computed for a friction coefficient equal to 0.01 and Young modulus equal to 10^9 Pa: a) first mode of the support at 3 kHz; b) second mode of the support at 3.5 kHz; c) third mode of the support at 5 kHz; d) mode of the support with deformation in the radial direction.

The three pairs of modes in the eigenfrequencies plots (Figure 3.6), at 2.6, 3.9 and 5.75 kHz, respectively (for the starting value of the Young modulus $E=10^9$ Pa), are the three double modes of the disc (0,3), (0,4) and (0,5).

An increase of the Young modulus of the pad affects the natural frequency of the mode with the antinode at the contact point, because it introduces an increasing stiffness at the contact point. On the contrary it does not affect the modes with a node at the contact point. Moreover, an increase of the pad Young modulus does not affect the support mode whose stiffness is much larger than the stiffness of the pad. The natural frequency of the mode (0,3+) increases up to the natural frequency of the support at 3 kHz and then to the one at 3.5 kHz. Likewise, the natural frequency of the mode (0,4+) increases up to the frequency of the third support mode at 5 kHz.

Figure 3.8-a and Figure 3.8-b show the deformed shapes of the mode (0,3+) for a Young modulus equal to 10^9 and 10^{10} Pa (1000 and 10000 MPa), respectively. Figure 3.8-c and Figure 3.8-d show the deformed shapes of the mode (0,4+) for the same values of the Young modulus of the pad.

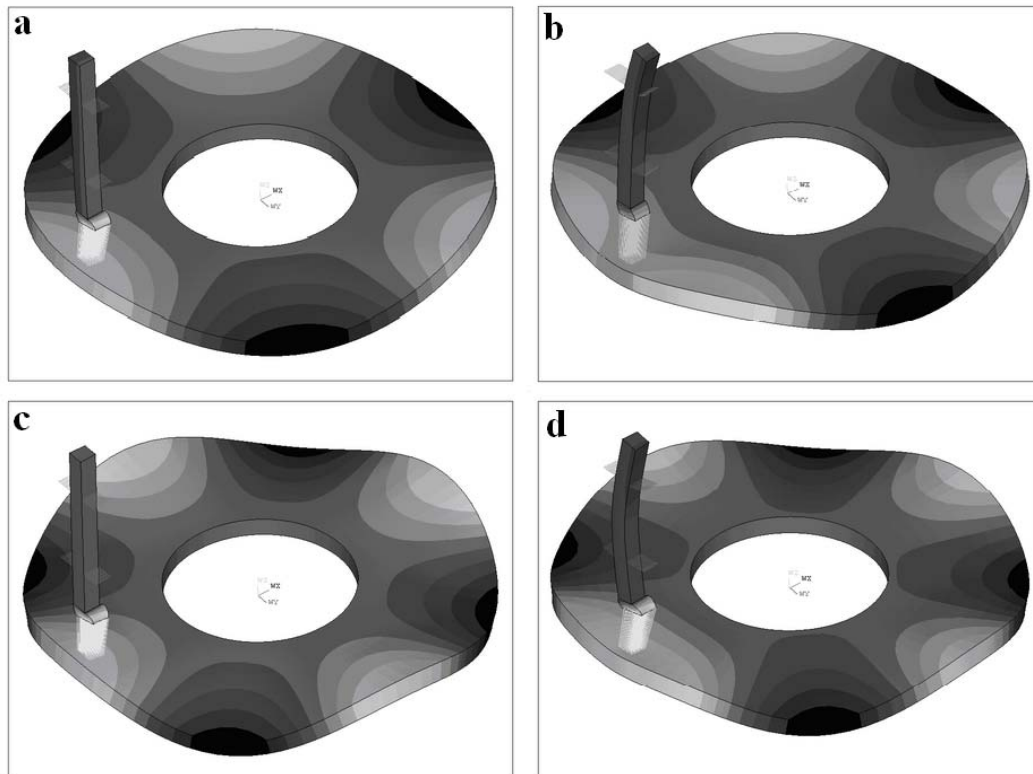


Figure 3.8 Behaviour of the disc modal shapes, computed with a friction coefficient equal to 0.01: a) Mode (0,3+) with Young modulus 10^9 Pa; b) Mode (0,3+) with Young modulus 10^{10} Pa; c) Mode (0,4+) with Young modulus 10^9 Pa; d) Mode (0,4+) with Young Modulus 10^{10} Pa.

Starting from the symmetric deformed shapes of the free disc, with three and four nodal diameters respectively, the angle between the two nodal radiuses that include the contact area becomes larger when the coupling with the beam increases, due to the increase of the contact stiffness. Therefore, the

increase of the contact pressure leads to a large increase of the natural frequencies related to the (n,m+) disc modes and to the non symmetric deformed shapes. A similar behaviour is observed by an experimental test on a simplified brake system, when changing the brake pressure [MASS 05b].

3.3.2 Stability analysis

Figure 3.9 and Figure 3.10 show the complex eigenvalues of the system in function of the Young modulus of the pad material, for a friction coefficient equal to 0.2 and 0.5 respectively. The grey dots represent eigenvalues with negative real part (stable behaviour). The black dots represent eigenvalues with positive real part (unstable behaviour). The analysis is performed in the frequency range between 2500 and 6000 Hz. In fact, in the whole frequency range of interest (i.e. between 1000 and 20000 Hz), only three unstable conditions are found at 3, 3.5 and 5 kHz respectively.

The solution is affected by numerical instabilities that depend on small parameter variations. Nevertheless, the complex eigenvalue analysis is robust enough to distinguish between such numerical instabilities and the mode-lock-in instabilities that occur only when two eigenfrequencies of the system coalesce. When two modes of the system coalesce (mode lock-in), they begin to keep equal frequencies for a variation of the parameter, while the real part of the eigenvalues moves opposite with respect to the starting value. One of the two modes becomes unstable with a positive real part. A further variation of the parameter leads to the lock-out between the two eigenvalues, the real parts return to the initial values and the imaginary parts split again (see **Figure 3.12**).

With a friction coefficient equal to 0.01 (**Figure 3.6**), there is not coalescing between the modes of the system. The regions with positive real eigenvalues are not found. In effect, a low friction coefficient is not able to couple sufficiently the normal and tangential stresses at the contact area so that it does not generate instability.

By increasing the friction coefficient to 0.2 (Figure 3.9), unstable regions appear between $10^{10.42}$ Pa (26300 MPa) and $10^{10.6}$ Pa (39800 MPa) at 5 kHz and between $10^{10.5}$ Pa (31600 MPa) and $10^{10.8}$ Pa (63100 MPa) at 3.5 kHz, respectively. For the Young modulus equal to $10^{9.62}$ Pa (4200 MPa) the mode (0,3+) crosses the first mode of the support at 3 kHz. However, due to the steep rise of the frequency of the (0,3+) mode, the range of values of the Young modulus bringing to instability is extremely small. When the friction coefficient is equal to 0.1, the instability at 3 kHz does not appear, and the ranges of the Young modulus that cause instability at 3.5 kHz and 5 kHz, are smaller, i.e. from $10^{10.46}$ Pa to $10^{10.54}$ Pa and from $10^{10.56}$ Pa to $10^{10.64}$ Pa, respectively (the eigenvalues plots for all the values of the friction coefficient are reported in Appendix A).

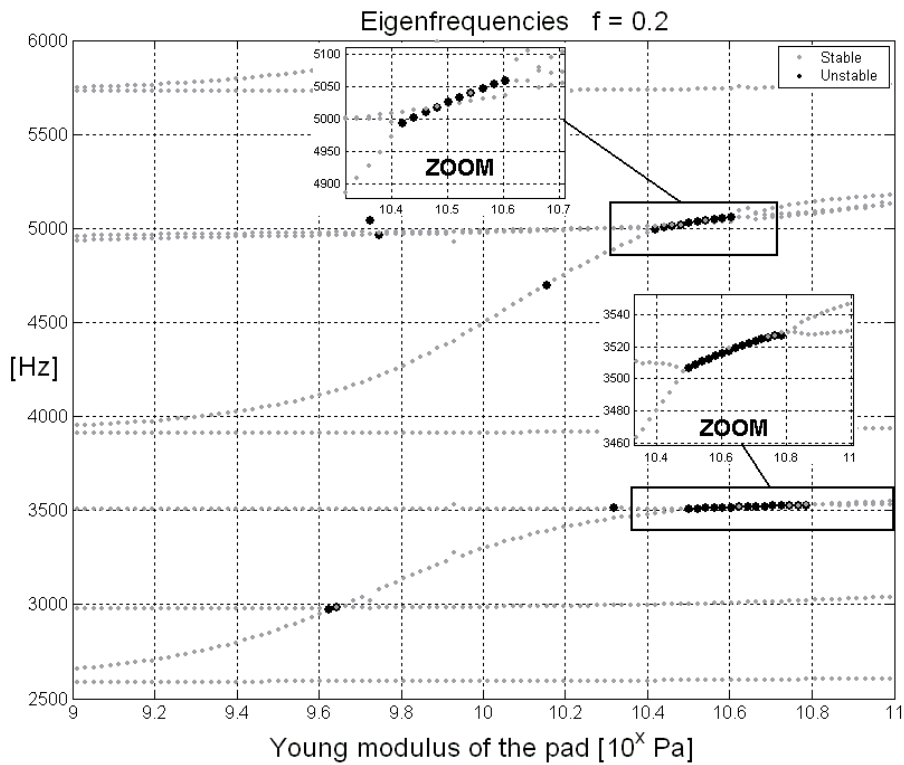


Figure 3.9 Eigenvalues analysis in function of the Young modulus of the pad (from 1 to 100 GPa) for a friction coefficient equal to 0.2.

By increasing the friction coefficient to 0.3, the unstable regions at 3.5 kHz and 5 kHz increase broadly and their upper limit falls over the range of interest of the pad Young modulus. For the friction coefficient ranging between 0.3 and 0.5 and between 0.5 and 0.7, only a small variation of the unstable area can be observed. In fact, by increasing the friction coefficient, the bound of the instability regions reach zones where the frequencies of the coalescing modes are too far away each other. In fact, a necessary condition to have mode lock-in is the proximity between two natural frequencies of the system. For the same reason the width of the unstable region at 3 kHz is always small, even for high values of the friction coefficient. In this region the rise of the (0,3+) mode is too steep, and the two modes frequencies are close enough to coalesce only in a narrow range of the Young modulus.

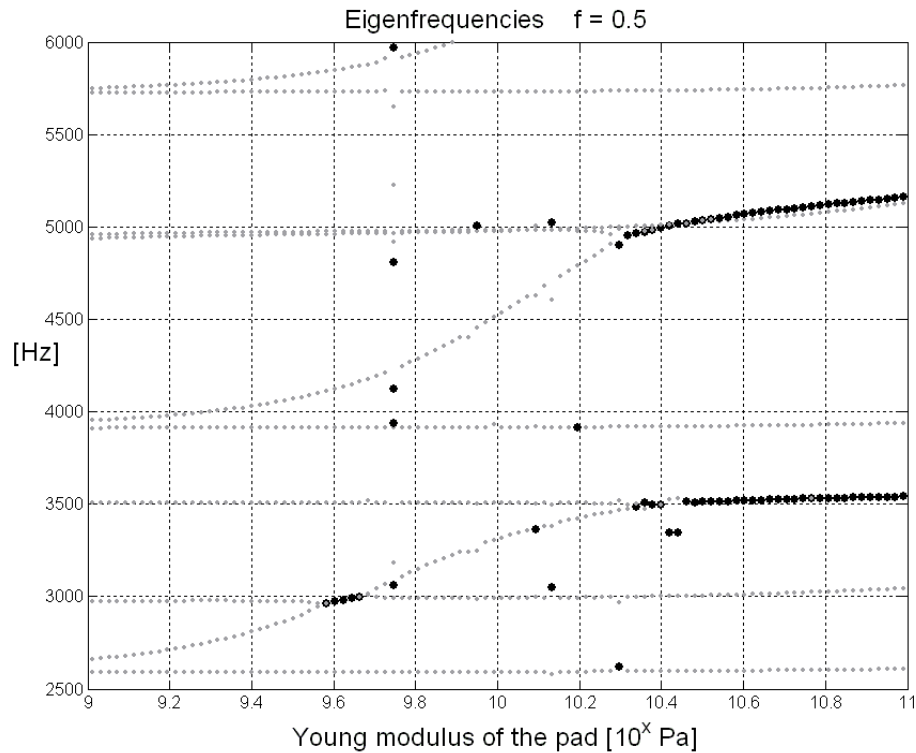


Figure 3.10 Eigenvalues analysis in function of the Young modulus of the pad (from 1 to 100 GPa) for a friction coefficient equal to 0.5.

Figure 3.11-a shows the unstable mode at 3 kHz, characterized by the (0,3+) deformed shape of the disc and the first mode of the support. Figure 3.11-b shows the unstable mode at 3.5 kHz, characterized by the (0,3+) mode of the disc, when it has completely lost its axial symmetry, and the second mode of the support. Figure 3.11-c, shows the unstable mode at 5 kHz, obtained by the coupling of the (0,4+) mode of the disc and the third mode of the support.



Figure 3.11 Unstable modes computed for a friction coefficient equal to 0.5: a) Unstable mode at 3 kHz ($10^{9.6}$ Pa); b) unstable mode at 3.5 kHz ($10^{10.6}$ Pa); c) unstable mode at 5 kHz ($10^{10.6}$ Pa).

3.3.3 Propensity to instability

In the complex eigenvalues approach, the friction forces are modeled by an asymmetric stiffness matrix. This method is still linear and cannot account for nonlinearities due to the disc rotation, instant contact stiffness, local detachment and local stick phenomena, materials nonlinearity, etc. Recent studies try to account for effects like disc rotation and non-uniform contact pressure distribution [ABU 05a 05b]. Usually this approach is a good indicator for potential squeal frequencies, but it gives a poor idea on the propensity of each squeal instability.

This suggests the need for an index of squeal propensity of the predicted unstable frequencies. Squeal indexes derived from the complex eigenvalue analysis relate usually the squeal propensity to the value of the real positive part of the eigenvalue. It is also possible to characterize the squeal robustness with respect to variations of the parameters, through the width of the range of the parameters that lead to unstable eigenvalues [GIAN 06c]. Nevertheless, these indexes do not take still into account the nonlinearities.

Moreover, the amplitude of the real part of the eigenvalue gives only the rate of growth of the vibration, while the effective strength of the squeal event is given by the amplitude of the final limit-cycle, when the nonlinearities are not negligible.

This section reports and comments locus plots of the unstable eigenvalues obtained by the linear model. The results are then compared with the instabilities obtained by the nonlinear model. For a friction coefficient equal to 0.01, no unstable behaviour is found. For a low value of the friction coefficient (i.e. $f=0.1$) the unstable range of the parameter is small. When increasing the friction coefficient up to 0.2 (Figure 3.9), the unstable range increases and, for a friction coefficient equal to 0.3, the unstable regions at 3.5 kHz and 5 kHz become larger and reach the upper limit for the considered Young modulus (i.e. 10^{11} Pa).

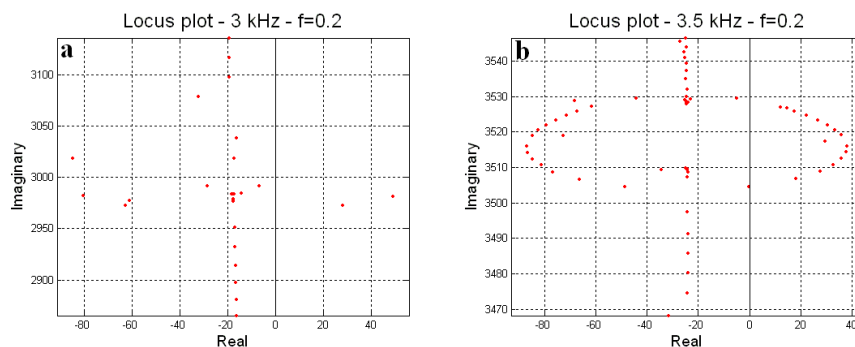


Figure 3.12 Locus plots for a friction coefficient equal to 0.2, for instabilities at a) 3 kHz and b) 3.5 kHz.

Figure 3.12 shows the locus plots for the unstable regions of the eigenvalues at 3 kHz (Figure 3.12-a) and 3.5 kHz (Figure 3.12-b), for the friction coefficient equal to 0.2 and for the Young modulus varying from $10^{9.58}$ Pa (3800 MPa) to $10^{9.7}$ Pa (5000 MPa) and from $10^{10.4}$ Pa (25100 MPa) to $10^{10.82}$ Pa (66100 MPa), respectively. Figure 3.13 shows the locus plots for the unstable regions at 3 kHz and 3.5 kHz for the friction coefficient equal to 0.3. The locus plots of the unstable regions for all the values of the friction coefficient are reported in Appendix B.

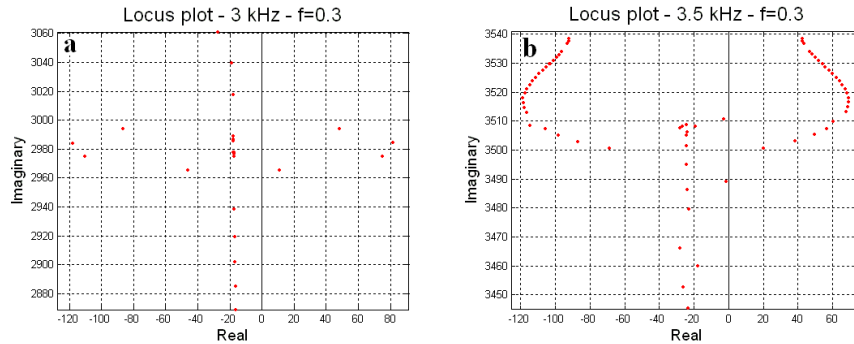


Figure 3.13 Locus plots for a friction coefficient equal to 0.3, for instabilities at a) 3 kHz and b) 3.5 kHz.

The locus plots show that an increase of the friction coefficient causes an increase of the absolute values of the real part of the eigenvalues. This happens because the friction contact forces, being proportional to the normal contact forces, cause the coupling between normal and tangential vibrations at the contact surface. Thus, the friction coefficient is the main parameter that sets the degree of coupling.

For the instability at 5 kHz, and friction coefficient equal to 0.2 (Figure 3.14), the real part of the eigenvalues first increases, when increasing the Young modulus up to a maximum value; afterwards, it decreases and increases again at a further variation of the Young modulus. Figure 3.14-a shows the unstable range of the eigenvalues for a friction coefficient equal to 0.2. Figure 3.14-b shows the locus plot for the same parameter range.

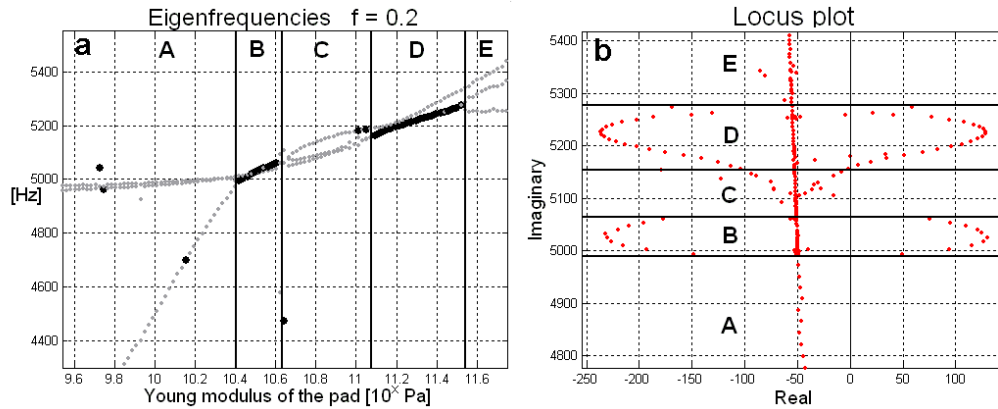


Figure 3.14 Behaviour of the real part of the eigenvalues in function of the difference between the natural frequencies, computed for a friction coefficient equal to 0.2 and Young modulus ranging from $10^{9.5}$ Pa to $10^{11.6}$ Pa: a) eigenfrequencies; b) locus plot.

This range can be divided into five zones:

- in zone A, the (0,4+) mode frequency increases and the modes are stable;
- in zone B, the (0,4+) mode reaches the third mode of the support and coalesces (lock-in) with it. The real part increases and then decreases;
- in zone C, the (0,4+) mode frequency continues to increase and the lock-out between the two modes is observed. In this zone the eigenvalues are stable. At the end of zone C, the (0,4+) mode frequency starts to stabilize for increasing values of the Young modulus, while the frequency of the third mode of the support starts to increase;
- in zone D, there is a second intersection between the two modes, bringing to a second lock-in and lock-out. The real part of the eigenvalues starts again to grow up and, after a maximum value, to decrease again;
- in zone E, after the mode lock-out, the two eigenfrequencies move away and the real part of the eigenvalues returns to the original value characterized by the structural damping.

When increasing the friction coefficient up to 0.3 the zone C disappears (Figure 3.15). The real part of the eigenvalues decreases and then increases again, but it does not become negative. This means that larger degrees of coupling between normal and friction forces, due to larger friction coefficients, induce coalescing of modes that are originally not too close in frequency.

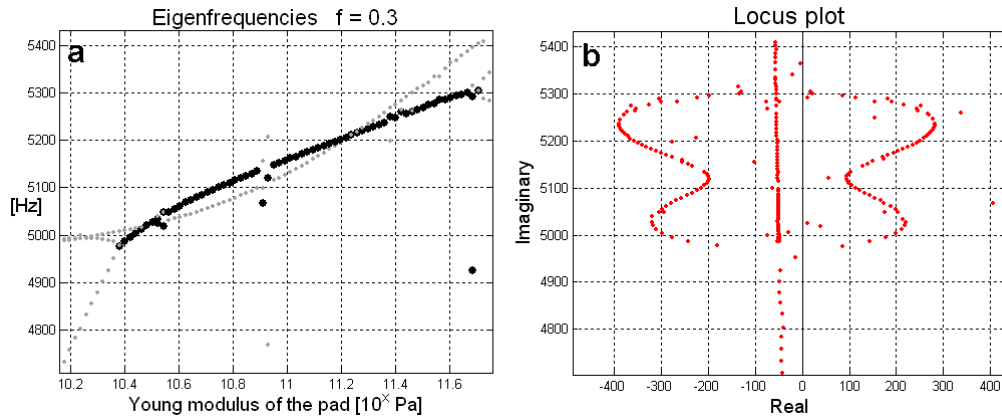


Figure 3.15 Behaviour of the real part of the eigenvalues in function of the difference between the natural frequencies, calculated for friction coefficient equal to 0.3 and Young modulus ranging from $10^{10.1}$ Pa to $10^{11.7}$ Pa: a) eigenfrequencies; b) locus plot.

In conclusion, the amplitude of the positive real part of the eigenvalues and the width of the coalescing (squeal) range are related to the proximity of the two coalescing modes and to the value of the friction coefficient, that couples the vibration of the support in the tangential direction and the vibration of the disc in the normal direction. Such results agree with the experimental evidences [MASS 06a].

3.4 Time analysis with the nonlinear contact model: braking simulation

3.4.1 Stability analysis

The values of the parameters characterizing the unstable regions of the system and identified by the modal approach can be introduced in the nonlinear model to study the nonlinear features of the squeal phenomenon in the time domain.

Nevertheless, aim of this section is to verify the agreement of the two models and the possibility of using the linear model approach to identify the proper parameters to introduce into the nonlinear model. Therefore, different values of the Young modulus of the pad and different values of the friction coefficient are used in the nonlinear model. These values are selected to cover both the stable and the unstable regions predicted by the complex eigenvalue analysis.

For each set of values the vibration of the system and the behaviour of the global forces (friction and normal loads) are analysed. The analysis of the system brings to distinguish the stable and unstable (squeal) conditions.

Figure 3.16-a shows the sum of the normal and tangential contact forces versus time for the Young modulus of the pad equal to $10^{10.2}$ Pa and coefficient of friction equal to 0.5. Figure 3.16-b shows the acceleration during the time simulation in the y-direction (relative velocity direction) of a node placed at the leading edge of the pad. The oscillations of the acceleration decrease in time after the contact between the pad and the disc occurs. Once the sum of the normal forces reaches the imposed maximum value (100 N), there are no remarkable oscillations. Within these values of the parameters, as predicted by the modal analysis, the system is stable.

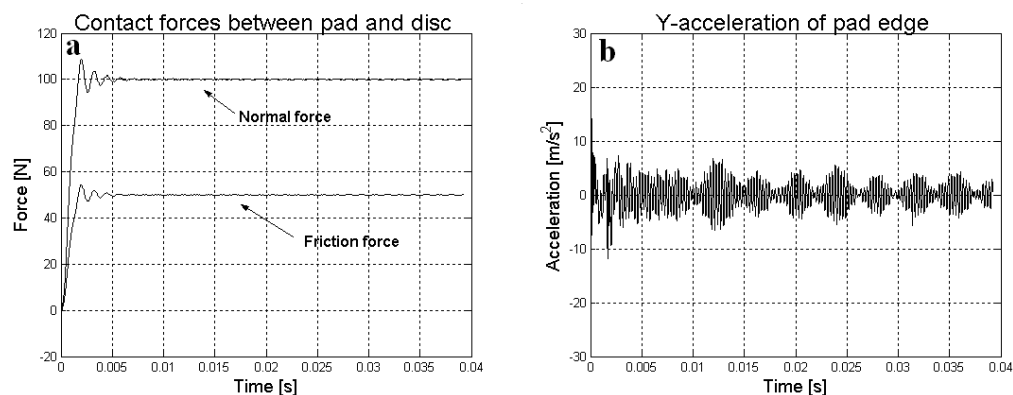


Figure 3.16 *Plast3 simulation for Young modulus of the pad equal to 16000 MPa and $f = 0.5$: a) sum of the contact forces; b) acceleration of the pad edge in the tangential direction. Stable behaviour.*

Figure 3.17-a and Figure 3.17-b show the same results described above for a Young modulus of the pad material equal to $10^{10.4}$ Pa (25100 MPa) and coefficient of friction equal to 0.5. With these values of the parameters an unstable state leading to the limit cycle, with strong vibration of the system, is determined. After the contact forces reach the stable value, a strong oscillation with exponential growth starts and develops until it reaches a maximum value.

Both the contact forces and the acceleration oscillations are harmonic. The exponential growth leading to a limit cycle agrees with the squeal behaviour observed during the experiments. The amplitude of oscillation of the tangential acceleration of the pad (Figure 3.17-b), calculated in the friction direction for a node belonging to the leading edge of the pad, has the same order of magnitude measured during the experiments on brake squeal [GIAN 04].

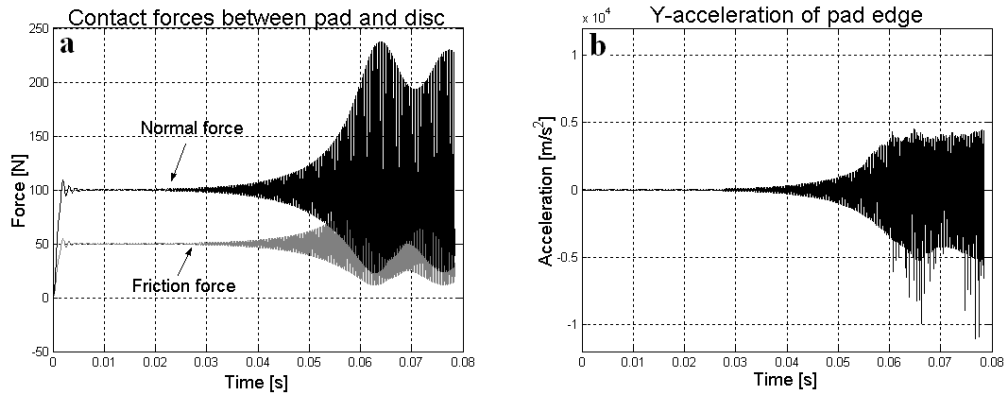


Figure 3.17 Plast3 simulation for Young modulus of the pad equal to 25100 MPa and $f = 0.5$: a) sum of contact forces; b) acceleration of the pad edge in the tangential direction. Unstable behaviour.

Figure 3.18-a shows the PSD (Power Spectral Density) of the acceleration. The vibration is characterized by one main frequency and its harmonics, as usual for squeal phenomena. The squeal frequency, 3430 Hz, corresponds to the eigenfrequency of the mode found to be unstable by the complex eigenvalue analysis. Moreover, the investigation of the system vibration shows that the system vibrates with the (0,3+) deformed shape of the disc. Figure 3.18-b shows the velocity of the system in the z-direction during the unstable condition. The vibrating deformed shape calculated with Plast3 coincides with the unstable mode calculated by Ansys (Figure 3.11-b).

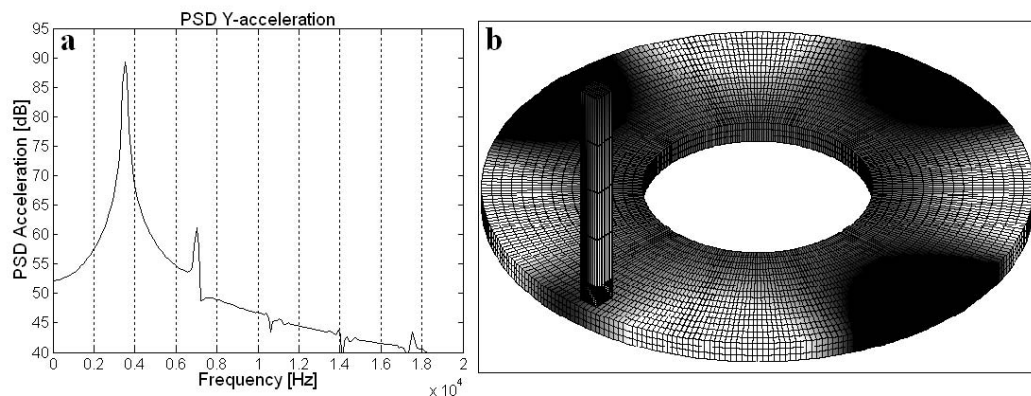


Figure 3.18 Plast3 simulation for Young modulus of the pad equal to 25100 MPa and $f = 0.5$: a) PSD of the pad acceleration; b) velocity distribution in the z-direction.

The same unstable condition is found for a Young modulus equal to $10^{10.6}$ Pa and friction coefficient equal to 0.5. For this value, the oscillation of the contact forces grows up until the pad starts to separate completely from the disc surface, and the contact forces reach zero (Figure 3.19-a). This behaviour can be explained by the large friction coefficient used for this simulation, the

low damping coefficients (proportional damping with $\alpha = 0.02$ and $\beta = 1e-7$), and by the neglected nonlinearities of the friction material. Likewise, during the eigenvalue analysis, the coupling of the modes becomes stronger and the real part of the eigenvalue increases. This brings to a larger amplitude of the system vibrations. Due to the detachments and the impacts with the disc, the PSD of the acceleration of the pad is not harmonic anymore (Figure 3.19-b).

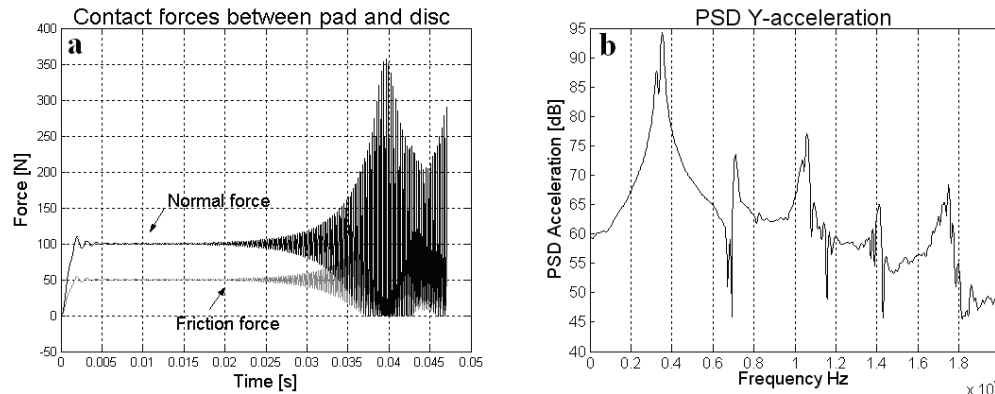


Figure 3.19 *Plast3 simulation for Young modulus of the pad equal to 39800 MPa and $f = 0.5$: a) sum of the contact forces; b) PSD of the pad acceleration.*

Table 3.2 resumes the unstable conditions found with Plast3 for different values of the Young modulus and friction coefficient.

		Young modulus						
		[MPa]	4300	4500	16000	25100	39800	70000
		[Pa]	$10^{9.63}$	$10^{9.65}$	$10^{10.2}$	$10^{10.4}$	$10^{10.6}$	$10^{10.85}$
Friction coefficient	0.01	STABLE	STABLE	STABLE	STABLE	STABLE	STABLE	STABLE
	0.1	STABLE	STABLE	STABLE	STABLE	STABLE	STABLE	STABLE
	0.2	STABLE	STABLE	STABLE	STABLE	STABLE	STABLE	STABLE
	0.3	STABLE	STABLE	STABLE	STABLE	UNSTABLE 3.5 kHz	UNSTABLE 3.5 kHz	UNSTABLE 3.5 kHz
	0.5	STABLE	STABLE	STABLE	UNSTABLE 3.5 kHz	UNSTABLE 3.5 kHz	UNSTABLE 3.5 kHz	UNSTABLE 3.5 kHz
	0.7	UNSTABLE 50 kHz	UNSTABLE 50 kHz	UNSTABLE 3.5 kHz				

Table 3.2 *Instabilities in braking simulations.*

The respective frequencies of the system vibrations are reported. As expected, the range of instability increases by increasing the friction coefficient, that couples the normal vibration of the disc with the tangential vibration of the

support. The unstable frequency (3.5 kHz) corresponds to the (0,3+) mode frequency when it reaches the bending mode frequency of the support, as showed by the eigenvalues analysis. As stated above, the amplitude of the system vibrations increases when the values of the parameters become closer (from 25100 to 39800 MPa) to the middle of the unstable range predicted by the eigenvalues analysis, i.e. when the real part of the unstable eigenvalue increases. Similarly, the amplitude of the system vibrations increases by increasing the friction coefficient.

The braking simulations show also an instability at 50 kHz for low values of the Young modulus of the pad (4300 and 4500 MPa) and high friction coefficient (0.7). This instability is not investigated here because it is not included in the frequency range of the squeal problem.

3.4.2 Local contact analysis

The braking simulations in the time domain are able to simulate the nonlinear behaviour at the contact, and allow to analyze the friction surface where no experimental data are available during braking events. In fact, the main lack in the experimental analysis dealing with mode lock-in is the need of some proof about the characterization of the “feed-back mechanism” that causes the self-excited vibrations of the system. Different theoretical approaches were proposed in the past: Mills [MILL 38] considered that a necessary condition for the onset of the unstable behaviour is the negative apparent damping due to the decreasing characteristic of the friction coefficient with respect to the sliding velocity. Other studies relating the squeal with the stick-slip phenomenon are based on the same relationship between relative velocity and friction coefficient. The unstable squeal cycle is considered by Spurr [SPUR 61], by using a constant friction coefficient and by relating the oscillations of the contact forces with the actual deformation of the model. As reported above, more recent works deal with the squeal instability as a modal instability.

The works by Spurr and North determine unstable conditions using a constant friction coefficient, and relate the self-excitation mechanism to the deformation of the model. In particular, the normal vibration of the disc mode at the contact point causes the oscillation of the normal force and, consequently, the oscillation of the friction force. This oscillation excites the tangential mode of the support that has the same frequency (lock-in frequency). Therefore a feed-back mechanism is needed to increase the energy of the vibrations.

The impossibility of an experimental analysis at the contact surface does not allow for a proof of this mechanism. Figure 3.20 and Figure 3.22 show the local contact forces calculated during braking simulation, in stable and unstable conditions, respectively. The dots represent the nodes of the pad at the contact surface with the disc. The arrows represent the local contact force

calculated at each node. The arrows bend toward the direction of the disc velocity because they are the sum of the normal and friction local forces.

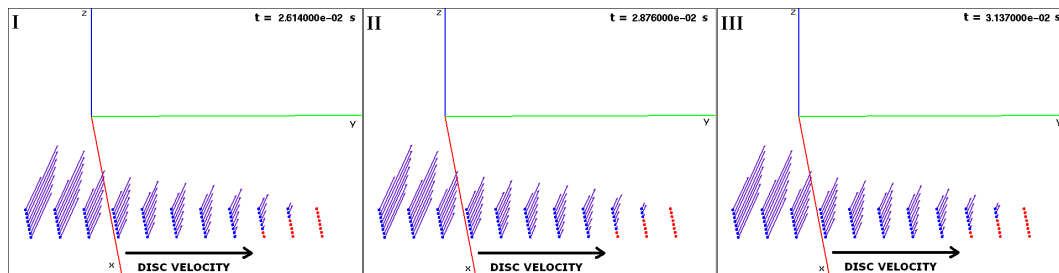


Figure 3.20 Local contact forces during braking simulation in stable condition, computed for three different time steps. Dots: nodes of the contact surface. Arrows: local contact forces computed at each contact node.

When a braking simulation is performed without squeal, the contact pressure remains approximately constant during the simulation (Figure 3.20 shows three different time steps). A non-homogeneous distribution of the contact force is due to the static bending deformation of the disc, because of the normal load, and to the tangential static deformation of the support and the pad, because of the friction load at the contact end. Therefore, a larger contact pressure is located at the leading edge, in correspondence of the inner contact radius. The effective predicted contact area coincides with the real contact area obtained during experimental brake tests on the experimental set-up in stable state (the worn out area in Figure 3.21).

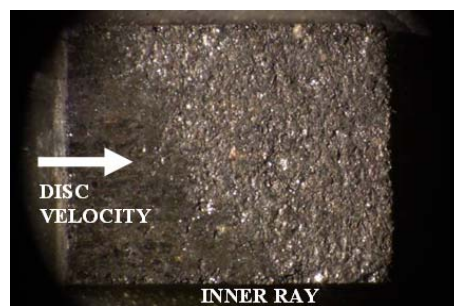


Figure 3.21 Contact surface of the friction pad after braking phase without squeal.

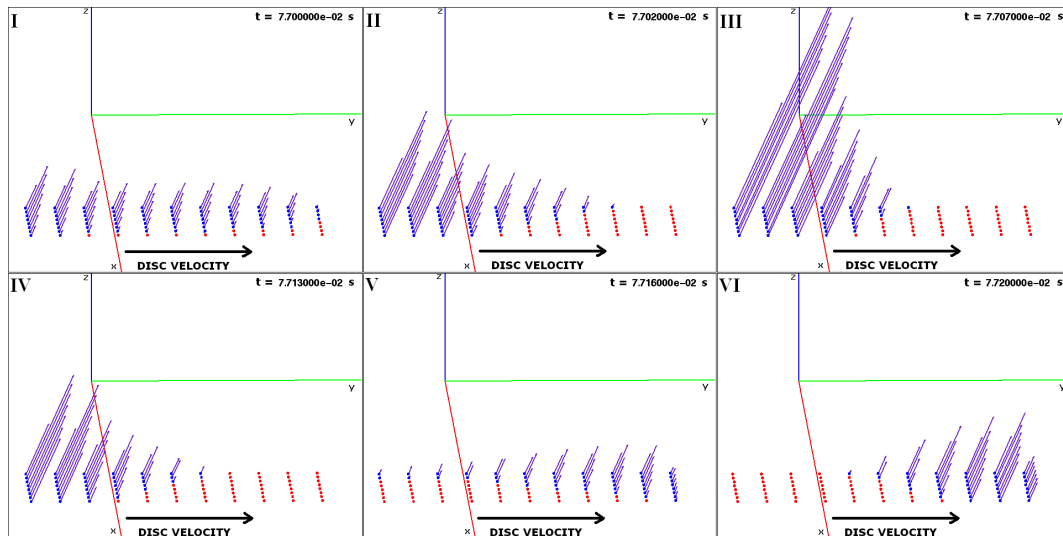


Figure 3.22 Local contact forces during braking simulation in the unstable condition at 3430 Hz calculated for six different time steps of the squeal limit cycle. Dots: nodes of the contact surface. Arrows: local contact forces. Detachment is detected where arrows miss.

Figure 3.22 shows six different time steps during a squeal unstable cycle at 3430 Hz. The oscillation of the local contact forces between the leading and trailing edges of the pad is due to the normal direction component of the bending deformation of the support, resulting in the local oscillation of both the normal and the tangential contact stresses.

Figure 3.23 shows the local normal stresses at five different time steps during the same unstable condition. The time steps are chosen to cover the period of vibration. The white area indicates the local detachment between pad and disc surface. The black area corresponds to the maximum of the contact pressure. The last graphic in Figure 3.23 shows the pressure distribution at the inner radius corresponding to the five time steps. As in the stable case, the highest peak of oscillation is located at the leading edge and the larger pressure is located at the inner radius.

This local oscillation of the normal stresses represents a reliable “feedback mechanism”, that is not related to the velocity dependence on the friction coefficient, while it is directly related to the deformed shapes of the unstable modes predicted by the eigenvalues extraction.

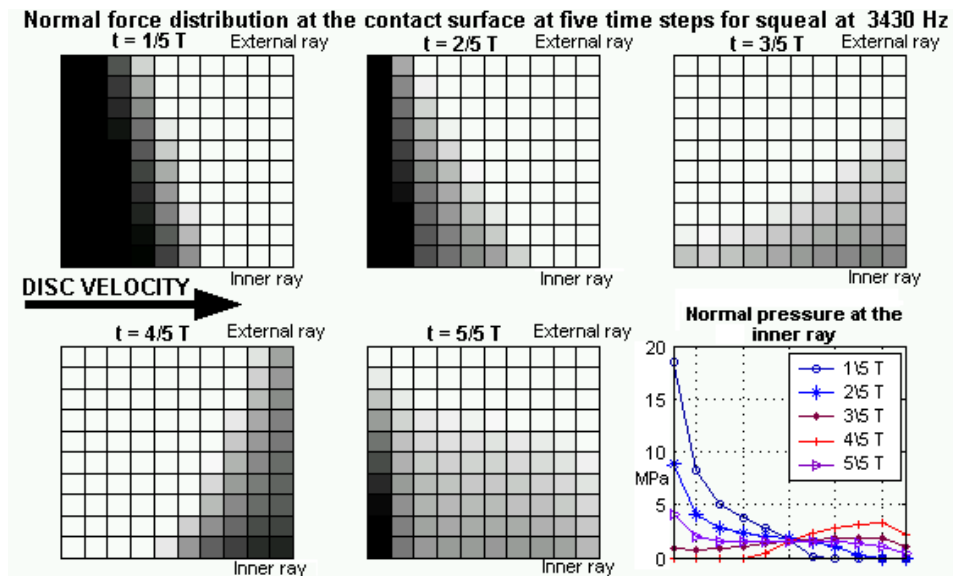


Figure 3.23 Local contact pressure distribution during instability at 3430 Hz calculated for five time steps of the squeal limit cycle ($T=1/3430$ s), and contact pressure at the inner ray.

3.5 Comparison of results

3.5.1 Prediction of the unstable regions of the parameters

The nonlinear time analysis shows two different behaviours of the system during brake simulations:

- a stable condition, characterized by no remarkable vibrations;
- an unstable condition, characterized by harmonic oscillations of the contact forces and the system vibrations.

The values of the parameters that lead to instability can be determined by the linear FEM at the onset of the “lock-in” mechanism, characterized by an eigenvalue with positive real part. The experimental analysis [MASS 06a] agrees with this approach that denotes the modal coupling between two modes as a necessary condition to have squeal.

A comparison between the unstable regions obtained by the eigenvalue extraction and by the nonlinear model underlines the validity of the two approaches and the limits of these numerical tools. In fact, both methods point out the instability at 3.5 kHz with similar values of the parameters. The same unstable deformed shape is calculated by the modal analysis (Figure 3.11-b) and by the time simulation (Figure 3.18-b). The eigenvalues extraction presents a maximum of the real part of the unstable eigenvalue in the central part of the unstable range, where the eigenfrequencies of the two coupling modes are the

closest. Likewise, the time simulation (braking simulation) shows an increase of the vibrations amplitude with values of the parameters that give a larger real part of the eigenvalue. Moreover, (as shown above) when the friction coefficient increases, both models predict an increasing amplitude (evaluated by the amplitude of the real part of the eigenvalue in the linear model and by the amplitude of the vibrations in the nonlinear model) and a wider unstable range of the instability at 3.5 kHz.

However, different amplitudes of the unstable ranges are predicted with the linear and the nonlinear models. Figure 3.24 resumes the predicted unstable regions calculated by the two models in function of the Young modulus of the pad and the friction coefficient.

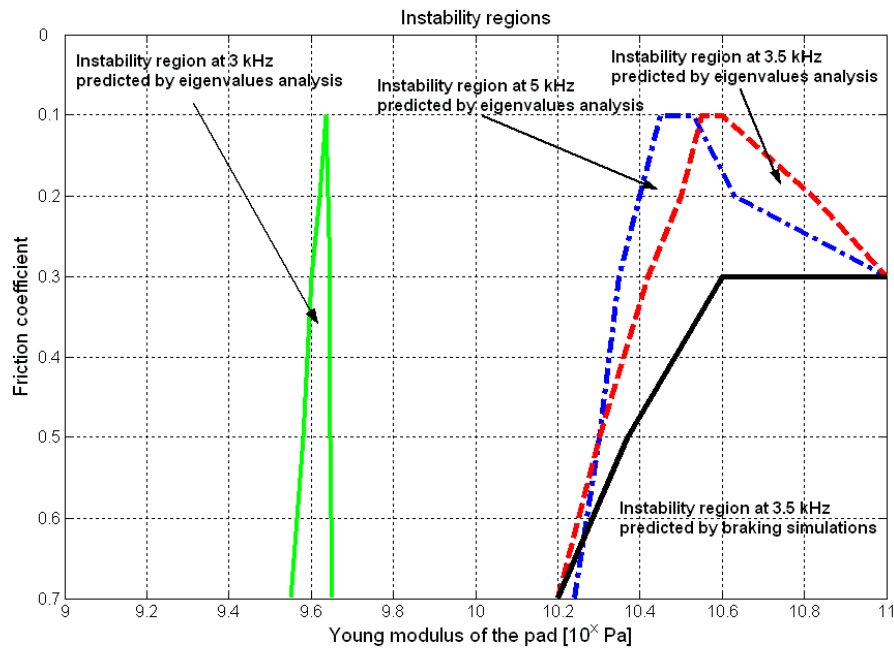


Figure 3.24 Unstable regions obtained with the linear and the nonlinear models. The area below the black line is the unstable region at 3.5 kHz predicted by the non linear model. Areas below the others curves are the instability regions at 3, 3.5 and 5 kHz predicted by the eigenvalues analysis.

The complex eigenvalue analysis predicts that the instability at 3.5 kHz rises in a region of values of the parameters wider than the one predicted by the time simulation.

Moreover, the instability predicted by the eigenvalues extraction at 3 kHz is not found by the nonlinear model, when using the same values of the system parameters. This can be ascribed to the low width of the unstable range predicted by the eigenvalues extraction and, especially, to the steepness of the variation of the $(0,3+)$ eigenfrequency with the increase of the Young modulus, that brings to an extremely tight range of the unstable parameters (**Figure 3.10**).

Also the instability at 5 kHz, predicted by the linear analysis for the same values of the parameters that lead to the instability at 3.5 kHz, is not recognized by the nonlinear analysis. In effect, the eigenvalues extraction predicts all the possible unstable modal couplings in the linear field, but does not include any nonlinear effect due to the contact.

While the absolute value of the eigenvalue can be considered as an index of the rate of growth of the instability, and the width of the unstable range as an index of the robustness of the instability for a single mode, these values can not be taken into account as a selection mechanism between two modes that become unstable for the same values of the driving parameters. In fact, the performed analysis shows that, even if the real part of the unstable eigenvalue at 5 kHz is larger than the real part of the unstable eigenvalue at 3.5 kHz, for every value of the parameters in the common unstable range, only the instability at 3.5 kHz rises during the braking simulations.

When comparing two instabilities for two different pairs of system modes, it is probably necessary to compare also the eigenvectors. In fact, the experimental analysis [MASS 06a] shows that the modes involved in the squeal phenomenon are those characterized by larger amplitudes of the deformed shape at the contact zone. However, this point needs further investigation to find a reliable squeal index that can be obtained from a linear analysis.

3.6 Conclusions

Two different methodologies are available in the literature for predicting brake squeal using the finite element method, i.e. the complex eigenvalue analysis and the dynamic transient analysis. Nevertheless, the two methods are always used separately rather than simultaneously.

The work presented in this chapter compares and combines the two different approaches for the analysis of squeal instability: the linear tool useful to predict the squeal onset in a wide range of driving parameters and the nonlinear model, able to reproduce the squeal phenomena in the time domain.

The same modal instability (3.5 kHz) is identified by the eigenvalues analysis and the time simulation, i.e. the same unstable frequencies and deformed shapes are identified. Nevertheless, an overprediction of the unstable regions calculated by the complex eigenvalue analysis is observed with respect to the nonlinear time simulations. Such overprediction is observed with respect to the experimental investigations as well (see Appendix E).

The results obtained by the nonlinear model agree with the squeal characteristics obtained during the experiments. In particular, the stabilization of the system vibrations at the limit cycle obtained by the experimental analysis [MASS 06a] is predicted here by introducing just contact nonlinearities in the numerical model.

Considering the same modal instability, there is a good agreement between the squeal index usually considered in the eigenvalues analysis and the results of the time simulation: a large friction coefficient means a large value of system vibrations and a high value of the real part of the unstable eigenvalue. In effect, the real part of the eigenvalue provides only the rate of growth of the vibration while the strength of the squeal event is given by the amplitude of the final limit cycle, obtained by introducing the contact nonlinearities. When comparing instabilities that involve different modes, the real part of the unstable eigenvalues is not a sufficient parameter to give a reliable index. A more accurate analysis of the unstable eigenvector, together with the eigenvalue, is necessary.

Squeal instability is detected with the standard Coulomb friction model, without any velocity-dependence of the friction coefficient and without the rise of stick-slip phenomena.

The analysis of the contact stresses (§ 3.4.2) highlights the “feed-back mechanism”, due to the system deformation at the contact surface that brings to self-excited vibrations.

The numerical analysis points out the same coupling conditions obtained by experimental works [MASS 06a], i.e. a large modal deformation at the contact point and the coalescence of two natural frequencies.

The obtained results confirm the need for both the numerical approaches; i.e. the use of both a linear (complex eigenvalue analysis) and a nonlinear (dynamic transient analysis) analysis for the study of brake squeal.

Chapter 4. Dynamic analysis

Chapter 4.	Dynamic analysis.....	113
4.1	Introduction.....	115
4.2	Experimental set-up.....	116
4.2.1	<i>Geometry of the TriboBrake</i>	116
4.2.2	<i>Dynamics of the set-up</i>	117
	Disc dynamics.....	117
	Support dynamics.....	119
	Pad dynamics.....	120
4.2.3	<i>Natural frequencies modulation for “modal tuning”</i>	122
4.3	Squeal phenomena.....	125
4.3.1	<i>Pad-disc squeal coupling</i>	126
4.3.2	<i>Support-disc squeal coupling</i>	128
4.4	Effects of modal damping on squeal instability.....	130
4.4.1	<i>Squeal suppression with damping</i>	131
4.4.2	<i>Increase of squeal propensity with modal damping</i>	132
4.4.3	<i>Phase of the squeal vibrations</i>	137
4.5	Conclusions.....	140

4.1 Introduction

This chapter presents an experimental analysis carried out on a simplified brake system and focused on correlating squeal characteristics with the dynamic behaviour of the system [MASS 06c]. Nowadays, the mode “lock-in” [NORT 72 76] [AKAY 00] between two modes of the system is one of the most accepted theories for the squeal mechanism. This section is aimed at verifying this approach to predict efficiently the squeal occurrence in a brake.

The experimental analysis is performed on the simplified set-up, named TriboBrake COLRIS, that has three main advantages with respect to commercial brake systems:

- 1) it can generate squeal noise easily;
- 2) it has a dynamics that can be easily measured;
- 3) it has a dynamics that can be easily adjusted.

The third point is particularly important to correlate the dynamics of the system to the squeal in a what-if analysis.

The modal behaviour of the set-up is first presented. The dynamics of the system is studied by considering the three main sub-structures of the brake (the caliper, the rotor, and the pad). Different approaches, studied to shift the natural frequencies of the system, are used to find different instability conditions, and the squeal conditions are related to a specific dynamic configuration of the system with specific values of the parameters, so that they are easily reproducible.

A clear distinction is made between squeal events involving the dynamics of the pad and squeal events involving the dynamics of the caliper.

The experimental analysis shows that the squeal occurrence in the experiments is always correlated to a modal coupling between one of the modes of the rotor and a mode of either the pad or the caliper. Therefore, to find an instability condition it is necessary to shift a specific mode of a substructure so that it falls close to a specific mode of another subsystem. The coincidence between two modes, is referred as “modal tuning”.

A further analysis on the effect of the modal damping on the squeal propensity is performed. Two opposite roles of the modal damping are described: a large modal damping can either prevent the rise of squeal instabilities or enlarge the squeal propensity of the brake apparatus. The robustness of the obtained squeal events permits a further analysis on the triggering mechanism of the squeal instability during braking.

4.2 Experimental set-up

4.2.1 Geometry of the TriboBrake

Since a real brake apparatus is characterized by geometry and dynamics that can be hardly controlled and understood, an experimental and theoretical study of a simplified experimental set-up is preferred. The set-up consists in a rotating disc (the disc brake rotor) and a small friction pad pushed against the disc by weights positioned on a rigid floating support (Figure 4.1).

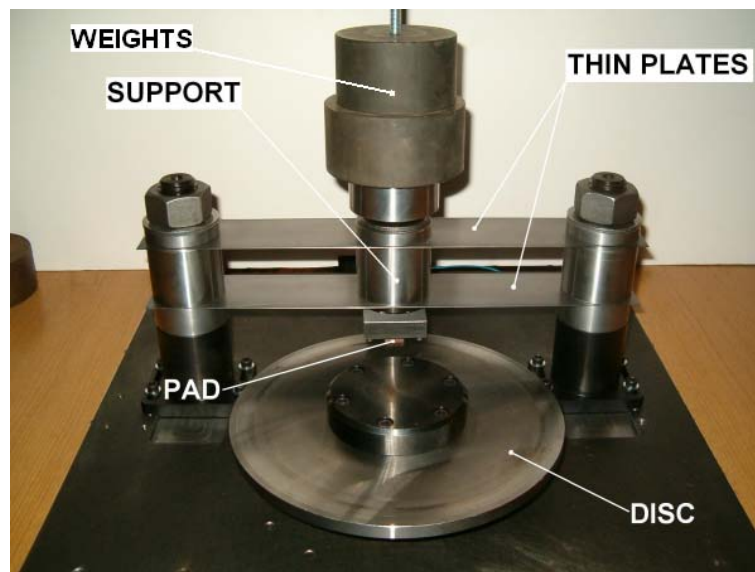


Figure 4.1 TriboBrake COLRIS, experimental rig.

The disc is made of steel (internal diameter 100 mm, external diameter 240 mm, thickness 10 mm) and is assembled with the shaft by two hubs of large thickness that assure a rigid behaviour of the connection in the frequency range of interest. The velocity of the motor can be adjusted to have a disc velocity between 5 and 100 rpm. The brake pad is made of a commercial brake friction material, obtained by machining standard brake pads. Reduced pad dimensions are adopted to simplify and control easily its dynamics. The support may host pads with different dimensions. When not differently specify the dimensions are $10 \times 10 \times 10 \text{ mm}^3$. The support (the central cylindrical body in the figure) is also made of steel and its shape is chosen to simplify its dynamics. The normal force between pad and disc (braking load) can be adjusted by adding weights on the top of the support, between 25 (the weight of the support) and 250 N. Two thin-plates hold the pad support in the tangential direction while allowing a negligible stiffness in the normal direction. Adjusting the normal load with weights (Figure 4.1) allows the pad surface to follow the disc oscillations, due to a possible not perfect planarity of the disc, and assures a constant value of the

contact normal force. A tri-axial force transducer is placed between the pad and the support. The transducer allows to measure the time history of the normal and tangential forces. It is important to note that these forces are not measured on the real contact surface, but above the brake pad. Thus, the pad dynamics influences the measured forces.

4.2.2 Dynamics of the set-up

The objective of this chapter is to show how the dynamics of a brake system influences squeal occurrence and squeal frequencies. Therefore, an investigation on the dynamics of the set-up is the first step of the work. Particular attention is focused on the bending modes of the disc (in the normal direction) and the bending modes of the support and the pad (in the tangential direction). It was shown in previous experiments [GIAN 06a] that these are the modes involved in squeal phenomena. Moreover, both an FEM analysis and experimental FRFs in the in-plane direction show that, in this simplified set-up, the in-plane modes of the disc are not involved in the squeal phenomenon, because they are out of the frequency ranges of the squeal occurring.

Three different substructures are considered in the analysis: the disc, the support and the pad. In the dynamics of the assembled system it is possible to recognize the combination of the dynamics of the disc and the support (because of the reduced contact surface between the two substructures and the consequent low coupling between them). Therefore, “disc modes” refer to the modes involving bending vibration of the disc, being the largest part of the energy concentrated in the disc. As well, “support modes” refer to the modes involving tangential vibration of the support. A further analysis allows to recognize the influence of the pad on the dynamics of the assembled system.

Disc dynamics

The EMA (Experimental Modal Analysis) is first performed on the disc to retrieve the bending dynamics of this substructure with and without contact with the pad. A SIMO (Single-Impulse-Multi-Output) analysis is performed by exciting the system with an instrumented hammer and acquiring the response of the disc with accelerometers in a grid made of 42 radius and 4 circumferences (168 points). The signals are acquired by the acquisition system PROSIG 5600 and elaborated with Matlab and ICATS software for modal analysis (Appendix C reports the acquisition parameters in detail). Figure 4.2 shows the FRF (Frequency Response Function) measured on the disc surface when the disc is in contact with the pad and a normal load of 200 N is applied. The double modes of the disc split in cosine modes (n,m+) and sine modes (n,m-). In Figure 4.2 the modes (0,3-) and (0,3+) are reported.

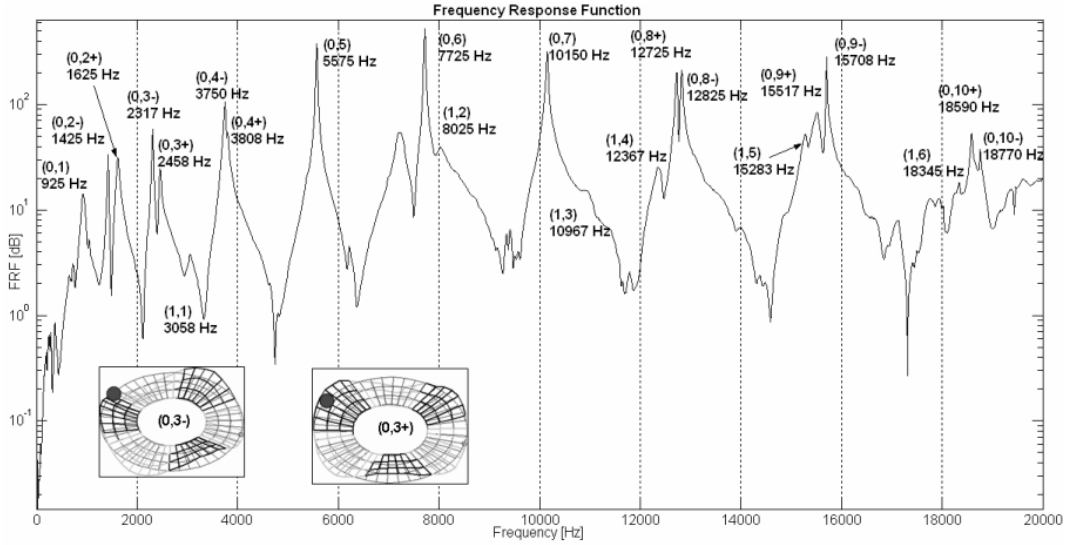


Figure 4.2 FRF of the set-up measured on the disc periphery when the pad is in contact the disc (coupled system) and samples of the disc deformed shapes (0,3) and (0,3+).

Figure 4.3 shows the modes of the disc that are involved in squeal instability (Appendix D reports all the measured modes). It is worth to note that all the disc modes involved in squeal are characterized by an antinode at the contact area with the pad.

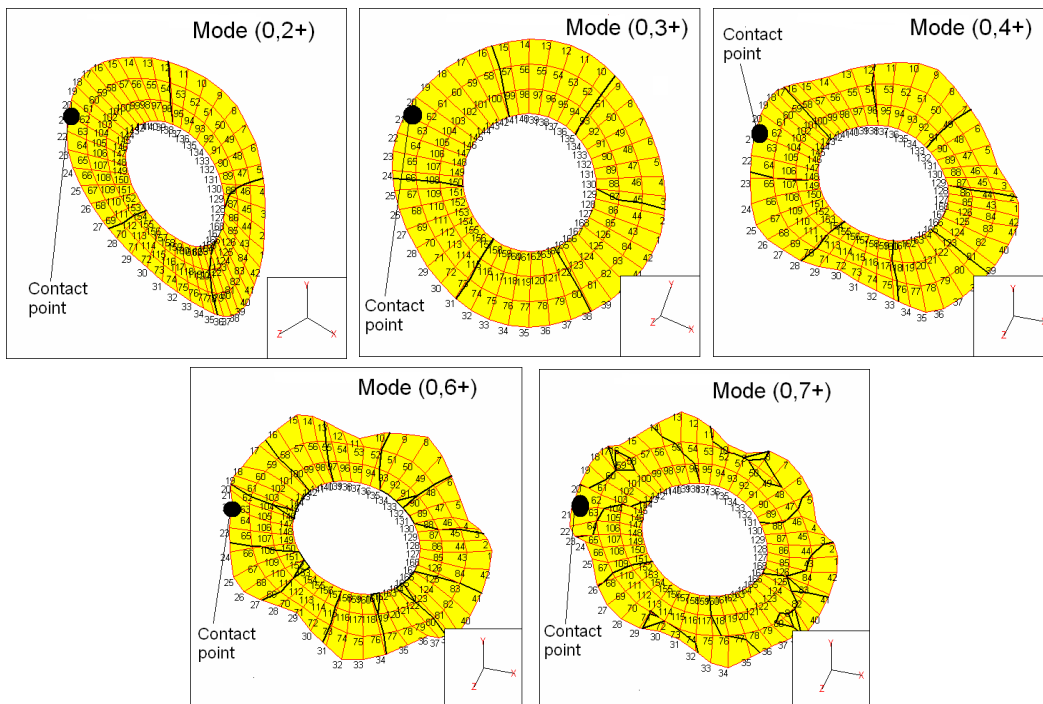


Figure 4.3 Bending modes that are involved in squeal coupling, calculated with ICATS software.

Support dynamics

Also the support modes are analyzed by a SIMO analysis, by exciting the support in the tangential direction, close to the contact area. In the frequency range of interest two rigid and three bending tangential modes of the support are recognized. Figure 4.4 shows the deformed shapes of the support in the tangential direction. The first and the second mode are rotational modes of the cylindrical body of the support, while the third, fourth and fifth mode are bending modes. It is worth to note that the second and the third mode are characterized by the largest deformation at the contact end (Figure 4.4).

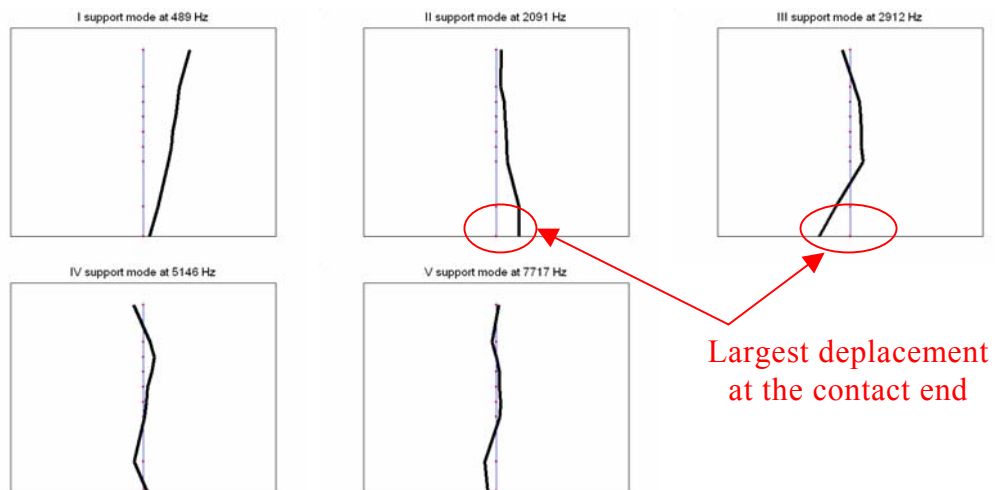


Figure 4.4 Tangential modes of the support in the frequency range of interest. The blue line is the undeformed grid of the cylindrical body of the support; the black line is the deformed shape.

This analysis is carried out with the coupled system, when the disc does not rotate. However, same peaks in frequency and same deformed shapes are found during brake simulations. The effect of the rotation of the disc is a reduction of the natural frequencies of about 500 Hz. Lower frequencies can be explained considering that the thin-plates holding the support have one end compressed during the braking phase. This introduces a lower stiffness in the support substructure that yields lower frequencies. A further effect of the disc rotation is the reduction of the modal damping of the tangential modes of the support. The modal dampings are calculated by the frequency domain decomposition of the tangential vibration of the support during the braking phase by the software Art&mis. Their values are 2,24% for the second mode and 0.96% for the third mode, respectively.

Table 4.1 lists the natural frequencies of the system obtained by the EMA, with a contact load equal to 25 N, and a friction pad with 10X10 mm contact surface is mounted.

MODE	FREQUENCY [Hz]	HYSTERTICAL DAMPING %	MODE	FREQUENCY [Hz]	HYSTERTICAL DAMPING %
I support	489	7,27	(0,5+)	5589	0,32
(0,1+)	925	5,36	(1,1)	7217	2,35
(0,2-)	1425	1,67	V support	7717	0,75
(0,2+)	1625	3,69	(0,6)	7725	0,26
II support	2091	0,72	(1,2)	8025	3,06
(0,3-)	2317	1,18	(0,7+)	10088	0,37
(0,3+)	2458	2,02	(0,7-)	10141	0,38
III support	2912	3,99	(1,4)	12367	1,07
(1,0)	3058	2,11	(0,8+)	12725	0,27
(0,4-)	3750	1,31	(0,8-)	12825	0,17
(0,4+)	3808	0,67	(1,5)	15283	0,58
IV support	5146	2,09	(0,9+)	15517	0,54
(0,5-)	5575	0,49	(0,9-)	15708	0,13

Table 4.1 System natural frequencies and modal damping of the set-up with normal load equal to 25 N.

Pad dynamics

The third substructure investigated is the friction pad. Its dynamics is easily recognized in the assembled dynamics. Figure 4.5 shows the PSD (Power Spectral Density) of the pad acceleration in the tangential direction during the braking phase (grey line). The first three peaks in frequency correspond to three support modes. The other two peaks at 4.5 and 11.5 kHz correspond to modes of the pad. A second test was made by dragging the pad, disassembled from the disc and the support, on a rigid surface. The black line in Figure 4.5 shows the PSD of the acceleration during this test. Only the two peaks related to the pad modes appear. An “output only” method based on the singular value decomposition is used to obtain information on the dynamic behaviour of the pad. When the disc rotates, it excites the pad vibration in a wide range of frequencies and the response is measured by an accelerometer or a laser vibrometer. The frequency domain decomposition obtained by the software Art&mis indicates a modal damping equal to 7% and 9%, for the first and the second mode of the pad, respectively.

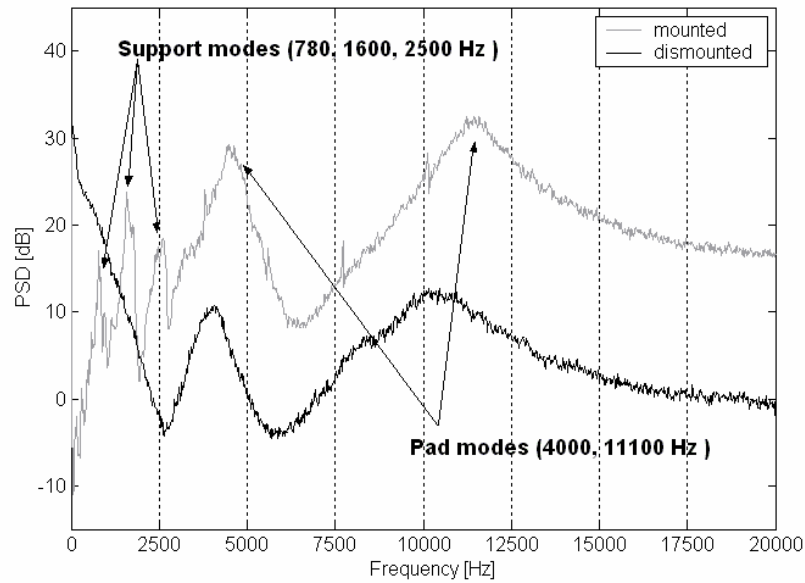


Figure 4.5 PSD of the pad acceleration during braking phase (grey), and in disassembled condition (black). Three peaks are due to the modes of the support and two peaks are due to the modes of the pad.

It is important to note the different dynamics of the friction pad with and without accelerometer. Figure 4.6 shows the PSD of the pad velocity along the friction direction when the accelerometer is attached to the pad and the PSD of the pad velocity when the accelerometer is not present. The velocity is measured by a laser vibrometer.

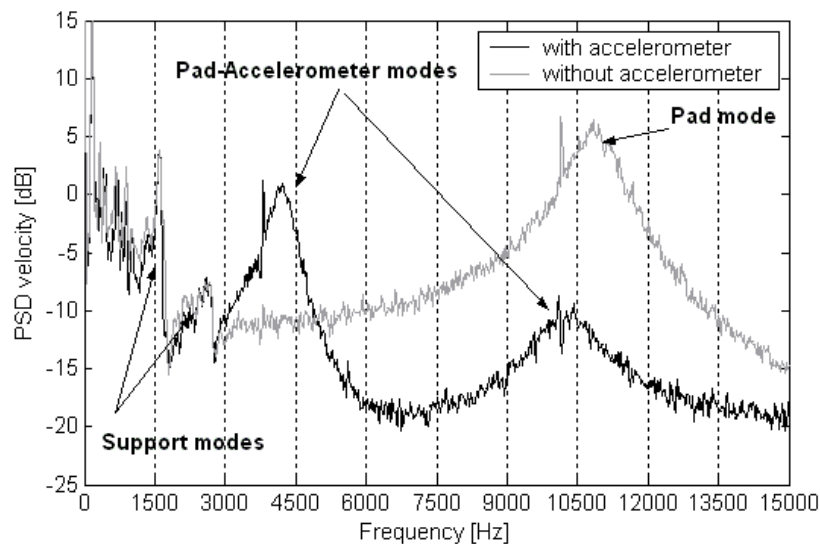


Figure 4.6 PSD of the pad velocity during braking phase: with the accelerometer attached at the leading side of the pad (black), and without accelerometer (grey).

An FE modal analysis allows to identify the pad modes characterized by the pad deformation in the tangential direction and large tangential oscillations at the contact surface, at the same frequencies obtained experimentally.

Without accelerometer the tangential dynamics of the pad is characterized by one tangential mode only in the studied range of frequencies (Figure 4.7-a); when introducing the lumped mass of the accelerometer two tangential modes of the assembly pad-accelerometer appear. The FE analysis allows to simulate such behaviour. When introducing the accelerometer, two tangential modes of the pad are recognized: one with the mass of the accelerometer rotating in phase with the pad (figure Figure 4.7-b) and the other one with the accelerometer rotating out of phase with respect to the pad (figure Figure 4.7-c).

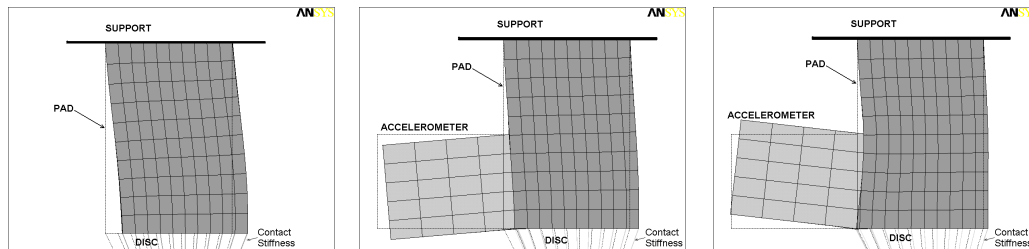


Figure 4.7 a) Pad mode at 11 kHz; b) Accelerometer-Pad mode at 4.5 kHz; Accelerometer-Pad mode at 10.5 kHz.

To have a large set of experimental data, it is useful to reproduce many different squeal events. The proposed experimental set-up achieves this goal: in fact, by controlling the driving parameters, different squeal conditions are allowed and reproduced easily.

4.2.3 Natural frequencies modulation for “modal tuning”

The proposed design allows to control the dynamics of the set-up by changing only few parameters. In order to tune the dynamics of the set-up to produce squeal, different driving parameters are chosen to shift the natural frequencies of the system: the load applied to the top of the support, the friction pad dimensions, the stiffness of the thin-plates, the insertion of damping material between the thin-plates and the support (Figure 4.1).

The variation of the normal load applied to the top of the support shifts the natural frequencies of the system. In particular, the double modes of the disc split at two different frequencies, and the split increases when the normal contact load increases. The dimension of the pad influences especially its natural frequencies. The stiffness of the thin plates affects the natural frequencies of the

support. The insertion of damping material between the thin plates and the support introduces modal damping and affects the natural frequencies of the pad.

Figure 4.8 shows the split values of the disc modes when a mass of 20 Kg is placed on the top of the support (225 N of normal load). The split $(\omega_{(n,m+)} - \omega_{(n,m-)})$ is defined positive when the (n,m+) mode is at higher frequency than the (n,m-) mode.

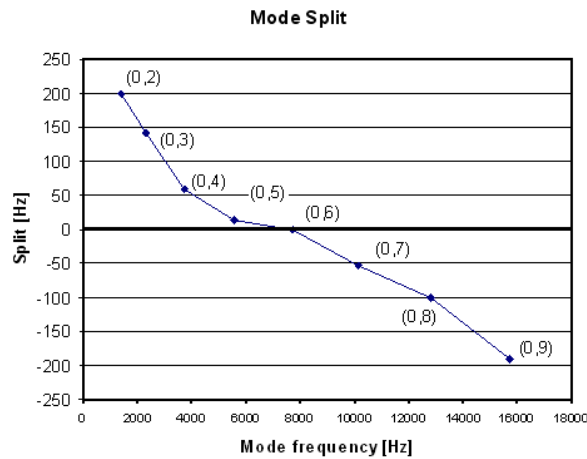


Figure 4.8 Split of the disc modes with 225 N of normal load.

The FRF of the disc presents a single peak when there is no contact with the pad; the separation of the double peaks increases by increasing the normal load. It is interesting to notice that the modal split is positive for the low frequency modes (Figure 4.9-a), almost zero for the mode with six nodal diameters, and negative for the high frequency modes (Figure 4.9-b). This behaviour is due to the mass and stiffness effects introduced by the contact with the pad. The (n,m-) mode has the contact area belonging to the nodal diameter so that it is not influenced too much by the contact, and its frequency remains almost constant. The (n,m+) mode has the contact area in the antinode of the disc. For the low frequency modes the add of stiffness due to the contact stiffness with the pad and support has more influence than the add of mass, and the natural frequency increases. The influence of the mass effect increases by increasing the frequency, and for high frequency modes the natural frequency decreases with the increase of the load.

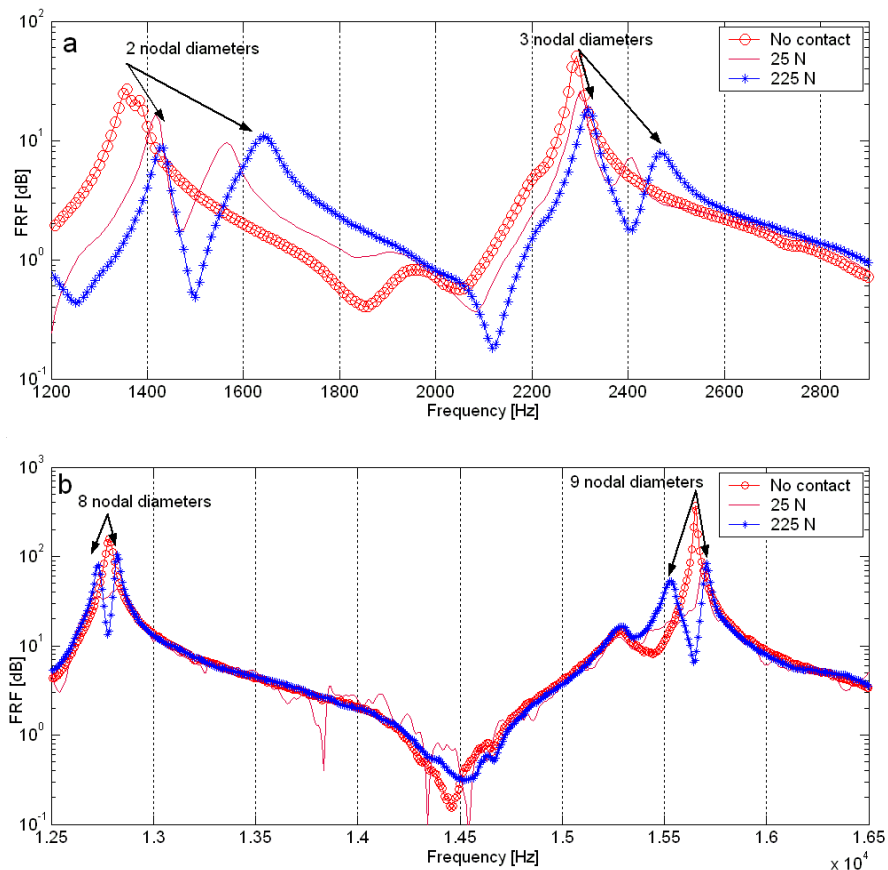


Figure 4.9 Split of double modes in function of the normal load for modes at low frequencies (a) and modes at high frequencies (b).

Adding weights to the top of the support changes the support natural frequencies as well. Moreover, because of the dependence of the properties of the friction material on the stress state of the material itself, and because of the increase of the contact stiffness with the load, the natural frequencies of the pad increase with the applied load. Table 4.2 shows the frequency ranges where the modes of the support and the pad fall, being the normal load varied from 25 N to 225 N. The contact surface of the pad is equal to 10x10 mm, and the thickness of the thin-plates is equal to 0.5 mm.

MODE	FREQUENCY RANGE [Hz]
II support mode	1500 - 2100
III support mode	2400 - 3150
I pad-accelerometer mode	3750 - 4500
II pad-accelerometer mode	10000 - 11800

Table 4.2 Support and pad frequency range for different load conditions.

Table 4.2 shows the second and third modes of the support, because only these two modes, that have a large vibration at the bottom end, where the

pad is in contact with the disc, are involved in the squeal phenomena. Since the dynamic instability is due to the coupling between one normal mode of the disc and one tangential mode of the support or pad, these modes are those characterized by highest coupling with the bending dynamics of the disc.

The thickness of the thin-plates does not affect the frequencies of the disc and pad modes, but affects the natural frequencies of the support (about 200 Hz when increasing the thickness from 0.5 to 1 mm).

By using different dimensions of the pad (8x8 mm², 10x10 mm², 10x15 mm², 10x20 mm²), the frequencies of the pad modes can be varied between 3700 and 5000 Hz for the first mode and between 10000 and 14000 for the second one.

The position of the accelerometer placed at the pad side affects the natural frequencies of the pad. The more the pad (lumped mass) is placed away from the connection with the support, the less is the value of the natural frequencies.

The introduction of rubber layers between the support and the thin plates, besides increasing the modal damping of the bending modes of the support, decreases the constraint stiffness of the pad in the tangential direction so that the natural frequency of the pad decreases of about 2 kHz.

4.3 Squeal phenomena

This section presents the results of an extensive experimental investigation aimed to find as many as possible squeal frequencies by changing the operational parameters of the set-up. During this investigation the dynamics of the system was monitored to relate its variation to the rising of instabilities. During the experiments the natural frequencies of the pad and the support are measured by looking at the PSD of the pad acceleration in the tangential direction. In fact, being the dynamics of the components already identified, the PSD allows to follow the real values of the natural frequencies of the pad and the support in the effective operating state, i.e. during the braking phase. On the contrary, the natural frequencies involving the bending vibrations of the disc are measured under brake application without disc rotation. However a preliminary test, carried out under brake application with disc rotation, assured a negligible effect of the rotation on these modes, that are the only rotor modes involved in the squeal in this set-up.

Five different squeal frequencies are found: 1566 Hz, 2467 Hz, 3767 Hz, 7850 Hz and 10150 Hz. These squeal conditions are obtained for defined values of the driving parameters, and all of them are easily reproducible.

Both the pad and the support present modes characterized by tangential vibrations along the contact surface. The experiments show that the disc

dynamics can couple either with the dynamics of the pad or with the dynamics of the support, bringing in both cases to squeal instabilities.

The experimental acquisitions are performed by lying the support over the rotating disc. The disc velocity is maintained at 10 rpm. In previous experiments it was shown that, over a limit value, the disc velocity affects only the amplitude of the system vibrations [MASS 03]. The global normal and tangential forces are acquired between the pad and support. The tangential acceleration at the leading side of the pad is measured. A microphone placed at 200 mm from the contact point measures the sound pressure level (Appendix C reports the acquisition details). The squeal events are recognized by the increase of vibrations of the system and by the harmonic sound emission that may overcome 100 dB.

4.3.1 Pad-disc squeal coupling

Each braking phase starts by lying the support over the disc (see Figure 4.17). The normal and friction forces show a starting ramp due to the initial contact between pad and disc (a slow non-physical decrease of the mean values of the forces is observed, and it is due to the discharging of the capacitive transducer). Then, the system vibrations and the sound pressure start to increase. The PSD of the pad acceleration and the sound pressure level reveal the harmonic nature of the system vibrations. After a small time (less than a second) the system vibration reaches its limit cycle.

Figure 4.10 presents a dynamic characterization of the pad when squeal occurs at 3767 Hz: the grey lines are the PSD of the pad acceleration in the tangential direction for different values of the normal load from 250 N to 45 N, while the dashed line is the measured FRF of the disc, obtained with normal load equal to 45 N. The amplitude of the peak related to the pad mode decreases with the decrease of normal load because the pad excitation in the tangential direction, due to the friction force, decreases proportionally to the normal load. By lowering the normal load, the first mode of the pad moves to lower frequencies and it gets close to the (0,4+) mode of the disc. This is caused by the lower contact stiffness between the pad and the disc.

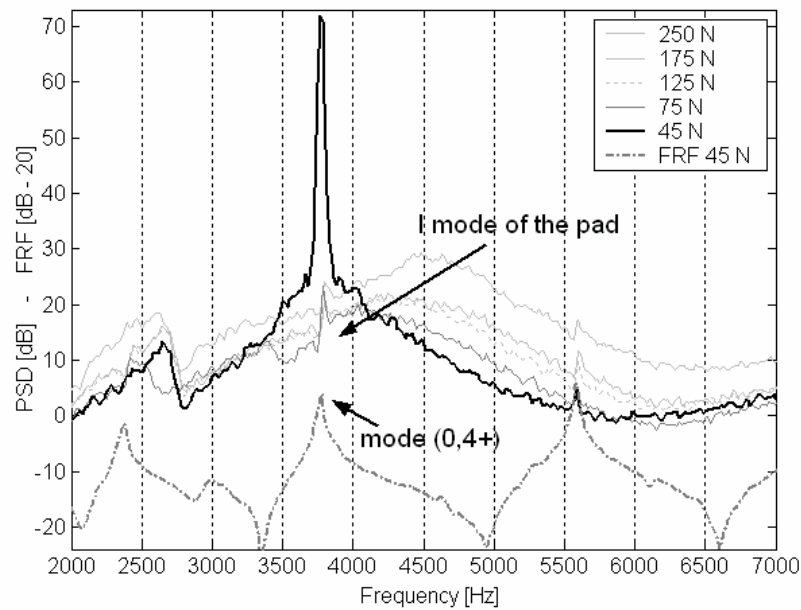


Figure 4.10 PSD of pad acceleration in function of the normal load, and FRF at the disc surface. By decreasing the load the natural frequency of the pad mode decreases up to the tuning with the natural frequency of the disc mode (squeal frequency).

It is important to notice that only when the natural frequency of the pad is close enough to one natural frequency of the disc, i.e. when the first natural frequency of the pad “tunes-in” with the natural frequency of the mode (0,4+), squeal happens (only the FRF for a 45 N normal load is plotted to make the graphic clear, but no coincidence between the natural frequencies is obtained for different values of the load).

In Figure 4.10 only the black line (PSD for 45 N of normal load) presents the frequency spectrum characteristic of the squeal phenomenon. Similar plots can be obtained by varying other parameters. This means that squeal instability can occur only when a coincidence of two system modes is obtained, as predicted by the complex modal analysis and by the lock-in theory. Other two squeal events due to the “tuning” between a natural frequency of the pad and a natural frequency of the disc are obtained at 7850 Hz when the frequency of the 2nd mode of the pad tunes with the frequency of the (0,6+) mode, and at 10150 Hz when the frequency of the 2nd mode of the pad tunes with the frequency of the (0,7+) mode. The former is obtained when the normal load is equal to 25 N, the dimensions of the pad is equal to 8x8 and the thickness of the thin-plates is equal to 0.5 mm; the second is obtained with a normal load equal to 45 N when introducing a thin layer of rubber between the support and the thin-plates. With this expedient the tangential stiffness of the pad mode

decreases and its natural frequency shifts to a lower frequency, becoming close to the (0,6+) mode.

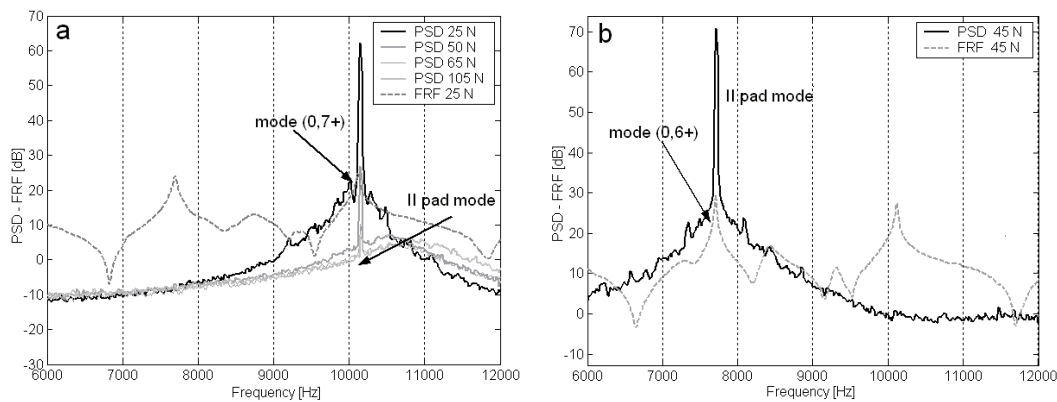


Figure 4.11 a) PSD of pad acceleration in the tangential direction for different load conditions and disc FRF (tuning at 10150 Hz); b) PSD of pad velocity in the tangential direction during squeal event at 7850 Hz and FRF disc.

4.3.2 Support-disc squeal coupling

Other squeal frequencies are obtained by the coupling of modes of the support characterized by tangential deformation and modes of the disc characterized by bending vibrations in the normal direction. Like in the previous cases, squeal arises only with the tuning between two natural frequencies. The modes of the support involved in squeal events are the second and the third mode. In fact, these modes are characterized by the largest vibration at the contact end, where coupling between the tangential vibrations of the pad surface and the normal vibrations of the disc occurs. Figure 4.12-a shows the PSD of the tangential acceleration of the pad when squeal at 1566 Hz occurs. The normal load is fixed at 200 N, the dimensions of the contact surface is $10 \times 10 \text{ mm}^2$. In these conditions the natural frequency of the second mode of the support tunes with the natural frequency of the (0,2+) mode of the disc, while there is no tuning between the third mode of the support and the (0,3+) mode of the disc. Therefore squeal occurs at the frequency of coincidence between the former modes (the dotted vertical line in the graphic).

Squeal at 2467 Hz (Figure 4.12-b) occurs when the normal load is equal to 250 N. Increasing the load from 200 to 250 N, the natural frequencies of the support increase and the third mode of the support tunes with the (0,3+) mode of the disc. Consequently, these two modes couple together and cause squeal, while the second mode of the support and the (0,2+) of the disc can no more couple together because they are not enough close in frequency.

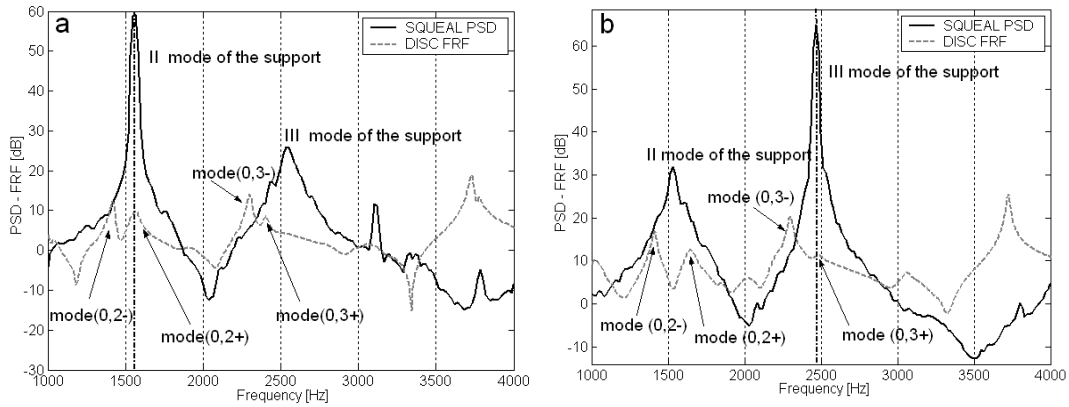


Figure 4.12 a) PSD of the pad acceleration during squeal at 1566 Hz and FRF of the disc (tuning between the second mode of the support and the (0,2+) disc mode); b) PSD of the pad acceleration during squeal at 2467 Hz and FRF of the disc (tuning between the third mode of the support and the (0,3+) disc mode).

Squeal events involving the support-disc coupling occur only when there is an exact tuning between the disc and the support natural frequencies. In fact, just by changing slightly the weighs configuration it is possible to obtain the results shown in Figure 4.13: the black line shows the PSD of the acceleration during squeal condition while the red line (circle marks) is the PSD when repositioning the normal load just a little off the support axis. The 3rd natural frequency of the support moves slightly (about 40 Hz) away from the (0,3+) mode of the disc, and squeal does not occur anymore.

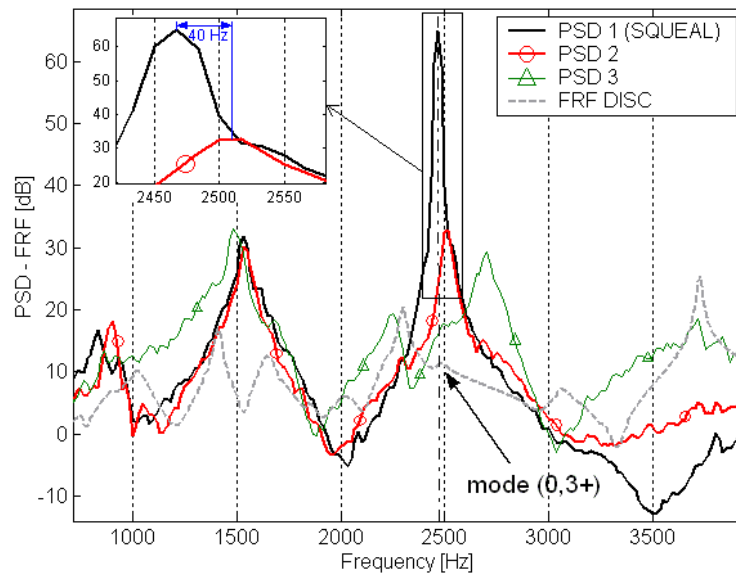


Figure 4.13 PSDs of the acceleration of the pad with three different weighs dispositions and FRF measured on the disc. Squeal appears only for precise tuning between the natural frequencies. For differences of just 40 Hz (zoom) squeal does not occur.

Figure 4.14 shows the disc modes involved in squeal events during experiments, along with the frequency ranges covered by the support and pad modes when changing the driving parameters. The bending modes of the disc, characterized by the antinode at the contact zone, that fall in the range of frequencies covered by the support and pad modes, may be involved in instability, and they become unstable when their frequencies tune with the corresponding support or pad natural frequencies. The $(0,5+)$ mode frequency of the disc does not fall in any range covered by the tangential modes of the pad or support and, consequently, it is not involved in squeal.

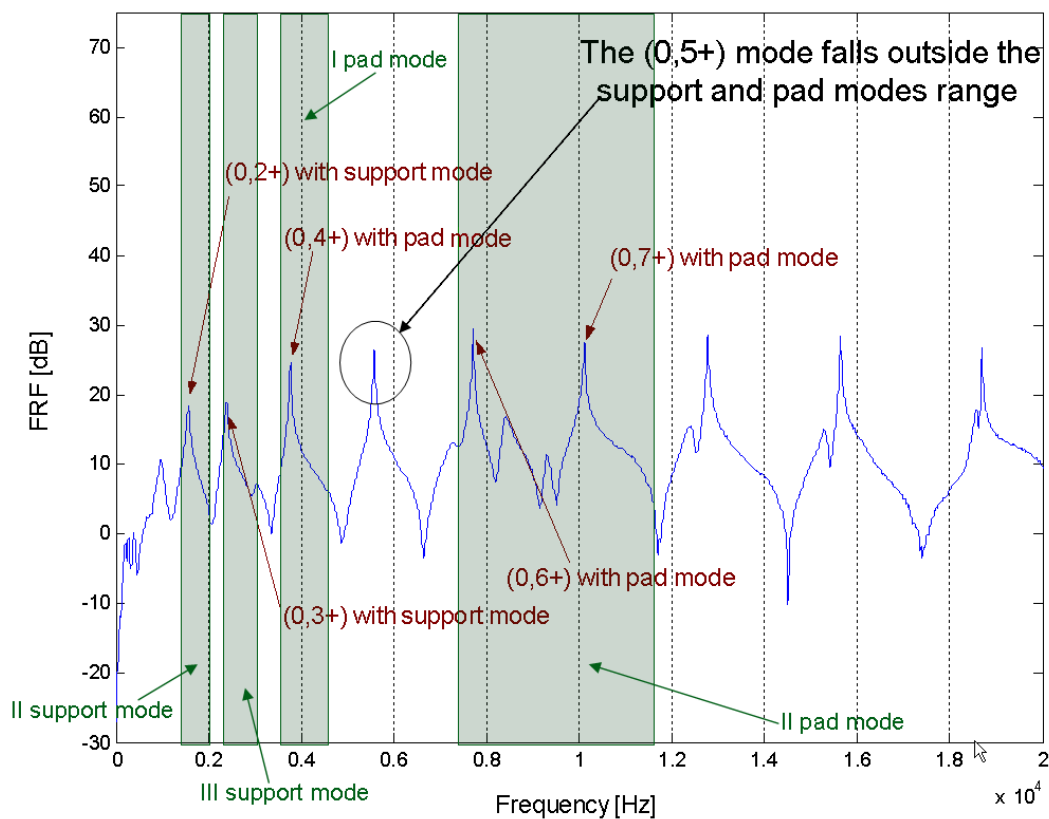


Figure 4.14 Modes involved in squeal instabilities. All the modes $(0,m+)$ of the disc that fall in the ranges of frequencies covered by the tangential modes of the pad and support are involved in squeal.

4.4 Effects of modal damping on squeal instability

This section describes two different, almost opposite, roles that the modal damping plays on squeal phenomenon. Experiments show that a higher

modal damping can either facilitate the rise of squeal or reduce the instability amplitude up to suppress it completely.

Moreover, a further proof that squeal is a dynamic instability, related to the dynamics of the mechanism, is brought by triggering its rise with an external impulse.

4.4.1 Squeal suppression with damping

In order to prevent squeal events, thin layers of rubber are introduced between the support and the thin-plates. The rubber introduces a high modal damping to the third mode of the support (2.7 kHz) that is characterized by its bending deformation. Figure 4.15-a shows the PSD of the tangential acceleration measured at the leading side of the pad when the values of the parameters are chosen to avoid squeal. As mentioned, the frequency peak at 2.7 kHz is extremely reduced by introducing rubber layers (from 28 dB to 8 dB). Figure 4.15-b suggests that the introduction of modal damping prevents the unstable coupling that involves the damped mode of the support. In fact, once the damping layers are introduced, it is not possible to obtain this squeal condition (black line), obtained without damping (grey line), by any change in the parameters.

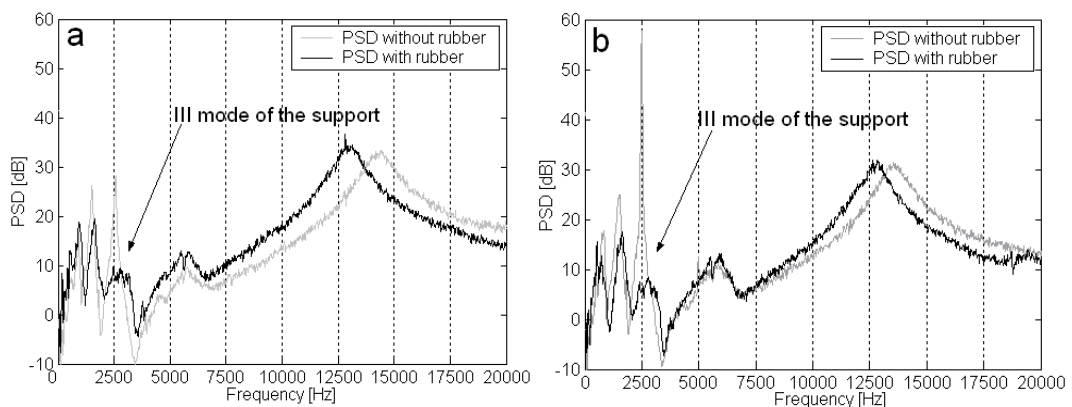


Figure 4.15 PSD of the pad acceleration with and without rubber layers respectively when: a) parameters are set to do not have squeal; b) parameters are set to have coupling between the third mode of the support and the (0,3+) mode of the disc (squeal at 2467 Hz).

On the contrary, when the values of the parameters are set to have coupling between the first mode of the pad and the (0,4+) mode of the disc, the introduction of the rubber layers does not affect the rise of squeal, that occurs as easily as without rubber (**Figure 4.16-a**).

This behaviour of the set-up is a demonstration of the fact that the disc modes can couple with modes of either the pad or the caliper. Introducing

solutions to avoid squeal caused by the coupling between modes of two substructures (support and disc in this case), can be useless to prevent squeal that can arise by the coupling between modes of two other substructures (pad and disc). Thus, brake design should take into account the dynamics of both the caliper and the pad. The introduction of thin plates between the back-plate of the pad and the piston, adopted on commercial brakes to prevent squeal, can introduce high contact damping [CHEN 05] in the tangential direction that avoids the modes of the caliper to couple with the modes of the disc, but can not affect the role of the dynamics of the pad.

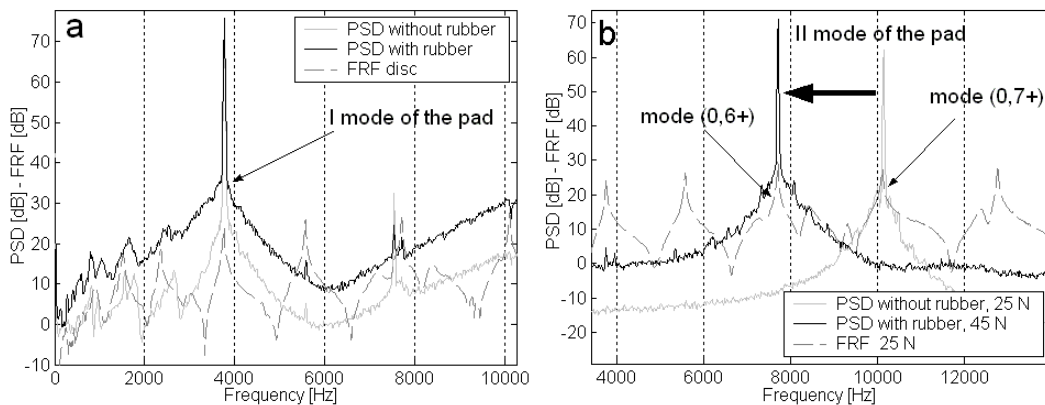


Figure 4.16 PSD of the pad acceleration with and without rubber layers respectively when: a) parameters are set to have coupling between the first mode of the pad and the (0,4+) mode of the disc (squeal at 3767 Hz); b) PSD of the pad velocity when parameters are set to have coupling between the second mode of the pad and the (0,6+) mode of the disc (squeal at 7850 Hz - black), with rubber ; and when parameters are set to have coupling between the second mode of the pad and the (0,7+) mode of the disc (squeal at 10150 Hz - grey), without rubber.

A different effect of the introduction of the rubber layer is the shift of the mode of the pad toward lower frequencies, due to the decrease of the tangential stiffness at the connection between the pad and the support. This effect is used to shift the natural frequency of the second mode of the pad from the coupling frequency with the (0,7+) mode of the disc (squeal at 10150 Hz) into the coupling frequency with the (0,6+) mode of the disc (squeal at 8850 Hz), as shown in **Figure 4.16-b**.

4.4.2 Increase of squeal propensity with modal damping

The previous section shows how an increase of modal damping can prevent the damped mode to participate in the squeal coupling. The following experiments will demonstrate also that a mode characterized by a large modal

damping can be more easily involved in squeal than a mode characterized by a small modal damping.

The modes of the support are characterized by a smaller modal damping than the modal damping of the pad. This is due to the large damping coefficient of the friction materials and appears on the PSDs of the pad acceleration showing two highly damped peaks (~ 4.5 kHz and 11.5 kHz) in corresponding to the two tangential modes of the pad (Figure 4.5).

As reported in section 4.3.2 when squeal occurs by coupling a mode of the support (modal damping equal to about 1-2%) with a mode of the disc, the instability rises only if there is an exact tuning between the two natural frequencies (Figure 4.13). On the contrary, when a mode of the pad (modal damping equal to about 7-9%) is involved in squeal (coupling with a mode of the disc) the behaviour of the instability is different and it can occur even when there is not exact tuning.

When there is exact tuning between the two modes, squeal occurs as soon as the braking phase starts; however, if the two modes are not perfectly tuned, squeal can still be triggered.

Thus, first the parameters of the set-up are set to have exact tuning between the (0,4+) mode of the disc and the first mode of the pad (squeal at 3767 Hz). With this configuration as soon as the pad engages the contact with the disc and the normal load reach the maximum value (starting ramp in Figure 4.17-a), the squeal oscillations increase exponentially up to the characteristic limit-cycle (Figure 4.17-c). A harmonic sound emission is measured and overcomes often the 100 dB (Figure 4.17-f).

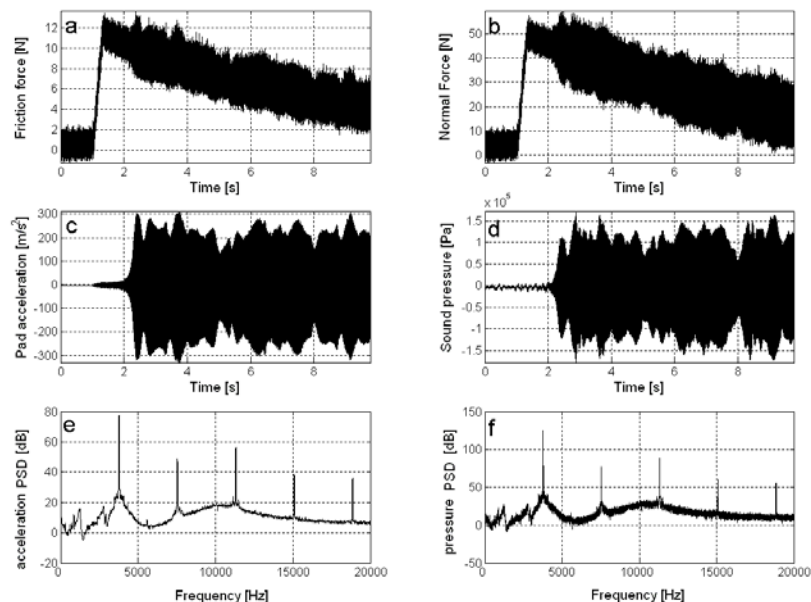


Figure 4.17 Squeal vibrations start as soon as the contact happens: a) friction (tangential) force; b) normal force; c) tangential acceleration of the pad; d) sound pressure; e) PSD of the acceleration; f) PSD of the sound pressure.

Then the normal load is changed from the tune-in value (45 N) and the brake simulation starts in “silent conditions” i.e. without squeal emission.

In “silent” conditions a hammer impulse is provided to the disc in the normal direction. Depending on the tuning level between the two modes (i.e. the distance between the two natural frequencies) three behaviours, described below, are found.

When the normal load increases from 45 N to 48 N (the two modes are off-tuning of about 40Hz), squeal starts only after the impulse is applied to the disc, as shown in Figure 4.18 and, after the impulse, the squeal doesn't stop. This means that with a highly damped mode, (i.e. the mode of the pad), the tune-in range of the mode is wide and squeal can still occur even if the two natural frequencies do not coincide exactly.

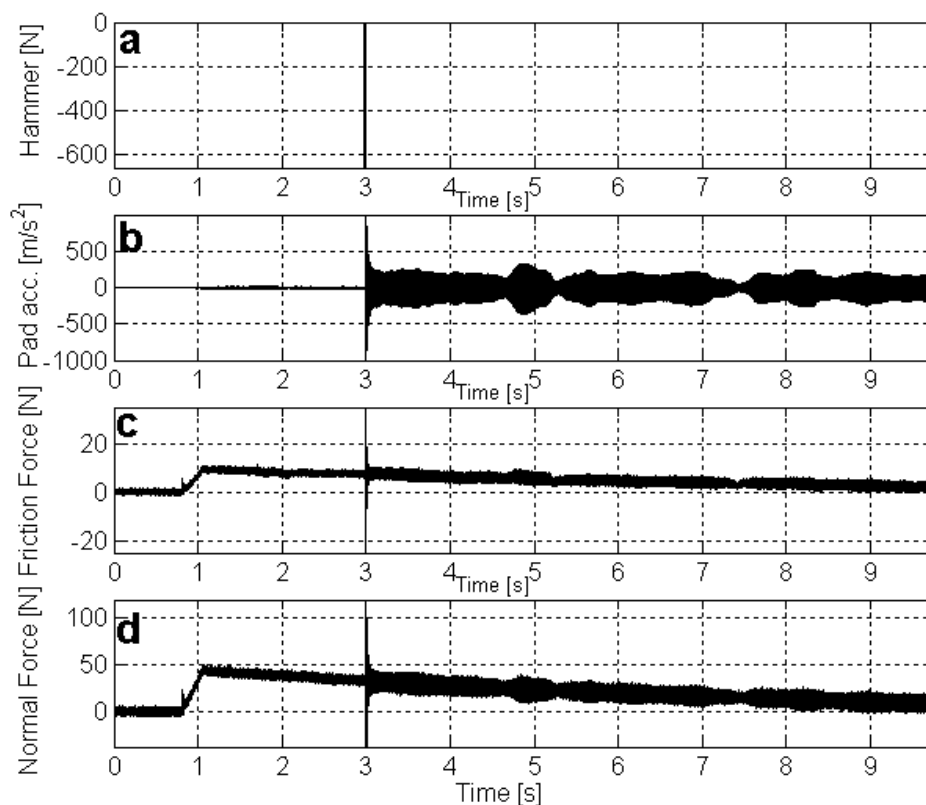


Figure 4.18 Squeal vibration starts after an impulse normal to the disc surface: a) hammer impulse; b) tangential acceleration of the pad; c) friction force; d) normal force.

The impulse is given in the opposite side of the contact with the pad, in order to excite all the modes with an antinode at the contact point. Figure 9 shows that, after the impact, the squeal starts and goes on until the disc is stopped.

Figure 4.19 shows these results and three different key-steps are identified: the grey band on the time history underlines the time range of the acceleration where the FFT of the tangential acceleration of the pad is calculated.

- Phase 1) before the impulse: a wide band noise with only two peaks related to the support modes and two highly damped peaks due to the pad modes is present (Figure 4.19-a);
- Phase 2) during the impulse: the FFT shows all the peaks due to the bending modes of the disc with an antinode at the contact surface (Figure 4.19-b);
- Phase 3) after the impact: only the frequency peak (squeal at 3767 Hz), coincident with the (0,4+) bending mode of the disc tuned with the 1st mode of the pad, and its harmonics are observed. (Figure 4.19-c).

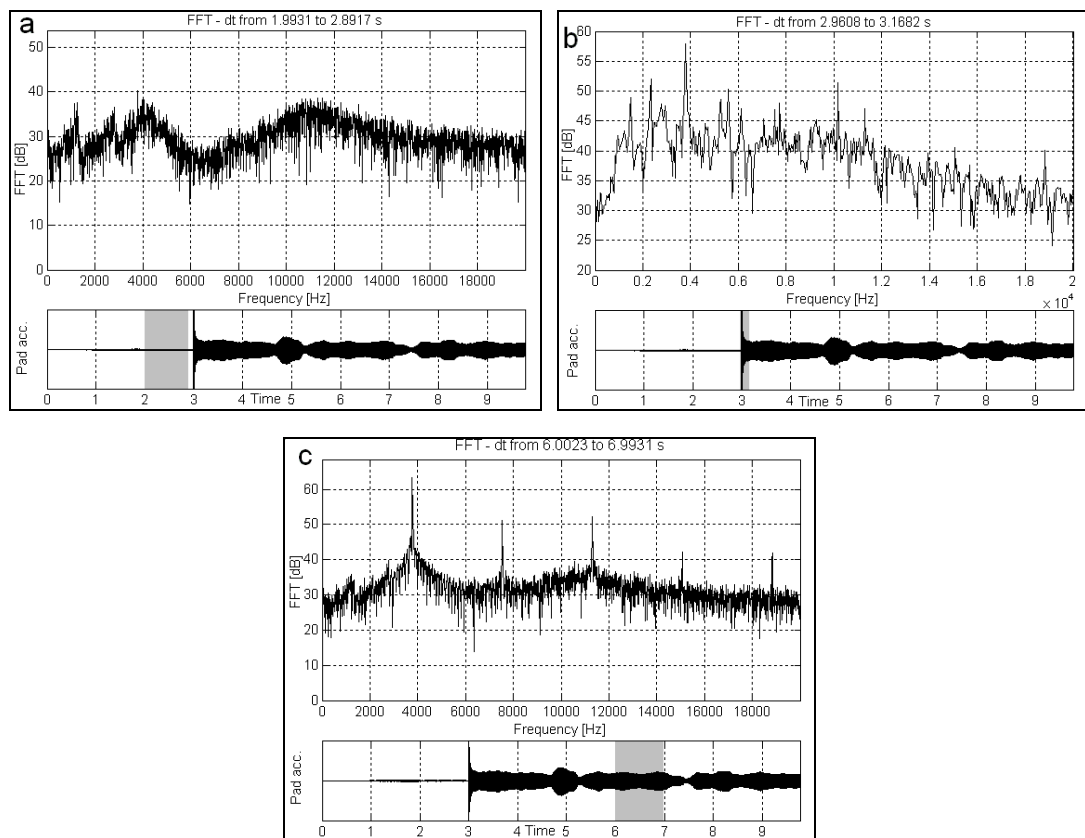


Figure 4.19 FFT of the pad acceleration during the hammer impulse test: a) before the impulse a stable behaviour is measured ; b) the impulse excite all the bending modes of the disc; c) after the impulse squeal occurs at the “tuning” frequency.

A different response of the system to the hammer impulse is obtained by increasing the normal load to 70 N and the 1st mode of the pad shifts about 300 Hz away from the (0,4+) disc mode. After every hammer impulse (Figure 4.20-a), squeal starts and stops after few seconds (Figure 4.20-b).

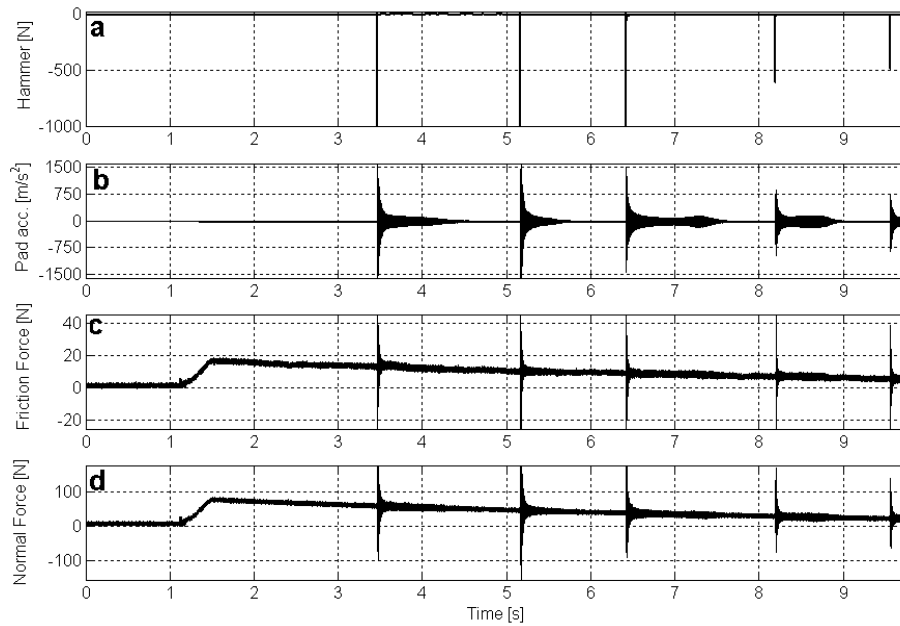


Figure 4.20 Squeal vibration starts after each impulse and stop after a while: a) hammer impulses; b) tangential acceleration of the pad; c) friction force; d) normal force.

If the normal load is equal to 120 N, so that the 1st mode of the pad shifts more than 400 Hz away from the (0,4+) disc mode, the hammer impulse does not trigger the squeal anymore (Figure 4.21), and the vibration of the systems decreases.

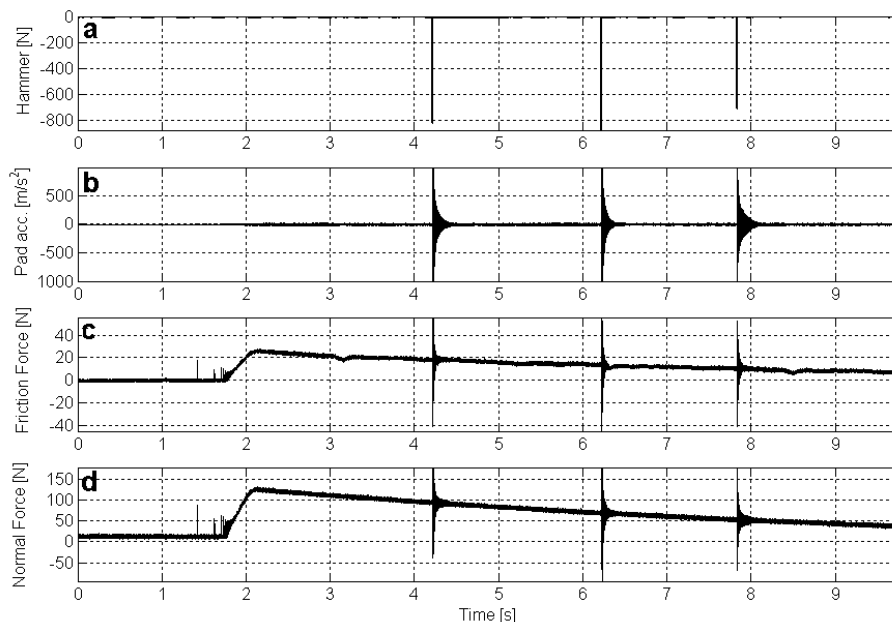


Figure 4.21 Squeal vibration does not start after the impulses: a) hammer impulses; b) tangential acceleration of the pad; c) friction force; d) normal force.

The same results that are obtained by exciting the bending modes of the disc, can be obtained as well by exciting the pad in the tangential direction by touching the disc surface in a point of the contact circumference with a humid wad. In this way it is possible to obtain an impulse in the friction force (Figure 4.22-b) when the humid point passes under the pad.

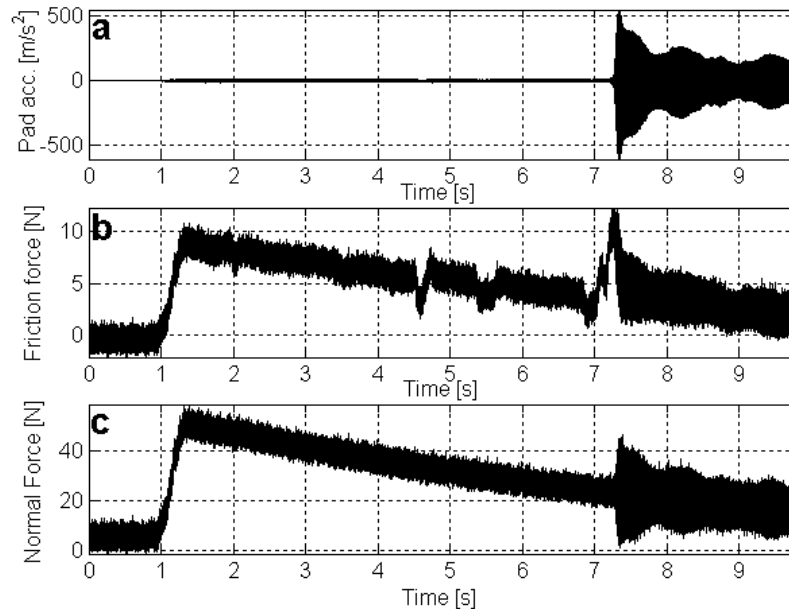


Figure 4.22 Squeal vibration starts after an impulse in the friction force provided by a perturbation in the friction coefficient (b).

Using this kind of excitation, phases 1 and 3, previously described, remain unchanged (Figure 4.19-a and Figure 4.19-c), while in the phase 2 only the frequency peak related to the disc mode, that is close to the pad mode, increases. Thus, the cause of instability is the excitation of one of the two modes that couple together. The impulse on the friction force excites the mode of the pad that couples with the (0,4+) bending mode of the disc. The hammer impulse on the disc surface excites the (0,4+) mode that couples with the mode of the pad. It is worth to notice that real brake in operating conditions are subjected to several circumstances that can trigger the instabilities, e.g. dirt on the disc surface, imperfections of the contact surfaces, vibrations coming from the connections with the vehicle, etc.

4.4.3 Phase of the squeal vibrations

The major effect of a large modal damping is the slow ramp of the phase response of the system around the natural frequency. Larger is the modal damping and more gradual is the shift of the phase of the system response at its

natural frequency. The dynamic instability is due to a phase relationship between the exciting force (friction force) and the response of the system (vibration of the pad surface in the tangential direction and vibration of the disc in the normal direction) that causes a self-excitation mechanism and brings to squeal. A correlation between the squeal and the phase differences between the vibrations of the system was already observed in [GIAN 06a]. Figure 4.23 shows the phase difference between the measured normal and tangential forces in the different analyzed cases. The difference of phase is calculated by performing the FFT of the global normal and friction forces and plotting the difference of the phases at the frequency of squeal, that is the frequency of the dynamic instability. When squeal occurs the difference of phase at the squeal frequency is found to be constant in time until squeal disappears. Each subplot in Figure 4.23 shows the acceleration of the system in time, together with the calculated difference of phase.

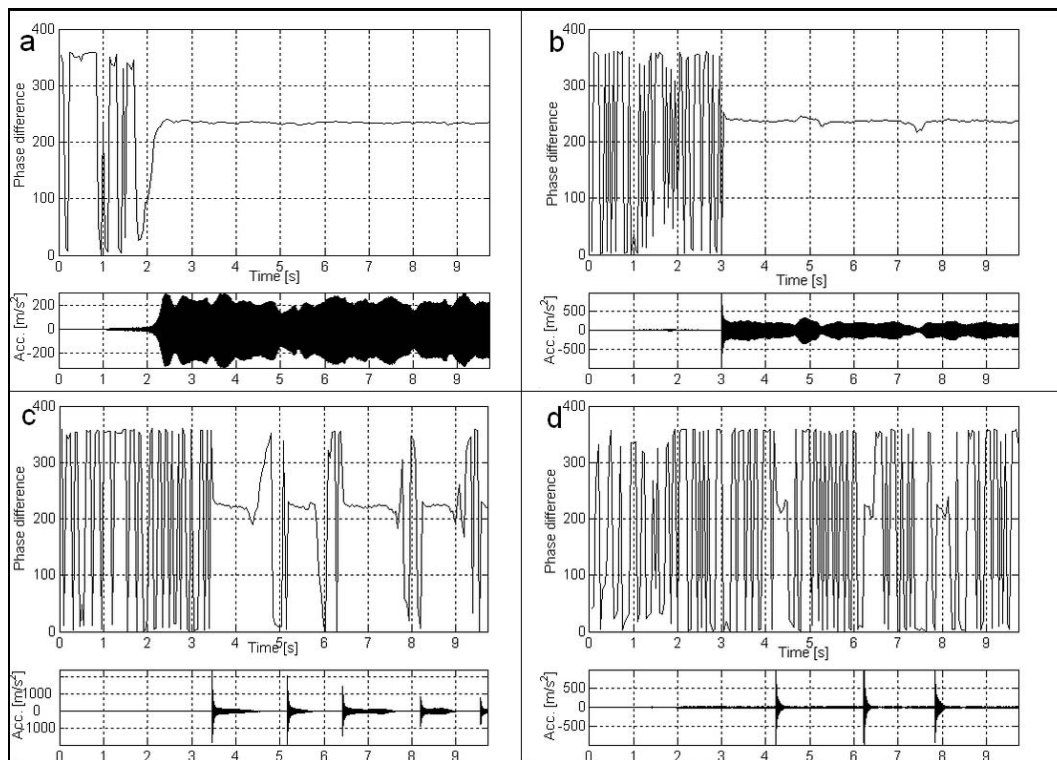


Figure 4.23 Behaviour of the phase difference between normal and friction forces calculated at the squeal frequencies (3767) over time, when the normal load is respectively equal to: a) 45 N with constant squeal; b) 48 N with constant squeal after the impulse; c) 70 N with momentary squeal after the impulses; d) 120 N without squeal.

At the contact surface the normal and friction forces are in phase and proportional. The measured tangential force presents a difference of phase with the normal load because it is measured between the pad and the support. Thus,

the dynamics of the pad is in between the contact point and the measured force. When the pad is excited in the tangential direction by the friction force, at a frequency close to its natural frequency, the pad vibrates with a maximum phase difference between these vibrations and the friction force.

When normal load is equal to 45 N and there is exact tuning between the two natural frequencies of the disc and pad, as soon as the pad gets in contact with the disc, squeal occurs and a constant phase difference of 240° is measured (Figure 4.23-a).

Changing the normal load from 45 N to 48 N, a continuous squeal can still occur but an external excitation is necessary to trigger the squeal. Once excited, the squeal vibrations of the set-up show a constant phase difference equal to 240 ° (Figure 4.23-b).

When the normal load is equal to 70 N it is not possible to have continuous squeal, but only temporary squeal occurs once the system is excited with an impulse, in these conditions, a phase difference equal to 230° is measured during the squeal emission (Figure 4.23-c).

With this value of normal load the two natural frequencies do not coincide and the squeal occurs at the natural frequency of the mode (0,4+).

When the normal load is equal to 120 N (Figure 4.23-d) the two natural frequencies are well separated, so that, when the system is excited with an impulse, squeal do not start, and the phase difference is equal to 215°.

It is worth to note that when there is not exact coincidence between the two natural frequencies, squeal happens at the frequency of the disc mode because of its lower modal damping.

Table 4.3 resumes the described cases, by reporting the normal load (boundary conditions), the frequency difference between the coupling modes (tune-in), the phase difference between the measured forces (phase response), and the system behaviour:

Normal load [N]	Frequency difference [Hz]	Phase difference [°]	Squeal behaviour
45	0	240	Constant squeal
48	≈40	240	Constant squeal after triggering
70	≈300	230	Temporary squeal after triggering
120	>400	215	No squeal

Table 4.3 *Resume of the behaviour of the system for the four different cases.*

These experiments show that a large modal damping can increase the possibility to have coupling between two modes of the system because it enlarges the tune-in range of the mode. Therefore, while it is useful to add damping material to reduce the modal response of the system, attention should be placed to the extended range of frequencies where the damped mode can couple with other modes. This explains why the disc-pad instability is characterized by a wider tune-in range between the modes with respect to the disc-support instability.

4.5 Conclusions

The proposed experimental set-up simplifies extremely the geometry of a real brake so that it is possible to have repeatable and consistent measurements.

Nevertheless, the set-up is able to reproduce, “at will”, squeal events that are qualitatively analogous to real brake squeals, and therefore can provide a reliable experimental insight into the squeal physics.

The simplified geometry of the TriboBrake allows also for an easy modelling by FE to predict and reproduce squeal events [MASS 06b].

The measurements presented in this chapter confirm the squeal phenomenon as a dynamic instability of the brake system. The dynamic analysis, together with the analysis of the squeal characteristics, relates the squeal phenomenon to a modal instability. In particular, squeal happens when a mode, characterized by large tangential vibrations at the pad contact surface, couples with a mode characterized by large bending vibration of the disc at the contact area.

These results agree with the mode lock-in theory and provide an experimental basis supporting the complex eigenvalue analysis as a tool for squeal prediction.

The presented analysis shows also that squeal can be easily triggered when the system dynamics is favourable, i.e. when there is tuning between two appropriate modes of the system. It is important to note that a brake apparatus is subjected to several circumstances that can trigger the instability.

An important distinction between dynamics of the pad and the support should be highlighted, because the experiments show that squeal can be obtained from the modal coupling between disc and either the pad or the support. During brake design for squeal suppression, this aspect should be taken in account.

Two different roles of the modal damping are finally described: a large modal damping can reduce the response of the damped mode and consequently prevent its participation to squeal coupling; however a high damped mode has more probability to couple with others modes that fall close to its natural

frequencies because its tune-in range is larger. This suggests to use carefully the add of damping in order to reduce squeal.

To conclude, it is important to note that the experiments do not show any direct dependence between squeal occurrence and the variation of a single parameter. In fact, since the squeal depends on the tuning between two modes of the brake apparatus, it is the modal distribution of the whole brake system that may, or may not induce the squeal instability. Moreover, the modal distribution depends on several global and local characteristics of the system in a non monotonic way. Therefore, in order to avoid squeal occurrence, the effectiveness of the changing of a single parameter must be evaluated in relation to the actual modal distribution with the aim of eliminating a possible tuning, without causing another one at a different frequency.

Chapter 5. Tribological analysis

Chapter 5.	Tribological analysis	143
5.1	Introduction.....	145
5.2	Dry friction contact between pad and disc.....	146
5.2.1	<i>First bodies.....</i>	<i>146</i>
5.2.2	<i>The role of the third body.....</i>	<i>148</i>
5.2.3	<i>Mechanism behaviour with and without squeal.....</i>	<i>151</i>
5.3	Contact surface topography	152
5.3.1	<i>Pad surface topography without squeal.....</i>	<i>152</i>
5.3.2	<i>Pad surface topography after squeal.....</i>	<i>153</i>
5.3.3	<i>Analysis of the superficial material of the pad after squeal.....</i>	<i>155</i>
5.3.4	<i>Disc surface topography</i>	<i>158</i>
5.4	Conclusions.....	159

5.1 Introduction

Several studies have been developed in the literature to relate the surface topography of both the disc and the pad to the occurring of squeal [ERIK 99] [BERG 99]. Rhee et al. [RHEE 89] hypothesized that squeal can be due to an effect of “local hammering” at the contact surface that excites a mode of the brake system. Chen et al. [CHEN 02b] explained the “local hammering” as material detachments or asperity formations and deformations. This tribological behaviour would be reached in the advanced phase of braking, when the friction coefficient reaches a larger value than the starting value. The critical friction coefficient found by Bergman et al. [BERG 99] is also related to local contact phenomena appearing after a consistent number of braking events. In their experimental analysis [CHEN 03] Chen et al. showed also a coincidence between the squeal frequency and a natural frequency of the system.

Despite squeal involves the dynamics of the whole mechanism[‡] as much as the local dynamics at the contact surface, including the STTs (Superficial Tribological Transformations) and the role of the third body, the dynamic and tribological analyses have been developed separately rather than simultaneously in the literature.

The work presented in this thesis is aimed to take into account both the tribological and dynamic aspects of the problem and to show how the dynamic behaviour of the mechanism affects the contact and vice versa.

In the previous experimental (§ 4) and numerical (§ 3) analysis, squeal is identified as a dynamic instability of the brake mechanism (first bodies), due to the modal coupling of two appropriate modes of the system. The vibrations of the first bodies are recovered by the experimental and numerical dynamic analysis. The local behaviour of the contact stresses is simulated by the numerical contact analysis.

This chapter presents a comparative investigation on the characteristics of the contact surfaces carried out under both silent and squealing conditions, i.e. after the braking phase with and without squeal. An analysis of the internal status of the pad material is presented too.

First, the analysis of the tribological triplet [BERT 01] is discussed. The material properties of the first bodies are presented and a preliminary analysis of the contact between the pad and the disc surfaces is performed to characterize the third body. The behaviour of the mechanism with and without squeal is then resumed.

[‡] In this chapter “mechanism” is referred to one of the three elements of the tribological triplet (mechanism, first bodies, third body).

The attention is focused on investigations (mainly post-mortem) of the third body and the STTs at the contact surfaces of both the pad and the disc, underlining the differences between the contact surface with and without squeal.

Finally, STTs and the third body are correlated with the behaviour of the local contact forces obtained by the numerical simulations and with the dynamic behaviour of the whole mechanism.

5.2 Dry friction contact between pad and disc

5.2.1 First bodies

The first bodies in contact are the brake disc and the brake pad that is assembled by the floating support.

The disc is made of steel with Young modulus equal to 210000 MPa and material density equal to 7800 kg/m³. The disc surface is finished with a linear straightening along one diameter direction that introduces a discontinuity in the roughness of the contact area when the disc is rotating. Such discontinuity affects the squeal amplitude that varies periodically with the period of the disc rotation. Nevertheless, the discontinuity is eliminated after some braking phases, when the disc surface is worn up by the sliding contact with the pad. The contact surface is placed horizontally so that the wear flow of the third body (the flow of the third body that definitively escapes from the contact) can be easily monitored.

The friction pad is obtained by machining commercial brake pads. The material of automotive brake pads are usually composites formed by hot compaction of powders that include many different components. Each component has different function and can be divided into four main categories: binders, structural materials, fillers and friction modifiers. Various modified phenol-formaldehyde resins are used as binders. Fibers (structural materials) can be classified as metallic, mineral, ceramic, or aramid, and include steel, copper, brass, potassium titanate, glass, organic material, and Kevlar. Fillers tend to be low-cost materials such as barium and antimony sulphates, kaolinite clays, magnesium and chromium oxides, and metal powders. Friction modifiers can be of inorganic, organic, or metallic composition. Graphite is a major modifier used to influence friction, but other modifiers include cashew nut dust, ground rubber, and carbon black. In the past, brake pads included asbestos fibres. Modern asbestos-free brake linings contain different inorganic compounds, though the metal compounds in use remained more or less the same.

Table 5.1 resumes the function of the different components and lists some example of used materials.

PAD COMPONENTS	FUNCTION	EXEMPLE
BINDER	Holds components and forms a thermally stable matrix	Phenolic resins, rubber (added to increase damping properties)
STRUCTURAL MATERIALS	Provide mechanical strength	Metal, carbon, glass, kevlar, mineral or ceramic fibres
FILLERS	Reduce cost and increase manufacturability	Mica, vermiculit, barium, etc.
FRICITION MODIFIERS	Ensure a stable frictional properties and control the wear rates of both the pad and the disc	Graphite, metal sulphides (stabilise the friction coefficient); Alumina, silica (abrasive particols that increase both the friction coefficient and the disc wear to give a better defined rubbing surface)

Table 5.1 Components of brake pad materials and their functions.

The brake pads used in the tests are automotive brake pads. The exact formulation of the friction material is unknown. Moreover, as the pad gradually wears, the different wear rates of the different components causes a different material composition at the contact surface. In particular, particles and fibers with high wear resistance (e.g. structural materials) resist better than the neighbouring material and form areas of high contact pressure.

Figure 5.1 shows a spectral analysis of the pad surface after braking. The analysis was carried out with a scanning electron microscope (SEM) model JEOL 840A equipped with an X-ray spectrometer. Because the SEM utilizes vacuum conditions and uses electrons to form an image, special preparations of the sample are necessary. Being a non-metal material the pad surface needs to be made conductive by covering the sample with a thin layer of conductive material.

An electric field and argon gas are used to extract gold atoms from the surface of a gold foil. The gold atoms fall and settle onto the surface of the sample producing a thin gold coating. Because of this, all the measured spectra show a high concentration of gold (Au).

The spectrum 1 is obtained by measuring a smooth contact area where a deposit of graphite forms a thin film over the contact surface and the spectrum analysis reveals a high concentration of carbon. The spectra 2 and 4 are measured at the fiber sections worn by the contact with the disc. High concentration of Sr, Zr and O are revealed, while a deep analysis shows also the presence of Cu, Fe and Si. Different kinds of fibers are adopted to compose the structural matrix of the material. The spectrum 3 is measured in an area not in contact with the disc and thus the oxides are not removed. This explains the high concentration of oxygen.

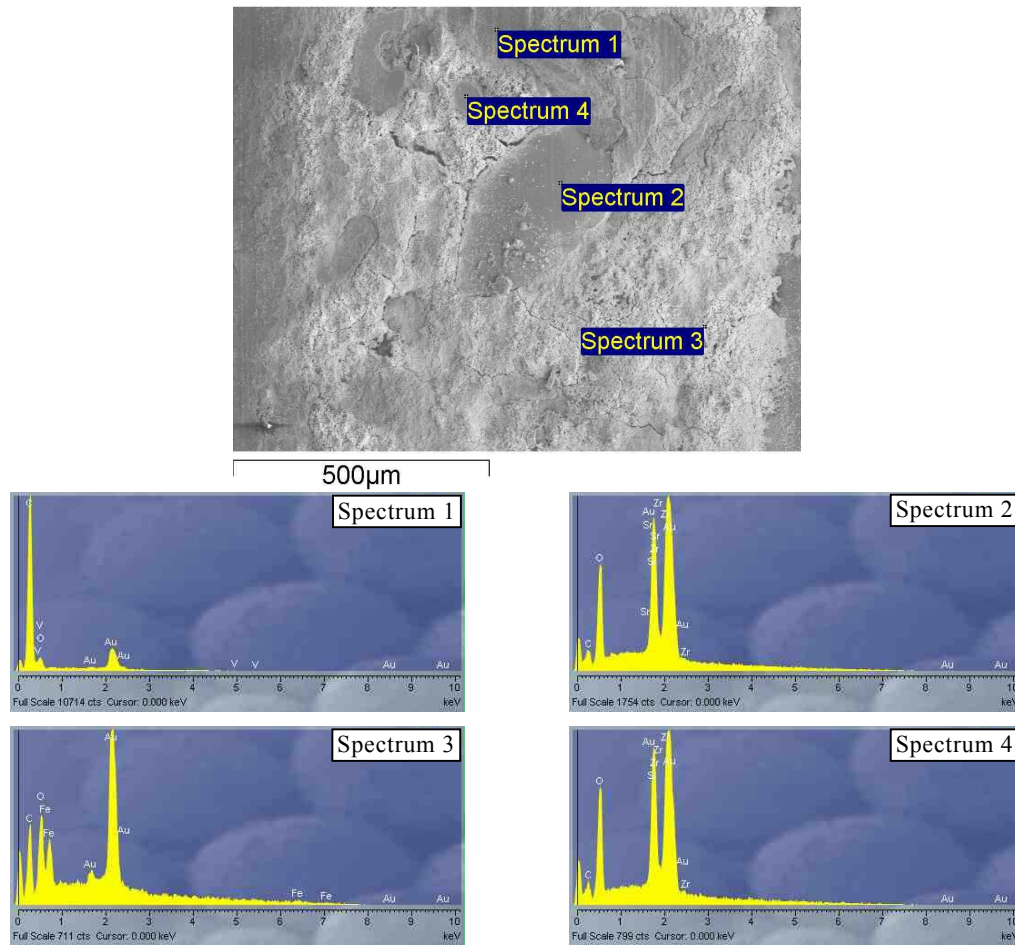


Figure 5.1 Spectral analysis of the pad contact surface.

5.2.2 The role of the third body

Particles coming from the pad and the disc constitute the third body [GODE 84] and have a key role in the tribological triplet [BERT 01]. The third body separates the first bodies, transmits the load between the first bodies and accommodates the relative velocity.

Figure 5.2 shows, on the left, the pad surface after few brake cycles (about 10 min of total time) and, on the right, the contact area after several brake cycles (about 100 min of total time). First, the contact area interests only a fraction of the pad surface, due to the disc and pad static deformations under the braking forces. The surface does not worn up uniformly and, after a while, it accommodates to the actual deformation of the first bodies (disc and pad). In Figure 5.2 a particular of the third body during the braking phase is shown. The flows of the tribological circuit are here:

- the internal source flow: particles detached from the pad and disc surface due to STTs, cracking, bonding, etc.;
- the internal flow: particles trapped into the contact that contribute to create the contact plateaus;
- the recirculation flow: the third body accumulated in front of the pad and the disc contact area, that can be reintroduced in the contact;
- the wear flow: the third body expelled laterally to the pad and the one in the front that is no more reintroduced into the contact.



Figure 5.2 Wear of the pad contact surface after a compressive brake time of 10 minutes (left) and 100 minutes (right), at 10 rpm; third body accumulated at the leading edge of the pad (center)

Only a limited fraction of the pad macroscopic contact surface is in contact with the disc. Eriksson et al.[ERIK 02] showed that the real contact between brake pads and disc consists of a number of small contact plateaus. The plateaus usually show signs of wear and sliding contact, including a pattern of parallel grooves along the direction of sliding (Figure 5.3). The nucleation of the contact plateaus takes place typically where the metal fibers come out from the surface, with hardness values considerably higher than the mean hardness of the pad composite. The third body agglomerates and compacts around the harder point, enlarging the effective area of the contact plateaus (Figure 5.3). A different kind of contact plateaus is observed where a large portion of the contact area is not interested by fibers and an uniform sliding area is in contact with the disc (see Figure 5.5-a). The area around the contact plateaus does not show signs of sliding contact.

With such configuration the contact load is concentrated in reduced areas where the effective contact pressure can reach extremely larger values with respect to the mean contact pressure calculated on the whole pad surface.

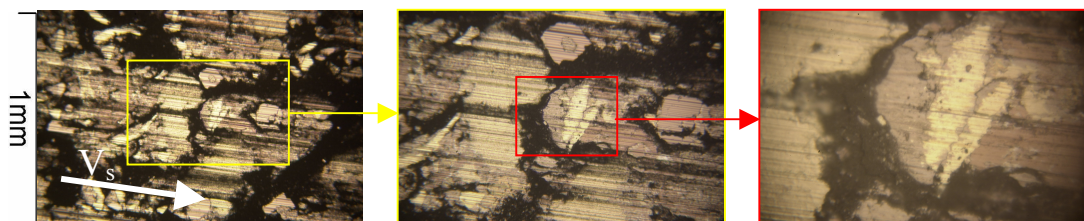


Figure 5.3 Three consecutive zooms of the pad contact surface characterized by contact plateaus. V_s is the sliding velocity.

Figure 5.4 shows a cut of the contact surface perpendicular to the sliding direction. After treatment with resin, the pad is cut in a plane normal to the sliding velocity to highlight the third body layer after brake events. The clear smooth area at the top of the figure is the resin. Then a layer (about $10\ \mu\text{m}$) of third body accommodates the pad and disc profiles and forms the contact surface. The parallel grooves due to the disc surface are recognizable on the top of the layer of third body, where the contact takes place.

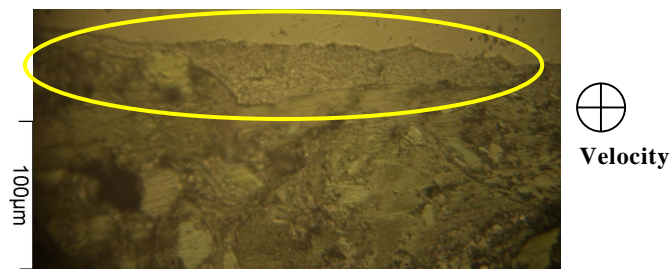


Figure 5.4 Layer of third body accommodating the pad and disc contact surfaces.

Figure 5.5-b shows the distribution of carbon (red), oxygen (blue) and iron (green) at the contact surface. The smooth areas, where the sliding between pad and disc happens, are characterized by a high concentration of carbon. In fact, in such areas the third body is mainly constituted by the graphite introduced into the friction composite to stabilize the friction coefficient. The areas not in contact with the disc are characterized by a strong oxidation, and, thus, by a high concentration of oxygen. The metallic fibers are also recognizable by the iron distribution.

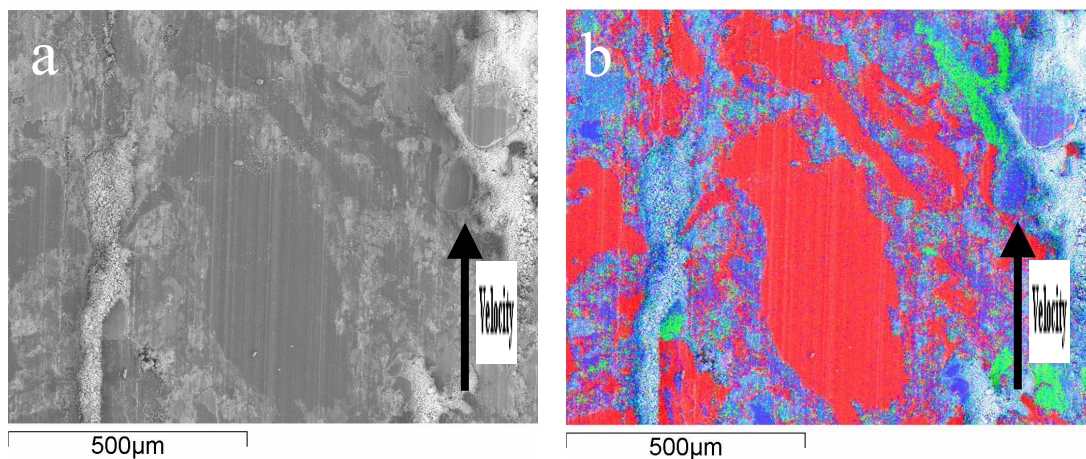


Figure 5.5 a) Contact surface; b) Carbon (red), oxygen (blue) and iron (green) composition at the contact surface.

The analysis underlines the importance of the third body in the contact topography between pad and disc.

5.2.3 Mechanism behaviour with and without squeal

Despite the behaviour of the mechanism during squeal is mainly described by the dynamic analysis (§ 4), in this section the effects on the contact configuration and the differences between the mechanism behaviour with and without squeal are considered.

Figure 5.2 (left) shows the contact distribution between pad and disc, highlighted by the worn area of the pad surface. The numerical analysis of the contact stresses shows the same distribution of contact pressure. In particular, Figure 3.20 shows the local contact stresses when squeal does not occur. The contact pressure is not uniformly distributed on the contact surface and the largest values are calculated at the leading edge, along the inner radius. In fact, because of the tangential deformation of the support under the friction torque (due to the friction force and the constraint at the connection with the thin plates), the contact force is the highest at the leading edge of the pad surface. The largest value of the contact pressure at the inner radius is due to the bending (static) deformation of the disc under the normal load.

It is important to notice that, despite the non uniform spatial distribution of the contact forces, the local values are almost constant in time when the squeal vibrations are absent (see Figure 3.20).

During squeal the system vibrates at the squeal frequency and the vibration shape is the one of the unstable mode, characterized by normal (bending) vibration of the disc and tangential vibration of either the support or the pad (see § 4). The effects at the contact area can be considered as the sum of the vibration of the disc contact surface and the vibration of the pad contact surface. While the disc surface is vibrating in the direction normal to the contact area, the pad surface is at the extremity of the support-pad assembly. Therefore, when the system vibrates with a tangential mode of either the pad or the support, the pad surface is characterized by both tangential and rotational vibrations. Being in contact with the disc surface, the normal component of the rotation produces a large local oscillation (at the squeal frequency) of the contact pressure that is both space and time depending. At the leading edge such oscillation ranges from zero to fifteen times the mean value of the contact pressure (see Figure 3.23). Moreover, considering that the real contact area is localized at the contact plateaus, the oscillation of the local contact forces can reach values even larger. Eriksson et al. [ERIK 02] assert that the average pressure on the plateaus can be five times higher than the average pad pressure.

In conclusion, during the squeal, the mechanism behaviour affects drastically the contact conditions by introducing large oscillations of the local

contact forces at the squeal frequency. On the contrary, without squeal, the mechanism behaviour affects only the spatial distribution of the local contact forces that remain constant in time.

5.3 Contact surface topography

5.3.1 Pad surface topography without squeal

A preliminary analysis of the contact surface of the pad after a braking phase without squeal is carried out by the SEM. After a consistent number of braking cycles (about 100 min) the whole pad surface is worn and the contact is localized along the whole surface (Figure 5.2). Nevertheless, the real contact area is localized at the contact plateaus. Figure 5.6 shows a contact plateau formed around a structural fiber that is composed by hard material. It is characterized by a compact smooth area with small parallel grooves along the sliding direction that are determined by the sliding with the disc. The plateau is surrounded by a no contact area where the material oxidation is visible.

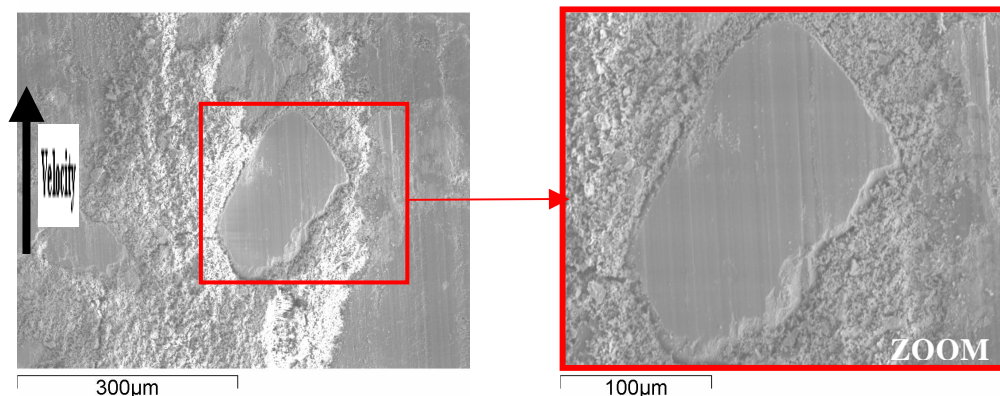


Figure 5.6 Contact plateau due to the hard material fiber at the contact surface.

Figure 5.7 shows a contact plateau formed in an area where fibers do not compare. In this case a layer of third body made of soft material is compressed and transmit the load between the contact surfaces. It is worth to notice that the parallel grooves determined by the sliding with the disc are more marked than in the previous case. In fact, the grooves on the disc surface are due to the localized contact with the structural fibers of the pad, where the local pressure reach the largest values and the disc material deforms plastically. Then, the contact plateaus made of soft material are modelled by the contact with the disc, forming the deep parallel grooves that are visible in Figure 5.7.

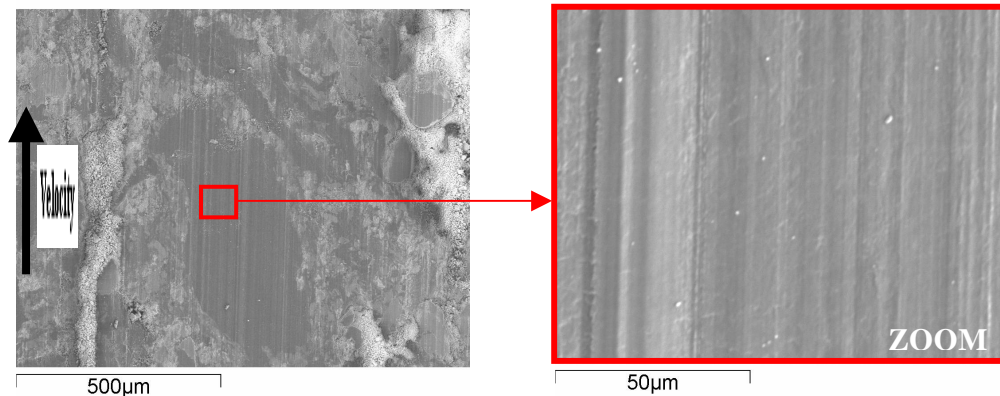


Figure 5.7 Contact plateau due to the third body accumulated over the soft pad components (no fibers in the contact area). The third body is compact.

Despite the pad topography obtained after braking events without squeal reveals a non-homogenous surface characterized by contact and non contact areas of different dimensions, the material results to be compact over both the smooth contact plateaus (Figure 5.8-a) and the rough non contact surface (Figure 5.8-b). No cracks or detachments are observed in the analysis.

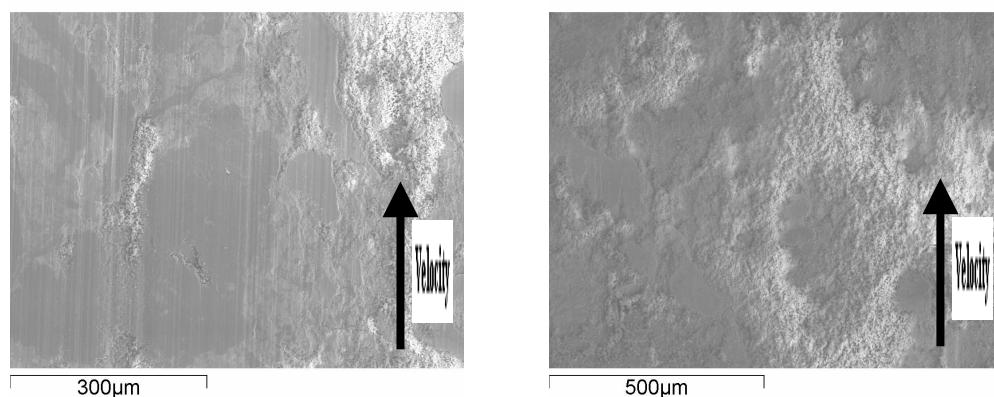


Figure 5.8 Contact plateaus (a) and no-contact area (b): the friction material at the contact surface is compact and no particular damages are detected.

5.3.2 Pad surface topography after squeal

The pad surface topography after squeal reveals a completely different aspect with respect to the topography without squeal.

The analysis is performed on a sample identical to the one used for the previous analysis, machined from the same brake pad. After the worn up of the pad to uniform the contact area, the values of the driving parameters are imposed to have squeal at 3767 Hz, i.e. when the first tangential mode of the pad

tunes in with the (0,4+) mode of the disc (see § 4). Several brake events with squeal are reproduced for a total time of about 20 min.

Figure 5.9 and Figure 5.10 show a material exfoliation at different scales. Figure 5.9 shows a large material exfoliation interesting an area larger than 1 mm^2 , while Figure 5.10 shows a contact plateau interested by exfoliations of the third body of some μm^2 . Most of the contact plateaus on the pad surface are characterized by a no compact third body, and even the areas not in contact with the disc present material detachments.

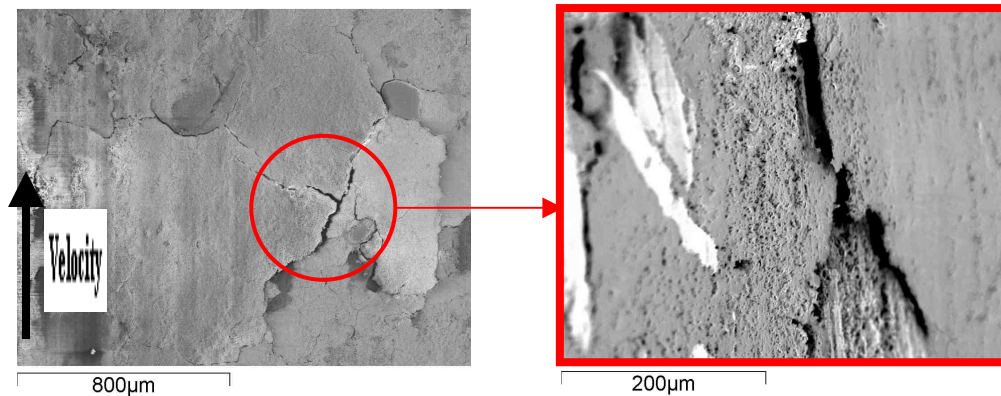


Figure 5.9 Material exfoliations at the contact surface after squeal; interested area more than 1 mm^2 .

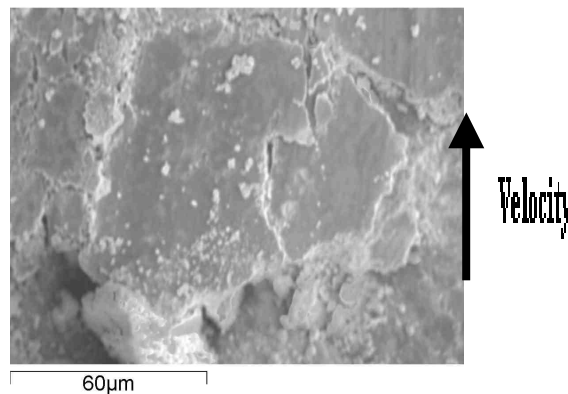


Figure 5.10 Micro-exfoliation of the third body (contact plateaus) after squeal.

Figure 5.11-a shows a contact plateau due to a superficial fiber with the surrounding no-contact area. The pad surface around the fiber is characterized by several cracks. Same results are shown in Figure 5.11-b where a contact plateau of soft material is interested by the cracks, together with the surrounding no-contact zone. The whole pad surface is characterized by superficial cracks or material exfoliations. Cracks can nucleate either in proximity of structural fibers or not.

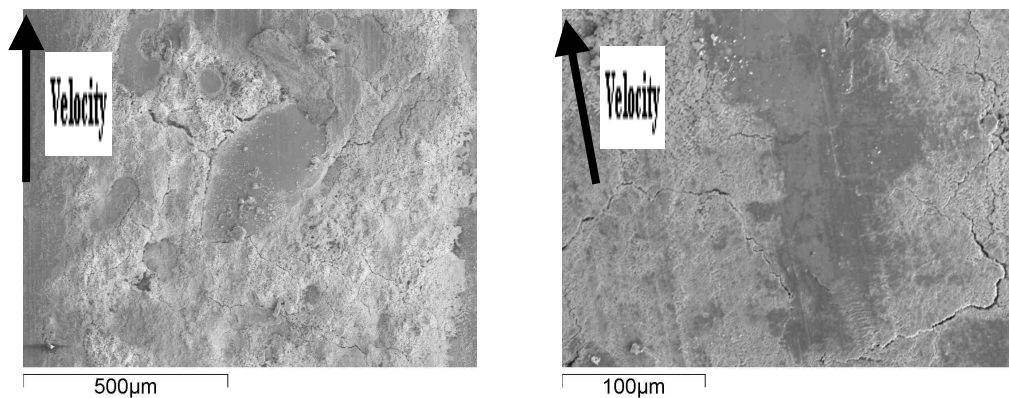


Figure 5.11 Superficial cracks both at the no-contact area (a) and at the contact plateaus (b), after squeal.

The topography of the pad surface highlights the effects of the system vibrations at the contact zone. The high frequency vibrations cause oscillations of the local contact stresses as evidenced by the numerical analysis (§ 3.4.2). Therefore, the pad material presents signs of fatigue, i.e. cracks and material exfoliations.

Once imposed the system parameters that bring to squeal (modal coupling), new tests were performed by cleaning the disc and pad surface to remove the detached third body: squeal is still obtained as soon as the brake starts. On the contrary, by changing the values of the macroscopic parameters, squeal does not occur. This means that the analyzed status of the contact surface is an effect and not a cause of squeal.

Nevertheless, for a new sample of friction pad, squeal does not occur at the beginning, for several braking cycles. This can be ascribed to a starting lower friction coefficient, due to surface contaminations and contact misalignments [CHEN 02b].

5.3.3 Analysis of the superficial material of the pad after squeal

In order to understand if the cracks and the material exfoliations interest only the superficial layer of the third body or also the pad, the friction pad was cut along the direction normal to the contact surface. Before cutting, the pad surface was fixed by immersing it into a specific resin. In the following figures the upper uniform grey zone is the resin and the third body layer is recognizable between the resin and the pad composite. Different kinds of superficial transformations are observed.

Figure 5.12 shows two cases where the third body layer is detached from the pad material. Such detachments can be due either to the squeal vibrations in operative conditions or to the successive treatment for the cutting, because the discontinuity between pad and third body is weak. Nevertheless,

these superficial detachments can correspond to the exfoliations visible in the pad topography before the cut of the sample, and are not observed in samples without squeal.

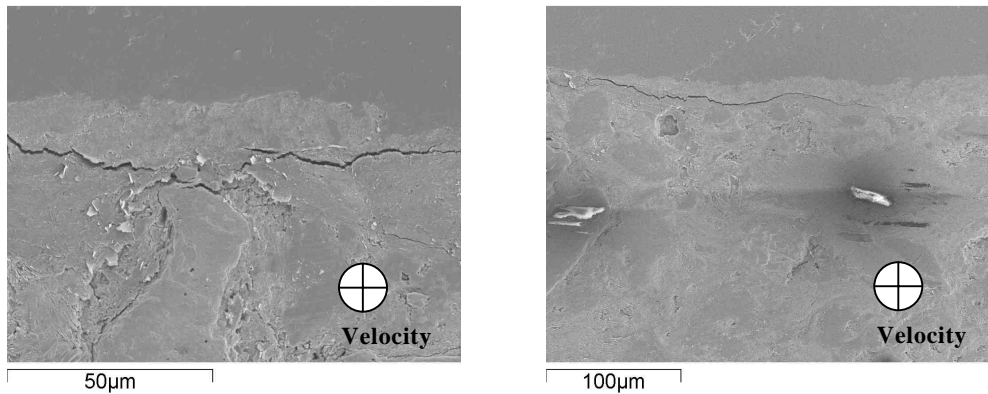


Figure 5.12 Section of the contact surface normal to the sliding direction, highlighting detachments of the third body layers after squeal.

Figure 5.13 shows further superficial detachments. In this case the detachment does not happen between the pad and the third body, but a thin layer of pad material detaches together with the third body layer. Thus, a crack parallel to the pad surface develops under the layer of third body, inside the pad material.

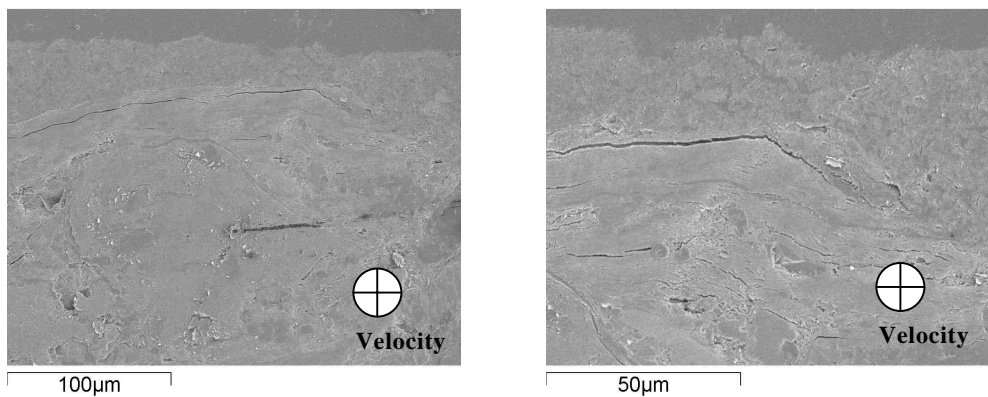


Figure 5.13 Detachments of layers of pad material under the third body, after squeal.

Moreover, the cracks do not interest only the surface of the pad and the discontinuity due to the third body layer. Starting from the contact surface several cracks develop inside the pad material up to a deepness of about ten μm . Figure 5.14 shows two examples.

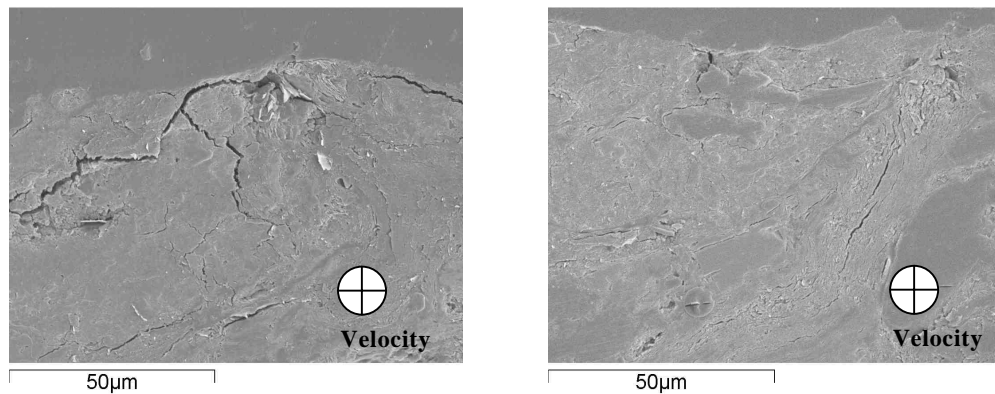


Figure 5.14 Superficial cracks develop inside the pad material, after squeal.

The material cracks can also nucleate inside the volume of the pad, close to the contact surface (Figure 5.15). In the first layer of pad material (about 400 μm from the contact surface) several cracks are observed without any preferential direction. The cracks follow the material composition by developing along areas filled by the same material component, where a high percentage of Si is recognized. This component expands throughout all the volume of the pad and the cracks develop along the direction of the continuous layers made of such component.

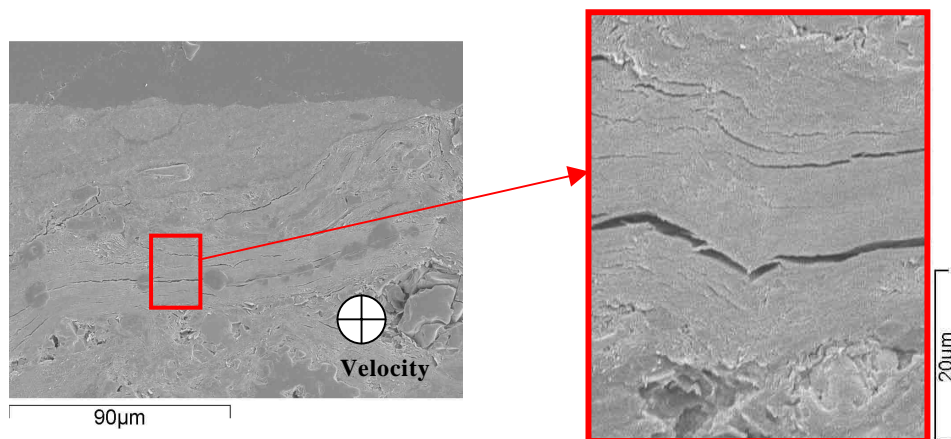


Figure 5.15 Internal cracks close to the pad surface developing along layers of pad composites.

The whole surface of the pad and the superficial layer mentioned above are interested by several cracks, while the internal volume of the pad is compact and does not present cracks.

The material exfoliations and the superficial and internal cracks close to the contact surface highlight the fatigue excitation of the pad material due to squeal vibrations. In fact, the high frequency (squeal at 3437 Hz) oscillations of

the contact stresses (shown by the numerical analysis of the contact stresses during squeal in Figure 3.22) cause fatigue in the superficial layer of the pad material and fragmentation of the third body layer.

5.3.4 Disc surface topography

Despite no relevant effects on the disc surface are observed, the topography of the contact surface after squeal is reported for completeness.

Being the disc machined with a linear straightening along a diameter direction, the initial roughness of the disc surface is not constant during the disc rotation. The roughness of the surface affects the squeal amplitude that oscillates with the periodicity of the disc rotation. In particular the squeal amplitude is lower when the roughness of the disc contact surface is higher, as shown also by Bergman et al. in [BERG 99]. This behaviour can be explained by the lower macroscopic friction coefficient due to the reduction of the real contact area, and to the frequent impacts between the pits of the disc surface and the contact plateaus, preventing them from growing to their normal “steady state” size [BERG 99].

Nevertheless, after a large number of runs, the starting roughness is worn up, and the disc surface is characterized by concentric circular grooves along the sliding direction. The grooves are formed because of the plastic deformation of the disc material where the contact with the hardest points (structural fibers) of the pad surface happens. During this stage the squeal amplitude is constant with the disc rotation.

The sample examined at SEM is not the disc surface, but a resin stamp of the contact surface of the disc that is previously obtained. The images from the SEM correspond to a negative film of the disc surface. Figure 5.16-a shows the disc surface after several brake cycles. The parallel grooves along the sliding direction are easily recognizable. Figure 5.16-b shows the boundary area between the contact zone (left) and the no-contact zone (right), where the linear straightening of the surface is not worn up.

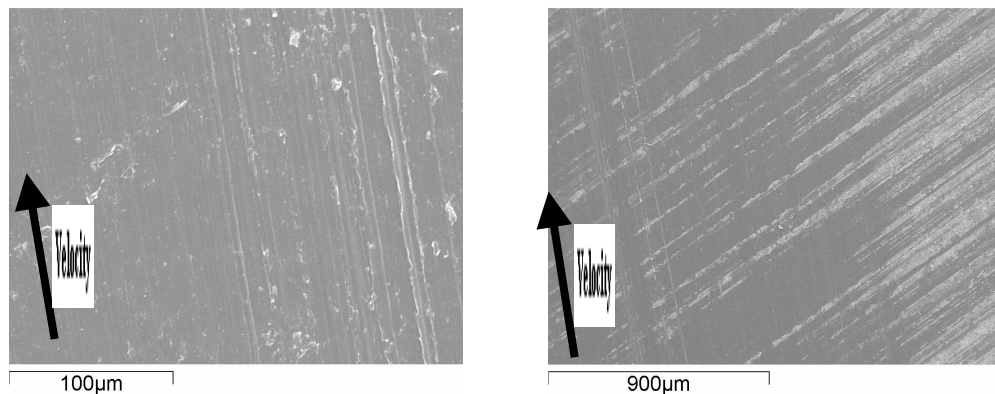


Figure 5.16 Grooves on the disc surface parallel to the sliding velocity after several brake cycles; b) boundary between the sliding zone and the no-contact zone, where the surface straightening is not worn out.

5.4 Conclusions

Despite the interdisciplinary nature of the squeal problems the dynamic and tribological approaches have been considered separately in the literature. The tribological work reported in this chapter is complementary to the dynamic analysis presented in chapter 4 and to the numerical analysis presented in chapter 3.

The analysis is addressed mainly to study the STTs and the role of the third body by highlighting the differences between contact surfaces with and without squeal. To understand the findings, the behavior of the mechanism, analyzed through the dynamic analysis, is taken into account.

After squeal events, the superficial layer of the pad material presents several signs of fatigue. Both exfoliations of the third body and cracks nucleated at the pad contact surface and inside the first layer of the pad material are observed. The cracks develop along certain material components.

On the contrary the disc surface topography is not affected by the squeal. The contact with the hardest points of the pad surface produces concentric grooves at the disc periphery, where the contact happens. The disc roughness, tangential to the sliding direction, affects the squeal amplitude, but is worn up after a number of brake cycles.

The comparison between the post mortem surface topography and the behaviour of the local contact forces calculated by numerical simulations (§ 3.4.2) permits to give an interpretation of the different characteristics of the pad topography with and without squeal and to validate physically the obtained numerical results.

The large oscillations of the contact stresses due to the high frequency vibrations of the mechanism, vibrating at its unstable mode, causes the rise of fatigue cracks and the fragmentation of the third body.

Tests were made to highlight that the status of the contact surface is an effect and not a cause of squeal. After finding the values of the parameters that bring to unstable modal coupling (squeal), the surface of both the disc and the pad are cleaned and squeal still occurs as soon as the contact happens. On the contrary, when the parameters are changed from the modal coupling configuration, squeal does not occur.

The fact that new pads do not squeal and need few preliminary braking cycles to be involved in the phenomenon can be ascribed to the need of a “steady state” size of the contact plateaus and an accommodating of the contact surfaces. In fact the low macroscopic friction coefficient due to the small effective contact surface, and the continuous impacts of the pits due to the surfaces roughness can prevent the rise of squeal.

The results of the tribological analysis highlight a further problem that can arise from squeal vibrations: the reduction of the pad life-time. In fact, the fragmentation of the third body (consider that some components of the third bodies are properly added to reduce the wear rate) and the fatigue damages of the superficial pad material can seriously affect the wear rate of the material and reduce the life-time of the friction pad.

Chapter 6. Concluding remarks

Chapter 6.	Concluding remarks.....	161
6.1	Summary	163
6.2	Original contributions.....	166
6.3	Future work.....	168

6.1 Summary

Despite brake squeal has been object of several studies since the first decades of the 20th century, there is not yet a commonly accepted understanding of the phenomenon. Difficulties are due both to its fugitive nature, in that it depends on slight changes in the system parameters that modify the system dynamics, and to the complicated mechanical interactions in brake systems, especially related to nonlinear contact problems at the friction interface.

Experimental, numerical and theoretical analyses are reported in the literature and are aimed to understand the physics of the problem and to predict and prevent the occurrence of squeal. Nevertheless, despite the interdisciplinary nature of such issue, involving dynamics, tribology, acoustics, etc., the analyses were mostly conducted separately in the specific disciplines.

Aim of this thesis is to provide a general approach to the problem, including numerical and experimental analyses in the dynamic and tribological domains. The dynamic (macro-scale) behaviour of the brake system, analyzed experimentally and numerically, is correlated with the local (micro-scale) behaviour of the contact, that is here analyzed by an experimental and numerical tribological analysis. The results allow to highlight a “feedback mechanism”, due to oscillations of the local contact forces and caused by the system deformation, that generates auto-excited squeal vibrations.

Because of the complexity of commercial brake systems the analysis is performed on a simplified brake apparatus, appropriately designed to obtain the following advantages:

- it permits to have robust and repeatable squeal events at different frequencies;
- it allows to reduce and control the influencing parameters;
- it allows to simplify, modify and monitor the system dynamics;
- it allows to conduct a tribological analysis on the contact surfaces;
- it allows an easy modelling with the FEM.

However, as a consequence of the use of the simplified set-up, the squeal events occurring during the experiments can only reflect a subset of squeal instabilities that may occur in real brakes. More precisely, because of the reduced dimensions of the pad, the disc-pad interaction is closer to that occurring in low frequency squeal, characterized by a wavelength of the disc deformed shape longer than the pad length.

The numerical analysis is performed by two different FEMs of the set-up: a linear FE model for squeal prediction in the frequency domain; a nonlinear FE model for squeal reproduction and analysis of the local contact stresses in the time domain. In the literature two main numerical approaches are available: the

complex eigenvalue analysis and the dynamic transient analysis. Nevertheless, these two methodologies, needing different models (linear and nonlinear respectively), were developed separately rather than simultaneously. The numerical work presented in this thesis combines these two methodologies:

- a linear model, through the complex eigenvalue analysis, is used to predict the unstable conditions (values of the parameters that bring to squeal). The method needs a lower computational effort to conduct the parametrical analysis;
- a nonlinear model, through the transient analysis, is used to analyze the time behaviour of the system vibrations and the local contact dynamics (stresses and deformations at the interface).

The linear model is developed by Ansys. To perform the transient analysis, a specific FE code Plast3 is used: it allows to introduce the contact nonlinearities between the disc and the pad and to calculate the local contact stresses distribution.

The two models are first compared and a check about the agreement of the unstable regions of the system parameters that lead to squeal, calculated with both the models, is performed. A good agreement is found, despite a characteristic over-prediction of squeal frequencies calculated by the linear model. The possibility to predict squeal events with a linear model means that squeal starts effectively in linear conditions. The mentioned over-prediction is also encountered by comparing the results from the complex eigenvalues analysis performed on the updated model and the experimental results (Appendix E). The over-prediction of the squeal frequencies can be ascribed to the linearity of the model. The results from the modal analysis are then compared with the dynamic experimental analysis to highlight the main features of the unstable modal coupling that leads to squeal.

A comparison is also performed between the squeal indexes that are generally adopted from the complex eigenvalue analysis and the squeal characteristics obtained by the transient analysis.

The nonlinear model is then used to analyze the behaviour of the contact stresses with and without squeal that are difficult to retrieve by experimental instrumentation. The numerical results are compared and validated with the experimental tribological evidences. The limit-cycle of the vibrations, characteristic of squeal, is reproduced by introducing only the contact nonlinearities in the model. Neither material nonlinearities or thermal effects have been considered.

The experimental analysis is performed to relate the actual (in operating conditions) system dynamics with the squeal occurrence. Several tests on different squeal frequencies and a parallel monitoring of the system dynamics are performed. The results are in good agreement with the “lock-in” theory that

considers squeal as a dynamic instability due to the unstable coupling of two modes of the system. The “tuning in frequency range” has been defined as the frequency band, around one natural frequency of the system, where the mode can couple with a second system mode. The frequency “tuning in” of two appropriate modes that are characterized by large tangential and normal deformations at the contact surface, are recognized to be necessary conditions for squeal to occur.

The study of the relationship between modal damping and squeal occurrence is also carried out, finding a double, almost opposite, role of the modal damping: it can either prevent the mode involved in squeal or enlarge the propensity of the mode involved in squeal coupling. The possibility to excite the instability by external impulses, and the phase difference between the measured signals depend on the frequency ‘tuning in’ rate between the two modes. This indicates the phase of the system response, excited close to its natural frequency, to be the cause of the apparent negative damping that brings to modal unstable vibrations.

The performed tribological experimental analysis highlights the different characteristics of the third body and the pad contact surface with and without squeal. A preliminary study of the contact surface and of the tribological triplet (first bodies, third body and mechanism) is reported. Cracks and material exfoliations of both the third body layer and the superficial material of the pad, are observed after squeal events. The material at the contact surface presents fatigue conditions, accordingly to the numerical results. Tests are performed to highlight that these STTs are consequences and not causes of the rise of squeal. However, the status of the contact surface can influence the rise of squeal by influencing the global friction coefficient. The analysis highlights a further problem that can be related to the presence of squeal vibrations during braking: the increase of the wear rate of the friction materials.

In conclusion, the work gives a general overview of the problem, concerning both dynamic and tribological aspects. Results from the performed numerical and experimental analyses converge together, characterizing the squeal as a dynamic instability of the brake system due to the unstable coupling between two appropriate modes. The coupling happens at the contact surface, where the oscillations of the local contact stresses, documented by fatigue phenomena, produce the “feed-back mechanism” that causes the auto-excited vibrations of the system. The friction coefficient allows to couple the normal vibrations of the disc with the tangential vibrations of both the pad and the support.

6.2 Original contributions

This thesis can be considered as a part of the research developed in the past years by several research groups to analyze and understand the physics of squeal by working on simplified brake systems. The nonlinear FE modelling and the tribological analysis have been jointed to this research guideline.

The main contributions introduced by the work object of this thesis to the actual state-of-art of the problem are considered in the following:

- the approach to the squeal problem through different and complementary methodologies, by developing both experiments and numerical analysis in the dynamic and tribological domains; this gives a general overview of the issue that implies both dynamic and tribological aspects;
- the numerical analysis combines together two different methodologies that, in the past, were developed separately: a linear model for the complex eigenvalue analysis and a nonlinear model for the dynamic transient analysis are here developed jointly. The combination of the two methodologies allows a parametrical analysis (squeal prediction) through the complex eigenvalue analysis, with low computational effort, and to analyze the vibration of the system and the contact stresses in the nonlinear domain by the transient analysis;
- the comparison of the instability prediction between the FE linear (frequency) analysis and the FE nonlinear (transient) analysis shows a good agreement, despite the squeal overprediction obtained by the linear model. Such overprediction is also obtained by the comparison with the experimental results;
- a distributed model of the contact is used for both the linear and the nonlinear analysis; in the nonlinear model the contact stresses are simulated by the Lagrange multipliers, introducing the contact nonlinearities;
- the contact nonlinearities (neither material nonlinearities or thermal effects are accounted for) allows to reproduce the characteristic limit-cycle of the squeal vibrations;
- the rise of squeal and the squeal vibrations are simulated by using a standard Coulomb friction model, without any velocity-dependence of the friction coefficient;
- considering the same modal instability, a good agreement is obtained between the squeal indexes usually adopted in the eigenvalues analysis and the results of the time simulation. When comparing instabilities that involve different modes, the real part of the unstable eigenvalues is not a sufficient parameter to give reliable squeal

indexes and a more accurate analysis of the unstable eigenvectors, together with the eigenvalues, is necessary;

- the numerical analysis of the contact stresses shows the local distribution with and without squeal. During squeal the oscillations of the contact forces (at the squeal frequency), due to the actual deformation of the system, are calculated. They explain the pad topography observed experimentally;
- the designed set-up allows for an accurate analysis of the dynamics and then for correlating the squeal occurrence with the “tuning in” between two appropriate modes of the system. Several robust and easily reproducible squeal frequencies are obtained;
- the dynamic analysis gives credit to the “lock-in” theory to explain squeal. The coupling between a bending mode of the disc and a tangential mode of either the pad or the support is recognized to be the cause of squeal;
- the “tuning in” between the two natural frequencies of the system and the large deformation at the contact surface are recognized to be necessary conditions for squeal coupling. This result agrees with the numerical findings;
- a clear distinction is obtained between squeal events due to the pad-disc coupling and the support (caliper)-disc coupling. Solutions to avoid one of them can be useless in order to avoid the other;
- a further proof that squeal is a dynamic instability is given by triggering its rise by an external impulse;
- the possibility to excite the instability by an external impulse, and the phase difference between the measured signals depend on the frequency ‘tuning in’ rate between the two modes. The phase of the response of the system, excited close to its natural frequency, has a key role in the unstable vibrations;
- a double, almost opposite role of the modal damping is shown: it can either prevent the damped mode to be involved in squeal or increase its propensity (“tuning in” range) to couple with other modes. Moreover, solutions to increase the modal damping can change the dynamics and then cause further squeal instabilities. Attention should be placed when adopting such solutions;
- the tribological analysis gives first a general overview of the tribological triplet. Then, the surface topography with and without squeal highlights the effects of the squeal vibrations on the contact surfaces;
- cracks and material exfoliations are observed after squeal events on both the third body layer and the superficial material of the pad. The

- pad material is under fatigue excitation due to the oscillation of the contact stresses at the squeal frequency, as calculated numerically;
- the cracks and the material exfoliations are observed to be an effect and not the cause of squeal;
 - the parallel dynamic analysis allows to take into account the role of the mechanism in the tribological analysis; the local oscillations of the contact stresses are related to the actual deformation of the mechanism during squeal;
 - the results show that the “feed-back mechanism” that causes the auto-excited vibrations of the system is due to the local oscillation of the contact forces, calculated numerically and highlighted by the experimental evidences. The friction coefficient couples the normal vibrations of the disc with the bending vibrations of the pad and the support;
 - the analysis of the contact surface highlights a further problem related to squeal: the damages of the pad surface and the fragmentation of the third body can increase the wear rate of the friction material;

The numerical and experimental results underline that squeal is an interdisciplinary issue where the tribological aspects and the dynamics of the mechanism are strongly related and, to fully understand the problem, they have to be jointly analyzed.

6.3 Future work

As asserted above this thesis is part of a wider research project. In the following the next steps of the research are reported.

The numerical and experimental results are qualitatively in agreement. Nevertheless, the numerical analysis, presented in Chapter 3, was carried out during the design and construction of the experimental set-up, and thus developed on a non updated model of the set-up. The analysis needs to be repeated on an updated model to be also quantitatively compared with the experimental evidences. An updating of the linear FE model has been already performed and the results have been compared with the experiments in Appendix E. A good agreement is found. The next step of the research program is the updating of the nonlinear model to compare quantitatively the time simulations with the experimental data.

The presented work highlights also the need of a quantitative analysis on the influence of both the modal damping and the amplitude of the eigenvector at the contact area on the squeal propensity.

Despite the use of the simplified set-up allows to study the physics of the problem, it also causes the mayor limit to the analysis. In fact, as asserted above, the results can be only extrapolated to the low frequency squeal because the dimensions of the friction pads are not accounted for. Therefore, to extend the findings to the high frequency squeal, the next step will consist in the use of commercial brake pads. Some results in this direction were already obtained and presented in [MASS 05b].

The presented work shows that squeal depends on the “tuning in” between two modes of the brake apparatus, i.e. on the modal distribution of the whole brake system. Nevertheless, the modal distribution depends on several global and local characteristics of the system and it is extremely sensitive to slight changes. In the mass production, for the same brake model, each brake system has unpredictable changes in the dynamics that can affects the squeal occurrence. Because of this, the author believes that solutions for squeal suppression should be addressed to reduce the squeal vibrations, after its occurrence, and not only to prevent the modal coupling that could result almost impossible. The influence of lumped discontinuities (lumped masses, stiffness) in the brake disc is actually under investigation.

Finally, the same dynamic and tribological analysis should be performed on a real brake apparatus to extend the results to commercial brake systems.

References

References

- [ABU 05a] Abu Bakar A.R., Ouyang H. and Siegel, J.E., *Brake pad surface topography Part I: Contact Pressure Distribution*, SAE paper n. 05BC-4, 2005.
- [ABU 05b] Abu Bakar A.R., Ouyang H. and Siegel, J.E., *Brake pad surface topography Part II: Squeal generation and prevention*, SAE paper n. 05BC-03, 2005.
- [ABU 06] Abu Bakar A.R., Ouyang H., *Complex eigenvalue analysis and dynamic transient analysis in predicting disc brake squeal*, International Journal of Vehicle Noise and Vibrations, 2006, Vol.2, No.3.
- [AKAY 00] Akay A., Wickert J., Xu Z., *Investigation of Mode Lock-In and friction interface*, Final Report, Department of mechanical engineering, Carnegie Mellon University, Pittsburgh, 2000.
- [AKAY 02] Akay A., *Acoustic of friction*, Journal of Acoustical Society of America, 2002, Vol. 111 (4), pp. 1525-1548.
- [ALLG 02] Allgaier R., Gaul L., Keiper W., Willnery K., Hoffmann N., *A study on brake squeal using a beam on disc*, Proceedings of the International Modal Analysis Conference – IMAC, 2002, Vol. 1, pp. 528-534.
- [ALLG 03] Allgaier R., *Experimentelle und numerische untersuchungen zum bremsenquietschen*, P.h.D. thesysis, University of Stuttgart, reihe12 Nr481, Stuttgart, 2003.
- [BAE 00] Bae J.C., Wickert J.A., *Free vibration of coupled disk-hat structures*, Journal of Sound and Vibration, 2000, Vol. 235 (1), pp. 117–132.
- [BAIL 00] Baillet L., Walter H., Brunet M., *A 3D contact algorithm for explicit dynamic F.E. code applied to the ironing process*, Metal Forming, 2000, pp. 141-147.
- [BAIL 02] Baillet L., Sassi T., *Finite element method with Lagrange multipliers for contact problems with friction*, Comptes Rendus de l'Académie des Sciences Paris, 2002, Series I,334 , pp. 917-922.
- [BAIL 05a] Baillet L., Link V., D'Errico S., et al., *Finite element simulation of dynamic instabilities in frictional sliding contact*, Transaction of ASME: Journal of Tribology, 2005, Vol. 127, pp. 652-657.
- [BAIL 05b] Baillet L., D'Errico S., Berthier Y., *Influence of sliding contact local dynamics on macroscopic friction coefficient variation*, Revue Européenne des Eléments Finis, 2005, Vol. 14/2-3, pp.305-321.
- [BAIL 06] Baillet L., D'Errico S., Laulagnet B., *Understanding of the squealing noise using the temporal finite element method*, Journal of Sound and Vibration, 2006, Vol. 292, pp.443-460.

References

- [BERG 99] Bergman F., Eriksson M., Jacobson S., *Influence of disc topography on generation of brake squeal*, *Wear*, 1999, Vol. 225-229, pp. 621-628.
- [BERT 01] Berthier Y., *Background on friction and wear*, Lemaître Handbook of Materials Behavior Models, Academic Press, 2001, Section 8.2, pp. 676-699.
- [CARP 91] Carpenter N.J., Taylor R.L., Katona M.G., *Lagrange constraints for transient finite element surface contact*, *International Journal for Numerical Methods in Engineering*, 1991, Vol. 32, pp. 130-128.
- [CHAN 94] Chan S.N., Mottershead J.E., Cartmell M.P., *Parametric resonances at subcritical speeds in discs with rotating frictional loads*, *Proceedings of the Institution of Mechanical Engineers Part*, 1994, C 208 (C6), pp. 417-425.
- [CHEN 00] Chen F., Chen S. E., Harwood P., *In-plane mode/friction process and their contribution to disc brake squeal at high frequency*, Technical Report 2000-01-2773, SAE, Warrendale, PA, 2000.
- [CHEN 02a] Chen F., Chern J., Swayze J., *Modal coupling and its effect on brake squeal*, Technical Report 2002-01-0922, SAE, Warrendale, PA, 2002.
- [CHEN 02b] Chen G.X., Zhou Z., Kapsa P., Vincent L., *Effect of surface topography on formation of squeal under reciprocating sliding*, *Wear* 253 (2002) 411-423.
- [CHEN 03] Chen G.X., Zhou Z., Kapsa P., Vincent L., *Experimental investigation into squeal under reciprocating sliding*, *Tribology*, 2003, Vol. 36, pp. 961-971.
- [CHEN 05] Chen W., Deng X., *Structural damping caused by micro-slip along frictional interfaces*, *International Journal of Mechanical Sciences*, 2005, Vol. 47, pp. 1191-1211.
- [CHER 02] Chern Y., Chen F. and Swayze J., *Nonlinear Brake Squeal Analysis*, 2002, SAE Paper 2002-01-3138.
- [CUNE 01] Cunefare K.A., Rye R., *Investigation of disc brake squeal via sound intensity and laser vibrometry*, Technical Report 2001-01-1604, SAE, Warrendale, PA, SAE, 2001.
- [DENO 01] Denou Y., Nishiwaki M., *First order analysis of low frequency disk brake squeal*, Technical Report 2001-01-3136, SAE, Warrendale, PA, 2001.
- [DERR 03] D'Errico S., *Modelisation de vibrations d'origine tribologique: application au freinage*, Mémoire de DEA, Institut National des Sciences Appliquées de Lyon, 2003, 74 p.
- [EARL 71] Earles S.W.E., Soar G.B., *Squeal noise in disc brakes*, in: *Vibration and Noise in Motor Vehicles*, Institution of Mechanical

- Engineers, London, England, 1971, Paper number C 101/71, pp. 61–69.
- [EARL 77] Earles S.W.E., *A mechanism of disc-brake squeal*, Technical Report 770181, SAE, Warrendale, PA, 1977.
- [EARL 84] Earles S.W.E., Badi M., *Oscillatory instabilities generated in a double-pin and disc undamped system: a mechanism of disc-brake squeal*, Proceedings of the Institution of Mechanical Engineers, 1984, C 198, pp. 43– 49.
- [EARL 87] Earles S.W.E., Chambers P.W., *Disc brake squeal noise generation: predicting its dependency on system parameters including damping*, International Journal of Vehicle Design, 1987, Vol. 8, pp. 538– 552.
- [ERIK 99] Eriksson M., Bergman F., Jacobson S., *Surface characteristic of brake pads after running under silent and squealing conditions*, Wear, 1999, Vol. 232, pp. 621-628.
- [ERIK 01] Eriksson M., Jacobson S., *Friction behaviour and squeal generation of disc brakes at low speeds*, Proceedings of the Institution of Mechanical Engineers, Part D: Journal of Automobile Engineering 2001, Vol. 215, pp. 1245– 1256.
- [ERIK 02] Eriksson M., Bergman F., Jacobson S., *On the nature of tribological contact in automotive brakes*, Wear, 2002, Vol. 252, pp. 26-36.
- [FELS 78] Felske A., Hoppe G., Matth.ai H., *Oscillations in squealing disc brakes-analysis of vibration modes byholographic interferometry*, Technical Report 780333, SAE, Warrendale, PA, 1978.
- [FIEL 93] Fieldhouse J.D., Newcomb P., *The application of holographic interferometry to the study of disc brake noise*, Technical Report 930805, SAE, Warrendale, PA, 1993.
- [FIEL 96] Fieldhouse J.D., Newcomb T.P., *Double pulsed holography used to investigate noisy brakes*, Optics and Lasers in Engineering, 1996, Vol. 25, No.6, pp. 455-494.
- [FOSB 59] Fosberry R.A.C., Holubecki Z., *Interim report on disc brake squeal*, Technical Report 1959/4, Motor Industry Research Association, Warwickshire, England, 1959.
- [FOSB 61] Fosberry R.A.C., Holubecki Z., *Disc brake squeal: its mechanism and suppression*, Technical Report 1961/1, Motor Industry Research Association, Warwickshire, England, 1961.
- [GIAN 04] Giannini O., Massi F., *An experimental study on the brake squeal noise*, Proc. ISMA 2004-International Conference on Noise and Vibration Engineering, Leuven, Belgium, 2004.

References

- [GIAN 05] Giannini O., Massi F., Sestieri A., *Experimental Characterization of the High Frequency Squeal on a Laboratory Brake Set-up*, Proceeding of IMAC XXIII, 2005, Paper No. 107, Orlando (FL), USA.
- [GIAN 06a] Giannini O., Akay A., Massi F., *Experimental analysis of brake squeal noise on a laboratory brake setup*, Journal of Sound and Vibration, 2006, Vol. 292, n° 1-2, pp. 1-20.
- [GIAN 06b] Giannini O., Massi F., *Uncertain finite element model for the brake squeal prediction*, International Modal Analysis Conference - IMAC-XXIV, St. Louis, MO, USA, 2006.
- [GIAN 06c] Giannini O., Sestieri A., *Predictive model of squeal noise occurring on a laboratory brake*, Journal of Sound and Vibration, 2006, Vol. 296, pp. 583-601.
- [GAUG 06] Gauger U., Hanss M., Gaul L., *On the inclusion of uncertain parameters in brake squeal analysis*, International Modal Analysis Conference - IMAC XXIV, Saint Louis, MO, USA, 2006
- [GODE 84] Godet M., *The third-body approach: a mechanical view of wear*, Wear, 1984, Vol. 100, pp. 437-452.
- [IBRA 00] Ibrahim R.A., Madhavan S., Qiao S.L., Chang W.K., *Experimental investigation of friction-induced noise in discbrake systems*, International Journal of Vehicle Design, 2000, Vol. 23 (3– 4), pp. 218-240.
- [ICHI 93] Ichiba Y., Nagasawa Y., *Experimental study on brake squeal*, Technical Report 930802, SAE, Warrendale, PA, 1993.
- [JARV 63] Jarvis R.P., Mills B., *Vibrations induced by friction*, Proceedings of the Institution of Mechanical Engineers, 1963, Vol. 178, No. 32, pp. 847–857.
- [KINK 03] Kinkaid N.M., O'Reilly O.M., Papadopoulos P., *Automotive disc brake squeal*, Journal of Sound and Vibration, 2003, Vol. 267, pp. 105-166.
- [LANG 93] Lang A.M., Smales H., *An approach to the solution of disc brake vibration problems*, in: Braking of Road Vehicles. Automobile Division of the Institution of Mechanical Engineers, Mechanical Engineering Publications Limited, Suffolk, England, 1993, pp. 223– 231.
- [LEE 03a] Lee Y.S., Brooks P.C., Barton D.C. and Crolla D.A., *A predictive tool to evaluate disc brake squeal propensity part 1: the model philosophy and the contact problem*, 2003, International Journal of Vehicle Design, Vol. 31, No. 3, pp.289–308.
- [LEE 03b] Lee Y.S., Brooks P.C., Barton D.C. and Crolla D.A., *A predictive tool to evaluate disc brake squeal propensity part 2: system*

- linearisation and modal analysis*, 2003, International Journal of Vehicle Design, Vol. 31, No. 3, pp.309–329.
- [LEE 03c] Lee Y.S., Brooks P.C., Barton D.C. and Crolla D.A., *A predictive tool to evaluate disc brake squeal propensity part 3: parametric design studies*, 2003, International Journal of Vehicle Design, Vol. 31, No. 3, pp.330–353.
- [LILE 89] Liles G.D., *Analysis of Disc Brake Squeal Using Finite Element Methods*, SAE Paper 891150, 1989.
- [MAHA 99] Mahajan S.K., Hu Y.K. and Zhang K., *Vehicle Disc Brake Squeal Simulations and Experience*, SAE Paper 1999-01-1738, 1999.
- [MASS 03] Massi F., *Studio del fenomeno dello "squeal" dei freni a disco tramite sperimentazione su un freno da laboratorio*, Master thesis in Mechanical Engineering - University of Rome "La Sapienza" - Carnegie Mellon University (Pittsburgh-PN), Rome, Italy, 2003.
- [MASS 05a] Massi F., Baillet L., *Numerical analysis of squeal instability*, Proc. International Conference on emerging technologies of noise and vibration analysis and control - NOVEM, Saint-Raphaël, France, 2005.
- [MASS 05b] Massi F., Giannini O., *Extension of a modal instability theory to real brake systems*, Proceeding of IMAC XXIII, 2005, Paper No 91, Orlando (FL), USA.
- [MASS 06a] Massi F., Giannini O., Baillet L., *Brake squeal as dynamic instability: an experimental investigation*, Journal of the Acoustical Society of America, 2006, Vol. 120 (3), pp. 1388-1399.
- [MASS 06b] Massi F., Baillet L., Giannini O., Sestieri A., *Brake squeal phenomenon: linear and non-linear numerical approach*, Mechanical Systems and Signal Processing, (Submitted 2006)
- [MASS 06c] Massi F., Baillet L., Giannini O., *Experimental analysis on squeal modal instability*, International Modal Analysis Conference - IMAC-XXIV, St. Louis, MO, USA, 2006.
- [MASS 06d] Massi F., Sestieri A., Baillet L., *The effect of modal damping on brake squeal instability*, The Thirteenth International Congress on Sound and Vibration - ICSV13, Vienna, Austria, 2006.
- [MASS 06e] Massi F., Baillet L., Sestieri A., *Linear and Nonlinear Numerical Approaches to Brake Squeal Noise*, The Fifth International Conference on Engineering Computational Technology - ECT2006, Las Palmas de Gran Canaria, Spain, 2006.
- [MASS 06f] Massi F., Baillet L., Giannini O., *Squeal prediction on a simplified brake system by complex eigenvalue analysis*, ISMA 2006-International Conference on Noise and Vibration Engineering, Leuven, Belgium, 2006.

References

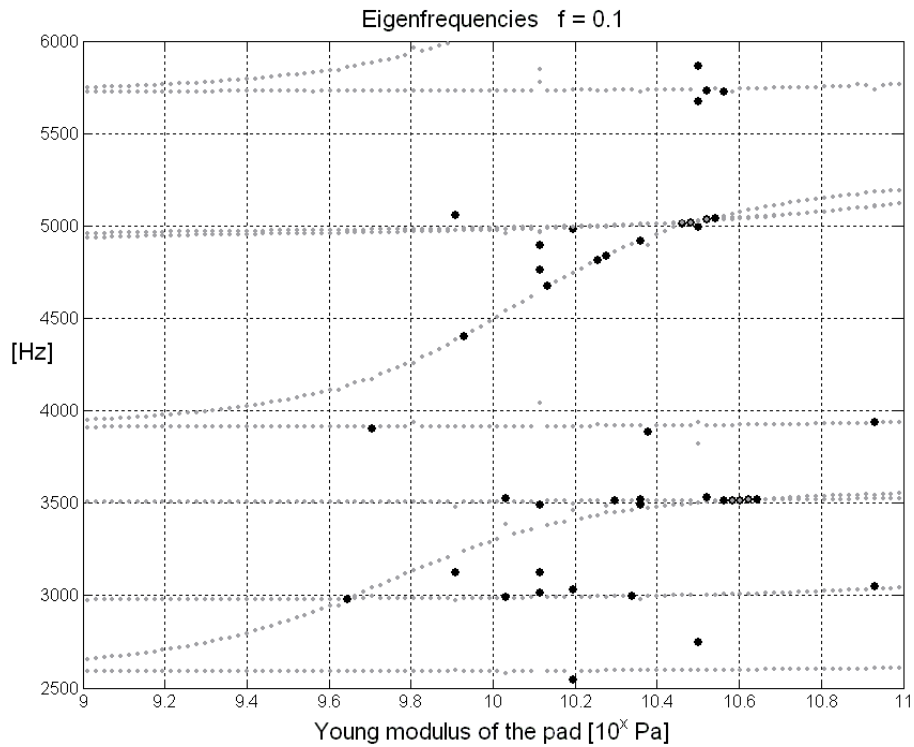
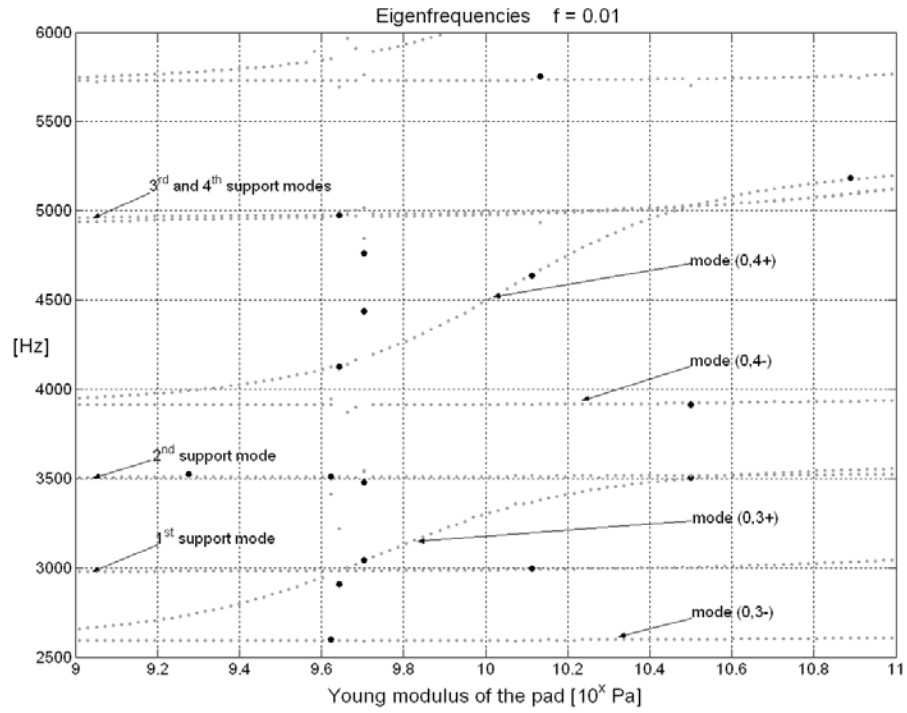
- [MATS 93] Matsuzaki M., Izumihara T., *Brake noise caused by longitudinal vibration of the disc rotor*, Technical Report 930804, SAE, Warrendale, PA, 1993.
- [MILL 38] Mills H.R., *Brake squeak*, Technical Report 9000 B, Institution of Automobile Engineers, 1938.
- [MILL 78] Millner N., *An analysis of disc brake squeal*, Technical Report 780332, SAE, Warrendale, PA, 1978.
- [MOTT 95] Mottershead J.E., Chan S.N., *Flutter instability of circular discs with frictional follower forces*, Transactions of the American Society of Mechanical Engineers Journal of Vibration and Acoustics, 1995, Vol. 117 (1), pp. 161– 163.
- [MOTT 97] Mottershead J.E., Ouyang H., Cartmell M.P. and Friswell M.I., *Parametric resonances in an annular disc, with a rotating system of distributed mass and elasticity; and the effects of friction and damping*, Proceedings of the Royal Society A: Mathematical, Physical and Engineering Sciences 1997, Vol. 453, n° 1956, pp. 1-19.
- [MOTT 98] Mottershead J.E., *Vibration- and friction-induced instability in disks*, Shock and Vibration Digest, 1998, Vol. 30 (1), pp. 14–31.
- [MURA 84] Murakami H., Tsunada N., Kitamura T., *A study concerned with a mechanism of disc-brake squeal*, Technical Report 841233, SAE, Warrendale, PA, 1984.
- [NAGY 94] Nagy L.I., Cheng J. and Hu Y., *A New Method Development to Predict Brake Squeal Occurrence*, SAE Paper 942258, 1994.
- [NISH 89] Nishiwaki M., Harada H., Okamura H., Ikeuchi T., *Study on disc brake squeal*, Technical Report 890864, SAE, Warrendale, PA, 1989.
- [NISH 93] Nishiwaki M., *Generalized theory of brake noise*, Proceedings of the Institution of Mechanical Engineers, Part D: Journal of Automobile Engineering. 1993, Vol. 207, n° 3, pp. 195–202.
- [NORT 72] North M.R., *Disc brake squeal-a theoretical model*, Technical Report 1972/5, Motor Industry Research Association, Warwickshire, England, 1972.
- [NORT 76] North M.R., *Disc brake squeal*, In: proc. conf. on braking of road vehicles-proceedings of a conference-institution of mechanical engineers, automobile division-institute of road transport engineers, Loughborough, 1976, pp. 169–176.
- [OUES 03] Oueslati A., Nguyen Q.S., Baillet L., *Stick-slip separation waves in unilateral and frictional contact*, Comptes Rendus Mecanique, 2003, Vol. 331 (2), pp. 133-140.
- [OUYA 98] Ouyang H., Mottershead J.E., Cartmell M.P. and Friswell M.I., *Friction-induced parametric resonances in discs: effect of a*

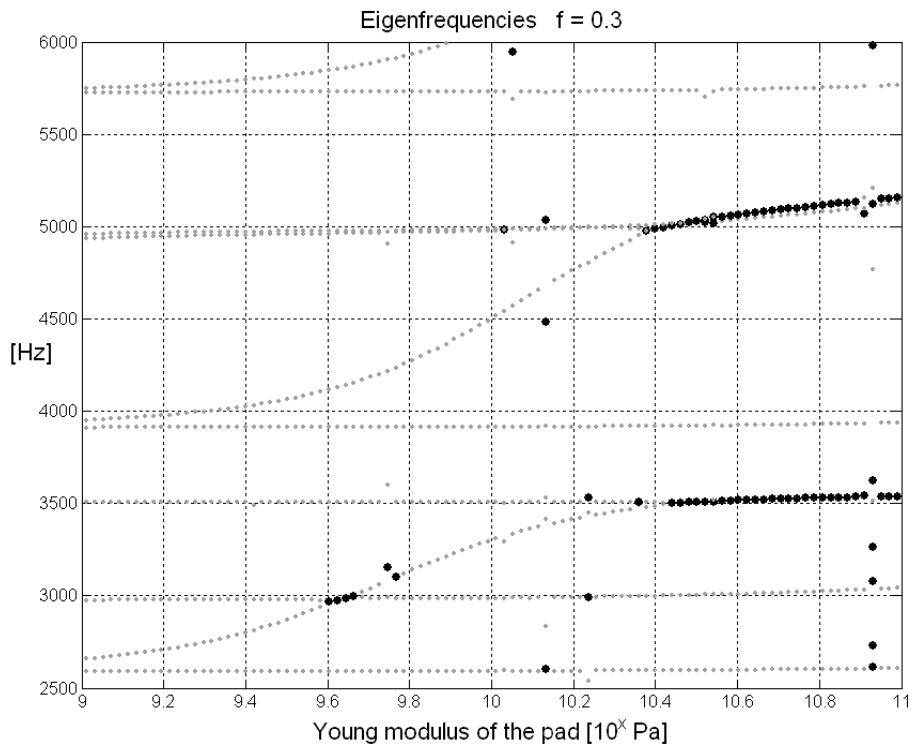
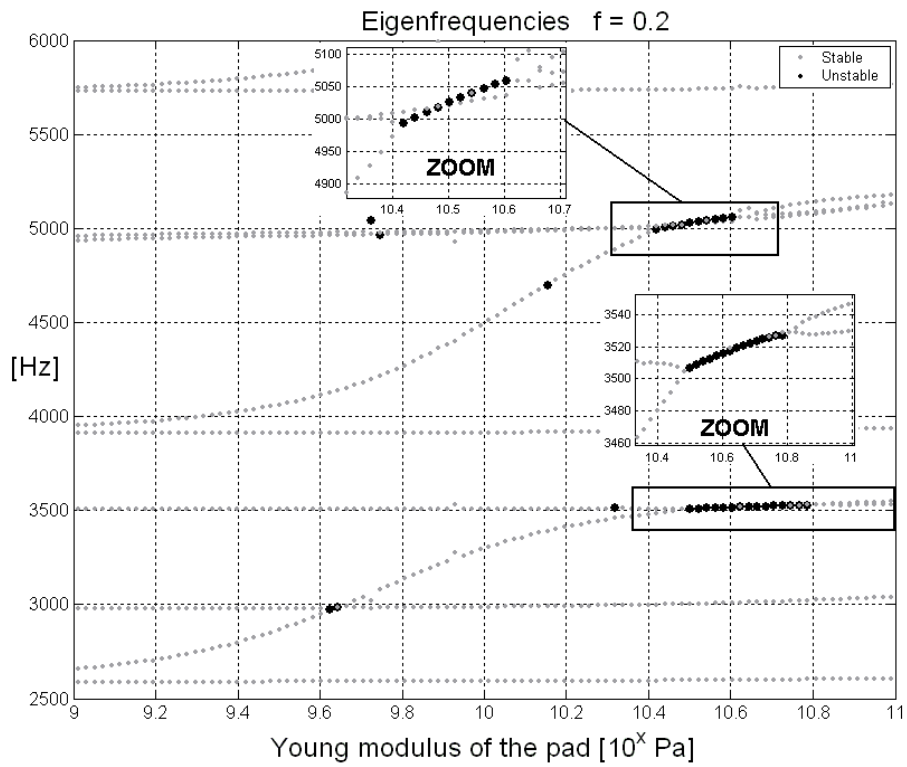
- negative friction-velocity relationship*, Journal of Sound and Vibration, 1998, Vol. 209(2), pp. 251-264.
- [OUYA 00] Ouyang H., Mottershead J.E., Brookfield D.J., James S., Cartmell M.P., *A methodology for the determination of dynamic instabilities in a car disc brake*, International Journal of Vehicle Design, 2000, Vol. 23 (3/4), pp. 241– 262.
- [OUYA 01] Ouyang H., Mottershead J.E., *A bounded region of disc-brake vibration instability*, Transactions of the American Society of Mechanical Engineers Journal of Vibration and Acoustics, 2001, Vol. 123 (4), pp. 543– 545.
- [OUYA 05] Ouyang H., Nack W., Yuan Y. and Chen F., *Numerical analysis of automotive disc brake squeal: a review*, 2005, International Journal of Vehicle Noise and Vibrations, Vol. 1, No. 3/4, pp.207–231.
- [RHEE 89] Rhee S.K., Tsang P.H.S., Wang Y.S., *Friction-induced noise and vibration of disc brakes*, Wear, 1989, Vol. 133, pp. 39-45.
- [RHEE 90] Rhee S.K., Jacko M.G., Tsang P.H.S., *The role of friction film in friction, wear, and noise of automotive brakes*, Technical Report 900004, SAE, Warrendale, PA, 1990.
- [RUDO 01] Rudolph M., Popp K., *Friction induced brake vibrations*, Proceedings of DETC'01, DETC2001/ VIB-21509, ASME, Pittsburgh, PA, 2001, pp. 1–10.
- [SHER 04] Sherif H.A., *Investigation on effect of surface topography of pad/disc assembly on squeal generation*, Wear, 2004, Vol. 257, pp. 687-695.
- [SUH 81] Suh N.P., Sin H.C., *The genesis of friction*, Wear, 1981, Vol. 69, pp. 91–114.
- [SPUR 61] Spurr R.T., *A theory of brake squeal*, Proceedings of the Automobile Division, Institution of Mechanical Engineers 1961–1962, 1961, Vol. 1, pp. 33–52.
- [TSEN 98] Tseng J.G., Wickert J.A., *Nonconservative stability of a friction loaded disk*, Transactions of the American Society for Mechanical Engineers Journal of Vibration and Acoustics, 1998, Vol. 120 (4), pp. 922–929.
- [TUCH 01] Tuchinda A., Hoffmann N. P., Ewins D. J. and Keiper W., *Mode Lock-in Characteristics and Instability Study of the Pin-On-Disc System*, Proceedings of the International Modal Analysis Conference – IMAC, 2001, Vol. 1, pp. 71–77.
- [TUCH 02] Tuchinda, A., Hoffmann, N. P., Ewins, D. J. and Keiper, W., *Effect of Pin Finite Width on Instability of Pin-On-Disc Systems*, Proceedings of the International Modal Analysis Conference – IMAC, 2002, Vol. 1, pp. 552-557.

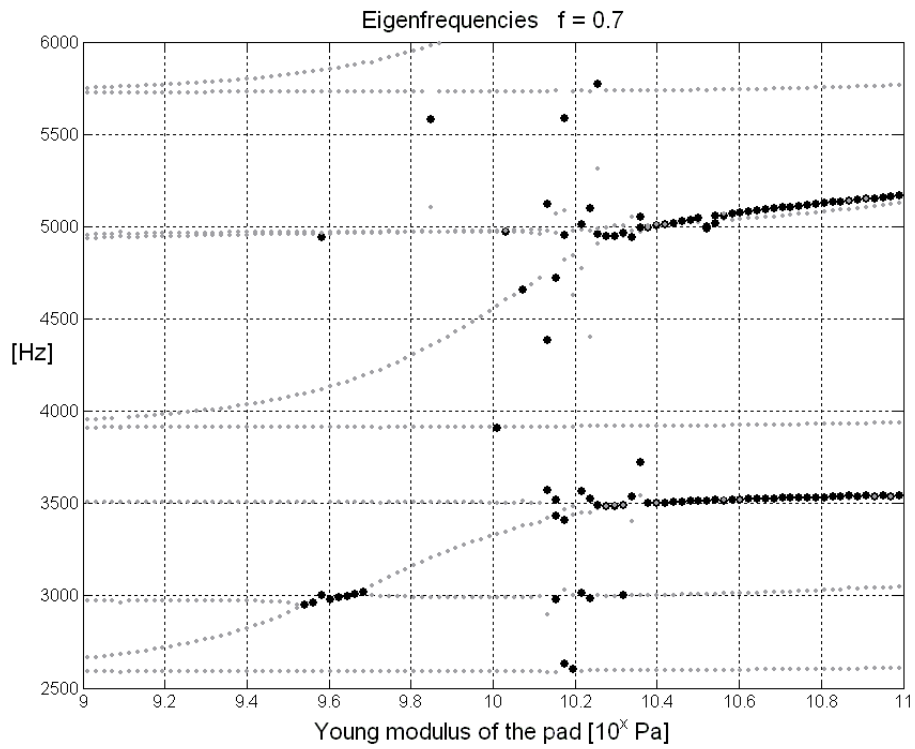
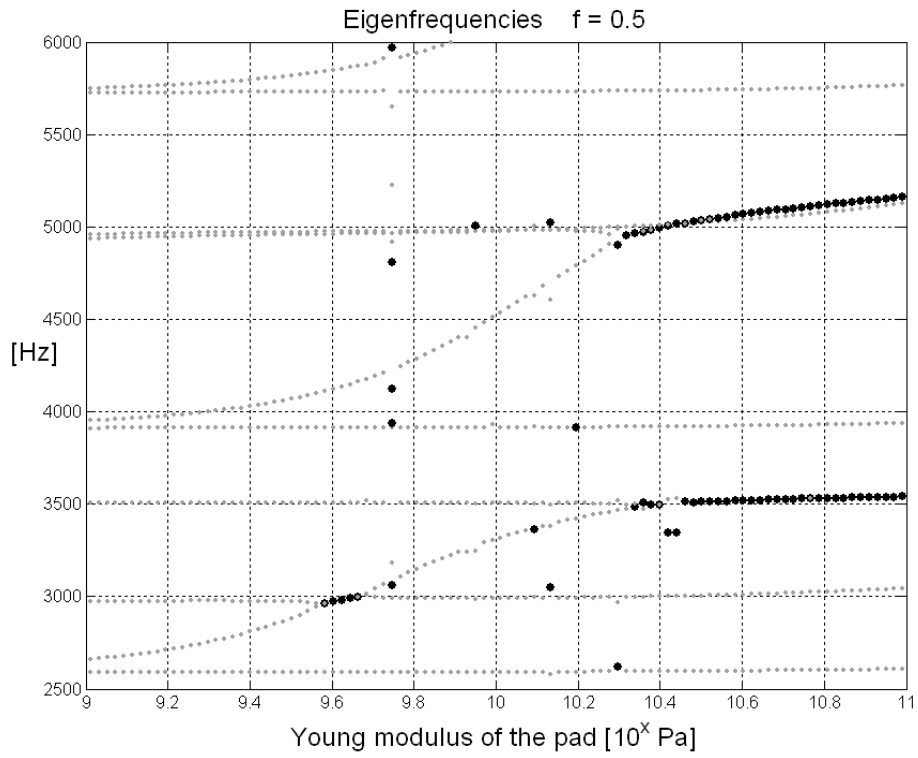
References

- [TZOU 98] Tzou K.I., Wickert J.A., Akay A., *In-plane vibration modes of arbitrary thick disks*, Transaction of ASME, 1998, Vol. 120, pp. 384-391.
- [VAN 01] Van der Auweraer H., Fischer M., Hendricx W., Pezzutto A., Garesci F., *Structural dynamics and multibody analysis of brake noise*, Proceedings of the International Modal Analysis Conference – *IMAC*, 2001, Vol. 1, pp. 558-563.
- [WRIG 02] Wriggers P., *Computational contact mechanics*, Somerset, New Jersey, USA: John Wiley & Sons, 2002, p. 464, ISBN 0471496804.

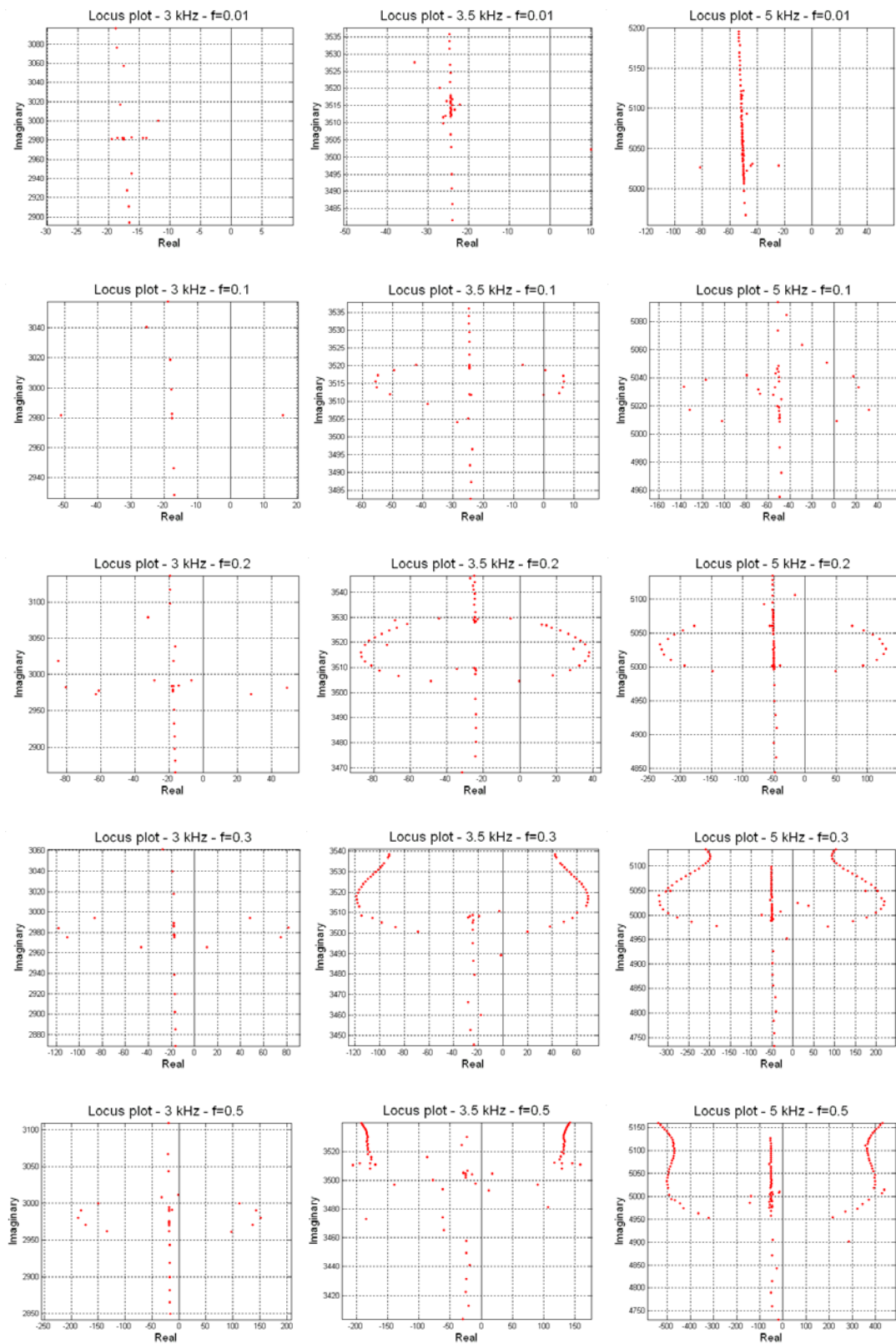
Appendix A. Eigenvalues plots with different friction coefficients

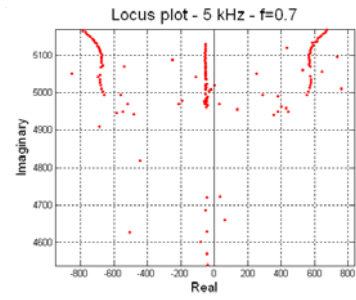
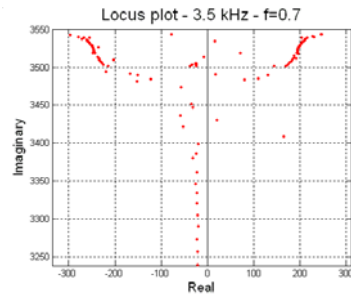
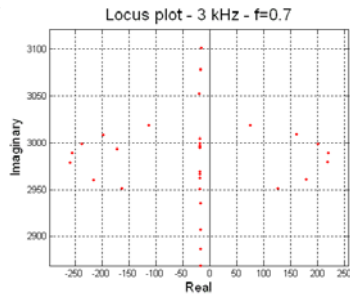






Appendix B. Locus plots of the unstable regions





Appendix C. Acquisition details

The EMAs of the brake assembly are performed by a SIMO method: the structure is excited with a hammer and the response is measured with accelerometers.

The disc is excited with the Bruel&Kjaer instrumented hammer, model 8202, that has a bandwidth of excitation limited to 7000Hz. Because the range of frequency of interest is larger than the frequency bandwidth of the hammer a preliminary comparison between different excitation methods must be performed:

- hammer impact with single impulse;
- white noise excitation with a shaker;
- hammer impact with random impulses.

The hammer impact with a single impulse does not modify the dynamics of the system (non intrusive method), but, as asserted above, gives good measurements just up to 7 kHz (bandwidth of the hammer).

The white noise excitation with the shaker allows to excite the system to higher frequencies, but modifies the dynamics of the system due to the stiffness and mass add of the force transducer (connection between shaker and structure). Moreover, particular attention must be placed to the response of the stinger, because of the high excitation frequency range.

Because of the low coupling between disc and pad (small area of contact), the modification of the system dynamics due to the connection with the shaker is not negligible. For this reason a hammer impact excitation with random impulses was preferred to excite the system. The randomness of the impulses that are provided to the structure and the major amount of energy with respect to the single impulse, allows to treat the signals to recover the FRFs up to 16 kHz, and observe the natural frequencies up to 20 kHz (Figure 4.2).

The response of the structure is measured on a radial grid of 168 points (4 circumferences per 42 radiuses) with Bruel&Kjaer (limit bandwidth 0-20 kHz) accelerometers, model 4393. The low mass of the accelerometers modifies slightly the dynamics of the system.

The signals in electric charge are then converted into voltage signals and amplified by Bruel&Kjaer amplifiers model 2635. The voltage signals are acquired by the acquisition system PROSIG 5600.

The following acquisition parameters are used:

Samples per second	40000	Hammer window	Rectangular
Acquisition time	20 s	Response window	Hanning

Table A.1 Acquisition parameters for EMA.

The FRFs at each single point are calculated with Matlab and the ICATS software is used to perform the modal analysis.

Squeal acquisitions are performed during the braking phase by measuring the following signals:

- the normal and tangential forces between support and pad by a tri-axial force transducer model PCB m260a01;
- the tangential acceleration measured at the leaning edge of the pad by a Bruel&Kjaer accelerometer and the laser vibrometer POLYTEC OFV 3001S;
- the pressure sound emission by a Bruel&Kjaer microphone placed at 200 mm from the periphery of the disc;

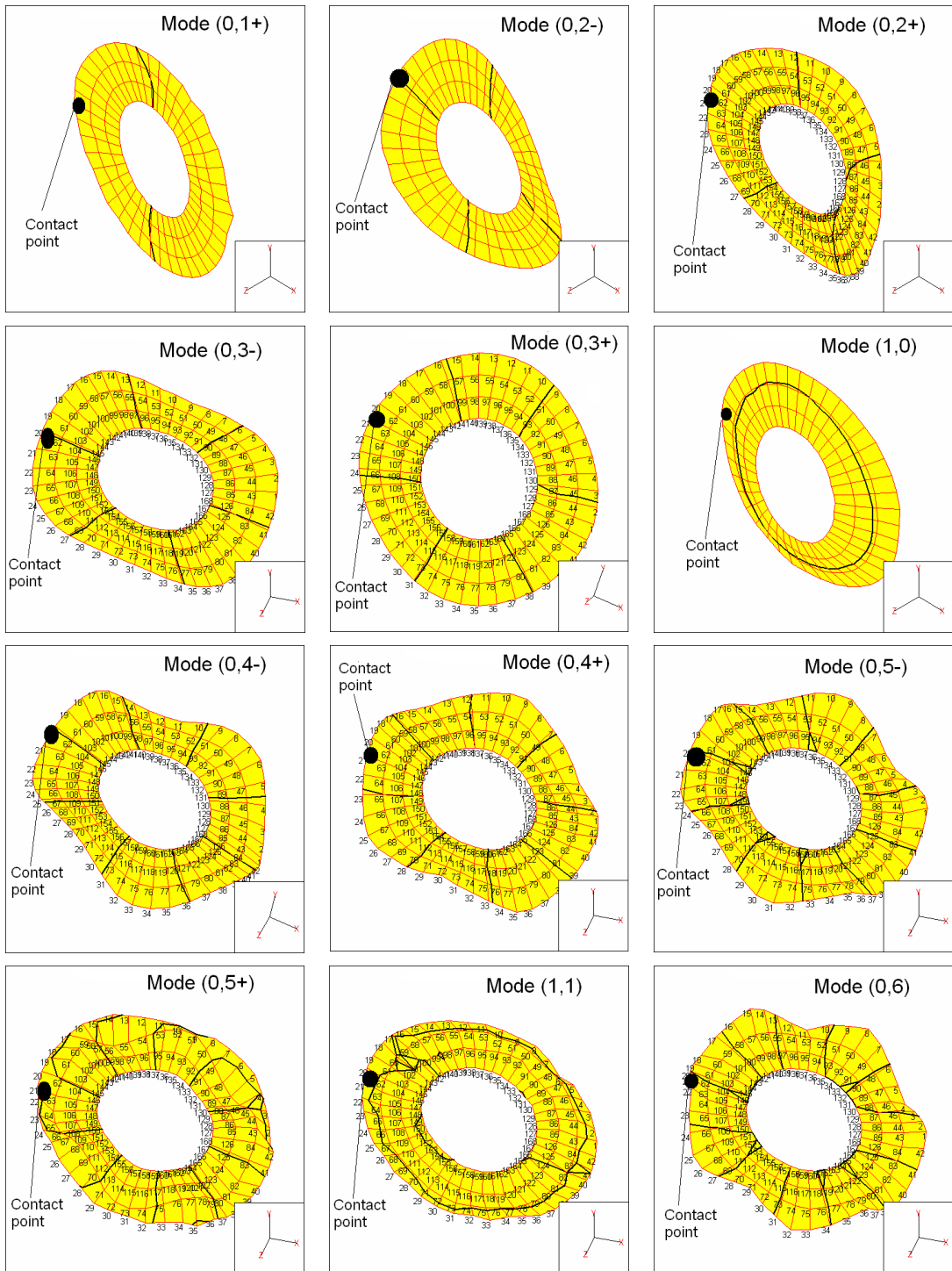
The following acquisition parameters are used:

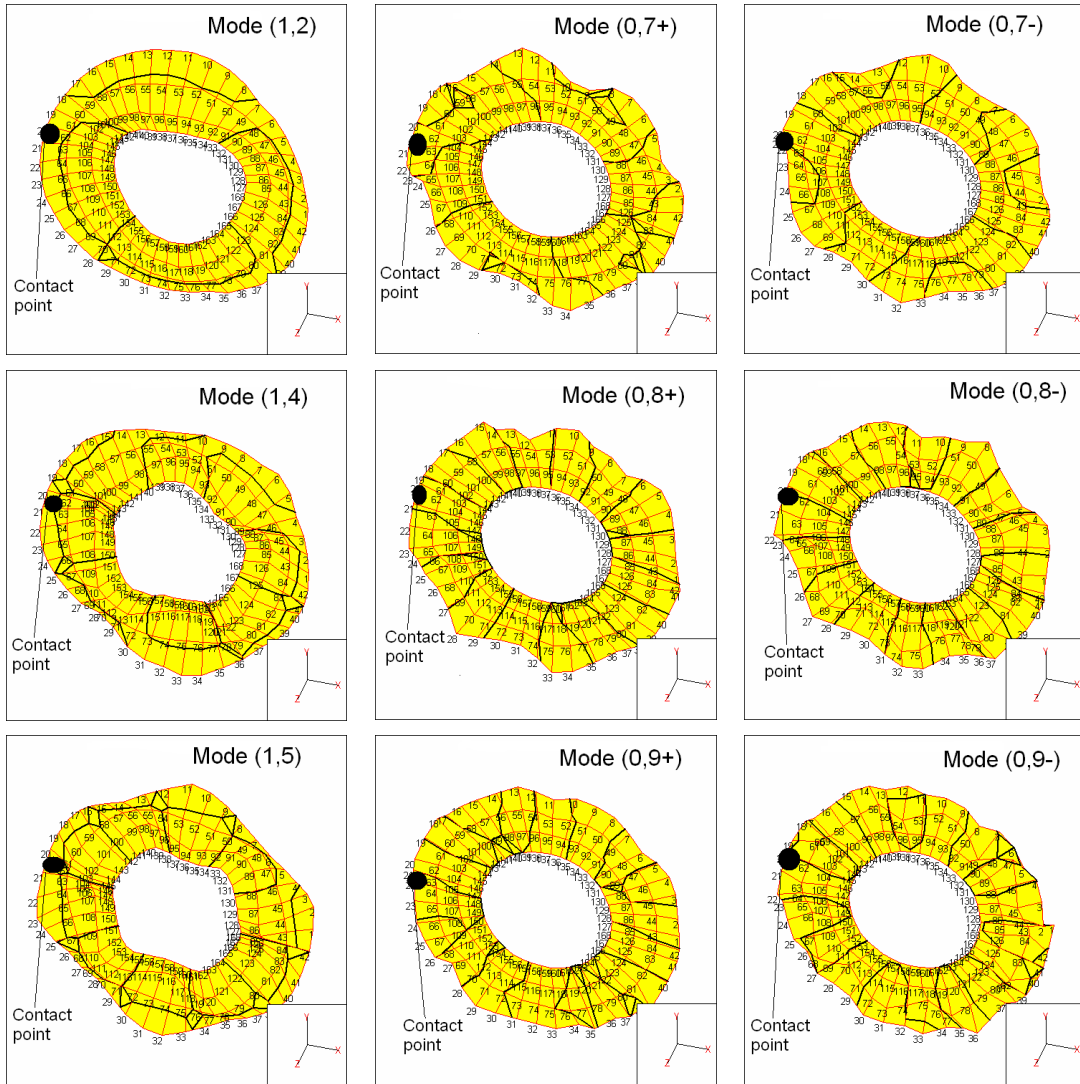
Samples per second	40000	Acceleration window	Hanning
Acquisition time	5-20 s	Force windows	Hanning
Microphone window	Rectangular		

Table C.2 Acquisition parameters for squeal measurements.

The signals are acquired by the PROSIG 5600 acquisition system and postprocessed in Matlab.

Appendix D. Modes of the disc under braking pressure





Appendix E. Linear model updating

Appendix E.	Linear model updating.....	199
E.1	Updating of the linear FE model	201
E.2	Prediction of squeal instabilities	203
<i>E.2.1</i>	<i>Support-disc squeal coupling</i>	<i>204</i>
<i>E.2.2</i>	<i>Pad-disc squeal coupling</i>	<i>205</i>
<i>E.2.3</i>	<i>Remarks.....</i>	<i>207</i>

E.1 Updating of the linear FE model

To fit the experimental apparatus, the FE model must be updated using the modal parameters obtained by the EMA (Experimental Modal Analysis). The updating process has been divided into two main steps: i) the updating of the disc without contact with the pad; ii) the updating of the whole brake assembly. In fact, the out-of-plane dynamics of the disc, involved in squeal, is influenced moderately by the low coupling due to the small contact surface, while the in-plane dynamics of the support and the pad are largely influenced by the contact with the disc. Moreover, the natural frequencies of the pad and the support are influenced significantly by the disc rotation so that the values measured in operating conditions (i.e. rotation of the disc under braking conditions) are considered for model updating.

The updating of the disc was carried out by a sensitivity analysis of the modal parameters to variations of both the material properties and the geometry. The reference dimensions of the disc are the physical dimensions of the brake disc in the experimental set-up. Because of the not perfectly rigid connection of the disc at its inner radius, the clamped condition in the model is not well represented by the real constraint conditions, resulting in lower frequencies of the modes (1,m) with respect to the modes (0,m). To reduce this effect the inner radius of the disc model is reduced with respect to the physical radius from 50 to 40 mm. The updated material properties are: Young modulus 197500 MPa; density 7800 kg/m³; Poisson ratio 0.3. The percentage error in the natural frequencies, after the updating, is less than 2% in the frequency range of interest (from 1 to 20 kHz). An error larger than 2% involves the modes (0,2) and (1,2) (4% and 8% respectively) because the constraint condition at the inner radius is still not adequate for these modes.

A further sensitivity analysis was performed on the model of the assembled system in order to update the model and to choose the driving parameters to be varied in the parametric analysis. To model the mass effect introduced by the weights positioned on the top of the support during the experiments, a layer of high density material is positioned on the top of the support model (Figure E.1).

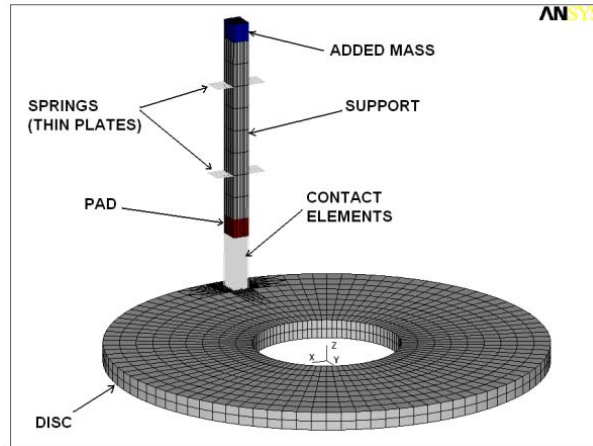


Figure E.1 Updated FE model of the experimental set-up.

Table E.1 resumes the main influence of different parameters on the model.

PARAMETERS	EIGENFREQUENCIES BEHAVIOR	PHYSICAL EFFECT
Young Modulus of the pad	Affects the eigenfrequencies of the pad, the eigenfrequencies of the support and the (m,n+) eigenfrequencies of the disc	Affects the pad stiffness and the coupling stiffness between support and disc at the contact point
Mass on the top of the support	A small add of mass affects the eigenfrequencies of the support. A further variation has a small effect on the eigenfrequencies	Changes the moment of inertia and the mass of the support
Contact stiffness	Small effect on the eigenfrequencies of the pad	Affects the boundary constraints of the pad. The stiffness of the pad affects the coupling between support and disc
Stiffness of the thin plates	Affects the eigenfrequencies of the support	Affects the stiffness of the constraints of the support in the tangential direction

Table E.1 Effects of different parameters on the model dynamics.

The updated model must consider the effect of the disc rotation in the system dynamics. The experimental analysis allowed to recognize the main effects of the rotation: a reduction of the support eigenfrequencies, due to the reduction of the tangential stiffness of the thin plates (two of them are under compression) and to the reduction of the tangential contact stiffness; a reduction of the pad eigenfrequencies, due to the reduction of the tangential contact stiffness; a negligible effect on the disc eigenfrequencies.

Because the analysis to perform is parametric, the variation of the natural frequencies in function of the main parameters is analyzed experimentally (see § 4), and then the driving parameters in the model are chosen so that the numerical eigenvalues cover the same range of variation. A

sensitivity analysis in function of the material properties of the support and in function of the parameters listed in Table E.1 is carried out. Finally, in order to reproduce the dynamics of the set-up and its variation in function of the experimental parameters, two different parameters in the model are varied simultaneously: the Young modulus of the pad material and the stiffness of the springs that hold the support (stiffness of the thin plates). The Young modulus of the pad material is very influential on the dynamics of the system at the contact zone. Moreover, the elastic properties of the pad materials are not well defined. The stiffness of the thin plates allows to modulate the tangential dynamics of the support. The following values of the parameters are introduced in the model: stiffness k of the single contact elements 2140 N/mm; density of the thin layer at the top of the support 20 Kg/cm³; Poisson ratio 0.3; density of the support 220539 Kg/m³; Young modulus of the support 2100 GPa; density of the pad 2500 Kg/m³; Young modulus of the pad ranging from 250 to 2500 MPa; stiffness of the single springs (thin plates) ranging from 3100 to 12900 N/mm.

Because of the combined linear and nonlinear numerical analysis of brake squeal, the compatibility between the two different FE models recommended a strong simplification of the FE model with respect to the experimental set-up. During the updating of the model the attention was focused particularly on the reproduction of its frequency behavior. The modes of the system are reproduced to simulate the main dynamic characteristics at the contact region, where the instability rises.

A MAC between the numerical and experimental modes was not yet implemented. Such analysis will be necessary when a quantitative analysis (that could reduce the overprediction of squeal occurrences) of the influence of modal damping and amplitude of the eigenvector at the contact area will be performed.

E.2 Prediction of squeal instabilities

The numerical eigenvalues extraction is performed by the Damped Method by ANSYS and repeated in function of the chosen driving parameters. The analysis is first performed in the frequency range from 900Hz to 20000Hz. Then, for clearness, the analysis is here reported only at the instability regions, because all the system modes are included in the eigenvalues extraction.

The value of the friction coefficient used in the analysis is retrieved from the experiments and is equal to 0.3. A detailed analysis of the relationship between friction coefficient and squeal prediction is reported in [MASS 06b].

E.2.1 Support-disc squeal coupling

Figure E.2 shows the complex eigenvalues of the system calculated between 1300 and 2600 Hz, when the Young modulus of the pad ranges from 300 to 2500 MPa, and the stiffness of the springs ranges from 3600 to 12900 N/mm. The grey dots represent eigenvalues with negative real part (stable behaviour); the black dots represent eigenvalues with positive real part (unstable behaviour).

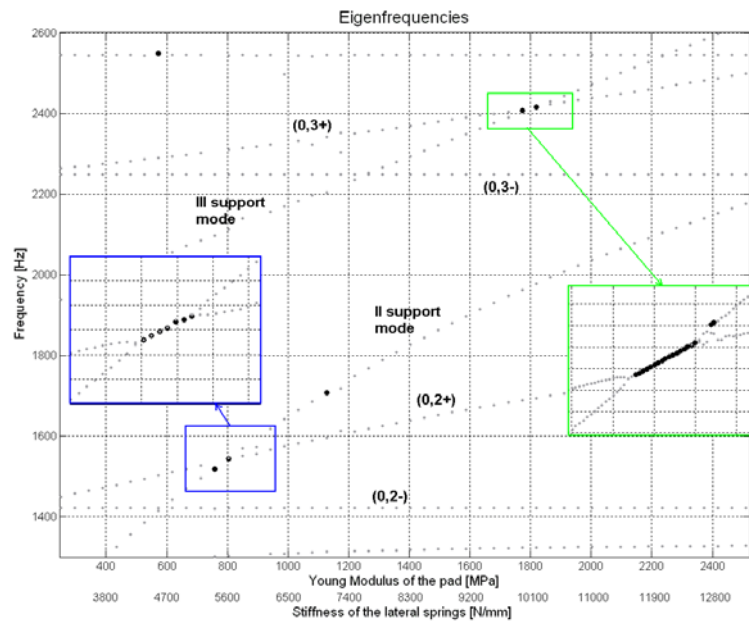


Figure E.2 Support-disc instabilities prediction by complex eigenvalue analysis.

The increase of the Young modulus of the pad causes an increase of the natural frequency of the modes $(0,m+)$, because it introduces an increasing stiffness at the contact point. On the contrary it does not affect the modes $(0,m-)$. Moreover, the increase of the spring stiffness together with the Young modulus affects the support modes whose natural frequencies increase and cross the natural frequencies of the $(0,m+)$ modes.

Two unstable regions appear around 1550 Hz (between 780 and 820 MPa), and around 2420 Hz (between 1770 and 1850 MPa), respectively. The former is due to the lock-in between the second mode of the support and the mode $(0,2+)$, while the latter is due to the lock-in between the third mode of the support and the mode $(0,3+)$. The predicted instabilities agree with the instabilities occurred during experiments, with an error percentage in frequency less than 0.2 % (see § 4). Figure E.3-a and E.3-b show the locus plot for the two unstable ranges. The updated FE model was able to predict all, and only, the

unstable couplings (squeal) between modes of the support and the disc obtained during experiments.

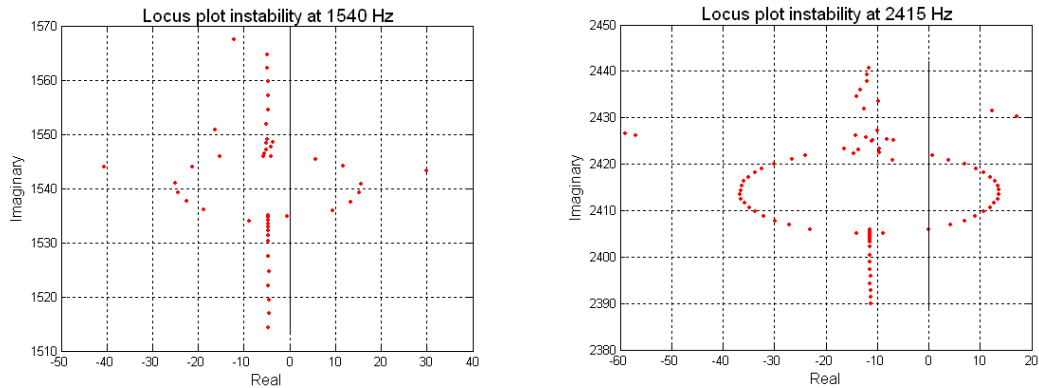


Figure E.3 Locus plot of the instabilities at: a) 1540 Hz; b) 2415 Hz.

E.2.2 Pad-disc squeal coupling

Squeal frequencies due to the coupling between modes of the pad and the disc fall in a higher frequency range with respect to those that involve modes of the support. This makes hard to predict the squeal instabilities, due to the large modal density of the system at such frequencies. Moreover the FE model does not include the lumped mass of the accelerometer, so that the pad has only one tangential mode in the considered frequency range. In fact, the configuration of the experimental set-up without accelerometer does not allow to have the squeal coupling at 3767 Hz, while the squeal couplings at 7850 Hz and at 10150 Hz still occur when the tangential mode of the pad “tunes in” with the modes (0,6+) and (0,7+).

Figure E.4 shows the eigenfrequencies and the locus plot between 7560 and 7750 Hz. In this frequency range the tangential mode of the pad reach the frequency of the mode (1,0) and the one of the mode (0,6+). As a result it couples with these two modes of the disc and two instabilities are predicted. The locus plot highlights the lock-in and lock-out points between the two pairs of modes.

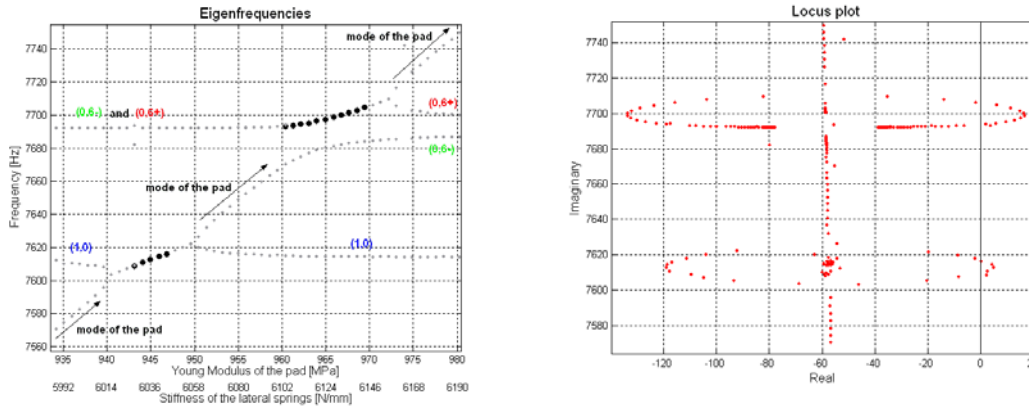


Figure E.4 a) Eigenfrequencies plot where the “lock-in” between the mode of the pad and the modes (0,1) and (0,6+) occurs; b) locus plot.

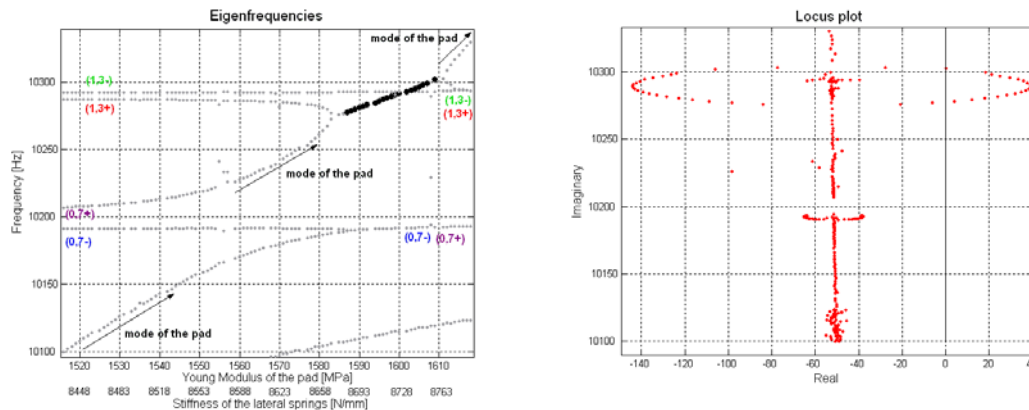


Figure E.5 a) Eigenfrequencies plot where the “lock-in” between the mode of the pad and the mode (1,3+) occurs; b) locus plot.

In the frequency range between 10 kHz and 10.5 kHz (Figure E.5), the numerical analysis shows an unstable lock-in between the mode of the pad and the (1,3+) mode that does not occur during the experiments. On the contrary, the experimental squeal of the (0,7+) mode is not reproduced by the numerical simulation. Nevertheless, the lock-in is found between the (0,7+) mode and the mode of the pad (at about 10.19 kHz) but it is not strong enough to push the eigenvalue toward the positive real semi-plane.

A further instability is predicted by the complex eigenvalue analysis when the mode of the pad crosses a longitudinal mode of the support (normal to the contact surface) at 8450 Hz.

In conclusion the analysis allowed predicting the lock-in frequencies obtained experimentally, with an over-prediction of the unstable couplings between the mode of the pad and modes of the disc. Moreover, the lock-in is predicted to occur between one mode characterized by tangential vibration at the contact area (bending modes of the support or of the pad) and one mode

characterized by normal vibrations (bending modes of the disc or longitudinal mode of the support).

E.2.3 Remarks

After the updating of the linear FE model, the parametric analysis is performed to retrieve the experimental squeal frequencies. The squeal frequencies, involving either the dynamics of the pad or the caliper that couples with the dynamics of the disc, are simulated. The complex eigenvalue analysis allowed to predict all the lock-in conditions that bring to squeal during experiments. Nevertheless, the complex eigenvalue analysis gives an over-prediction of the squeal frequencies by predicting the lock-in between pairs of modes not recognized during the tests. This can be due either to the simplification of the FE model that does not allow to reproduce the modes exactly, or to the linearity of the FE model that does not account for nonlinear effects. In fact, the over-prediction is recognized also by comparing the linear and nonlinear models.

As discussed above, the analysis highlights that two main conditions are necessary for squeal occurrence: i) the tuning-in between two natural frequencies of an in-plane mode and an out-of-plane mode of the system; ii) a large amplitude of the unstable mode in both the in-plane direction and the out-of-plane direction at the contact area, where the contact forces behave as follower forces.

Despite the over-prediction, the agreement with the experimental results demonstrates that the linear model is useful to conduct a parametrical analysis, with low computational effort, and predict all the possible unstable modal couplings that can bring to squeal.